

Lipids as Trans Acting Factors for the Transport of Integral Membrane Proteins

Dissertation

Submitted to the
combined Faculties for the Natural Sciences and
for Mathematics of the
Ruperta-Carola University of Heidelberg, Germany
for the degree of Doctor of Natural Sciences

Presented by

Diplom-Biochemiker

Marcel Fischer

born in Stadthagen, Germany

Dissertation

Submitted to the
combined Faculties for the Natural Sciences and
for Mathematics of the
Ruperta-Carola University of Heidelberg, Germany
for the degree of Doctor of Natural Sciences

Marcel Fischer

2009

Oral Examination:

Declarations

I hereby declare that I have written the submitted dissertation myself and in this process have used no other sources or materials than those expressly indicated.

I hereby declare that I have not applied to be examined at any other institution, nor have I used the dissertation in this or any other form at any other institution as an examination paper, nor submitted it to any other faculty as a dissertation.

Heidelberg, April 30, 2009

Marcel Fischer

Lipids as Trans Acting Factors for the Transport of Integral Membrane Proteins

Referees:

PD Dr. Matthias Seedorf

Professor Dr. Blanche Schwappach

**„Einen Vorgang oder einen Charakter verfremden
heißt zunächst einfach, dem Vorgang oder dem Charakter
das Selbstverständliche, Bekannte, Einleuchtende zu nehmen
und über ihn Staunen und Neugierde zu erzeugen.“**

Bertolt Brecht

Summary

Ist2 is an integral, polytopic membrane protein of *Saccharomyces cerevisiae*. Some of the *IST2* mRNA is localized to the bud tip of the daughter cell, where the protein is locally translated at the cortical endoplasmic reticulum (ER). After its translation in mother cells, Ist2 rapidly accumulates at domains of the cortical ER. This cortical localization is mediated by a protein signal localized within the last 69 amino acids of the cytosolic Ist2 C-terminus (cortical sorting signal of Ist2, CSS^{Ist2}). In particular, certain hydrophobic and basic amino acids, which form an amphipathic helix, are important for Ist2 transport. The CSS^{Ist2} is a dominant sorting signal, it can redirect different Golgi- and ER localized membrane proteins efficiently to domains of the cortical ER. Ist2 localizes to the cortical ER independently of a functional secretory pathway (*sec*). Moreover, Ist2 is accessible to proteases added to intact yeast cells, suggesting a *sec*-independent transport mechanism from domains of the cortical ER to the plasma membrane (PM).

The aim of this thesis was to identify the molecular mechanism responsible for the efficient transport of Ist2 to the yeast cortical ER. I was able to show that the soluble CSS^{Ist2} *in vivo* binds to the yeast PM. This membrane binding could be identified as an interaction between the CSS^{Ist2} and lipids of the PM. *In vitro* binding assays using liposomes of a defined composition revealed phosphoinositides (PIPs) as the lipid class showing the strongest interaction with CSS^{Ist2}. This protein-lipid interaction depends on certain basic residues of the CSS^{Ist2} and its multimerization.

The PIP showing the strongest enrichment at the PM is Phosphatidylinositol[4,5]-biphosphate (PtdIns[4,5]P₂). Therefore, I replaced the cortical sorting signal of Ist2 by a characterized PtdIns[4,5]P₂ binding domain from Phospholipase C- δ_1 . The chimeric protein localized under all tested conditions like wild type Ist2 and complements cell wall defects of *ist2*-knockout strains caused by calcofluor white.

My data show that a binding of PM lipids is necessary and sufficient for the transport of Ist2 to the cortical ER. After translation of Ist2 the CSS^{Ist2} serves as a lipid-binding domain, which efficiently anchors the protein at organelle junctions between the ER and the PM.

Fusion proteins of different Golgi- and ER localized membrane proteins and the PtdIns[4,5]P₂ binding domain from Phospholipase C- δ_1 are efficiently redirected to the cortical ER. This novel sorting mechanism for integral membrane proteins is dominant over signals responsible for ER export and dominant over the proteasomal degradation of unstable ER proteins. This demonstrates the efficiency of protein sorting via protein-lipid interactions.

Zusammenfassung

Ist2 ist ein integrales, polytopisches Membranprotein in *Saccharomyces cerevisiae*. Ein Teil der *IST2* mRNA wird zur Spitze der Tochterzelle transportiert, wo das Protein lokal am kortikalen endoplasmatischen Retikulum (ER) translatiert wird. Nach der Translation in Mutterzellen akkumuliert Ist2 sehr schnell in Domänen des kortikalen ERs. Für diese kortikale Lokalisation ist ein Protein-Signal ausreichend, das sich in den letzten 69 Aminosäuren des cytosolisch orientierten C-Terminus von Ist2 befindet (kortikales Sortierungssignal von Ist2, CSS^{Ist2}). Vor allem hydrophobe und basische Aminosäuren, die eine amphipathische Helix bilden, sind von Bedeutung für den Transport von Ist2. Das CSS^{Ist2} wirkt als dominantes Signal über andere Proteinsortierungssignale, so kann es verschiedene Golgi- und ER-Membranproteine effizient in Domänen des kortikalen ERs umleiten. Die Lokalisation von Ist2 im kortikalen ER ist unabhängig von einem funktionellen sekretorischen Weg (*sec*). Ist2 ist zugänglich für Proteasen, die zu intakten Hefezellen zugegeben werden. Daher wurde für Ist2 ein *sec*-unabhängiger Transportweg von Domänen des kortikalen ERs zur Plasmamembran (PM) vorgeschlagen.

Das Ziel dieser Doktorarbeit bestand in der Aufklärung des molekularen Mechanismus, der für den effizienten Transport von Ist2 zum kortikalen ER verantwortlich ist. Ich konnte zeigen, dass das lösliche CSS^{Ist2} *in vivo* an die Hefe-PM bindet. Diese Membranbindung konnte als eine Interaktion des CSS^{Ist2} mit Lipiden der PM identifiziert werden. Durch *in vitro*-Versuche mit Liposomen definierter Zusammensetzung konnte ich Phosphatidylinositolphosphate (PIPs) als die Lipidklasse identifizieren, die die stärkste Interaktion mit CSS^{Ist2} aufweist. Diese Protein-Lipid-Interaktion hängt von basischen Resten des CSS^{Ist2}, sowie dessen Multimerisierung ab.

Das an der PM am stärksten angereicherte PIP ist Phosphatidylinositol[4,5]-bisphosphat (PtdIns[4,5]P₂). Daher ersetzte ich das kortikale Sortierungssignal von Ist2 durch eine charakterisierte PtdIns[4,5]P₂-Bindungsdomäne aus Phospholipase C- δ_1 . Das chimäre Protein lokalisiert unter allen getesteten Bedingungen wie Wildtyp-Ist2 und komplementiert durch das Reagenz Calcofluor weiß hervorgerufene Zellwanddefekte von *ist2-knockout*-Stämmen.

Diese Daten zeigen, dass für den Transport von Ist2 zum kortikalen ER die Bindung von Lipiden der PM notwendig und ausreichend ist. Nach der Translation von Ist2 dient das CSS^{Ist2} als Lipid-Bindungsdomäne, die das Protein effizient an Kontakten zwischen ER und PM verankert.

Fusionsproteine aus verschiedenen Golgi- und ER-Membranproteinen und der PtdIns[4,5]P₂-Bindungsdomäne aus Phospholipase C- δ_1 werden effizient in das kortikale ER umgeleitet. Dieser neu entdeckte Sortierungsmechanismus für integrale Membranproteine ist dominant über Signale für den Export von Proteinen aus dem ER und dominant über den proteasomalen Abbau instabiler ER-Proteine, was die Effizienz der Proteinsortierung durch Protein-Lipid-Interaktionen aufzeigt.

Table of Contents

1 Introduction	1
1.1 The endoplasmic reticulum	1
<u>1.1.1 ER morphology of <i>Saccharomyces cerevisiae</i></u>	3
<u>1.1.2 ER - organelle junctions in <i>Saccharomyces cerevisiae</i></u>	5
1.2 Intracellular transport	6
<u>1.2.1 The secretory pathway</u>	7
<u>1.2.2 ER export and retrieval signals</u>	10
<u>1.2.3 Unconventional secretion of proteins</u>	12
1.3 Lipids in <i>Saccharomyces cerevisiae</i>	14
<u>1.3.1 Lipid content</u>	14
<u>1.3.2 Transport and transfer of lipids</u>	16
<u>1.3.3 Lipids and organelle identity</u>	17
<u>1.3.4 Phosphoinositides</u>	19
<u>1.3.5 Lipid-binding motifs and domains</u>	21
1.4 The Ist2 protein	23
<u>1.4.1 The TMEM16 superfamily</u>	23
<u>1.4.2 Structure and function of Ist2</u>	24
<u>1.4.3 Localization of Ist2</u>	24
<u>1.4.4 Biosynthesis of Ist2</u>	25
<u>1.4.5 Mapping of the cortical sorting signal of Ist2</u>	27
1.5. Aim of this thesis	30
2 Results	31
2.1 Genetic identification of factors involved in Ist2 transport to the cell periphery	31
<u>2.1.1. Results</u>	32
<u>2.1.2. Materials</u>	34
<u>2.1.3. Methods</u>	35
2.2 Biochemical characterization of the cortical sorting signal	38
<u>2.2.1. Results</u>	38
<u>2.2.2. Materials</u>	40
<u>2.2.3. Methods</u>	40
2.3 Results and publications of this cumulative dissertation	42
<u>2.3.1. A signal comprising a basic cluster and an amphipathic α-helix interacts with lipids and is required for the transport of Ist2 to the yeast cortical ER.</u>	43
<u>2.3.2. Binding of plasma membrane lipids recruits the yeast integral membrane protein Ist2 to the cortical ER.</u>	64

<u>3 Discussion</u>	103
3.1 Lipid mediated sorting of integral membrane proteins	103
<u>3.1.1 The cortical sorting signal of Ist2 is a lipid-binding motif</u>	103
<u>3.1.2 Transport to subdomains of the ER is a novel transport mechanism</u>	105
3.2 Signals and factors involved in Ist2 sorting	108
3.3 Structural properties and multimerization of Ist2	112
<u>3.3.1 Domains within the CSS^{Ist2}</u>	112
<u>3.3.2 Multimerization of Ist2</u>	114
3.4 Model for Ist2 transport to the cortical ER.....	116
3.5 Localization and function of Ist2	118
3.6 Lipid mediated sorting of eukaryotic membrane proteins.....	121
3.7 Future perspectives	123
<u>4 Abbreviation list</u>	124
<u>5 List of tables and figures</u>	127
5.1 List of tables	127
5.2 List of figures.....	127
<u>6 References</u>	128
<u>7 Acknowledgements</u>	150

1 Introduction

The most crucial event in the evolution of eukaryotes was the generation of different compartments within one cell. This compartmentalization led to the partition of the cell into different reaction chambers, or organelles, each surrounded by membranes consisting of a lipid bilayer. Many cellular processes in eukaryotes, such as transcription, protein synthesis or energy metabolism, are restricted to only one or very few cellular compartments. However, in order to function as one entity, eukaryotic cells have evolved several transport pathways between the different organelles. Proteins that fulfill certain functions in particular organelles carry specific signals targeting them to their respective compartment. Many integral membrane proteins and most secreted proteins possess a signal sequence, which cotranslationally targets them to the endoplasmic reticulum (ER). After translocation into the ER these proteins are further transported into downstream compartments of the secretory pathway via *bulk flow* or making use of ER export signals. Alternatively, proteins can be kept in the ER via retention signals.

Here, I describe a novel mechanism of protein distribution on the level of the ER. This mechanism, which is used by the yeast integral membrane protein Ist2, is based on a binding to plasma membrane (PM) lipids at organelle junctions between the ER and the PM. This mechanism leads to efficient protein sorting into the cortical subcompartment of the yeast ER.

1.1 The endoplasmic reticulum

All eukaryotic cells have an ER. It consists of a continuous network of sheets and tubular structures with a common luminal space. The ER forms the nuclear envelope, which is interconnected to peripheral ER structures. The morphology and shape of the peripheral ER, however, is highly variable. In yeast the peripheral ER forms a stable meshwork-like structure beneath the PM, whereas in higher eukaryotes the peripheral ER consists of mostly tubular structures distributed throughout the cytoplasm (Shibata et al., 2006; Staehelin, 1997).

The ER can be subdivided into the rough endoplasmic reticulum (rER) and the smooth endoplasmic reticulum (sER), which fulfill different tasks. The rER is defined by the presence of membrane bound ribosomes (Palade 1958; Adelman et al., 1973). It therefore is the site, at which the biosynthesis of membrane and secretory proteins takes place. Moreover, the rER is associated with processes directly linked to protein translation, such as N-linked protein glycosylation and protein quality control (Ellgaard and Helenius, 2003; Gething, 1999; Helenius and Aebi, 2002).

The sER is free of ribosomes. In liver cells the sER is involved in different detoxification processes and in muscle cells it is the site of calcium release from the sarcoplasmic reticulum (Rossi et al., 2008; Voeltz et al., 2002). The transitional ER, from which vesicle budding occurs (see chapter 1.2.1), is also part of the sER.

The ER is closely adjacent to almost all other organelles of a cell. These ER-organelle junctions (ERJs) are relatively stable (Voeltz et al., 2002) and include contacts to the PM, the Golgi apparatus, endosomes, vacuole (plants, yeast) or lysosomes (mammalian cells), lipid droplets and mitochondria (Fig. 1; (Levine, 2004; Staehelin, 1997)).

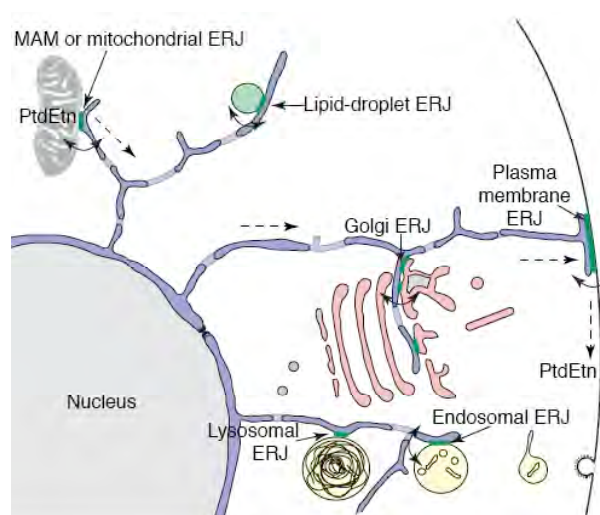


Figure 1: ER-organelle junctions (ERJs). The ER is closely adjacent to mitochondria (mitochondrial associated membranes [MAM]), the Golgi apparatus, the PM, endosomes, lysosomes and lipid droplets. Lipid transfer of phosphatidylethanolamine (PtdEtn) supposedly occurs at mitochondrial ERJs. Adapted from (Levine, 2004).

ERJs are also part of the sER and have been linked to lipid transfer between the ER and its adjacent organelles, coupling of enzyme reactions as well as coupling of calcium ion exchange. The latter one seems to be particularly important in organelle junctions between the ER and the PM, coupling calcium ion flux over the membranes of these two organelles. A curious example for calcium ion exchange between sER and the cell exterior is the interaction of the PM localized calcium channel Orai with the ER localized calcium sensing proteins stromal interaction molecule 1 (STIM1) and STIM2 (Putney et al., 2007; Lewis 2007; Frischauf et al., 2008). Upon drop of ER calcium concentration, STIM proteins undergo a conformational change, multimerize and interact with the Orai channel at the PM (Brandman et al., 2007; Navarro-Borelly et al., 2008). This leads to a massive recruitment of ER to the cell periphery and establishes stable junctions between ER and PM (Liou et al., 2005; Wu 2006; Brandman et al., 2007). The interaction between STIM proteins and Orai couples Orai mediated calcium influx from the extracellular space to calcium import into the ER via the mammalian sarcoplasmic/endoplasmic reticulum calcium ATPase (SERCA) system.

Almost all major classes of lipids are synthesized at the ER. Phosphatidylcholine (PtdCho), phosphatidylserine (PtdSer) and phosphatidylethanolamine (PtdEtn) as well as phosphatidylinositol (PtdIns) and sterols are synthesized in the cytosolic leaflet of the ER membrane, from where they are transported to other organelles of the cell via vesicular transport of specific carrier proteins. Scramblases, floppases and flippases work as phospholipid translocators, which exchange these molecules between the two leaflets of the lipid bilayer (Daleke, 2003). The site of lipid synthesis has not clearly been linked to the rER or the sER. However, in steroid producing cells the sER is exhibiting the highest enzyme activity for sterol synthesis (Voeltz et al., 2002). In yeast, organelle junctions between the sER and mitochondria, as well as junctions between the sER and the PM, exhibit strongly enriched enzyme activities of PtdSer-synthase and PtdIns-synthase (Gaigg et al., 1995; Pichler et al., 2001).

1.1.1 ER morphology of *Saccharomyces cerevisiae*

The budding yeast *Saccharomyces cerevisiae* (*S. cerevisiae*) is a polarized cell. During vegetative growth the actin cytoskeleton underlies several rearrangements within one cell cycle. Upon G1 and S phase, actin cables within the cytosol of the mother cell are oriented towards the growing bud, and they are interconnected with highly concentrated cortical actin patches in the daughter cell (Madden and Snyder, 1998). As a consequence of actin polarization, certain mRNAs (Aronov et al., 2007; Shepard et al., 2003) as well as exocytic vesicles (Johnston et al., 1991) are transported along the actin cytoskeleton into the daughter cell in a directed manner. During vegetative growth the polarized actin cables serve as tracks for myosin-dependent transport into the daughter cell. To maintain the polarity between mother and daughter cell, the yeast PM and the ER are compartmentalized into a mother and a bud domain. A ring of septin filaments at the bud neck establishes this compartmentalization (Barral et al., 2000; Faty et al., 2002; Takizawa et al., 2000).

As the yeast cell is polarized towards the bud, the ER faces the task to be inherited into the daughter cell in a polarized manner as well. The ER of *S. cerevisiae* can be subdivided into two morphologically distinct structures. The perinuclear ER is surrounding the nucleus. Via tubular ER, the perinuclear ER is connected to the peripheral cortical ER. Unlike in mammalian cells, the yeast cortical ER is stably underlying the PM (Preuss et al., 1991; Prinz et al., 2000). During the cell cycle, both perinuclear and cortical ER are inherited into the daughter cell in a highly efficient manner.

Inheritance of cortical ER starts in the early S-phase, when the newly emerging bud acquires segregating cytoplasmic ER tubules from the mother cell. These tubules are oriented along the mother-bud axis and move into the daughter cell along the polarized actin cables. The ER is attached to actin via the adaptor protein She3 and its motor protein

Myo4 (Estrada et al., 2003; Lowe and Barr, 2007; Prinz et al., 2000). After its transport into the daughter cell, the first domain of cortical ER is stably associated to the apical bud tip (Fehrenbacher et al., 2002). Proteins that are required or involved in this stable association are Scs2, Sec3, Aux1/Swa2, reticulons (Rtn1, Rtn2, Yop1) and translocon components (Sec61, Seb1, Sss1). Scs2 is an integral ER membrane protein, which carries a cytosolic N-terminal domain and a C-terminal transmembrane region. Wild type Scs2 localizes to perinuclear and cortical ER with a preference to the tips of small buds and sites of incipient budding, if the protein expressed at low level (Loewen et al., 2007). Lacking its transmembrane domain, Scs2 localizes to the bud tip of daughter cells during S-phase. Cells lacking Scs2 show a disturbed distribution of cortical ER in mother and, more severe, in daughter cells (Loewen et al., 2007). Sec3, a component of the yeast exocyst complex, was suggested to be an anchor for ER tubules moving into the daughter cell (Du et al., 2004; Wiederkehr et al., 2003). Reticulons exhibit a role in structuring ER tubules (Voeltz et al., 2006). Rtn1 interacts with the exocyst component Sec6 and might target ER tubules to the bud tip of daughter cells (De Craene et al., 2006). Similarly, the translocon components Sec61, Seb1 and Sss1 interact genetically and Seb1 (the yeast β -subunit of the translocation channel, see 1.2.1) interacts physically with the exocyst complex, thus providing an additional molecular bridge between ER and the bud tip (Guo and Novick, 2004; Toikkanen et al., 2003). Cells lacking Aux1/Swa2 show a delay in cortical ER inheritance (Du et al., 2001). However, the exact molecular impact of Aux1/Swa2 in cortical ER inheritance is still unclear.

After anchorage at the bud tip, the inherited cortical ER tubules are distributed along the bud cortex during late S and G2 phase of the cell cycle, finally forming a reticular network beneath the PM. One molecular component involved in this process, although not fully understood mechanistically, is Ice2. ER tubules fail to distribute along the bud cortex in the absence of Ice2 (Estrada de Martin et al., 2005).

As the nuclear envelope in yeast does not break down during mitosis, the perinuclear ER has to be partitioned between mother and daughter cell as an intact organelle. During S and G2 stage, the small and medium sized daughter cells still lack perinuclear ER (Fehrenbacher et al., 2002). At the end of G2 phase, the nucleus and the surrounding perinuclear ER are positioned at the bud neck. In a multi-stage process, which involves extension of the perinuclear ER towards both tips of mother and daughter cells, the perinuclear ER is distributed between mother and daughter cell during M phase in a microtubule-dependent manner (Fehrenbacher et al., 2002). Despite these dramatic reorganizations of the yeast ER, it still remains one entity with a common luminal space.

During all stages of the cell cycle luminal proteins are diffusible throughout the whole ER (Prinz et al., 2000; Luedeke et al., 2005). Integral membrane proteins, as shown for a green fluorescent protein (GFP) labeled version of the translocon component Sec61, can diffuse within the perinuclear and cortical ER of mother cells and exchange between both

compartments with diffusion rates similar to ER luminal proteins. However, diffusion of Sec61-GFP between the mother and the daughter cell is 10-fold slower than diffusion within each of these compartments, which is a consequence of the septin barrier in the bud neck (Luedeke et al., 2005).

1.1.2 ER - organelle junctions in *Saccharomyces cerevisiae*

As higher eukaryotic cells (Fig. 1, (Voeltz et al., 2002; Levine et al., 2004)), yeast exhibits a variety of junctions between the sER and other organelles. These ERJs include mitochondrial associated membranes (MAMs; (Gaigg et al., 1995)), PM associated membranes (PAMs; (Pichler et al., 2001)), associations between ER and Lipid droplets (Perktold et al., 2007) and junctions between ER and the vacuole (NV junctions; (Kvam and Goldfarb, 2006; Pan et al., 2000)).

In *S. cerevisiae* ER-organelle junctions are defined as sites with less than 30 nm distance between the organelles, as judged from electron microscopy or electron tomography (Gaigg et al., 1995; Perktold et al., 2007; Pichler et al., 2001). Electron tomography revealed the extent of organelle junctions in fixed yeast cells. Although the number of ERJs varies between chemically or cryofixed cells, the largest number of ERJs was observed between ER and PM as well as between ER and mitochondria (Table 1; (Perktold et al., 2007)).

Table 1: Number of ERJs per cell. The number of junctions (distance < 30 nm) between the ER and other organelles in either chemically or cryofixed cells was counted subsequent to electron tomography. Adapted from (Perktold et al., 2007).

ER contacts to	cryofixed cells	chemically fixed cells
mitochondria	11	79
plasma membrane	10	1139
lipid particles	1	14
vacuole	4	2

A variety of biological processes associated to ERJs have been suggested in yeast and mammalian cells. In yeast most studies suggest that ERJs are involved in nonvesicular lipid transfer between ER and associated organelles. MAMs exhibit a significantly higher capacity to synthesize PtdIns and PtdSer as compared to microsomal or mitochondrial fractions (Pichler et al., 2001). As mitochondria are not connected to the secretory pathway, they have to acquire some of their lipids via nonvesicular transport. MAMs have therefore been suggested to be the site of lipid transfer between the ER and mitochondria (Achleitner et al., 1999; Gaigg et al., 1995; Levine, 2004; Voelker, 2005; Voeltz et al., 2002).

Similar to MAMs, the PM associated fraction of the ER is enriched in PtdIns- and PtdSer-synthase activity (Pichler et al., 2001). There is increasing evidence that nonvesicular transport of lipids, in particular sterols, occurs at PAMs (Baumann et al., 2005; Li and Prinz, 2004; Schnabl et al., 2005). Proteins from the Oxysterol binding protein homologue (Osh) family might mediate the bidirectional sterol transport between ER and PM (see 1.3.2; (Im et al., 2005; Raychaudhuri et al., 2006)).

The biological significance of associations between ER and lipid particles is not understood yet. Some studies assume that lipid particles are directly derived from the ER membrane (Athenstaedt and Daum, 2006; Ploegh, 2007).

NV junctions mediate a process called piecemeal microautophagy of the nucleus (PMN), leading to the degradation of certain nuclear material in the vacuole for autophagic recycling (Roberts et al., 2003). Tsc13, an enoyl reductase, and Osh1, an oxysterol binding protein, maintain the local lipid composition at NV junctions. The process of PMN is facilitated by this local lipid composition (Kvam and Goldfarb, 2004; Kvam and Goldfarb, 2006; Levine and Munro, 2001).

Although a variety of possible functions in several cellular processes have been proposed for these ER-organelle junctions, the molecular bridges connecting the organelles remain largely unknown. Beside the interaction of reticulons and translocon components with the exocyst complex during cortical ER inheritance, only two ERJs have been characterized with respect to their molecular nature. The interaction of the ER protein Nvj1 and the vacuolar protein Vac8 maintains NV junctions in yeast (Kvam and Goldfarb, 2006; Pan et al., 2000). In mammalian cells it was recently shown that Mitofusin 2 at the ER and Mitofusin 1 or 2 at the mitochondria tether ER-mitochondria contacts (de Brito and Scorrano, 2008). These contacts are a prerequisite of inositol triphosphate (IP₃) generated calcium flux from the ER into mitochondria (de Brito and Scorrano, 2008). However, whether in yeast ER-mitochondria contacts are also maintained by the only Mitofusin orthologue Fzo1 (source: www.yeastgenome.org), still remains unclear.

1.2 Intracellular transport

Except for few mitochondrial proteins, the fate of all proteins in yeast and in mammals begins in the cytosol. The mRNA is translated on cytosolic ribosomes into the corresponding protein sequence, which destines the cellular compartment, to which the protein is localized. Proteins lacking a sorting signal remain within the cytosol. However, many proteins carry sorting signals within their amino acid sequence, which directs them from the cytosol into the nucleus, to mitochondria, chloroplasts, peroxisomes or the ER. One of the most complex intracellular machineries is the secretory pathway, a membrane system that interconnects the ER, the Golgi apparatus, lysosomes/vacuoles, endosomes and

the cell exterior via vesicular transport. Many components of the vesicular transport machinery interconnecting the secretory pathway have been identified via genetic approaches in *S. cerevisiae* in the early 80's (Novick et al., 1980; Schekman and Novick, 2004).

1.2.1 The secretory pathway

Within their lifetime, the vast majority of secretory and integral membrane proteins are inserted into the ER (Fig. 2 a) and from there distributed to their specific compartment along the secretory pathway (Fig. 2 bcde).

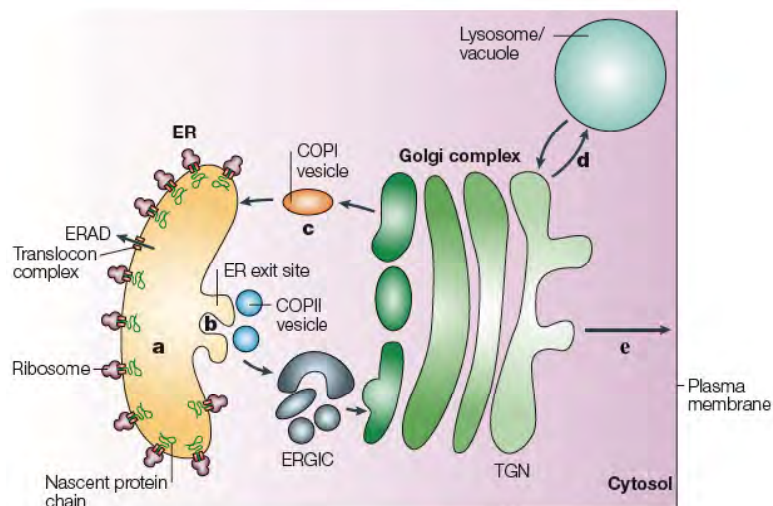


Figure 2: Overview of the early secretory pathway. Secretory proteins are synthesized at ER bound ribosomes and translocated into the ER (a). Misfolded proteins undergo ER associated degradation (ERAD). Proteins travel from ER exit sites (b) through an ER to Golgi intermediate compartment (ERGIC) to the Golgi apparatus via coat protein complex (COP) II vesicles. Retrograde transport from the Golgi apparatus to the ER takes place in COPI vesicles (c). Further anterograde transport from the trans Golgi network (TGN) targets the lysosome/vacuole (d) or the PM (e). Adapted from (Ellgaard and Helenius, 2003).

Translocation into the ER

Synthesis of proteins starts at free ribosomes in the cytosol. For proteins destined to be ER inserted, the secretory pathway begins with a targeting to the ER membrane followed by their co- or posttranslational translocation into the ER (Blobel and Dobberstein, 1975; Borgese et al., 2003; Ng et al., 1996; Pool, 2003). Cotranslationally inserted proteins possess a mostly N-terminal signal sequence, which is exposed to the cytosol upon emerging as a nascent chain from the ribosome. This hydrophobic signal sequence is recognized and bound by the signal recognition particle (SRP), leading to a translational arrest (Keenan et al., 2001). The SRP subsequently targets the nascent protein/ribosome

complex to the SRP receptor at the cytosolic side of the ER membrane (Keenan et al., 2001; Miller et al., 1993; Pool et al., 2002). Protein translocation occurs through the aqueous channel of the translocation complex, which is built by the heterotrimeric Sec61 complex (Gorlich et al., 1992; Osborne et al., 2005; Simon and Blobel, 1991; Van den Berg et al., 2004).

Protein modifications in the ER

Several mechanisms in the ER ensure the proper folding of translocated proteins. Protein Disulfide Isomerase ensures the oxidation of free sulfhydryl groups to cystine bonds. The chaperon BiP (yeast: Kar2) posttranslationally assists protein translocation and folding of luminal proteins (Gething, 1999). Most proteins synthesized at the ER carry N-linked glycosylations. To asparagine residues of the consensus sequence [Asn-X-Ser] or [Asn-X-Thr] a precursor oligosaccharide consisting of 14 sugars is covalently bound (Knauer and Lehle, 1999). This core glycosylation is thought to mark the folding state of the protein. The carbohydrate binding ER chaperones Calnexin and Calreticulin retain incompletely folded Glycoproteins in the ER. Glycoproteins undergo several cycles of deglycosylation and subsequent glycosylation until they are released as fully folded proteins (Caramelo and Parodi, 2008).

Luminal proteins, which fail to fold or to assemble properly, or membrane proteins improperly inserted into the ER membrane are undergoing a process called ER associated degradation (ERAD). Misfolded proteins are retrotranslocated into the cytosol, deglycosylated, ubiquitinated and degraded in the proteasome (Nishikawa et al., 2005; Romisch, 2005; Tsai et al., 2002). There is increasing evidence that proteins from the Derlin family assist in retrotranslocation (Vembar and Brodsky, 2008; Wahlman et al., 2007).

Export of proteins from the ER

Correctly folded and assembled proteins that carry an ER export signal (see list in 1.2.2) are actively concentrated at ER exit sites. These sites, also referred to as transitional ER, are part of the sER (Voeltz et al., 2002). Most transmembrane spanning proteins expose their ER exit signal to the cytosol. ER luminal proteins are attached to cargo receptors, which convey ER exit signals to the cytosolic side of the ER membrane (Barlowe, 2003; Lee et al., 2004).

Transport from the ER to the Golgi apparatus takes place in coat protein complex (COP) II vesicles (Barlowe et al., 1994; Lee et al., 2004). The assembly of COPII coated vesicles starts with a nucleotide exchange in cytosolic Sar1-GDP to Sar1-GTP, thereby inducing a conformational change in Sar1. This exposes the Sar1 amphipathic helix, which inserts into

the cytoplasmic leaflet of the ER membrane (Bielli et al., 2005; Lee et al., 2005). Membrane bound Sar1 subsequently binds to a heterodimeric complex of Sec23 and Sec24, of which Sec23 interacts with Sar1, whereas Sec24 recognizes membrane proteins carrying ER exit signals or cargo receptors for ER luminal proteins. By these interactions, secretory proteins are selectively concentrated at sites prone to vesicle formation. The subsequent recruitment of the Sec13/Sec31 heterodimer and the assembly of more of the aforementioned COPII components is bending the membrane, finally leading to vesicle formation (Lee et al., 2004; Stagg et al., 2006). After budding off the ER membrane, the coat of the COPII vesicle disassembles. This shedding event is triggered by hydrolysis of Sar1 bound GTP. The GTP hydrolysis is accelerated by other components of the COPII coat (Antonny et al., 2001).

Transport to downstream organelles of the secretory pathway

For fusion of the shedded vesicle with its acceptor compartment, the vesicle is tethered to the target membrane via Rab-GTPases. Upon vesicle shedding, active Rab-GTP is exposed to the cytosolic side of the vesicle and interacts with its respective Rab effector on the target membrane. This tethers vesicle and target membrane into such a small distance that SNARE (soluble N-ethylmaleimide sensitive factor (NSF) attachment protein (SNAP) receptor) mediated vesicle fusion can occur (Sollner et al., 1993; Wickner and Schekman, 2008). A tetrameric complex of one v-SNARE on the vesicle and three t-SNAREs on the target membrane leads to a four helix bundle formation catalyzing the fusion between vesicle and target membrane (Malsam et al., 2008; Sorensen et al., 2006). After membrane fusion, the cargo proteins are released into the lumen or the membrane of the acceptor compartment. The cargo receptors are backtransported and recycled. The ATPase NSF (Sec18 in yeast) disassembles the helix bundle of SNARE proteins and the SNAREs are recycled through SNAPs (Malsam et al., 2008; Wickner and Schekman, 2008; Zhao et al., 2007).

The process as described here interconnects all compartments along the secretory pathway. Transport from the ER to the Golgi apparatus occurs in COPII vesicles as described above. From the Golgi apparatus cargo can be transported back to the ER, forward to the PM or to the endosomes, from where the protein can reach the lysosome/vacuole of the cell. Transport steps from the Golgi apparatus to other compartments are carried out using COPI vesicles. The assembly of COPI vesicles occurs in a similar manner as for COPII vesicles except using other molecular players. The GTPase involved in COPI vesicle formation is Arf, which uses a posttranslationally added myristoyl group for membrane insertion. The other components of the COPI coat are the subunits of the coatomer complex (Lippincott-Schwartz and Liu, 2006).

Transport pathways between particular organelles are tightly regulated on the level of cargo selection, vesicle tethering and vesicle fusion. Organelle specific Rab proteins with their respective receptors as well as highly specific pairs of v-SNAREs and t-SNAREs ensure a directed transport of secretory proteins along the secretory pathway from the ER through the Golgi apparatus to the exterior of the cell (Brandhorst et al., 2006; Cai et al., 2007).

1.2.2 ER export and retrieval signals

Proteins use a wide variety of domains and motifs in order to localize to specific cellular compartments. These signals can act as a cotranslational targeting sequence as described above or they can determine the localization of a readily folded protein posttranslationally. For example cytosolic proteins can enter the nucleus via nuclear localization signals or they can be recruited to specific membranes via lipid-binding motifs (see 1.3.5). Membrane proteins carry signals that lead to their localization in particular organelles. As this thesis focuses on protein transport on the level of the ER, signals necessary for export from the ER or retrieval to the ER from the Golgi apparatus are described in this paragraph.

Export from the ER

For ER export integral membrane proteins expose their export signals into the cytosol. However, soluble proteins in the ER lumen, as well as Glycosylphosphatidylinositol (GPI)-anchored proteins, cannot expose signals to the cytosol due to a lack of transmembrane regions. Some soluble secretory proteins are transported via passive processes. This *bulk flow* export is used by amylase and chymotrypsinogen in pancreatic exocrine cells (Martinez-Menarguez et al., 1999; Wieland et al., 1987). However, most luminal and membrane proteins are concentrated up to 50-fold higher than the *bulk flow* rate for ER export (Lee et al., 2004). Many secretory proteins bind to receptors in the ER lumen. These receptors carry a transmembrane region and expose ER export signals on the cytosolic side of the ER membrane. The best described cargo receptors for luminal proteins are ERGIC53 (Emp46/Emp47 in yeast), p24 proteins and Erv29 (Appenzeller et al., 1999; Barlowe, 2003; Belden and Barlowe, 2001; Nichols et al., 1998; Sato and Nakano, 2002; Schimmoller et al., 1995). Up to this point, no common ER export signal was found in secreted luminal proteins. However, they share the mechanism of binding to a receptor, which transduces the ER export signal to the cytoplasmic side of the ER membrane.

For cargo receptors as well as for membrane proteins, the family of Sec24 proteins is thought to function as the binding site of COPII vesicles (Barlowe, 2003). In mammalian

cells there are four isoforms of Sec24, yeast has beside Sec24 two homologous proteins, Lst1 and Iss1 (Barlowe, 2003; Pagano et al., 1999). The variety of Sec24 proteins might enable them to select different cargo receptors and exported membrane proteins (Miller et al., 2003). The characterized ER export signals of transmembrane cargo can be subdivided into two classes: Di-acidic motifs and di-hydrophobic motifs (Table 2).

Table 2: Characterized ER export signals for transmembrane proteins. Underlined residues are required for ER export. Numbering from the C-terminus, which corresponds to (-1). From (Barlowe, 2003).

Export signal	Protein
Di-acidic motifs:	
<u>Y</u> <u>T</u> <u>D</u> <u>I</u> <u>E</u> <u>M</u> <u>N</u> <u>R</u> <u>L</u> <u>G</u> <u>K</u> (-1)	VSV-G
ANSEC <u>Y</u> ENEVAL (-45)	Kir2.1
QSP <u>I</u> QL <u>K</u> D <u>L</u> ESQI (-1)	Sys1
AEKMD <u>I</u> D <u>I</u> TGR (-34)	Gap1
Di-hydrophobic motifs:	
YIMYRSQQEAAAK <u>K</u> <u>F</u> F (-1)	ERGIC53
<u>Y</u> YMERINQDIKK <u>V</u> <u>K</u> <u>L</u> L (-1)	Emp46
YLRR <u>F</u> F <u>K</u> AKKLIE (-1)	p24 δ 1
YQPDDKTKG <u>I</u> LDR (-1)	Erv41
KLFYKAQRSIWGKKSQ (-1)	Erv46

ER export of the vesicular stomatitis virus glycoprotein (VSV-G) depends on a YTDIEM motif within its cytoplasmic C-terminus. This motif is necessary for ER export and a transfer to ER resident proteins makes these being exported from the ER (Sevier et al., 2000). Cytosolically exposed DXE-like di-acidic motifs are also found in other ER-exported proteins in mammalian cells (Kir2.1) as well as in yeast (Sys1, Gap1) (Ma et al., 2001; Malkus et al., 2002; Votsmeier and Gallwitz, 2001).

Many ER exported membrane proteins do not carry di-acidic motifs, but a pair of large hydrophobic residues, which often are aromatic. The export of ERGIC53 from the ER depends on a pair of phenylalanines in its C-terminus (Kappeler et al., 1997). The yeast orthologues Emp46 and Emp47 both carry a di-leucine motif instead, which functions as an ER export signal in combination with tyrosine residues 10-15 amino acids upstream the C-terminus (Sato and Nakano, 2002).

Many proteins carrying di-hydrophobic motifs for ER export are oligomeric complexes and can only exit the ER as such (Barlowe, 2003). Emp47 is required in yeast for Emp46 export from the ER in a process depending on heterooligomerization between both molecules via a coiled-coil domain mediating their assembly (Sato and Nakano, 2003). The potassium channel Kir 3.1 in mammalian cells does not expose any mapped ER exit signals, but via heterotetramerization with Kir3.2A and Kir3.4, which carry ER export signals, the protein is efficiently transported to the cell surface (Ma et al., 2002).

Retrieval to the ER

Soluble proteins, which are shuttling between ER and Golgi apparatus, or ER luminal proteins coincidentally transported to the Golgi apparatus via *bulk flow* undergo retrograde transport from the Golgi apparatus to the ER via COPI vesicles. These proteins carry a specific and highly conserved KDEL (yeast: HDEL) retrieval signal at their C-terminus. The KDEL (HDEL) sequence interacts with the transmembraneous KDEL receptor (yeast: Erd2), which mediates backtransport to the ER. The KDEL receptor exhibits a cytosolic di-lysine ER-retrieval signal, which, in combination with a phosphoserine residue, mediates retrograde transport to the ER (Cabrera et al., 2003).

The di-lysine ER-retrieval signal in the KDEL receptor is a frequent feature of membrane proteins, which are transported from the Golgi apparatus to the ER. The di-lysine signal consensus sequence KKXX or KXXKXX at the C-terminus of the particular protein directly interacts with Coatamer (Cosson and Letourneur, 1994), leading to transport to the ER via COPI vesicles.

Another motif for ER retrieval is the exposure of a twin-arginine signal with the consensus sequence RXR (Zerangue et al., 1999). This signal directly interacts with the COPI coat as well. It is particularly well characterized in the trafficking of potassium channels. The activity of the RXR signal is strongly dependent on the multimeric state of the protein (Michelsen et al., 2005) and its activity is conserved in yeast, although endogenous yeast proteins using this mechanism are not yet identified (Michelsen et al., 2006).

The cystic fibrosis transmembrane conductance regulator (CFTR) protein is localized at the PM of epithelial cells. Upon deletion of a Phenylalanine (Δ F508-mutant), the protein localizes to the ER due to the loss of a functional ER-exit signal (Wang et al., 2004). CFTR Δ F508 is subject to ER quality control and is degraded via the ERAD machinery. However, the mutation of RXR-signals in the CFTR Δ F508-mutant leads to PM targeting of this mutant protein (Hegedus et al., 2006). Therefore, Arg-based signals might have a function in coupling the folding status of a membrane protein to its forward transport (Michelsen et al., 2005).

14-3-3 proteins can regulate the activity of RXR based signals in mammalian cells as well as in yeast (Michelsen et al., 2006; Mrowiec and Schwappach, 2006; Yuan et al., 2003).

1.2.3 Unconventional secretion of proteins

A small but increasing number of proteins is secreted to the cell exterior by unconventional routes or non-classical pathways (Nickel and Rabouille, 2009; Nickel and Sedorf, 2008). The biological significance of unconventional secretion still remains elusive for many substrates of such pathways. However, some proteins, which are simply too large to fit into

a COPII vesicle, might use different mechanisms for ER export (Fromme and Schekman, 2005). Proteins secreted independently from the ER/Golgi-System might need to avoid glycosylation or proteolytic processing in the Golgi apparatus for their function or they might become toxic to the cells upon secretion via the secretory pathway.

Firstly, soluble proteins, which are via a signal peptide inserted into the ER lumen, can be secreted via mechanisms partly independent of COPII components. However, all of the proteins in this class are inserted into the ER and are transported via the Golgi apparatus to the cell exterior. Proteins using this pathway are for example procollagen-I (Stephens and Pepperkok, 2002), the chylomicron protein Apo-B (Gusarova et al., 2003; Siddiqi et al., 2003), the potassium channel Kv4 (Hasdemir et al., 2005) and the yeast protein Hsp150 (Fatal et al., 2004; Karhinen et al., 2005). Procollagen I and Apo-B are too large to be exported from the ER via COPII vesicles, which are roughly 60 nm in diameter (Barlowe et al., 1994). Therefore, these proteins are thought to be secreted from the ER via transport pathways dependent on Sar1, but partly independent of certain COPII components (Fromme and Schekman, 2005).

Secondly, some cytoplasmic proteins lacking an ER targeting signal are secreted independently from the ER/Golgi system. Their secretion is insensitive to the Golgi apparatus-disassembling reagent Brefeldin A (BFA) treatment and they lack ER/Golgi modifications. Proteins of this group are for example Interleukin 1 α and 1 β (Rubartelli et al., 1990; Siders et al., 1993), Galectin 1 and 3 (Cooper and Barondes, 1990; Sato et al., 1993; Seelenmeyer et al., 2005) and fibroblast growth factor 2 (FGF-2). These proteins use a variety of different mechanisms for their secretion (reviewed in (Nickel and Rabouille, 2009; Nickel and Seedorf, 2008)). Secretion of FGF-2 occurs through a direct translocation from the cytosol to the cell exterior in an ATP-independent manner (Schafer et al., 2004). FGF-2 is translocated in a folded state (Backhaus et al., 2004). Heparan sulfate proteoglycans (HSPGs) act as a crucial molecular trap in the cell exterior via a high affinity interaction with FGF-2 (Zehe et al., 2006). The PM lipid Phosphatidylinositol(4,5)-bisphosphate (PtdIns[4,5]P₂) is involved in FGF-2 secretion. Depletion of PtdIns[4,5]P₂ led to a decrease in FGF-2 secretion, corroborating the secretion decrease by mutations in the proposed PtdIns[4,5]P₂ binding pocket of FGF-2 (Temmerman et al., 2008). After a PtdIns[4,5]P₂-dependent docking step to the PM, FGF-2 might be translocated into the extracellular space via specific transporters or by HSPG-driven passive diffusion through transient hydrophilic pores (Nickel and Seedorf, 2008). Unconventional secretion in yeast independent of the ER/Golgi System was reported for the mating peptide α -factor. This peptide, which lacks a transmembrane region, is intracellularly bound to the PM via prenylation. Translocation to the exterior space is mediated via the ABC-transporter Ste6 (Chen et al., 1997; McGrath and Varshavsky, 1989).

There are some integral membrane proteins, which were described to undergo unconventional transport mechanisms to the PM (Nickel and Seedorf, 2008). The cell

surface exposure of the tyrosine phosphatase CD45 as well as the PM localization of certain cell adhesion molecules in neuroblastoma cells is BFA insensitive (Baldwin and Ostergaard, 2002; Bonnon et al., 2003). However, the molecular mechanism underlying these transport pathways is still unknown. In yeast the polytopic, ER inserted membrane protein Ist2 (see section 1.4) is accessible for external proteases. The transport of Ist2 into protease sensitive domains is independent of several components of the secretory pathway as well as of NSF (Sec18 in yeast). Therefore, a direct *sec*-independent transport pathway from the ER to the PM was proposed (Juschke et al., 2004; Juschke et al., 2005).

1.3 Lipids in *Saccharomyces cerevisiae*

Eukaryotic cells have a complex intramembrane system with membranes consisting of lipid bilayers. As these membranes have to segregate particular organelles from the aqueous environment, they are made up of lipids exposing a hydrophilic headgroup to the aqueous phase and carrying aliphatic side chains, which form the hydrophobic plane of the membrane. The lipid bilayer is intersected by channels, pores and other integral membrane proteins. These proteins ensure flux of ions, mediate transport processes or energy retrieval. To ensure organelle identity, not only proteins are localized in specific compartments, also the lipid composition of diverse organelles is distinct. In addition, the lipid compound of both leaflets of the membrane is different leading to specific lipid mixtures of each membrane on each organelle.

This chapter describes the cellular organelles of *S. cerevisiae* with respect to the specific lipid composition of their membranes. In particular the role of phosphoinositides (PIPs) as markers for organelle identity and its metabolism in yeast is discussed.

1.3.1 Lipid content

The endomembrane system of *S. cerevisiae* is made of lipids from the three major lipid classes glycerophospholipids, ceramides and sterols. In addition, glycolipids in the outer leaflet of the PM are involved in cell wall integrity (Tyorinoja et al., 1974) and non-polar lipids as triacylglycerol and sterylesters fulfill storage functions in lipid particles (Rajakumari et al., 2008).

The biosynthesis of the major four glycerophospholipids in yeast (PtdSer, PtdEtn, PtdCho and PtdIns) starts from Cytidin diphosphate-diacylglycerol (CDP-DAG). Upon transfer of one serine molecule to CDP-DAG, PtdSer is synthesized from the PtdSer-synthase Cho1 in the cytosolic leaflet of the ER and the outer mitochondrial membrane (Kohlwein et al., 1988; Kuchler et al., 1986). The negatively charged PtdSer is highly enriched to the

cytosolic leaflet of the PM, where it makes up 40% of the total glycerophospholipid content (Pichler et al., 2001). Yeast strains lacking PtdSer are viable if supplemented with choline and ethanolamine. These strains exhibit defects in tryptophane uptake and metabolism (Nakamura et al., 2000).

In the Kennedy Pathway, PtdSer is the precursor of PtdEtn and PtdCho. Psd1 and Psd2 decarboxylate PtdSer, yielding PtdEtn. Psd1 is exclusively localized to the inner mitochondrial membrane, whereas Psd2 exhibits its activity in the Golgi/vacuolar membrane (Voelker, 1997). Mitochondria are slightly enriched in PtdEtn content compared to fractions of the secretory pathway system (Pichler et al., 2001). Yeast cells lacking PtdEtn exhibit transport defects of the PM proteins Can1 and Pma1 (Opekarova et al., 2005).

Methylation of PtdEtn via Cho2 and Opi3 yields PtdCho. The enzyme activities from Cho2 and Opi3 have been characterized in microsomal membranes (Gaynor and Carman, 1990). PtdCho is the major constituent of the ER and mitochondrial membranes, making up to 50% of the total glycerophospholipid content. In the PM PtdCho is less abundant (Pichler et al., 2001).

The PtdIns-synthase Pis1 catalyzes the synthesis of PtdIns from inositol and CDP-DAG in the cytosolic leaflet of the ER and the outer mitochondrial membrane (Nikawa and Yamashita, 1997). PtdIns is enriched in the ER compared to mitochondria and the PM (Pichler et al., 2001). PtdIns can be phosphorylated from various PtdIns-kinases yielding PIPs (see 1.3.4).

Additional less abundant glycerophospholipids of yeast membranes are phosphatidic acid (PA), which is the precursor of CDP-DAG, and Cardiolipin, which regulates the respiratory chain in the inner mitochondrial membrane (Joshi et al., 2009).

S. cerevisiae does not have any sphingomyelin as higher eukaryotes. Instead, the only sphingolipids present in yeast are three kinds of ceramides, inositol-phosphoceramide (IPC), mannose-inositol-phosphoceramide (MIPC), and mannose-(inositol phosphate)₂-ceramide (M(IP)₂C) (Cowart and Obeid, 2007). These complex ceramides are thought to be involved in the formation of detergent-insoluble membranes (DIMs) in the PM, where they are strongly enriched (Cowart and Obeid, 2007; Dickson and Lester, 2002). They have been linked to endocytosis (Zanolari et al., 2000), signaling processes (Zhang et al., 2004) and the trafficking of GPI-anchored and PM proteins (Chung et al., 2003; Gaigg et al., 2005; Horvath et al., 1994; Mitsui et al., 2009). The enzymes involved in the different conversions and synthesis steps leading to IPC, MIPS and (M(IP)₂C) have been localized to the ER and, for later steps in the sphingolipid biosynthesis, to the Golgi apparatus (Dickson and Lester, 2002).

Unlike higher eukaryotic cells, *S. cerevisiae* does not have cholesterol, but ergosterol as its main sterol. Although the multi-step process of sterol biosynthesis occurs at the ER, the concentration of sterols in the ER is very low. In contrast, ergosterol is highly enriched in

the PM (Pichler et al., 2001), the PM ergosterol fraction was assumed to make up 60-80% of the total cellular sterol content (Schulz and Prinz, 2007; Sullivan et al., 2006). The PM sterols are a major structural component, where they form DIMs. Although sterol starvation is hard to control, ergosterol was suggested to be necessary for transport of tryptophane permease and uracil permease to the PM (Pineau et al., 2008).

1.3.2 Transport and transfer of lipids

As a consequence of vesicle transport within the cell, lipids are exchanged between different organelles of the secretory pathway. However, most lipids are not evenly distributed throughout the secretory pathway, but are enriched at certain organelles as discussed above. Probably the strongest enrichment of any lipid is established by ergosterol. Ergosterol is synthesized in the ER, but almost 60-80% of total cellular ergosterol resides in the PM (Schulz and Prinz, 2007; Sullivan et al., 2006). Therefore, mechanisms that establish and maintain the accumulation of certain lipids on particular organelles must exist. On the one hand, lipids can in principle directly be enriched at certain organelles by the activity of the enzymes generating them. This mechanism is widely used for PIPs, which are generated by phosphorylation of PtdIns. The kinases achieving this phosphorylation exhibit their activity only on particular organelles, leading to an enrichment of differently phosphorylated PIP species on different organelles ((Strahl and Thorner, 2007) see also 1.3.3). On the other hand, lipids can directly be transferred from one membrane to another in nonvesicular transport pathways. As lipids are hydrophobic, a passive migration of a lipid molecule from one membrane to another through the aqueous cytosol without the help of carrier proteins can be excluded from the thermodynamic point of view. Therefore, lipid carrier proteins execute the exchange of lipids between two organelles. The two best-investigated systems are the sterol transporters from the Osh protein family (Schulz and Prinz, 2007) and the PtdIns transfer proteins (PITPs; (Mousley et al., 2007)).

In mammalian cells as well as in yeast, there is a gradient of sterol concentration along the secretory pathway (Daum et al., 1998; Orci et al., 1981). From the ER, the sterol concentration increases and reaches its highest concentration at the PM. At least in mammalian cells cholesterol, as well as sphingomyelin, are partially excluded from COPI vesicles (Brugger et al., 2000). However, exclusion from COPI vesicles cannot be the solely mechanism for sterol concentration at the PM, because transport of sterols from the ER to the PM is independent of BFA in mammalian cells (Urbani and Simoni, 1990) and independent of Sec18 (the yeast NSF) dependent vesicle trafficking in yeast (Baumann et al., 2005). The sterol transport proteins maintaining this transport are proteins from the Osh family, which in yeast has seven members (Osh1-Osh7). Mutants depleted of all seven Osh

proteins show a severe decline in sterol transport between ER and PM in both directions and severely altered sterol distribution (Beh and Rine, 2004; Raychaudhuri et al., 2006). Osh4 can *in vitro* move sterols between liposomes, a process specifically enhanced by the presence of PtdIns[4,5]P₂ (Raychaudhuri et al., 2006). This is consistent with the fact that many Osh proteins have N-terminal lipid-binding motifs (see 1.3.5) for PIPs (Schulz and Prinz, 2007).

The major yeast PITP is the Sec14 protein. Sec14 is on the one hand an essential peripheral Golgi membrane protein and is necessary for membrane trafficking events in the trans Golgi network (TGN; Cleves et al., 1991). On the other hand, Sec14 was found to transfer PtdIns or PtdCho monomers between membranes *in vitro* (Bankaitis et al., 1990; Bankaitis et al., 1989). However, despite strong *in vitro* data, there is poor research about whether this process is relevant *in vivo* (Mousley et al., 2007). The connection of Sec14 to non-vesicular lipid transport was suggested from genetic data showing that the ablation of the essential Sec14 can be compensated either by ablation of Osh4 (Fang et al., 1996) or by certain mutations in the biogenesis pathway of PtdCho (Cleves et al., 1991).

The non-vesicular transport of lipids is thought to occur at sites, in which two organelles are closely adjacent to each other. In particular ERJs were proposed to be the site, at which lipid carrier proteins act. Beside the suggestive fact that transfer processes are facilitated if donor and acceptor membrane are in proximity, MAMs and PAMs were indeed found to have particular high enzyme activities for PtdSer-synthase and PtdIns-synthase (Gaigg et al., 1995; Pichler et al., 2001). As mitochondria are not connected to the secretory pathway, they have to acquire many of their lipids via nonvesicular transport pathways. However, the exact molecular mechanisms for lipid transfer between ER and mitochondria are still poorly known.

PAMs are enriched in enzymes generating ergosterol precursors (Pichler et al., 2001). This suggests a connection between these sites to nonvesicular transport of sterols by Osh proteins. The proteins Osh1-3 do indeed localize to specific domains of the yeast ER, a process dependent on the expression level of Scs2 (Loewen et al., 2003). Scs2 is involved in cortical ER inheritance and morphology (Loewen et al., 2007). This directly links sterol transport to the inheritance of cortical ER, two processes occurring at the interface between cortical ER and PM.

1.3.3 Lipids and organelle identity

Integral membrane proteins carry signals, which determine their localization to particular organelles. Some of these signals have been described in 1.2.2. However, many proteins that mediate traffic between organelles or fulfill other functions at specific compartments are peripheral membrane proteins, which are recruited from the cytosol to the cytosolic

surface of the organelle. For precise function, these proteins have to be tethered to the right organelle in an extremely specific manner. Thus, the cytosolic surface of organelles carries hallmarks, which can recruit proteins in a specific manner. These hallmarks are generated either by organelle-specific GTPases from the Rab- and Arf families or by specific lipids, in particular PIPs (reviewed in (Behnia and Munro, 2005; Di Paolo and De Camilli, 2006; Munro, 2002)).

In yeast, 11 Rab-GTPases have been identified (Ypt-Genes). Their localization is limited to particular organelles and for some of them (e.g. Ypt31) variations in localization within one cell cycle were observed (Buvelot Frei et al., 2006). In a similar manner like Rab-GTPases, Arf-GTPases can work as proteins that determine the identity of organelles. In COPII vesicle formation the Arf GTPase Sar1 inserts into the cytoplasmic leaflet of the ER membrane (Bielli et al., 2005; Lee et al., 2005). This localization then works as a hallmark for the recruitment of further COPII components, specifically tethering them to sites of vesicle formation (see 1.2.1).

Beside proteins from the Rab and Arf-family, lipids can serve as specific marker molecules as well. In particular PIPs are restricted to the cytosolic leaflet of certain organelles. PIPs are phosphorylated derivatives of PtdIns. PtdIns is present in all organelles of the secretory pathway and slightly enriched in the ER (Pichler et al., 2001). PtdIns carries an inositol sugar esterified to the phosphorylated headgroup of DAG. The inositol can be further phosphorylated by kinases at the 3, 4 or 5-OH-group of the sugar ring (Fig. 3).

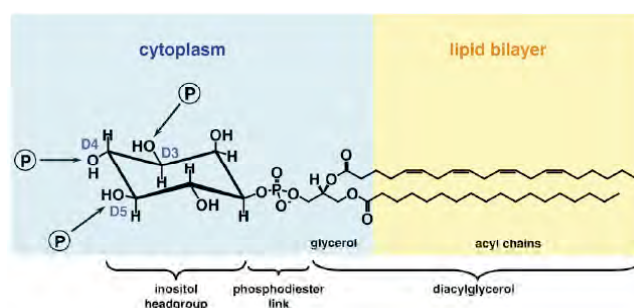


Figure 3: Structure of PtdIns and possible phosphorylation sites at the inositol ring. From (Strahl and Thorner, 2007).

The kinases catalyzing the phosphorylation of PtdIns, are restricted to specific organelles. Of the seven possible mono-, bis- and triphosphorylated PIPs, four have been identified in yeast, all of them are enriched in particular organelles (Fig. 4; reviewed in (Strahl and Thorner, 2007)). The enzymes involved in PIP metabolism and catabolism are described in 1.3.4.

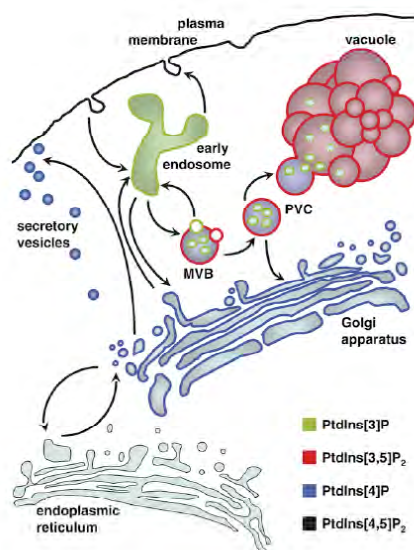


Figure 4: Distribution of PIPs in yeast. PtdIns[3]P is found in the vacuole and especially in early endosomes, PtdIns[4]P is mainly localized at the Golgi apparatus, PtdIns[4,5]P₂ at the PM and PtdIns[3,5]P₂ at the vacuole. MVB = multivesicular body; PVC = prevacuolar compartment; from (Strahl and Thorner, 2007).

A variety of different proteins in mammalian cells as well as in yeast cells are recruited from the cytosol to particular organelles via lipid-binding domains (see 1.3.5) or via electrostatic interactions between basic protein clusters and the negatively charged phosphate groups of PIPs (Di Paolo and De Camilli, 2006; Heo et al., 2006).

The combination of specific proteins and lipids on the surface of each organelle provides an identity for spatial recognition from the cytosol. The usage of GTPases and phosphorylated lipids as markers for such identity is suggested to confer not only accuracy, but also plasticity to a vesicular compartment, allowing it to lose or gain its identity (Behnia and Munro, 2005).

1.3.4 Phosphoinositides

PIPs do not only function in organelle identity. They are also necessary for IP₃ signaling, the arrangement of the cytoskeleton, transport of vesicles and a variety of other essential and nonessential processes (Strahl and Thorner, 2007). Yeast has four different PIPs: PtdIns[3]P, PtdIns[4]P, PtdIns[4,5]P₂ and PtdIns[3,5]P₂. They are synthesized from PtdIns by in total six different kinases and can be dephosphorylated by seven different phosphatases.

PtdIns[3]P is generated from PtdIns, in a reaction catalyzed by the kinase Vps34 (Schu et al., 1993). Cells lacking Vps34 are viable, but are temperature sensitive. They exhibit defects in protein sorting to the vacuole, but possess an intact secretory pathway (Robinson et al., 1988; Rothman et al., 1989; Schu et al., 1993). PtdIns[3]P is mainly localized in

punctuate structures corresponding to prevacuolar endosomes, but also to the vacuole (Burd and Emr, 1998; Gillooly et al., 2000). It is necessary for protein sorting processes at the vacuole by interacting with the vacuolar t-SNARE Vam7 (Cheever et al., 2001) and components of the retromer complex necessary for the retrieval of cargo from the prevacuolar compartment (PVC) to the Golgi apparatus (Burda et al., 2002). Furthermore, the PtdIns[3]P effectors Cvt13 and Cvt20 are components of the pexophagy machinery, an autophagic process of peroxisomes (Nice et al., 2002). In addition, PtdIns[3]P is necessary in the generation of multivesicular bodies (MVBs; (Katzmann et al., 2003)). Hydrolysis of PtdIns[3]P to PtdIns occurs upon invagination of PtdIns[3]P containing vesicles into the vacuole, where it is hydrolyzed by the phosphatases Ymr1, Inp52 and Inp53 (Parrish et al., 2004).

The only PtdIns[3]P kinase in yeast is Fab1 (Yamamoto et al., 1995). Fab1 generates PtdIns[3,5]P₂, which is localized at endosomes and the vacuole. Cells lacking Fab1 exhibit growth defects at 25°C and they are temperature sensitive. These cells have extremely enlarged vacuoles, defects in vacuolar protein sorting (Gary et al., 1998; Yamamoto et al., 1995) as well as in vacuolar acidification and inheritance (Yamamoto et al., 1995; Zheng et al., 1998). The number of binucleate cells is strongly enhanced in Fab1 mutant cells (Palmer et al., 1990). However, this effect might be caused by the sterical hindrance of chromosome segregation due to the enlarged vacuole (Strahl and Thorner, 2007). A hyperosmotic shock in wild type cells leads to a rapid increase in PtdIns[3,5]P₂ (Dove et al., 1997). Furthermore, PtdIns[3,5]P₂ is important in protein sorting to MVBs (Odorizzi et al., 1998). PtdIns[3,5]P₂ can be hydrolyzed in the vacuole by the phosphatases Fig1, Inp52 and Inp53.

Yeast has three PtdIns kinases generating PtdIns[4]P: Stt4, Pik1 and Lsb6. PtdIns[4]P is highest concentrated in punctuate structures corresponding to the Golgi apparatus (Stefan et al., 2002). However, the Golgi apparatus PtdIns[4]P pool is exclusively made by Pik1. Pik1 is an essential protein, it can shuttle between nucleus, cytosol and the Golgi apparatus (Sciorra et al., 2005; Strahl and Thorner, 2007). Although Pik1 makes some PtdIns[4]P in the nucleus (Strahl et al., 2005), its function in this organelle is still not understood. PtdIns[4]P in the Golgi apparatus is necessary for transport from the Golgi apparatus to the PM within the secretory pathway (Audhya et al., 2000; Demmel et al., 2008; Hama et al., 1999; Walch-Solimena and Novick, 1999). The PtdIns[4]P pool also regulates the localization and function of the Oxysterol binding protein Osh4 (Li et al., 2002), linking protein transport along the secretory pathway with non-vesicular transport of sterols. Lsb6 localizes partly to the PM, but also to the vacuole (Strahl and Thorner, 2007). Where in particular Lsb6 generates PtdIns[4]P is unclear. Lsb6 is necessary for endosome motility, suggesting a minor pool of PtdIns[4]P being generated at these organelles (Chang et al., 2005). The third kinase generating PtdIns[4]P is Stt4 (Cutler et al., 1997; Yoshida et al., 1994). Stt4 is an essential protein localizing to the PM (Audhya and Emr, 2002), where it

generates a local pool of PtdIns[4]P, which is thought to be rapidly further phosphorylated by Mss4 gaining PtdIns[4,5]P₂ (see below). Therefore, most phenotypes associated with PtdIns[4]P decrease at the PM are a consequence of PtdIns[4,5]P₂ decrease. Moreover, the activity of Stt4 is directly involved in cell wall integrity, heat shock responses via protein kinase C (Audhya et al., 2000; Paravicini et al., 1992) and translation initiation (Cameroni et al., 2006). PtdIns[4]P can be hydrolyzed by the phosphatases Inp52, Inp53 and Sac1. The latter one is the only PIP phosphatase, which is an integral membrane protein (Konrad et al., 2002). Sac1 regulates a PtdIns[4]P pool in late endocytic pathways (Tahirovic et al., 2005) as well as PtdIns[4]P pools at ER and in the Golgi apparatus upon response to available nutrients (Faulhammer et al., 2005).

PtdIns[4,5]P₂ is exclusively made at the PM from PtdIns[4]P by the action of the PM localized kinase Mss4 (Audhya 2002, Homma 1998). Mss4 is an essential protein, the use of temperature sensitive (*ts*) alleles have shown various cellular processes depending on PtdIns[4,5]P₂. PtdIns[4,5]P₂ is necessary for proper organization of the actin cytoskeleton and such in polarized growth (Audhya and Emr, 2002; Audhya et al., 2004; Desrivieres et al., 1998; Homma et al., 1998). It is important for endocytosis (Desrivieres et al., 1998), Tor2-dependent signaling (Audhya et al., 2004) and recruitment of Rom2 (Audhya et al., 2000), which activates protein kinase C signaling pathways. Overexpression of Mss4 rescues several temperature sensitive *sec*-mutants (Novick et al., 1980) in the late secretory pathway, in particular the exocyst complex members Sec8, Sec10 and Sec1 (Routt et al., 2005). This suggests a role of PtdIns[4,5]P₂ in fusion of secretory vesicles with the PM. PtdIns[4,5]P₂ is substrate for phospholipase C (Plc1 in yeast), which generates the second messengers DAG and IP₃ activating a signaling pathway, finally leading to the release of calcium from the ER lumen. Beside breakdown by Plc1, PtdIns[4,5]P₂ can be hydrolyzed by the phosphatases Inp51, Inp52, Inp53 and Inp54 to PtdIns[4]P.

1.3.5 Lipid-binding motifs and domains

Many peripheral membrane proteins are tethered to certain organelles using lipid-binding domains or motifs (Di Paolo and De Camilli, 2006; Lemmon, 2008). In mammals as well as in yeast lipid-binding proteins can affect various cellular processes: Anchoring of the cytoskeleton (Yin and Janmey, 2003), endocytosis (Wenk and De Camilli, 2004) or Golgi trafficking (Odorizzi et al., 2000). Various globular lipid-binding domains have been characterized (Table 3), yeast has 91 proteins carrying such domains, human more than 500 (Lemmon, 2008). Most characterized lipid-binding domains target proteins to PIPs, but there are also domains binding to phosphatidylserine or unpolar lipids (Shi et al., 2004; Zhang et al., 1995).

Table 3: Lipid-binding domains, their targets and examples of proteins carrying lipid-binding domains. From (Di Paolo and De Camilli, 2006).

Module	Specificity	Examples of proteins
A/ENTH	PtdIns(4)P	EpsinR
	PtdIns(3,5)P ₂	Ent3p, Ent5p
	PtdIns(4,5)P ₂	AP180, CALM, epsin, HIP
C2	PtdIns(4,5)P ₂	Synaptotagmin
FERM	PtdIns(4,5)P ₂	Ezrin, moesin, radixin, talin
FYVE	PtdIns(3)P	EEA1, Hrs, SARA, PIKfyve
GRAM	PtdIns(3,5)P ₂	Myotubularin
PDZ	PtdIns(4,5)P ₂	Syntenin
PH	PtdIns(4)P	FAPP1/2, OSBP
	PtdIns(3,4)P ₂	AKT/PKB, TAPP1,2
	PtdIns(4,5)P ₂	PLCδ1, dynamin
	PtdIns(3,4,5)P ₃	BTK, AKT/PKB, ARNO, GRP1
PHD	PtdIns(5)P	ING2
PTB	PtdIns(4,5)P ₂	Dab1, ARH, SHC
	PtdIns(3,4,5)P ₃	SHC
PX	PtdIns(3)P	SNX2,3,7,13
	PtdIns(5)P	SNX13
	PtdIns(3,4)P ₂	p47PHOX
	PtdIns(4,5)P ₂	Class II PI(3)kinase
	PtdIns(3,4,5)P ₃	CISK

Lipid-binding domains specifically bind to their targets using a defined structure. However, although pleckstrin homology (PH) domains from different proteins have structural homologies, their affinity for lipids is largely different in PH domains from diverse proteins. For example the PH domain from the δ_1 subunit of Phospholipase C (PLC- δ_1 -PH) binds to PtdIns[4,5]P₂ (Lemmon et al., 1995), whereas the PH domain from the four-phosphate adaptor protein 1 (FAPP1-PH) is rather specific for PtdIns[4]P (Levine and Munro, 2002). Many lipid-binding domains were cocrystallized with the headgroups of their lipid targets, providing insight into the structural requirements for this protein-lipid interaction (Ferguson et al., 1995).

In addition to well-defined structural domains, polybasic clusters can serve as lipid-binding motifs targeting proteins to specific organelles as well. As the headgroups of PIPs are negatively charged (the valence of PtdIns[4,5]P₂ is -4 at pH 7; (McLaughlin and Murray, 2005)), lysine- and arginine-rich clusters of proteins can interact with PIPs and such be recruited to membranes. In particular, the binding of many small GTPases to the PM is mediated by interactions between polybasic clusters at the C-terminus of the proteins and PtdIns[4,5]P₂ and PtdIns[3,4,5]P₃ at the PM of mammalian cells (Heo et al., 2006). Also in yeast proteins with polybasic clusters can be recruited to particular organelles. For example, the yeast integral type II membrane protein Etf1 binds PtdIns[3]P via a polybasic cluster of lysine residues near its transmembrane region (Wurmser and Emr, 2002). Etf1 is also one of the very few examples of integral membrane proteins that carry lipid-binding motifs or domains. The vast majority of proteins experimentally verified to bind to lipids are cytosolic proteins, which are transiently recruited to membranes. Some cytosolic proteins recruited to membranes carry, in addition to their lipid-binding motifs, amphipathic helices or posttranslational lipid modifications as myristoylation, thereby stabilizing their binding to lipids (Heo et al., 2006).

In general the interaction between PIPs and their lipid-binding proteins is a low affinity interaction. The so called “coincidence detection” model suggests that a physiologically relevant high affinity interaction between proteins and lipids is a consequence of the integration of many low affinity interactions. This can be achieved by multiple lipid-binding domains in one protein, additional binding sites for other factors beside lipids, a homo- or heterooligomerization of lipid-binding proteins or by clustering of lipids within the organelle membrane (Carlton and Cullen, 2005; Di Paolo and De Camilli, 2006; Krauss and Haucke, 2007).

1.4 The Ist2 protein

1.4.1 The TMEM16 superfamily

The mammalian transmembrane protein with unknown function (TMEM) 16 family has 10 members. They are referred to as TMEM16A-K or Anoctamin 1-10. The TMEM16 family is conserved among higher eukaryotes. Human and mouse TMEM16A have an identity of 91% (Yang et al., 2008). Members of the TMEM16 family are also found in *Drosophila melanogaster* and, with less similarity, in *S. cerevisiae* (Caputo et al., 2008). The closest yeast relative to the TMEM16 family is the Ist2 protein. However, Ist2 and human TMEM16 members share a rather low overall identity of 15-20%. Nonetheless, other yeast proteins do not share any significant similarity to mammalian TMEM16 proteins (source: <http://www.ncbi.nlm.nih.gov/blast/Blast.cgi>).

TMEM16 members are multispinning membrane proteins. TMEM16A-G and TMEM16J are annotated to have eight predicted transmembrane (TM) domains with a long N- and a short C-terminus facing the cytosol. All members share a domain of unknown function (DUF) 590 domain, which is covering the three C-terminal transmembrane regions (source: <http://pfam.sanger.ac.uk/>). TMEM16 proteins can undergo alternative splicing (Caputo et al., 2008) in mammalian cells.

The localization of TMEM16 proteins varies within the members of this protein family. Mouse TMEM16A localizes to the PM of HEK293 cells (Rock 2007; Schroeder et al., 2008; Yang et al., 2008). TMEM16E is localized at the ER (Mizuta et al., 2007). TMEM16G localizes to the PM, whereas a shorter splice-variant lacking its transmembrane domains localizes to the cytoplasm (Bera et al., 2004).

The human, mouse and xenopus family members TMEM16A and TMEM16B were recently identified as calcium activated chloride channels (CaCC; (Caputo et al., 2008; Yang et al., 2008)) or subunits of such (Schroeder et al., 2008). Mouse TMEM16A exhibits its function as a CaCC with outward rectification (Schroeder et al., 2008; Yang et al., 2008). TMEM16A is involved in fluid secretion and necessary for normal development of the murine trachea (Rock et al., 2008). Mutations in human TMEM16E cause

gnathodiaphyseal dysplasia, a disease leading to fragility of tubular bones (Mizuta et al., 2007).

1.4.2 Structure and function of Ist2

Like most members of the TMEM family in higher eukaryotes, the yeast Ist2 protein has eight predicted transmembrane domains (Krogh et al., 2001) with N- and C-terminus facing the cytosol (Juschke et al., 2004). However, compared to mammalian TMEM16 proteins, Ist2 does not have a long N-terminus, but a long C-terminus (Fig. 5).

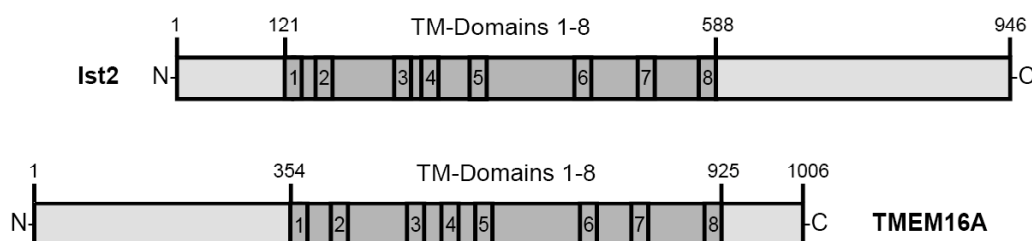


Figure 5: Alignment of Ist2 and the *abcd* splice variant (Caputo et al., 2008) of TMEM16A. The shared homologous DUF590 domain covers the amino acids 369-605 from Ist2 and 669-928 from TMEM16A (source: <http://pfam.sanger.ac.uk/>).

High throughput experiments suggest an ubiquitination of Ist2 and the amino acids T726, S729, S924 and S926 to be phosphorylated (Ficarro et al., 2002; Peng et al., 2003).

Ist2 is encoded from the open reading frame *YBR086c* and was initially named increased sodium tolerance protein 2, because an *ist2*-knockout shows a tolerance towards 1 M sodium chloride as compared to wild type cells (Entian et al., 1999). Beside its similarity to CaCC proteins and the NaCl tolerance of *ist2Δ* strains, Ist2 was suggested to play a role in ion homeostasis (Kim et al., 2005). Moreover, Ist2 was identified to be a dosage repressor of cells expressing strongly decreased levels of Irr1, an essential component of the cohesin complex (Bialkowska and Kurlandzka, 2002). How Ist2 is involved in sister chromatid cohesion on the molecular level has not been studied in detail.

However, although Ist2 was suggested to play a role in ion homeostasis and sister chromatid cohesion, the exact function of the protein is unknown.

1.4.3 Localization of Ist2

GFP-Ist2 localizes in patch like structures in the cell periphery (Juschke et al., 2004; Takizawa et al., 2000). Fluorescence microscopy initially suggested that Ist2 is localized at the PM. (Takizawa et al., 2000). However, GFP-Ist2 colocalizes with the ER marker Dpm1-CFP in patch like structures at the cortical ER of yeast cells (Juschke et al., 2004).

The cortical ER and the PM are closely apposed to each other. The distance between both organelles is below the diffraction barrier of light microscopy. Therefore, they cannot be distinguished via fluorescence microscopy. In order to further discriminate, whether Ist2 is a PM or a cortical ER protein, protease protection and cell fractionation experiments were carried out (Juschke et al., 2004). GFP-Ist2 is accessible to proteases given to intact yeast cells. Pronase and Trypsin were able to digest GFP-Ist2 in intact cells or spheroplasts, respectively. The resulting fragments correspond to digestion in protein domains that are either extracellular or ER luminal (Juschke et al., 2004). Moreover, in cell fractionation experiments, GFP-Ist2 cofractionates rather with the PM protein Pma1 than with the ER protein Dpm1-CFP (Juschke et al., 2004). However, in protease protection and cell fractionation experiments the used control ER protein was Dpm1-CFP, which localizes to both perinuclear and cortical ER.

These experiments show that GFP-Ist2 localizes to membranes that are accessible to external proteases and which cofractionate with the PM. This can either be the PM, or subdomains of the cortical ER that are protease accessible and share biophysical properties with the PM in cell fractionation experiments. Ist2 might also be present in both the PM and subdomains of the cortical ER.

1.4.4 Biosynthesis of Ist2

In *S. cerevisiae* roughly 50 mRNAs are localized to the bud tip of the daughter cell (Aronov et al., 2007; Oeffinger et al., 2007; Shepard et al., 2003). The mRNA localization machinery consists of the mRNA binding protein She2, which recognizes stem-loop motifs on substrate mRNAs in the nucleus (Bohl et al., 2000). After export of the nucleus, the adaptor molecule She3 binds the She2/mRNA-complex in the cytosol. She3 interacts with the type V Myosin Myo4 (She1), which transports localized mRNAs into the bud tip along the polarized actin cytoskeleton (Takizawa and Vale, 2000). The components of the mRNA transport machinery are not essential for vegetative growth.

The phenomenon of mRNA localization was also observed for the *IST2* mRNA (Juschke et al., 2004; Takizawa et al., 2000). The localization element is encoded by the mRNA nucleotides corresponding to the amino acids 898-928 of the mature Ist2 protein. This region forms the stem-loop recognized by She2 (Olivier et al., 2005). The mRNA localization of Ist2 coincides with the inheritance of cortical ER tubules into the daughter cell (Lange et al., 2008; Schmid et al., 2006). Whether the stem loop motif initiates a translational arrest during mRNA transport as shown for other localized mRNAs in yeast (Bohl et al., 2000; Jansen et al., 1996) is unclear in the case of *IST2* mRNA.

In wild type cells the *IST2* mRNA is concentrated at the bud tip and translated at the cortical ER of the daughter cell (Juschke et al., 2004). The deletion of She1 or She2 led to

a dispersed distribution of *IST2* mRNA throughout the mother and the daughter cell and the Ist2 protein expression in daughter cells was very weak (Juschke et al., 2004). As small- and medium sized daughter cells lack perinuclear ER and *IST2* mRNA is localized into the daughter cell, a local translation of Ist2 at the cortical ER of daughter cells was postulated (Juschke et al., 2004).

This local synthesis of Ist2 is restricted to the cortical ER at the bud tip of daughter cells. Therefore, this local synthesis might be linked to an unconventional transport pathway of Ist2. The protein would then subsequent to its local translation be transported to subdomains of the cortical ER or even to the PM. In order to test whether Ist2 is transported along the secretory pathway as other well described peripheral membrane proteins, experiments in *sec*-mutants (Novick et al., 1980) were carried out. The peripheral localization of Ist2 is independent of the function of the secretory pathway. Neither vesicle fusion with the PM (investigated in a *sec1^{ts}* allele), vesicle generation at the Golgi apparatus (*sec7^{ts}*) or the ER (*sec12^{ts}* and *sec23^{ts}*), nor SNARE mediated transport processes (*sec18^{ts}*) are a prerequisite for the transport of GFP-Ist2 to the cell periphery (Juschke et al., 2004; Juschke et al., 2005). This establishes that the peripheral localization of Ist2 is independent of any vesicular transport events along the classical secretory pathway. Instead, Ist2 follows a novel, *sec*-independent transport pathway to the cell periphery (Juschke et al., 2004; Juschke et al., 2005).

She2 binds to a stem-loop motif from the localized *ASH1* mRNA with a K_D of 210nM (Niessing et al., 2004). As the cellular concentration of She2 was estimated to be 230nM (Niessing et al., 2004), roughly half of this particular stem-loop motif is supposedly bound by She2. As the *ASH1* mRNA contains four localization elements (Chartrand et al., 1999), the majority of *ASH1* mRNA is bound to She2 and is transported into the bud tip. The stem-loop motifs of *ASH1* and *IST2* mRNA show structural similarities (Olivier et al., 2005). However, the *IST2* mRNA only has one localization element (Olivier et al., 2005). Assuming a similar affinity of She2 to the localization elements in *ASH1* and *IST2* mRNA, only half of the *IST2* mRNA should be bound to She2 according to this rough estimation. Therefore, two distinct pools of *IST2* mRNA might exist, one pool being transported to the bud tip of daughter cells and the other pool being not localized. Immunofluorescence of newly synthesized HA-Ist2 revealed that indeed a significant amount of this protein is also translated at the perinuclear ER of mother cells (Maass et al., 2009). This perinuclear pool is transported to the cell periphery rapidly after translation (Maass et al., 2009). These experiments established that two pools of *IST2* mRNA exist. One pool of *IST2* mRNA is localized to the bud-tip of daughter cells, where it is locally translated. The second pool can be translated at the perinuclear ER of mother cells. The mature Ist2 protein generated from this second pool is rapidly transported to the cell periphery subsequent to translation. The signal for *sec*-independent transport of Ist2 to the cell periphery could lie within the *IST2* mRNA and depend on the mRNA transport and local translation of the protein.

Alternatively, the transport signals of Ist2 could be present within the Ist2 protein sequence and act as a posttranslational transport mechanism. An coupling of *IST2* mRNA transport to the localization of the Ist2 protein could, however, be ruled out by three lines of evidence: (1) *Sec*-independent transport of the protein also occurred in cells lacking the mRNA transport machinery (Juschke et al., 2004). (2) A change of the mRNA structure within the She2 binding motif while maintaining the Ist2 protein sequence led to peripheral accumulation of the protein (Franz et al., 2007) as well. (3) The pool of Ist2 translated at the perinuclear ER of mother cells is not a substrate for the mRNA transport machinery, but nonetheless rapidly accumulates at the cell periphery (Maass et al., 2009). These three experiments establish that the *IST2* mRNA localization is no prerequisite for the accumulation of the Ist2 protein at the cell periphery. Therefore, the cortical sorting signal has to be encoded within the protein sequence of Ist2, acting independent of mRNA transport.

1.4.5 Mapping of the cortical sorting signal of Ist2

Expression of GFP-Ist2 lacking its C-terminal cytosolic domain, controlled by its endogenous promoter, led to a distribution of the protein in the perinuclear and cortical ER (Juschke et al., 2005). Moreover, fusion of the cytosolic C-terminus of Ist2 (amino acids 589-946; Ist2^c) to the cytosolic C-terminus of other ER and Golgi resident transmembrane spanning proteins led to an accumulation of these Ist2^c-tagged reporter proteins at the cell periphery. For example, the PIP phosphatase GFP-Sac1 localized to the ER, whereas GFP-Sac1-Ist2^c was localized in patch-like structures in the yeast cell periphery (Juschke et al., 2005). This transport was independent of a functional secretory pathway and the fusion protein was protease accessible. These data suggest that the information for peripheral targeting and localization to protease accessible domains is located within the cytosolic C-terminus of Ist2. Other proteins that can be redirected to the cell periphery via Ist2^c are Prm1, which upon mating is localized to cell-cell contacts, an ER resident truncated version of Ste6 and the Golgi proteins Kex2 and Sys1 (Juschke et al., 2005) (Franz A., Diploma Thesis 2005; Franz A., personal communication).

Two lines of evidence revealed that Ist2 is a dominant sorting signal. (1) Proteins carrying well-characterized sorting signals, for example Sys1 with its DXE motif and Kex2, which carries a tyrosine Golgi retention signal (Wilcox et al., 1992), can efficiently be redirected via Ist2^c from the Golgi apparatus to the cell periphery. This is also true under conditions, where ER export is blocked. Therefore, Ist2^c is dominant over the ER export signal in Sys1 (Franz A., personal communication) and the Golgi retention signal of Kex2 on the level of protein distribution in the ER (Franz et al., 2007). (2) Ist2^c can redirect the chloride channel Gef1 to the cell periphery. Gef1 is a homodimer (Dutzler et al., 2002; Middleton et al.,

1996). Gef1 localizes to endosomes and the prevacuolar compartment under wild type conditions. During maturation Gef1 is cleaved by the furin protease Kex2 in the Golgi apparatus (Wachter and Schwappach, 2005). Upon parallel expression of wild type Gef1 and Gef1-Ist2^c heterodimers were formed, which localized to the cell periphery. The peripheral localization was maintained upon block of the secretory pathway and Gef1 was not proteolytically processed by Kex2 (Juschke et al., 2005). This indicates that Ist2^c is a dominant signal redirecting the untagged Gef1 via heterodimerization.

Further studies revealed that the minimal signal required for the efficient peripheral transport of the reporter proteins Kex2, Sys1 and a truncated version of Ste6 to the cell periphery are the C-terminal 69 amino acids of Ist2 (Franz et al., 2007), defining this sequence as the cortical sorting signal of Ist2 (CSS^{Ist2}). The CSS^{Ist2} can be subdivided into the T/H/S-cluster and the K/L-sequence (Fig. 6). The T/H/S-cluster, which corresponds to the Ist2 amino acids 878-928, has three amino acid stretches of threonine, histidine and serine. Within the mRNA sequence of the T/H/S-cluster, the binding site for She2 is present (see 1.4.4). The K/L-sequence, corresponding to the Ist2 amino acids 929-946, is extremely basic and mostly comprised of lysine and leucine residues (Fig. 6).

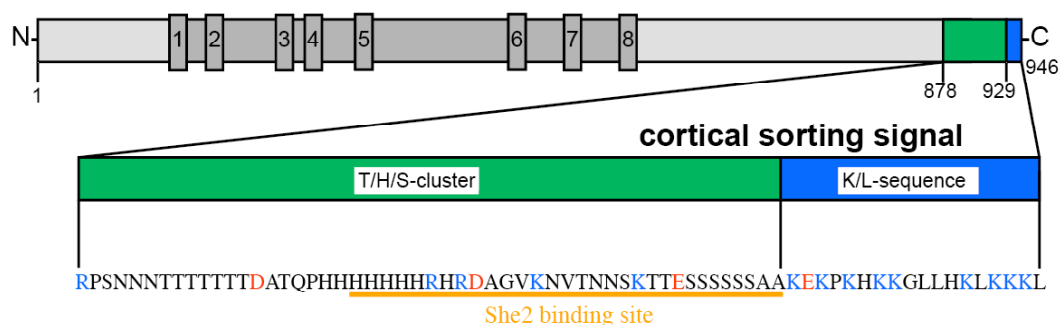


Figure 6: Ist2 and its cortical sorting signal. The transmembrane regions are labeled 1-8. The cortical sorting signal comprises amino acids 878-946, the T/H/S-cluster (green) amino acids 878-928 and the K/L-sequence amino acids 929-946 (blue). The She2-binding sites covers amino acids 898-928. In the sequence of the CSS^{Ist2} acidic amino acids are labeled red, basic amino acids are labeled blue.

The T/H/S-cluster can functionally be replaced by a tetramerization domain from the Gcn4-pLI Leucine Zipper (Harbury et al., 1993). This tetramerization domain forms a coiled-coil structure (cc). The reporter protein Kex2-cc-GFP-Ist2 929-946 is efficiently transported to cell periphery. However, replacement of the T/H/S-cluster with an unrelated sequence from the ABC transporter Ste6 led to a partial intracellular accumulation of Kex2-Ste6 100-150-GFP-Ist2 929-946 (Franz et al., 2007; Franz A., personal communication). These data suggest a multimerization function within the T/H/S-cluster. Indeed, Ist2 does multimerize, because coexpressed HA-Ist2 and myc-Ist2 can be co-immunoprecipitated (Franz et al., 2007).

Expression of YFP-Ist2 1-928, which lacks the K/L sequence, led to a distribution of the protein in the perinuclear and cortical ER (Franz et al., 2007). Furthermore, a screen for

mutations in Ist2-YFP revealed that single amino acid mutations, which lead to a mislocalization of the protein, can exclusively been found in the K/L sequence of Ist2 (Maass et al., 2009). This suggests that the K/L sequence has a crucial role in the sorting of the Ist2 protein.

1.5. Aim of this thesis

Subsequent to its translation, the Ist2 protein rapidly accumulates at the cortical ER independently of its mRNA transport (Franz et al., 2007; Maass et al., 2009).

The aim of this thesis was to find the molecular mechanism responsible for this transport step of Ist2 by the answering of two major questions:

- (1) Which cellular molecules are involved in the rapid accumulation of Ist2 at the cell periphery after protein translation? In order to identify such trans acting factors, I conducted a genetic screen with the *S. cerevisiae* knockout library. Moreover, I performed a large variety of biochemical experiments searching for transport factors for the accumulation of Ist2 at the cell periphery.
- (2) Which structural properties within the Ist2 sorting signal are responsible for its peripheral transport? In order to identify structural motifs within Ist2, I performed limited proteolysis experiments and circular dichroism spectroscopy.

2 Results

The aim of this thesis was to find the molecular mechanism responsible for the rapid of Ist2 to the cortical ER, which occurs independently of the *IST2* mRNA localization. My results can be subdivided into three parts: (1) In order to identify cellular factors involved in the accumulation of Ist2 at the cortical ER, I screened the yeast knockout library for strains, in which the localization of GFP-Ist2 is altered. I was able to show that the knockout of a single, nonessential gene in *S. cerevisiae* gene does not impair the transport of GFP-Ist2 to the cell periphery. (2) In order to find domain borders within the cytosolic C-terminus of Ist2, I performed limited proteolysis experiments followed by mass spectrometry. I could show that Ist2 is protease accessible in a threonine stretch after the amino acid T886. (3) In order to identify the molecular mechanism responsible for the accumulation of Ist2 at the cell periphery, I used a variety of biochemical approaches. These experiments finally led to the observation that the CSS^{Ist2} is a lipid-binding motif. CSS^{Ist2} binds to lipids of the PM *in vivo* as well as *in vitro*. In the Ist2 protein, the CSS^{Ist2} can functionally be replaced by a PtdIns[4,5]P₂ binding PH domain from the δ_1 subunit of Phospholipase C. After translation, Ist2 accumulates at the cell periphery via a binding to PIPs at the PM, thereby anchoring the protein in domains of the cortical ER. I was able to show that protein sorting via lipid binding of adjacent organelles is a dominant mechanism for the distribution of proteins within the ER. This novel sorting mechanism for integral membrane proteins can also be applied to a variety of reporter proteins. These findings were published in two papers, which are attached in section 2.3.

2.1 Genetic identification of factors involved in Ist2 transport to the cell periphery

In order to identify cellular factors responsible for the accumulation of Ist2 at the cortical ER, I screened a yeast knockout library for knockout strains, in which the peripheral localization of Ist2 is altered. For this study I used GFP-Ist2 as a reporter and a read-out based on fluorescence microscopy. In wild type cells GFP-Ist2 localizes in patch-like structures of the yeast cell periphery (Juschke et al., 2004). A mislocalization of GFP-Ist2 in perinuclear ER structures would indicate a particular knockout strain, in which the corresponding gene product is involved in the transport of GFP-Ist2 from the perinuclear ER to the cortical ER. When this study was designed, it was not yet found that the *IST2* mRNA localization is no prerequisite for the accumulation of the Ist2 protein at the cell periphery (Franz et al., 2007). Therefore, GFP-Ist2 was chosen as a reporter, which exhibits mRNA localization. The mRNA of the used GFP-Ist2 reporter is localized to the

bud tip and translated locally at the cortical ER of daughter cells. However, although a majority of this reporter might be locally translated at the cortical ER, GFP-Ist2 allows the distinction between perinuclear localization and peripheral localization of the protein under steady state conditions.

Yeast knockout libraries, which cover the majority of nonessential genes, are commercially available. These libraries are provided in 96-well-plates, each well contains a different strain with a particular nonessential gene knocked out. Yeast contains 8632 open reading frames (ORFs), of which 6607 are annotated to cover verified (4766), uncharacterized (1030) or dubious (811) genes. Of these 6607 genes the deletion of 1179 is fatal for haploid yeast cells. The remaining 5428 genes are nonessential for vegetative growth under standard conditions. However, these numbers may slightly differ depending on growth conditions and strain background (source: www.yeastgenome.org).

2.1.1. Results

For this study I used the EUROSCARF knockout library. It contains 4850 different deletion mutants in the BY4741 strain background. Of these, 4827 knockout strains could be transformed with a plasmid encoding for GFP-Ist2 controlled by the *IST2* promoter. The residual 23 strains could not be transformed under standard lab conditions. The 4827 transformed strains were grown in selective medium in 96-well-plates over night and screened via fluorescence microscopy. From 4827 strains 4808 showed a patch-like localization of GFP-Ist2 in the cell periphery, similar as in wild type yeast strains. In four strains GFP-Ist2 was poorly expressed in daughter cells, four strains showed alterations of Ist2 distribution within the cell periphery and in 11 strains the expression level of Ist2 was strongly altered (Table 4).

Table 4: Phenotypes observed in the yeast knockout library screen. 4827 strains were transformed with a plasmid encoding for GFP-Ist2. Protein localization was determined via fluorescence microscopy.

Observed phenotype:	Deleted ORF:	Corresponding gene:	Additional comments:
Patch-like localization in the cell periphery	4808 different ORFs		Wild type-like localization
Weak expression in daughter cells	<i>YAL029C</i> <i>YKL130C</i> <i>YBR130C</i> <i>YOR035C</i>	<i>MYO4/SHE1</i> <i>SHE2</i> <i>SHE3</i> <i>SHE4</i>	

Altered distribution in the cell periphery	<i>YAR018C</i> <i>YPL050C</i>	<i>KIN3</i> <i>MNN9</i>	PM and/or cortical ER exhibit some invaginations into the cell, Ist2 localizes patch like to cell periphery and these invaginations.
	<i>YIL090W</i>	<i>ICE2</i>	GFP-Ist2 is only present on one side of the daughter cell.
	<i>YER120W</i>	<i>SCS2</i>	GFP-Ist2 is not present at the apical pole of the daughter cell and sometimes not present at the apical pole of the mother cell.
Altered expression level of GFP-Ist2	<i>YJL080C</i> <i>YOR371C</i> <i>YHR034C</i> <i>YHR093W</i> <i>YJR055W</i> <i>YJL184W</i> <i>YKR061W</i>	<i>SCP160</i> <i>GPB1</i> <i>PIH1</i> <i>AHT1</i> <i>HIT1</i> <i>GON7</i> <i>KTR2</i>	Weak expression level in all cells
	<i>YJL124C</i>	<i>LSM1</i>	Strong expression level in some cells
	<i>YOR290C</i> <i>YPR046W</i> <i>YDR485C</i>	<i>SNF2</i> <i>MCM16</i> <i>VPS72</i>	Strong expression level in all cells

In four knockout strains Ist2 was weakly expressed in daughter cells. The corresponding knocked out genes were *SHE1*, *SHE2*, *SHE3* and *SHE4*, which encode proteins that are part of the mRNA localization machinery. In these strains the mRNA of GFP-Ist2 is not localized and few protein is translated in the daughter cell. This phenomenon was already described for *she1Δ* and *she2Δ* cells (Juschke et al, 2004). Therefore, these strains served as an internal control that a localization of GFP-Ist2 that differs from the localization in wild type cells could be identified via this unbiased screen.

KIN3 and *MNN9* encode for a protein kinase with unknown cellular function and for a subunit of the mannosyltransferase complex, respectively (source: www.yeastgenome.org). Knockouts of these genes led to invaginations from peripheral membranes into the cell interior. Ist2 localized in a patch like manner to the cell periphery as well as to these invaginations. This localization of GFP-Ist2 differs from the localization in wild type cells. These differences are, however, most probably a secondary effect of the invaginations of peripheral membranes, in which GFP-Ist2 resides and were not followed up further.

In *ice2Δ* cells and *scs2Δ* cells the cortical ER inheritance is impaired (Estrada de Martin et al., 2005; Loewen et al., 2007). GFP-Ist2 in these strains localizes to the cell periphery, but is not present at the apical poles of daughter and some mother cells in *scs2Δ* cells. In *ice2Δ* cells GFP-Ist2 is only present on one side of the daughter cell. At least for *scs2Δ* cells it was shown that GFP-Ist2 only resides in sites of the cell periphery, at which cortical ER is present (Maass K., PhD Thesis 2008). Therefore, in these cells the localization of GFP-Ist2 can be explained as a consequence of defects in the distribution of cortical ER.

In 11 knockout strains the expression level of GFP-Ist2 was altered. However, as the localization of Ist2 remained unchanged, these phenotypes were not characterized on the molecular level. These phenotypes might be caused by defects in the distribution of the used plasmid or by cellular defects of the transcription or translation machinery.

Despite some mislocalizations within the cell periphery and alterations in expression levels, in all strains GFP-Ist2 localized in patch like-structure in the cell periphery. An accumulation of GFP-Ist2 at the perinuclear ER or other intracellular organelles was not detectable for any strain. From this dataset, it can be concluded that a single, nonessential gene is not solely responsible for the transport of GFP-Ist2 from the perinuclear ER to the cortical ER. However, within the cell periphery GFP-Ist2 is only accumulating at sites, at which cortical ER is present, as judged from *scs2Δ* cells. From this screen no factor that is solely responsible for the rapid transport of the Ist2 protein from the perinuclear ER to the cortical ER could be identified. Cellular factors involved in this process might be essential components, which are not included in knockout libraries. Furthermore, these factors might be redundant and therefore been missed in this screen, which only focused on the localization of GFP-Ist2 in cells with a single gene knocked out. Alternatively, the usage of an Ist2 reporter, of which the mRNA is not localized (e.g. GFP-Ist2 with a changed codon usage within the She2-binding site), might lead to a higher amount of protein synthesized at the perinuclear ER of mother cells. Such a reporter might be more sensitive to detect differences in the distribution of the reporter protein between cortical and perinuclear ER.

2.1.2. Materials

Chemicals and reagents:

All used chemicals were purchased from Serva (Heidelberg), Roth (Karlsruhe), Merck (Darmstadt) or Sigma (Munich). Restriction enzymes were from New England Biolabs (Frankfurt), T4 DNA Ligase from Roche (Mannheim). Single strand DNA from salmon sperm was from Sigma.

Kits for plasmid purification in Miniprep and Maxiprep scale were from Qiagen (Hilden) and Macherey-Nagel (Düren), respectively. Kits for DNA extraction from agarose gels were from Qiagen.

Media:

Escherichia coli (*E. coli*) were grown in lysogeny-broth (LB)-Medium (Sambrook and Russell, 2001). For selection purpose 100 µg/ml Ampicillin (Sigma) was added. Yeast cells were grown in yeast peptone dextrose (YPD)-Medium (Sambrook and Russell, 2001)

before transformation and after transformation in Hartwell-complete (HC)-Medium lacking leucine (Sambrook and Russell, 2001).

BactoTryptone and yeast extract for preparation of LB and YPD-Medium were from Becton Dickinson (Heidelberg). For growth of *E. coli* and yeast cells on culture plates 2% Agar (Invitrogen, Karlsruhe) was added to the respective medium.

Plasmid:

The plasmid used for this screen encodes for yEGFP3-Ist2 controlled by the *IST2* promoter and the *IST2* 3'UTR (pMF6). pMF6 was generated by subcloning a SacI/XhoI fragment from pCJ100 (Jüschke C., PhD Thesis 2005) into pRS315 (Sikorski and Hieter, 1989). pMF6 carries the *LEU2* gene and a centromeric *CEN6* DNA fragment, which confers the distribution of the plasmids upon cell division. The plasmid was verified via sequencing.

***E. coli* strain:**

For plasmid amplification DH5 α -cells of the following genotype were used:

F⁻ Φ 80*lacZ* Δ M15 Δ (*lacZYA-argF*)U169 *deoR recA1 endA1 hsdR17*(r_k⁻, m_k⁺) *phoA supE44 thi-1 gyrA96 relA1*

Yeast knockout library:

The used yeast knockout library was from EUROSCARF (Frankfurt). It contains 4850 different deletion mutants in the BY4741 strain background provided in 96-well plates. The genotype of the BY4741 wild type strain is the following:

MAT a; *his3* Δ 1; *leu2* Δ 0; *met15* Δ 0; *ura3* Δ 0

Each knockout strain has its corresponding coding sequence replaced by a kanMX4 cassette (Winzeler et al., 1999). kanMX4 encodes for a protein conferring resistance to the fungal antibiotic G418 (Baudin et al., 1993; Wach et al., 1994).

2.1.3. Methods

Restriction digest of DNA:

3 μg of DNA was cut with 10 U of each used restriction enzyme. The reaction had a total volume of 20 μl and was carried out for 1 h in the recommended buffer. Subsequent to digestion the DNA was analyzed via agarose gelelectrophoresis.

Agarose gelelectrophoresis:

For the analysis of DNA fragments these were subjected to agarose gelelectrophoresis. Agarose gels were poured in a concentration of 0.8% (w/v) agarose in TAE buffer (90 mM Tris-acetate pH 8.0; 2 mM EDTA). To analyze the DNA, 2 μg ethidium bromide was added per 1 ml Gel. The DNA was taken up in DNA loading buffer (50% (v/v) Glycerol; 0.1% (w/v) bromophenol blue in TAE buffer). The gels were run at a voltage of 70 V. As a marker the 1 kb ladder (Invitrogen) was used.

Subsequent to electrophoresis the gels were analyzed on a UV-Transilluminator (Bio-Rad, Munich) and the respective bands were cut out with a scalpel.

Gel extraction:

The extraction of DNA from agarose gels was performed using the QIAquick Gel Extraction Kit (Qiagen) according to the manufacturer's protocol.

Measurements of DNA concentration:

DNA concentration was measured in a NanoDrop ND-1000 Spectrophotometer (Thermo scientific, Dreieich). The absorption of 1 μl DNA solution at 260 nm was measured and the DNA concentration calculated.

Ligation:

For ligation of DNA fragments 30 fmol vector backbone and 60 fmol vector insert were ligated over night at 16°C. Each reaction (10 μl volume) contained 10 U T4 DNA Ligase and the respective buffer.

Transformation of *E. coli*:

E. coli cells were transformed with DNA using electroporation. Electroporation cuvettes (peqlab, Erlangen) were filled with 1 μl DNA solution and 45 μl competent bacteria solution. The cells were pulsed at 2,5 kV, 200 Ω and 25 μF in the GenePulser (Bio-Rad). The transformed bacteria were recovered for 50 min in 950 μl LB-Medium and streaked out on selective LB-plates containing Ampicillin.

Growth of *E. coli*:

E. coli was inoculated from a culture plate into LB-medium containing Ampicillin and grown overnight shaking at 150 rpm at 37°C.

DNA preparation from *E. coli*:

Preparation of DNA was performed using the QIAprep Spin Miniprep Kit for 50 ml of bacterial culture or the Nucleobond AX Maxiprep Kit for 500 ml of bacterial culture. DNA preparations were performed according to the manufacturer's protocol. The plasmid was stored in sterile water at -20°C.

Yeast knockout library:

The yeast knockout library was stored as stocks in 20% (v/v) glycerol at -80°C. In order to grow the cells, the 96-well-plates were mildly thawed and the cell suspension was stamped onto angular YPD-plates. The cells were grown for two days at 25°C. For transformation with pMF6 the grown colonies were transferred via a stamp into a fresh 96 well plate, each well containing 100 µl sterile water. The cell suspension was centrifuged in a plate centrifuge (Eppendorf, Hamburg) at 3000 g for 10 min. The supernatant was discarded and the pellets were resuspended in 50 µl transformation mix per well:

transformation mix:

1.5 ml Lithium Acetate (1 M)

5 mg single strand DNA

3 µg plasmid

ad 5 ml sterile water

After addition of the transformation mix, 100 µl 50% (w/v) polyethylene glycol was added to each well. The cells were incubated for 3 h at 42°C and subsequently centrifuged at 3000 g for 10 min. The supernatant was discarded, the cells were resuspended in 150 µl HC-medium lacking leucine and grown for 2 days at 25°C. The cells were then centrifuged at 3000 g for 10 min, the supernatant was discarded, the pellet was stamped onto angular HC-leucine plates and grown for 3 days.

For fluorescence microscopy the transformed cells were transferred into a fresh 96-well plate and grown over night in 150 µl HC-leucine medium. On the next morning the cells were centrifuged at 3000 g for 10 min and 1 µl of the pellet was subjected to fluorescence microscopy.

Fluorescence microscopy:

1 μ l yeast cell suspension was mounted onto a glass slide and covered with a coverslip. Cells were observed with an inverted microscope (DM IRE2, Leica Microsystems, Wetzlar), using an oil immersion objective (HCX PL APO CS 100/1.4 0.7, Leica). Pictures were taken using a Hamamatsu ORCA-ER CCD camera using Openlab software. For fluorescence microscopy a GFP 470/40 (excitation) filter was used. Picture processing was performed with Adobe Photoshop.

2.2 Biochemical characterization of the cortical sorting signal

In order to map functional domains within the cytosolic C-terminus of Ist2, I performed limited proteolysis experiments. The cytosolic C-terminus is predicted to be rather unstructured (Cole et al., 2008), except the C-terminal 11 amino acids of Ist2, which are predicted to form an amphipathic helix (Sapay et al., 2006). The only functional domain described within the Ist2 C-terminus is the CSS^{Ist2}. Therefore, at least one domain border that segregates the CSS^{Ist2} from the residual Ist2 protein might be found via limited proteolysis experiments within the predicted unstructured cytosolic C-terminus of Ist2. The cortical sorting signal of Ist2 was defined as the last 69 amino acids of Ist2. This is the minimal C-terminal part of Ist2, which redirects reporter proteins efficiently to the cell periphery (Franz et al., 2007). However, as the structure of Ist2 or its cytosolic C-terminus is not solved yet, it is unclear, whether the CSS^{Ist2} is really folded as a structural domain, thereby defining the Ist2 sorting signal as a functional entity at the C-terminus of Ist2.

2.2.1. Results

Assuming that borders between certain protein domains are better accessible for proteases than readily folded protein domains, digesting the entire cytosolic C-terminus of Ist2 (Fig. 5) with a limited amount of protease should result in peptide fragments corresponding to rather folded domains within the Ist2 C-terminus. As a substrate for proteolysis, I used recombinant glutathione-S-transferase (GST)-Ist2 589-946 (GST-Ist2^c; (Maass K., PhD Thesis 2008)). GST-Ist2^c was incubated with different concentrations of Proteinase K (Fig. 7, lanes 1-7), the proteolysis mix was precipitated with trichloro acetic acid (TCA) and subjected to sodium dodecyl sulfate polyacrylamide-gel electrophoresis (SDS-PAGE). Recombinant GST and Proteinase K without substrate served as loading controls (Fig. 7, lanes 8/9).

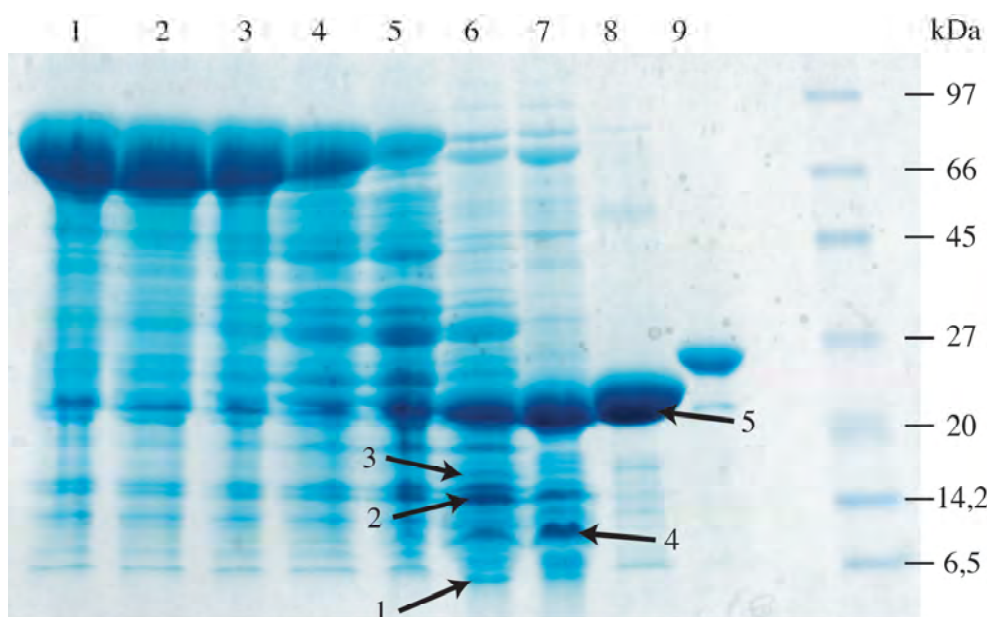


Fig. 7: Limited proteolysis of GST-Ist2 589-946. 150 μg GST-Ist2 589-946 was digested with different Proteinase K concentrations. Proteolysis occurred for 60 min at 25°C and was stopped with Phenylmethylsulfonyl fluoride (PMSF). The TCA precipitated pellet was subjected to SDS-PAGE on a 10-17% gradient gel. Lane 1: no Proteinase K; lane 2: 1 $\mu\text{g}/\text{ml}$ Proteinase K; lane 3: 3 $\mu\text{g}/\text{ml}$ Proteinase K; lane 4: 10 $\mu\text{g}/\text{ml}$ Proteinase K; lane 5: 30 $\mu\text{g}/\text{ml}$ Proteinase K; lane 6: 100 $\mu\text{g}/\text{ml}$ Proteinase K; lane 7: 300 $\mu\text{g}/\text{ml}$ Proteinase K; lane 8: 150 μg GST, no Proteinase K; lane 9: 30 μg Proteinase K, no substrate. The gel was Coomassie stained. Bands labeled with 1-5 were subjected to mass spectrometry.

Upon increasing concentration of Proteinase K, a prominent band at >20 kDa appeared, which corresponds to the size of GST (compare lane 8). Additional bands in the molecular range of 5-15 kDa appeared as well (see arrowheads 1-4). These bands might correspond to domains in the Ist2 C-terminus. In order to check, to which protein sequence in the Ist2 C-terminus the bands 1-4 correspond, they were analyzed via mass spectrometry. Band 5 containing only GST served as a specificity control.

The bands were cut out, digested in the gel with trypsin, purified by High Performance Liquid Chromatography (HPLC) and analyzed via Electrospray Ionization Mass Spectrometry (ESI-MS). It has to be noted that after the unspecific digestion with proteinase K the bands for mass spectrometry were subjected to a tryptic in-gel digest. Trypsin cleaves specifically after lysine and arginine residues. Therefore, most of the identified peptides start after such residues or end with these amino acids, as a consequence of the tryptic digest. However, cleavage after other residues indicates a region, which was cleaved by proteinase K. Figure 8 shows the amino acid sequence of Ist2 589-946 with the peptides, which were identified in mass spectrometry, underlined and labeled A-G:

```

589 KSSHDDVANGIVPKHVVNVQNPQKQEVFEKIPSPFNSNNEKELVQRKGSANEKLNHQLG
649 EKQPASSANGYEAHAATHANNDPSSLSSASSPSLSSSSSSSKTGAVKAVDNDTAGSAGKK
709 PLATESTEKRNLSLVKVPVTVGSYGVAGATLPETIPTSAKNYYLRFDEDEGKSIRDAKSSAESS
769 NATNNNTLGTESFKLLPDGDAVDALSRKIDQIPKIAVTGGENNENTQAKDDAATKTPLIKD
829 ANIKPVVNAAVNDNQSKVSVATEQTKKTEVSTDKNGPSRSISTKETEKDSARPSNNNTTTTE
889 TTDATQPHHHHHHRHRDAGVKNVTNNSKGTTSSSSSSAAKEKPKHKKGLLHKLKKKL

```

Fig. 8: Peptides identified via mass spectrometry. The bands 1-5 from Fig. 7 were subjected to mass spectrometry. The sequence of Ist2 589-946 is drawn, the peptides identified via mass spectrometry are underlined with A-G. For peptides that start after lysine residues, this lysine residue is marked blue. In the bands 1 and 5 from Fig. 7 only peptides corresponding to GST were found. In band 2 the Peptides D, E and G were found, in band 3 the peptides A and traces of B and C were found. In band 4 the peptides F and G were identified.

As expected, the mass spectrometry from band 5 from Fig. 7 identified only peptides corresponding to GST (not shown in Fig. 8). Also in band 1 only GST-peptides were found, probably because band 1 is a digestion product of GST. In the bands 2-4 peptides corresponding to the C-terminus of Ist2 could be identified (Fig. 8). Peptide A and traces of the peptides B and C were found in band 3 from Fig. 7. The peptides D, E and G could be found in band 2, band 4 contained the peptides F and G.

Only one peptide that does not start with lysine residues could be identified. This is peptide F, which starts with the threonine residue at position 887. Therefore, the threonine stretch within the T/H/S-cluster of Ist2 (see Fig. 6) seems to be accessible to proteinase K indicating a domain border being present in this region of the protein.

2.2.2. Materials

All used chemicals were purchased from Serva (Heidelberg), Roth (Karlsruhe), Merck (Darmstadt) or Sigma (Munich). Proteinase K was from Merck. GST-Ist2 589-946 was from K. Maass (Maass K., PhD Thesis 2008).

2.2.3. Methods

Limited proteolysis:

To GST-Ist2 589-946 the appropriate amount of Proteinase K was added in a volume of 100 μ l. As the reaction buffer PBS (Sambrook and Russell, 2001) was used. Limited proteolysis was performed at 25°C for 60 min shaking at 300 rpm. The reaction was stopped by the addition of 10 μ l Phenyl-methylsulfonyl fluoride (PMSF; 100 mM).

Samples were precipitated with 110 μ l 20% (v/v) TCA for 15 min on ice and centrifuged at 13000 g for 5 min.

SDS-PAGE:

The pellet from the TCA precipitation was taken up in SDS-sample buffer (330 mM Tris-HCl, pH 6.8; 2% (v/v) β -Mercaptoethanol, 2% (w/v) SDS, 0.1% (w/v) bromophenol blue, 10% (w/v) glycerol) and boiled for 5 minutes at 95°C. The solubilized protein was loaded onto one lane of a 10-17% gradient gel, which was poured using a gradient mixer. As a protein marker prestained protein marker (New England Biolabs) was used. The SDS-Gel was run in electrophoresis buffer (192 mM glycine, 25 mM Tris, 0.1% (v/v) SDS).

Protein detection was performed using Coomassie staining. The gel was incubated in Coomassie staining solution (0.25% (w/v) Coomassie brilliant blue S250, 40% (v/v) Ethanol, 10% (v/v) acetic acid) over night. On the next day it was destained via multiple incubation steps in Coomassie destaining solution (40% (v/v) Ethanol, 10% (v/v) acetic acid). The gel was stored in water.

Mass spectrometry:

The bands of interest from the Coomassie stained gel were cut out with a scalpel. Gel slices were reduced, alkylated and subjected to a tryptic digest (Catrein et al., 2005) using a Digest pro MS liquid handling system (Intavis AG, Cologne). The peptides were eluted from the gel with 50% (v/v) acetonitrile/0.1% (v/v) trifluoro acetic acid (TFA) and dried in a SpeedVac centrifuge (Thermo scientific). Peptides were taken up in 30 μ l 0.1% (v/v) TFA and purified via a nanoHPLC system coupled to an ESI LTQ Orbitrap mass spectrometer (Thermo scientific). Data processing was performed using the Mascot software (Matrix Science, London) and handcurated.

2.3 Results and publications of this cumulative dissertation

The cumulative dissertation

Lipids as Trans Acting Factors for the Transport of Integral Membrane Proteins

by

Diplom-Biochemiker

Marcel Fischer

born in Stadthagen, Germany

is based on the following publications:

1) A signal comprising a basic cluster and an amphipathic α -helix interacts with lipids and is required for the transport of Ist2 to the yeast cortical ER.

Kiran Maass*, Marcel Fischer*, Markus Seiler, Koen Temmerman, Walter Nickel and Matthias Seedorf.

* joined first authorship

J Cell Sci. 2009 Mar 1;122(Pt 5):625-35.

Contribution of M. Fischer to the experimental data: 45%

Written by M. Seedorf

2) Binding of plasma membrane lipids recruits the yeast integral membrane protein Ist2 to the cortical ER.

Marcel Fischer, Koen Temmerman, Ebru Ercan, Walter Nickel and Matthias Seedorf.

Traffic. 2009; in press.

Contribution of M. Fischer to the experimental data: 90%

Written by M. Fischer

The work in these two publications covers 90% of the total results obtained within this thesis.

Heidelberg, April 30, 2009

PD Dr. Matthias Seedorf

A signal comprising a basic cluster and an amphipathic α -helix interacts with lipids and is required for the transport of Ist2 to the yeast cortical ER

Kiran Maass^{1,*}, Marcel André Fischer^{1,*}, Markus Seiler², Koen Temmerman³, Walter Nickel³ and Matthias Seedorf^{1,‡}

¹Zentrum für Molekulare Biologie der Universität Heidelberg (ZMBH), Im Neuenheimer Feld 282, D-69120 Heidelberg, Germany

²European Molecular Biology Laboratory (EMBL) Heidelberg, Meyerhofstrasse 1, D-69117 Heidelberg, Germany

³Heidelberg University Biochemistry Center (BZH), Im Neuenheimer Feld 328, D-69120 Heidelberg, Germany

*These authors contributed equally to this work

‡Author for correspondence (e-mail: m.seedorf@zmbh.uni-heidelberg.de)

Accepted 2 November 2008

Journal of Cell Science 122, 625–635 Published by The Company of Biologists 2009

doi:10.1242/jcs.036012

Summary

The yeast integral membrane protein Ist2 is encoded by a bud-localised mRNA and accumulates at patch-like domains of the cell periphery, either at the cortical ER or at ER-associated domains of the plasma membrane. Transport of *IST2* mRNA and local protein synthesis are not prerequisite for this localisation, indicating that Ist2 can travel through the general ER to membranes at the cell periphery. Here, we describe that the accumulation of Ist2 at the cortical ER requires a cytosolically exposed complex sorting signal that can interact with lipids at the yeast plasma membrane. Binding of the Ist2 sorting signal to lipids and rapid and efficient transport of Ist2 from perinuclear to cortical ER depend on a cluster of lysine residues, the formation of an amphipathic α -helix and a patch of hydrophobic side chains positioned at one side of the

amphipathic α -helix. We suggest that a direct interaction of the Ist2 sorting signal with lipids at the plasma membrane places Ist2 at contact sites between cortical ER and plasma membrane. This provides a physical link of an integral membrane protein of the cortical ER with the plasma membrane and might allow direct transport of proteins from cortical ER to domains of the plasma membrane.

Supplementary material available online at <http://jcs.biologists.org/cgi/content/full/122/5/625/DC1>

Key words: Cortical ER, Plasma membrane, Sorting signal, Lipid binding, Sec-independent trafficking

Introduction

The endoplasmic reticulum (ER) is an organelle that forms contacts with many other membranes, and these contacts are specialised for traffic of both material and information (Levine and Loewen, 2006). One example of such direct transport is the exchange of lipids between the ER and plasma membrane. Experiments in *Saccharomyces cerevisiae* show that a non-vesicular exchange of lipids occurs between the ER and plasma membrane (Baumann et al., 2005; Raychaudhuri et al., 2006; Schnabl et al., 2005). The yeast cortical ER is in contact with the plasma membrane at many positions, where such a direct exchange of molecules between cortical ER and plasma membrane might occur (Perktold et al., 2007; Pichler et al., 2001). However, little is known about the molecular components of ER-to-plasma-membrane contact sites and the sorting of ER membrane proteins to these or to other domains of the yeast cortical ER.

The yeast *S. cerevisiae* has two main ER types: the perinuclear ER and the cortical ER (Voeltz et al., 2002). The cortical ER is a peripheral meshwork of membrane tubules underlying the plasma membrane, with only a few cytoplasmic tubules connecting the cortical ER to the perinuclear ER (Koning et al., 1993; Preuss et al., 1991; Prinz et al., 2000). However, the entire ER is one continuum, as shown by free diffusion of luminal GFP and the

mobility of integral ER membrane proteins (Luedeke et al., 2005). The movement of the translocon component Sec61, the SNARE Sec22 and 3-hydroxy-3-methylglutaryl-coenzyme A reductase (Hmg1) between the cortical and perinuclear ER of mother cells is only ten times slower than the free diffusion of GFP in the ER lumen (Luedeke et al., 2005). Fluorescence loss in photobleaching experiments in mother cells revealed that half of the Sec61 exchanges between cortical and perinuclear ER in less than 20 seconds. Between the ER of mother and daughter cells this exchange occurs within minutes (Luedeke et al., 2005).

Based on mRNA transport and local translation, the cortical ER of daughter cells is the main site for synthesis of a number of membrane proteins encoded by localised mRNAs (Aronov et al., 2007; Shepard et al., 2003; Takizawa et al., 2000). One of these localised mRNAs encodes the polytopic membrane protein Ist2, which localises to patch-like domains of the cell periphery (Juschke et al., 2004; Takizawa et al., 2000). By fluorescence microscopy, these domains colocalise with the ER protein Dpm1 (Juschke et al., 2004). However, cell fractionation and protease protection experiments indicate a localisation of Ist2 at the plasma membrane (Juschke et al., 2004). Transport of Ist2 to these peripheral domains occurs independently of the classical secretory pathway on a route that bypasses the Golgi (Juschke et al., 2004;

Juschke et al., 2005). This transport requires the cytosolically exposed C-terminal domain of Ist2 (Juschke et al., 2005). Without this domain, Ist2 accumulates at punctuated structures of the perinuclear and cortical ER (Franz et al., 2007; Juschke et al., 2005). When attached to a cytosolically oriented C-terminus of a membrane protein, a protein sorting of the C-terminal 69 amino acid signal is sufficient for sec-independent transport to the cell periphery (Franz et al., 2007). Transport of Ist2 can operate independently of *IST2* mRNA localisation (Franz et al., 2007), indicating that the Ist2 sorting signal leads to the accumulation of Ist2 at the cortical ER from where the protein may reach ER-associated domains of the plasma membrane.

In this study, we found that a certain amount of Ist2 localises for a short period at the perinuclear ER of mother cells, and we identified specific residues required for rapid movement from the perinuclear to the cortical ER. These residues are part of a sorting signal that binds lipids at the plasma membrane, suggesting that the interaction between the Ist2 sorting signal and lipids localises Ist2 at the cortical ER.

Results

Insertion of Ist2 into the perinuclear ER of mother cells

Is all Ist2 synthesised at the cortical ER of daughter cells as a consequence of mRNA localisation, or does synthesis also take place at the perinuclear ER of mother cells? Since *GAL1*-promoter-induced, fluorescent-protein-tagged Ist2 appeared at peripheral patches without any staining of the perinuclear ER (Fig. 1A) (Juschke et al., 2004; Juschke et al., 2005; Takizawa et al., 2000), we argued that if Ist2 is inserted into the perinuclear ER, the protein leaves this part of the organelle before maturation of the fluorescent proteins. To analyse this, we localised *GAL1*-induced Ist2 with an N-terminal hemagglutinin (HA) tag by indirect immunofluorescence. HA-Ist2 was synthesised 30 minutes after galactose induction, as detected by western-blotting (Fig. 1B). After 40 minutes, *ist2Δ* cells frequently showed HA-Ist2 staining at buds, and at patches in the periphery of budded and unbudded cells (Fig. 1C). 40% of the unbudded cells and 18% of budded cells showed additional perinuclear HA-Ist2 staining (indicated with arrows in Fig. 1C, quantification at the 0-minute time point in Fig. 1D). The transport of *IST2* mRNA to the bud cortical ER is probably responsible for the reduced number of budded cells with perinuclear HA-Ist2 staining compared with unbudded cells with this staining. Detection of *GAL1*-induced YFP-Ist2 at the perinuclear ER with an antibody against the C-terminal domain of Ist2 confirmed that a detectable pool of YFP-Ist2 is also inserted into the perinuclear ER (supplementary material Fig. S1). This pool is not detected by YFP fluorescence in living cells (Fig. 1A), probably because of the slow maturation of YFP.

How long does this pool of Ist2 remain at the perinuclear ER? To address this question, we stopped protein synthesis by adding cycloheximide, took a sample every three minutes, fixed the cells with formaldehyde and localised HA-Ist2 by immunofluorescence with antibodies against HA. Within the first 3 minutes, the number of unbudded cells with perinuclear ER staining was reduced from 40% to 21%, indicating that Ist2 reached the cell periphery rapidly (Fig. 1D). Repression of *HA-IST2* transcription by glucose resulted in a similar disappearance of HA-Ist2 from the perinuclear ER. After a 10 minute treatment with glucose, the number of unbudded cells with detectable HA-Ist2 at the perinuclear ER dropped from 50% to 26% (not shown). These data confirm the cycloheximide results and demonstrate that some of the newly synthesised Ist2 spends a

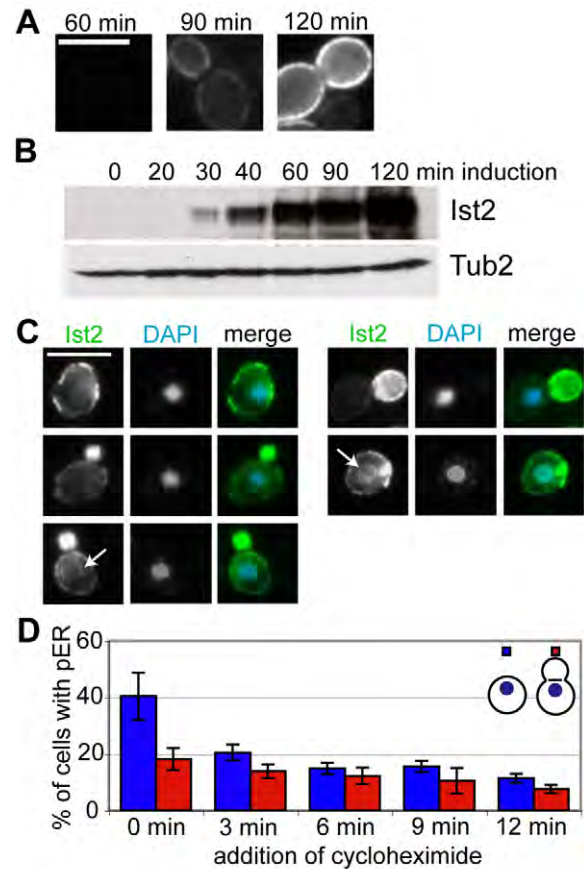


Fig. 1. The sorting of Ist2 starts with rapid accumulation at the cortical ER. (A) Fluorescence of *GAL1*-controlled YFP-Ist2 in living *ist2Δ* cells at 60, 90 and 120 minutes after galactose induction in YEAP medium at 25°C. Scale bar: 5 μm. (B) Western blot of total extract from 0.2 OD₆₀₀ *ist2Δ* cells grown for the indicated time in 2% galactose at 25°C expressing HA-Ist2 under control of the *GAL1* promoter with antibodies against HA and tubulin (Tub2). (C) Immunofluorescence of cells expressing HA-Ist2 at different stages of the cell cycle after 40 minutes of galactose induction at 25°C. Nuclei are stained with DAPI. (D) Quantification of the percentage of cells (mean ± s.d.) with a detectable perinuclear HA-Ist2 signal after 40 minutes of galactose induction at 25°C. For the indicated times, 100 μg/ml cycloheximide was added to the galactose-induced cultures before fixation with formaldehyde. The percentage of cells with perinuclear HA-Ist2 (pER) in unbudded cells is shown in blue and in budded cells in red.

limited time at the perinuclear ER before it accumulates at the cell periphery.

Basic residues at the C-terminus of Ist2 are required for trafficking to the cortical ER

Ist2 from *S. cerevisiae* comprises 946 residues and has eight transmembrane domains and a domain, named DUF590, of unknown function (Fig. 2A) (Galindo and Vacquier, 2005). The cytosol-oriented C-terminal domain of Ist2 contains a complex protein-sorting signal comprising the C-terminal 69 residues of Ist2 (Franz et al., 2007). This signal consists of two parts. Its N-terminus contains a cluster of single amino acid repeats with multiple threonine, histidine and serine residues (T/H/S cluster) (Fig. 2A). Its C-terminus consists of a basic region, which is rich in lysine and leucine residues (K/L-sequence). The C-terminal 11 residues of the K/L-sequence (K936-L946) are predicted to form an

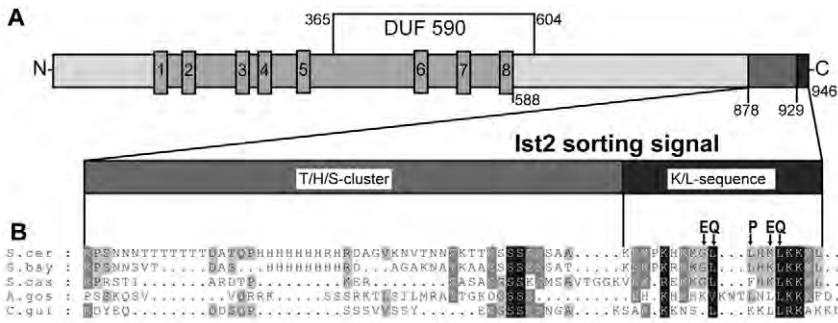


Fig. 2. Features of the Ist2 protein. (A) Schematic overview of features of the Ist2 protein from *S. cerevisiae*. The transmembrane domains (1-8), the position of the DUF590 domain and the cytosol-orientated Ist2 sorting signal are shown. (B) Alignment of the Ist2 sorting signal (residues 878-946 of *S. cerevisiae*) with C-termini of Ist2 homologues from a selection of related yeast species. The residues in bold on top of the *S. cerevisiae* sequence indicate single mutations that cause mislocalisation of Ist2. The conserved positions are shown in shaded boxes.

amphipathic α -helix (Sapay et al., 2006), of which the three most C-terminally located lysines and L946 fit the consensus of a lysine ER-retrieval signal (Fig. 2B).

To identify the residues that are essential for the function of the Ist2 sorting signal, we screened for mutants that mislocalised to a perinuclear or punctuated peripheral distribution. Among other

mutations, we identified five single residue exchanges in the K/L-sequence that caused such mislocalisation (G937E, L938Q, L939P, K941E and L942Q) (Fig. 2B). These mutations fall into three different categories: change from a basic into an acidic residue, loss of a hydrophobic side chain and change of a secondary structure by the introduction of a helix-breaking proline residue. An alignment of a selection of closely related yeast species revealed that the K/L sequence is better conserved than the upstream T/H/S cluster (Fig. 2B).

We tested the effects of these three types of mutation individually. Using fluorescence microscopy it is not possible to discriminate whether a protein is at the plasma membrane or at the underlying cortical ER. Therefore, we use the term 'cell periphery' to describe localisation at plasma membrane or cortical ER. To determine whether the isolated Ist2 alleles localise to the general ER or to membranes at the cell periphery, we used *sec23-1* mutant cells, which fail to form COPII vesicles and accumulate proliferated ER structures (Novick et al., 1980). Since the proliferated cortical ER of these cells detaches from the cell periphery, a trapping of mutated Ist2 at the general ER becomes visible. The *sec23-1* phenotype was monitored by the expression of *GALI*-induced hexose transporter (Hxt1-CFP). At the non-permissive temperature of 37°C Hxt1-CFP was trapped at proliferated ER structures, whereas at 25°C, Hxt1-CFP reached the plasma membrane, from where it entered the vacuole via endocytosis (Fig. 3A). At permissive and non-permissive conditions, *GALI*-induced YFP-Ist2 localised exclusively to the cell periphery (Fig. 3A). A deletion of the K/L sequence (residues 929-946) resulted, at 25°C, in an accumulation at perinuclear ER and at peripheral dots, indicating that the K/L sequence is required for sorting from the

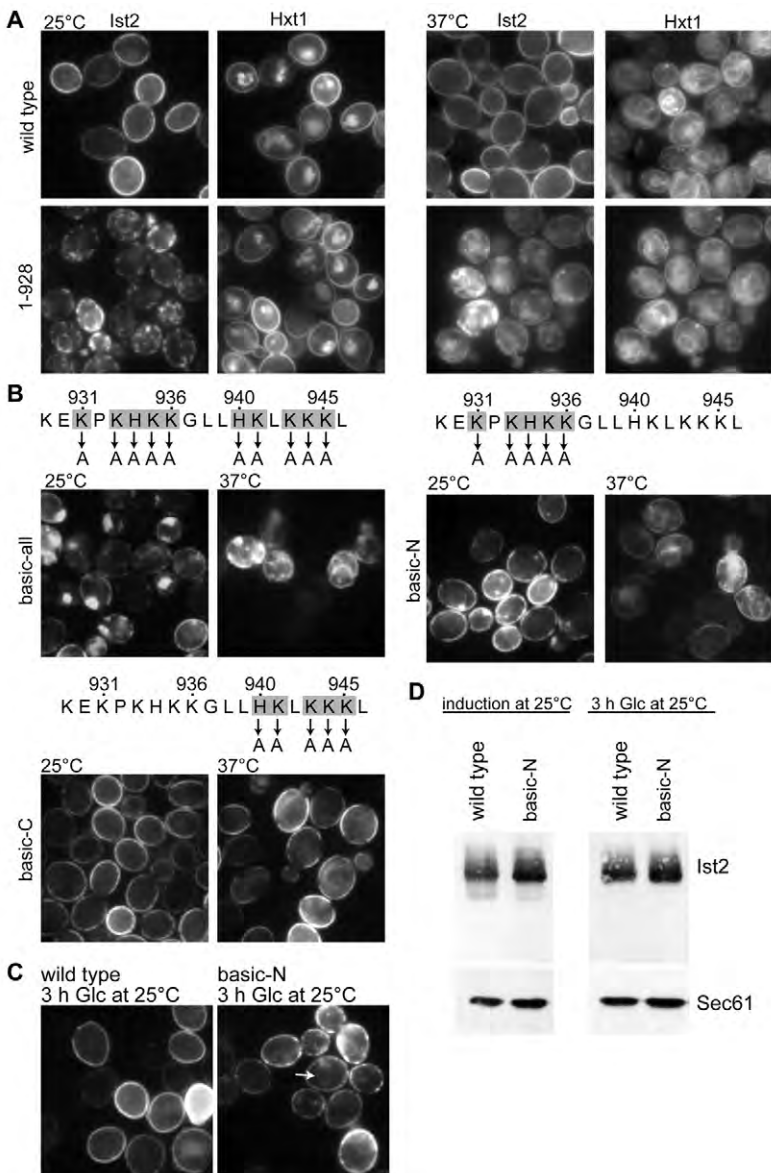


Fig. 3. Mutation of certain basic residues traps Ist2 at the perinuclear ER. (A) Localisation of YFP-tagged wild-type Ist2 and a C-terminal deletion (1-928) of YFP-Ist2 in *sec23-1* cells after 120 minutes of induction with galactose at 25°C and 37°C with coexpression of *GALI*-induced Hxt1-CFP in *sec23-1* cells. (B) Localisation of the indicated YFP-tagged Ist2 mutants in *sec23-1* cells after 120 minutes of induction with galactose at 25°C and 37°C. The mutated residues are indicated in shaded boxes. (C) Localisation of YFP-Ist2 and YFP-Ist2 basic-N in *ist2Δ* cells 120 minutes after addition of galactose and further incubation for 3 hours in glucose (Glc) at 25°C. (D) Quantification of Ist2 expression shown in C: total proteins from 0.1 OD₆₀₀ unit cells were separated by SDS-PAGE and analysed by western blotting with antibodies recognising Ist2 or Sec61.

perinuclear to the cortical ER. At 37°C, YFP-Ist2₁₋₉₂₈ and Hxt1-CFP were trapped at proliferated ER structures (Fig. 3A).

A mutation of C-terminally located K931, K933, H934, K935, K936, H940, K941, K943, K944, K945 to A (basic-all) resulted in an accumulation in ill-defined large dots and other intracellular structures at 25°C (Fig. 3B). Upon the shift to 37°C, most of the protein was trapped at the proliferating ER. Next, we exchanged either four of the N- or C-terminal basic residues with alanines. Mutation of K931, K933, H934, K935, K936 to A (basic-N) caused at 25°C a weak staining of structures resembling perinuclear ER in addition to the accumulation at the cell periphery. Mutations of H940, K941, K943, K944, K945 to A (basic-C) showed no phenotype, suggesting that if the N-terminal part of the basic cluster is present, the C-terminal part has only a minor contribution to Ist2 sorting. Taken together, these results suggest that positive charges are indeed important for the peripheral accumulation of Ist2 and that the lysine residues have a position-dependent function.

To characterise the function of the lysine residues further, we mutated single lysine residues of the N-terminal part of the basic cluster to alanines. The mutation K936A caused partial punctuated accumulation in a few cells at 25°C, whereas the mutation K935A and the double mutation K933A/H934A had no effect (supplementary material Fig. S2A). The K936A mutation, however, increased the trapping of Ist2 if combined with a mutation in the C-terminal part (supplementary material Fig. S2B). Mutations of three lysines or two lysines and a histidine in K931-K935 were tolerated (supplementary material Fig. S3A), whereas a K931A/K933A/H934A/K935A mutation caused some perinuclear accumulation at 25°C (supplementary material Fig. S3B). However, compared with the basic-N mutant, less of the K931A/K933A/H934A/K935A mutant was trapped at the proliferated ER at 37°C (compare Fig. 3B and supplementary material Fig. S3B). These results indicate an additive effect of K936 and the C-terminal part of the basic cluster as well as a position-dependent requirement of at least two lysines and/or one histidine in the N-terminal part in cooperation with several lysine residues in the C-terminal part.

To investigate whether transport of the Ist2 basic-N mutant from the perinuclear ER to the cell periphery was simply delayed or whether the protein could not leave the perinuclear ER, we induced the synthesis of Ist2 basic-N for 120 minutes at 25°C. After a 180 minute shift into glucose medium, Ist2 basic-N was not degraded but maintained its perinuclear localisation (Fig. 3C, indicated by arrow). Under the same conditions, wild-type YFP-Ist2 reached the cell periphery without any visible intracellular accumulation. This localisation and the quantification of Ist2 proteins by western blotting (Fig. 3D), indicated that the mutation of the N-terminal cluster of basic residues did not affect the stability of Ist2 and showed that this mutation abolished trafficking of Ist2 from the perinuclear ER to the cortical ER.

Mutation of hydrophobic residues traps Ist2 at specific ER domains

As a second category of mutations causing intracellular accumulations of Ist2, we identified mutations of the hydrophobic positions L938 and L942 (L938Q, L942Q). Most *sec23-1* cells expressing YFP-Ist2 L942Q at 25°C showed punctuated accumulation at perinuclear and peripheral structures and a trapping at the proliferating ER at 37°C (supplementary material Fig. S4). We observed a heterogeneous phenotype, because some cells showed a localisation only at the cell periphery (quantification in

supplementary material Table S1). A comparison of two clones with different expression revealed that the degree of punctuated accumulation at 25°C depends on the amount of Ist2 L942Q synthesis (supplementary material Fig. S4). In cells with high expression, the accumulation of Ist2 L942Q in dots was more pronounced. This accumulation in large dots was observed at both 25°C and 37°C. Importantly, we never saw such punctuated localisation for wild-type Ist2, which was induced similarly.

Next, we asked whether the hydrophobicity at position 942 influences the peripheral accumulation. Exchange of L942 to alanine, valine or methionine at 25°C led to accumulation in one or two dots in 72-89% of cells (supplementary material Fig. S5, Table S2). Compared with the L942Q mutant, these dots disappeared in cells shifted to 37°C, although small amounts of Ist2 remained at proliferated ER structures. Exchange of L942 to tryptophan and phenylalanine resulted in only 12% and 25%, respectively, of cells in punctuated accumulation. The mutation to isoleucine had no effect. As a next step, we determined whether the remaining leucines also contribute to the peripheral accumulation of Ist2. Mutation of L938 or L939 to alanine and valine led to punctuated protein accumulation, which was similar to that observed for L942 (supplementary material Fig. S6). A combination of mutations of the neighbouring L938 and L939 to alanine or valine increased this phenotype, whereas double mutation of L938 and L939 to isoleucine was tolerated. Compared with positions 938, 939 and 942, the mutation of L946 had the mildest effect.

To analyse at which membranes the punctuated Ist2 was trapped, we colocalised mCherry-tagged Ist2 L942Q (red) with GFP-tagged proteins characteristic for specific organelles (green). mCherry-Ist2 L942Q dots showed no overlap with Sed5, Gef1 and Kex2 (supplementary material Fig. S7). Instead of mCherry-Ist2 L942Q, we used GFP-tagged Ist2 L942Q (green) for colocalisation with Sec7-RFP (red). Similarly to Sed5, Gef1 and Kex2, we observed no overlap between Ist2 L942Q and Sec7 (supplementary material Fig. S7). A statistical analysis of Ist2 L942Q dots revealed an average distance of five pixels (0.4 µm) between the maximum signal intensity of an Ist2 L942Q dot and the nearest Sec7, Sed5, Gef1 or Kex2 dot, indicating that Ist2 L942Q was not trapped at either the Golgi (Sec7, Sed5, Gef1 and Kex2) or in endosomes (Gef1 and Kex2) (supplementary material Fig. S8A). Fractionation of mCherry-Ist2 L942Q by separation on a 20-60% sucrose density gradient revealed that the majority of Ist2 L942Q cofractionated with rough ER and plasma membrane markers (Sec61 and Pma1) in fraction 8, whereas the Golgi-modified forms of Emp47 migrated in fractions 4-6 (supplementary material Fig. S9A,B). Under these conditions, rough ER and plasma membrane do not separate. Emp47 shuttles between the ER and Golgi (Schroder et al., 1995) and Sed5-GFP showed a similar partial separation from mCherry-Ist2 L942Q into Golgi fractions (supplementary material Fig. S9C). No difference was observed for Ist2 L942Q compared with the wild type, when separated on a sucrose gradient under these conditions (data not shown).

Ist2 L942Q dots colocalised with Scs2-containing ER at bud tips, cortical and perinuclear ER (Fig. 4, indicated by arrows). Scs2 is an integral ER membrane protein that functions as an adaptor for lipid-transfer proteins and in the anchorage of ER at the bud cortex (Loewen et al., 2003; Loewen et al., 2007). Some Scs2, which showed a normal ER distribution in cells overexpressing wild-type Ist2, was recruited to the dots containing Ist2 L942Q. An even stronger recruitment into Ist2 L942Q dots was observed for the integral ER membrane proteins Dpm1 and Sec63 (Fig. 4).

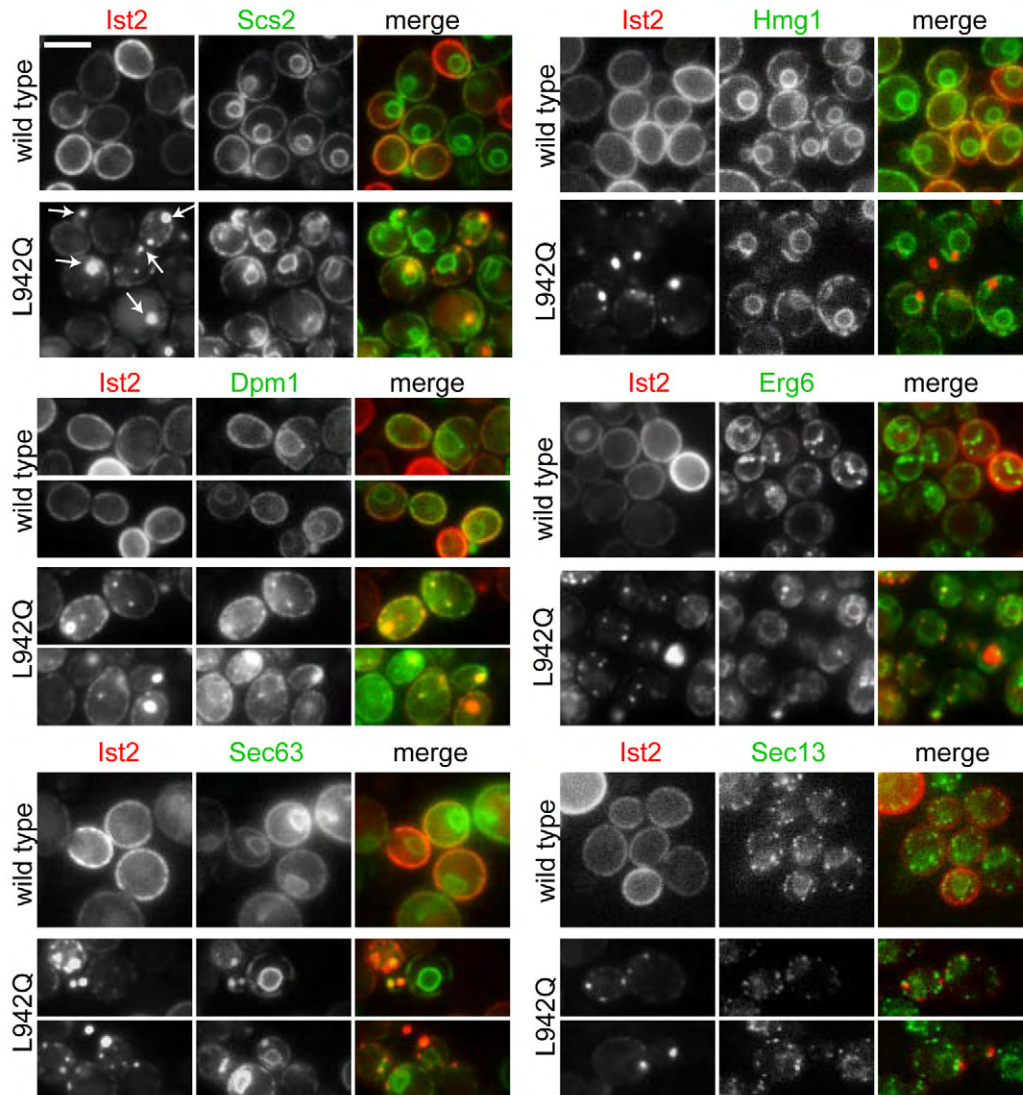


Fig. 4. Mutation of the Ist2 sorting signal causes trapping at ER domains. Localisation of *GALI*-induced wild-type mCherry-Ist2 or mCherry-Ist2 L942Q (in red) in strains coexpressing either GFP-tagged Scs2, Dpm1, Sec63, Hmg1, Erg6 or Sec13 (in green) in *ist2Δ* cells after induction with galactose at 25°C for 120 minutes. Scale bar: 5 μm.

In Dpm1-GFP coexpressing cells, mCherry-Ist2 L942Q had reproducibly more peripheral signal, whereas all other strains showed more accumulation of Ist2 L942Q in dots. The reason for this variability remains unknown. The distance of the maximum signal intensities between Ist2 L942Q dots and Scs2, Dpm1 or Sec63 signals at the ER were zero to one pixel, indicating that these proteins colocalise (supplementary material Fig. S8B). In comparison with Scs2, Dpm1 and Sec63, the recruitment of Hmg1 to Ist2-L942Q-positive dots occurred less frequently (supplementary material Fig. S8B). The enzyme Hmg1 is involved in the first step of ergosterol lipid biosynthesis (Basson et al., 1986). At the light microscopic level, all tested ER proteins localised to the perinuclear and cortical ER.

Some of the Ist2 L942Q dots were closely adjacent to Erg6, which localises to the ER and ER-derived lipid droplets (Athenstaedt et al., 1999). However, many of the punctuated Erg6-positive lipid droplets were clearly separated from Ist2 L942Q, indicating that Ist2 L942Q did not accumulate at lipid droplets (Fig. 4; supplementary material Fig. S8C). A total of 90% of Sec13 dots, which stain the ER exit sites containing COPII, showed a separation from Ist2 L942Q, with a distance of maximal signal intensities of

three or more pixels (Fig. 4; supplementary material Fig. S8C). Sucrose density centrifugation revealed that more than 65% of Sec13-GFP was separated from Ist2 L942Q (supplementary material Fig. S9D).

In summary, the mutation of hydrophobic residues abolished the transport of Ist2 to patch-like domains at the cell periphery. The colocalisation and fractionation experiments clearly indicate that the Ist2 L942Q mutation led to a dot-like accumulation at perinuclear, tubular and cortical ER domains. The intracellular Ist2 L942Q dots were often located at positions where ER tubules emerge from the perinuclear ER in the direction of the cortical ER (colocalisation of Ist2 L942Q with Scs2 and Dpm1) (Fig. 4).

Next, we investigated whether the Ist2 L942Q dots correspond to aggregated protein. Expression of YFP-Ist2 L942Q for 3 hours resulted in a 1.7-fold upregulation of Kar2, whereas expression of wild-type YFP-Ist2 had no effect on Kar2 levels (supplementary material Fig. S10A,B). This suggests that an aggregation of YFP-Ist2 L942Q might cause the observed trapping at the ER. However, antibody staining of endogenous Kar2 in cells expressing mCherry-Ist2 L942Q did not result in a massive recruitment of Kar2 to these structures (supplementary material Fig. S10C,D).

Mutations of single leucines into less hydrophobic and bulky residues in *sec23-1* cells at 25°C led to a punctuated accumulation at specific ER domains. At 37°C, most of these punctuated structures were dissolved, and we observed a slight accumulation at intracellular ER structures (supplementary material Figs S5 and S6). Is the observed disappearance of punctuated Ist2 at 37°C just a matter of protein concentration or is it a temperature- and energy-dependent effect? To exclude a temperature- and energy-dependent effect? To exclude a temperature- and energy-dependent effect on protein concentration, we induced the expression of Ist2 L942V at 25°C for 120 minutes, stopped new transcription of *IST2* mRNA by the addition of glucose and kept the cells at 25°C or 37°C (supplementary material Fig. S11). After 60 minutes in glucose at 25°C, most cells maintained one to two Ist2 L942V dots, whereas most of these dots disappeared at 37°C. This mobilisation of trapped Ist2 was reduced in ATP-depleted cells poisoned with 10 mM sodium azide, indicating that higher temperatures mobilise trapped Ist2 L942V in an energy-dependent manner.

Hydrophobic residues function as part of an amphipathic α -helix

We identified a L939P mutation as a third category of mutations causing intracellular accumulations of Ist2. If the hydrophobic residues L938, L939 and L942 function as part of an amphipathic α -helix, the introduction of a helix-breaking proline is expected to abolish the function of this amphipathic α -helix. All four leucines in the K/L sequence are predicted to locate on one side of an amphipathic α -helix as illustrated by a helical wheel projection (Fig. 5). According to the prediction program 'AmphipaSeek', this short amphipathic α -helix comprises residues K936 to L946 (Sapay et al., 2006). The four hydrophobic side chains of L938, L939, L942

and L946 will be located within an angle of 120 degrees in the helix. According to the Ist2 sequence of *Ashbya gossypii* (Fig. 2B), we inserted three extra residues (alanines) after position L938. This insertion added one extra helical turn without changing the hydrophobic patch and had no effect on the localisation of Ist2 (Fig. 5A). Similarly, an insertion of four alanines after position G937 resulting in an arrangement of leucines as in wild-type Ist2, had no effect. To test whether the concentration of hydrophobic residues at one side of the helix is required for Ist2 trafficking, we changed the distribution of hydrophobic side chains. As seen in the helical projection, a mutation of LLxxL to LxxLL inserted a positive residue in the hydrophobic patch. This caused an accumulation in dots at 25°C and weak trapping at the proliferated ER at 37°C (Fig. 5B). Such an arrangement of hydrophobic residues exists in the Ist2 sequences of *Candida guilliermondii* and other more distantly related yeast species (Fig. 2B). Additional spreading of the leucine residues by insertion of one or two alanines between K941 and L942 had a stronger effect with a more pronounced accumulation at proliferated ER at 37°C.

In summary, it is possible to add at least one extra loop to the α -helical structure without losing its function for trafficking of Ist2 to the cell periphery, as long as there is no disturbance in the hydrophobicity of side chains and the hydrophobic and basic residues are positioned of two opposite sides of an α -helix. To validate whether the extreme C-terminus of Ist2 forms is indeed an α -helix, we determined the secondary structure of a peptide encoding the last 14 residues of Ist2, starting with K933. We performed secondary structure determination with this peptide by circular dichroism (CD) spectroscopy. In aqueous solution (potassium phosphate buffer), the CD spectrum suggested a random

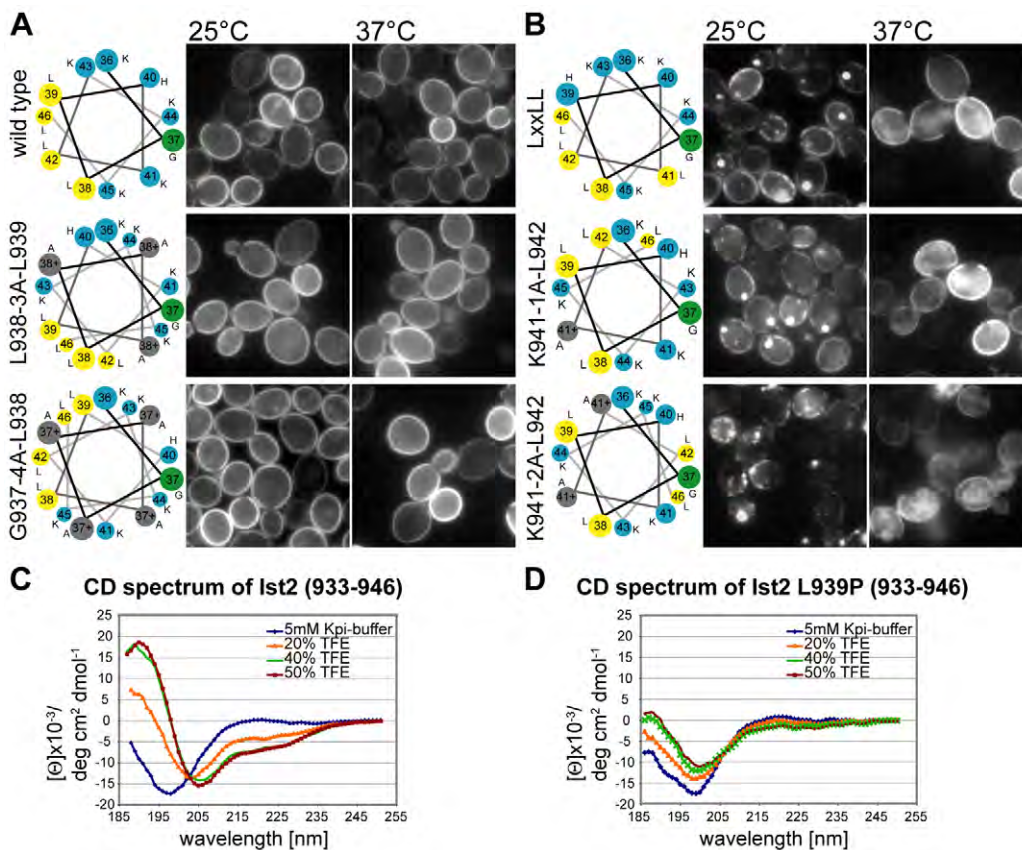


Fig. 5. Hydrophobic residues of the Ist2 sorting signal function as an amphipathic α -helix. (A) Presentation of residues K936-L946 as helical wheel projection. Hydrophobic leucines are marked in yellow, basic residues in blue, glycine in green and inserted alanines in grey. Depicted are wild-type Ist2, a mutant with an insertion of three alanines after position L938 and a mutant with insertion of four alanines after position G937. (B) Ist2 mutants with an exchange in the order of the leucine residues resulting in LxxLL and with an insertion of one or two alanines after position K941. The expression of the constructs in A and B was induced in *sec23-1* cells for 120 minutes with galactose at 25°C or 37°C. (C,D) Secondary structure determination of the Ist2 933-946 peptide (C) and Ist2 L939P 933-946 peptide (D) by CD in 5 mM potassium phosphate buffer or in 20%, 40% and 50% TFE buffered with 5 mM potassium phosphate, respectively. The given spectra are the means of five measurements.

coil conformation (Fig. 5C, blue curve). When solved in increasing concentrations of trifluoroethanol (TFE), we recorded a conversion from a disordered state into an α -helical structure at 20% (v/v) TFE. At 40% and 50% TFE, a maximal conversion into an α -helical structure was reached, compared with reference spectra (Chen et al., 1974). However, a rough estimation of the α -helical content for the K933-L946 peptide in 50% (v/v) TFE suggested that parts of the peptide remained unstructured. To confirm that this partially α -helical conformation is required for sorting to the periphery, we tested the secondary structure of a K933-L946 peptide with a L939P mutation, which we had identified in our initial screen (Fig. 2B). In *sec23-1* cells, newly synthesised Ist2 L939P accumulated at dot-like intracellular ER structures (supplementary material Fig. S12). The presence of a proline at this position abolished the TFE-induced partial conversion into an α -helical structure, supporting the idea that the C-terminus of the Ist2-sorting signal forms an amphipathic α -helix.

The Ist2 sorting signal interacts with membranes

Since many examples are known where basic sequences and amphipathic α -helices mediate membrane binding (Ford et al., 2002; Heo et al., 2006; Lee et al., 2005), we wondered whether the Ist2 sorting signal, which lacks a transmembrane domain, shows any direct interactions with membranes. Therefore, we expressed a fusion of GFP with the last 69 residues of Ist2 in *ist2* Δ cells. Compared with GFP, which localised at the cytosol and the nucleus, some of the GFP-Ist2 (878-946) accumulated at the entire cell periphery. Compared with the patch-like staining of full-length GFP-Ist2, GFP-Ist2 (878-946) showed a smooth rim staining (Fig. 6A), suggesting that the Ist2 sorting signal binds to the plasma membrane. In addition, large amounts of GFP-Ist2 (878-946) were seen in the cytosol and at the nucleolus (data not shown). The association of the Ist2 sorting signal with the plasma membrane became more obvious after an induction of *GALI*-driven GFP-Ist2 (878-946) synthesis followed by 8 hours of repression (Fig. 6B). When attached to the C-terminus of a minimal integral ER membrane protein comprising luminal YFP and the first transmembrane domain from Sec63, the Ist2 sorting signal targeted the vast majority of this reporter to the cell periphery, whereas the same reporter without Ist2 sorting signal showed a strong accumulation at the perinuclear ER (supplementary material Fig. S13).

Cell fractionation of yeast cells expressing GFP and GFP-Ist2 (878-946) showed a binding of some GFP-Ist2 (878-946) to membranes, whereas all GFP remained in the supernatant (Fig. 6C). A floatation of the majority of GFP-Ist2 (878-946) from the bottom of a sucrose-step gradient into lighter fractions confirmed the membrane association of GFP-Ist2 (878-946) (supplementary material Fig. S14A). As marker for the floatation of membranes we used the ER protein Sec61. This association of GFP-Ist2 (878-946) with membranes was abolished by 500 mM potassium acetate, demonstrating an electrostatic interaction between the Ist2 sorting signal and membranes (supplementary material Fig. S14B).

Binding of the Ist2 sorting signal to membranes occurs independently of a protein receptor but requires lipids

We purified GFP-Ist2 (878-946) via an N-terminal His₆ tag from bacteria and reconstituted binding of GFP-Ist2 (878-946) to membranes isolated from *ist2* Δ cells. Similarly to the previous cell fractionation experiments, a significant amount of recombinant GFP-Ist2 (878-946) was found in the membrane fraction. Treatment of membranes with proteinase K before incubation with purified

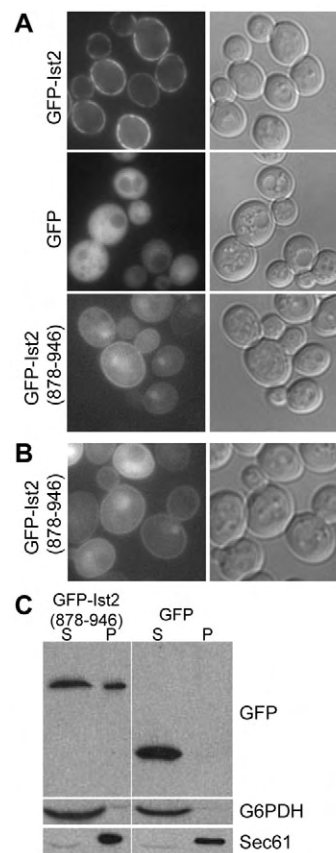


Fig. 6. The sorting signal of Ist2 binds to peripheral yeast membranes.

(A) Localisation of GFP-Ist2, GFP and GFP-Ist2 (878-946) under control of the *IST2* promoter in *ist2* Δ cells. (B) Localisation of *GALI*-induced GFP-Ist2 (878-946) in *ist2* Δ cells after addition of galactose for 3 hours and further incubation for 8 hours in glucose. (C) Supernatant and 25,000 g membrane pellet of *ist2* Δ cells expressing GFP or GFP-Ist2 (878-946) under the control of the *IST2* promoter. Proteins from 1 OD₆₀₀ unit supernatant (S) and pellet (P) were analysed by western blotting with antibodies against GFP, G6PDH and Sec61.

GFP-Ist2 (878-946) had no influence on this binding (Fig. 7A), indicating that lipids, but not proteins, are essential for the interaction between the Ist2 sorting signal and membranes. To confirm an interaction between the Ist2 sorting signal and lipids, we prepared artificial liposomes with an average diameter of 200 nm from a lipid mixture resembling the plasma membrane. Incubation of liposomes with 15 μ g purified GFP and GFP-Ist2 (878-946), and recovery of liposomes by centrifugation showed that 30.5% of GFP-Ist2 (878-946) was found in the pellet fraction, whereas GFP remained in the supernatant (Fig. 7B). According to a recently published procedure (Temmerman and Nickel, 2009), we measured the liposome-bound GFP fluorescence by FACS. Rhodamine-phosphatidylethanolamine-labelled liposomes were sorted into the red channel of a FACS and the amount of GFP fluorescence was determined. The GFP fluorescence of GFP-Ist2 (878-946) bound to liposomes was set to 100 (Fig. 7C). Mutation of the hydrophobic residues resulted in a 2.5- to 5-fold reduction of binding with the strongest effect caused by the L939P mutation. Compared with this moderate loss of binding to liposomes, mutation of the first basic cluster to alanines and the rearrangement of basic and hydrophobic residues in the amphipathic α -helix had a much more severe effect.

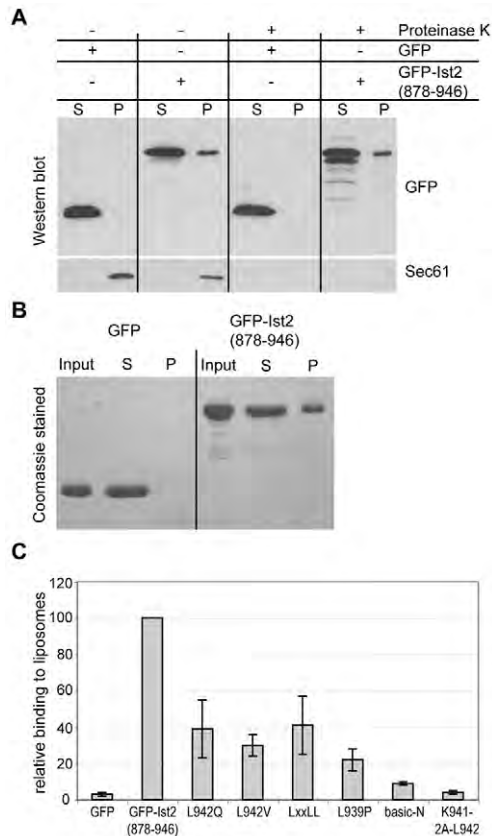


Fig. 7. The sorting signal of Ist2 binds to lipids. (A) Pellet fraction of 25,000 g membranes of *ist2Δ* cells was treated either with buffer or proteinase K and incubated with recombinant GFP or GFP-Ist2 (878-946). The reactions were separated into supernatant and pellet fraction, analysed by western blotting with antibodies against GFP and Sec61. (B) Binding of recombinant GFP and GFP-Ist2 (878-946) to liposomes. Liposomes were incubated with 15 μg recombinant protein in 100 μl buffer and fractionated into supernatant and pellet. (C) Binding of recombinant GFP, GFP-Ist2 (878-946) and different mutants of GFP-Ist2 (878-946) to liposomes. Liposomes were incubated with 15 μg recombinant protein in 100 μl buffer, sorted via flow cytometry and GFP fluorescence was detected. The relative GFP fluorescence of GFP-Ist2 (878-946) bound to liposomes was set to 100. Values are means ± s.d.

Considered together, these data suggest that basic residues of the Ist2 sorting signal are involved in an electrostatic interaction between the Ist2 sorting signal and lipids at the plasma membrane, and that these interactions trap Ist2 at sites of the cortical ER adjacent to the plasma membrane.

Discussion

We identified a sorting signal responsible for the rapid transport of Ist2 from the general ER to specific domains of the cortical ER. A certain fraction of wild-type Ist2 was detected by immunofluorescence at the perinuclear ER for a short period and was transported to the cell periphery within minutes. This transport was faster than the maturation of fluorescence proteins. In living cells the detection of fluorescent-protein-tagged wild-type Ist2 was limited to peripheral membranes without any apparent accumulation at perinuclear or tubular ER or at any other intracellular structures. This was observed under all tested conditions [strong induction by the *GALI* promoter at temperatures between 16°C (not shown) and 37°C in wild-type and *sec23-1* cells]. When expressed as a soluble

GFP-fusion in *ist2Δ* yeast cells, the Ist2 sorting signal partially accumulated in a smooth peripheral pattern, suggesting that this sequence interacts directly with the plasma membrane. Since the cortical ER is in close proximity to the plasma membrane at many positions (Perktold et al., 2007; Pichler et al., 2001; Preuss et al., 1991), we suggest that the sorting signal of ER-located Ist2 can bridge the distance between these two membranes.

In vitro reconstitution experiments with purified Ist2 sorting signal and either protease-treated yeast membranes or liposomes confirmed direct binding of the Ist2 sorting signal to lipids. Cell fractionation experiments showed that this interaction is electrostatic, which is consistent with the idea that basic residues of the Ist2 sorting signal interact with negatively charged lipids. Based on the combination of the mutational analysis of the Ist2 sorting signal and the in vitro reconstitution experiments, we suggest that a certain arrangement of a number of lysine residues at the C-terminus of the Ist2 sorting signal creates a surface for the binding of lipids located in the plasma membrane.

Mutation of a cluster of basic residues located N-terminal of the predicted amphipathic α -helix (K931A/K933A/H934A/K935A/K936A) caused a weak perinuclear accumulation of Ist2. Since Ist2 with this mutation is a stable protein, we explain the observed perinuclear localisation with a loss of binding to negatively charged lipids at the plasma membrane. The highly abundant, negatively charged head groups of phosphatidylserine and phosphatidylinositol-4,5-bisphosphate at the cytoplasmic side of the plasma membrane are strong candidates for direct interaction with the Ist2 sorting signal (Behnia and Munro, 2005; McLaughlin et al., 2002).

Additionally, the mutational analysis of the Ist2 sorting signal revealed that an arrangement of the hydrophobic positions L938, L939 and L942 at one side of the amphipathic α -helix is also required for sorting of Ist2. The observed partial transition of an Ist2 peptide from an unstructured sequence into an α -helix in the presence of TFE supports the idea that in a certain environment, for example, at membranes, the C-terminus of the Ist2 sorting signal forms a short three-turn α -helix. Although the precise effect of TFE on peptides remains unclear, it is suggested that TFE mimics certain biophysical properties of a membrane environment (Sonnichsen et al., 1992). Single mutation of L938, L939 or L942 led to a punctuated accumulation of Ist2 at the perinuclear, tubular and cortical ER. High expression and low temperature increased the punctuated accumulation of these Ist2 alleles. Accumulation of these Ist2 alleles at distinct sites distributed over the entire ER might be a consequence of misfolding of the Ist2 sorting signal, which results in a local expansion of the ER and the recruitment of a large subset of ER proteins. This is consistent with the moderate upregulation of Kar2, which is a consequence of the unfolded protein response (Normington et al., 1989). However, a severe misfolding of the Ist2 sorting signal seems unlikely, because energy and elevated temperature dissolved most of the Ist2 L942V accumulations, Ist2 L942Q dots showed no massive recruitment of Kar2, and the majority of Ist2 L942Q cofractionated with ER and plasma membrane markers on sucrose density gradients. Compared with the exchange of lysine residues to alanines and the structural changes of the amphipathic α -helices, the loss of hydrophobic positions had only a moderate effect on the binding of the Ist2 sorting signal to lipids, but caused a severe accumulation at specific domains of perinuclear, tubular and cortical ER.

Since our previous work has shown that a multimerisation domain could replace the N-terminal part of the Ist2 sorting signal (residues

878-928) (Franz et al., 2007), it is likely that the Ist2 sorting signal adopts a specific structure and functions in a multimeric state. In such a scenario, the hydrophobic positions of two or more amphipathic α -helices might form a hydrophobic interface, which leads to proper positioning of lysine residues for multivalent binding to negatively charged lipids. The observation that mutations in hydrophobic residues caused punctuated accumulations at all sites of the ER, and not only at the cortical ER, favours this model. Alternatively, a penetration of the hydrophobic residues into the acyl chain core of membranes might lead to bending of the plasma membrane towards the associated cortical ER (McMahon and Gallop, 2005). In a very speculative model, this might drive a transient fusion of cortical ER and plasma membrane. Thereby, Ist2 could reach the cell surface by diffusion. The observed increased sodium tolerance in cells without Ist2 protein (Entian et al., 1999) is consistent with such a postulated transient connection of ER and plasma membrane.

At this point, we cannot answer whether Ist2 is transported to ER-adjacent domains of the plasma membrane or whether Ist2 remains at a unique plasma-membrane-associated domain of the cortical ER. Our previous work showed that Ist2 is accessible for external proteases under conditions where other ER proteins remain undigested (Juschke et al., 2004; Juschke et al., 2005). However, an exclusive localisation at cortical ER and a direct interaction with specific domains of the plasma membrane might increase the sensitivity of Ist2 for digestion by external protease.

To our knowledge, the Ist2 sorting signal is the first signal described that mediates a rapid and efficient accumulation of integral membrane proteins at the yeast cortical ER via a direct interaction with lipids of the plasma membrane. This connection might lead to formation of a transient fusion pore, allowing the transfer of Ist2 from ER to plasma membrane. Alternatively, Ist2 might remain at domains of the cortical ER, where it could connect ER and plasma membrane to allow the direct exchange of molecules or information between these two membranes.

Materials and Methods

Yeast strains, media and plasmids

Preparation of media and yeast transformation was carried out as described (Juschke et al., 2005). All cells were grown to mid log phase. The strains MSY367 [*sec23-1*, *pGAL1-HXT1-CFP::TRP1* (Franz et al., 2007)] and CJY3 [*ist2Δ::HIS3MX6* (Juschke et al., 2004)] are isogenic derivatives of W303 (Thomas and Rothstein, 1989). BY4741 and its isogenic derivative JY3 (*ist2Δ::kanMX4*) were purchased from Euroscarf. Plasmids are described in supplementary material Table S3.

Sequences and alignments

The sequences refer to Ist2 from *S. cerevisiae* (P38250), *A. gossypii* (Q75B72) *S. bayanus* (6.143), *S. castelli* (718.21) (Byrne and Wolfe, 2005) and *C. guilliermondii* (PGUG_03099.1; <http://www.broad.mit.edu>). The alignments were based on ClustalW output (Chenna et al., 2003) that was manually edited in Genedoc version 2.6 to correct some obvious alignment errors.

Random mutagenesis and screening for mislocalised Ist2

To identify the residues in the C-terminal domain of Ist2 that are essential for sorting to the cell periphery, we constructed an integrative plasmid that contains 2205 nucleotides of the 3' of the *IST2* open reading frame followed by EYFP [in pPS1891 (Damelin and Silver, 2000)]. From this plasmid, we generated by error-prone PCR a library with mutations in the sequence encoding residues 787-942 of Ist2 and recombined these plasmids into the *IST2* locus of a BY4741 wild-type strain. Out of approximately 500 clones, 20 showed perinuclear and punctuated mislocalisation of Ist2-YFP. Sequencing revealed a clustering of mutations in the K/L sequence in clones that mislocalised.

Fluorescence microscopy

Yeast cells expressing constructs under *GAL1* control were grown overnight at 25°C in medium supplemented with 2% (w/v) raffinose. For induction, 2% galactose (w/v) was added. GFP-tagged constructs from Fig. 6, as well as all YFP- and CFP-tagged

constructs were visualised using an inverted microscope (Leica DM IRE2) equipped with a HCX PL APO CS $\times 100/1.4$ 0.7 oil-immersion objective (Leica), a camera (Hamamatsu ORCA-ER CCD) and the Openlab software package (Improvision). mCherry-tagged and all other GFP-tagged constructs were visualised using a wide-field epifluorescence microscope (Axio Imager.A1; Carl Zeiss MicroImaging) equipped with a plan-Fluar $\times 100/1.45$ oil-immersion objective (Carl Zeiss MicroImaging), a camera (Cascade:IK; Photometrics) and MetaMorph software (Universal Imaging). The following filters were used: YFP 510/20 nm (excitation) and 560/40 nm (emission), CFP 436/20 (excitation) and 480/40 nm (emission), GFP 470/40 (excitation) and 525/50 nm (emission) (Leica DM IRE2), mCherry 565/55 nm (excitation) and 650/75 nm (emission) and GFP 470/30 nm (excitation) and 515/30 nm (emission) (Axio Imager). All images were processed with Adobe Photoshop. All experiments were repeated at least three times and representative images are shown. The statistical analysis of the colocalisation data was performed using the program ImageJ (<http://rsb.info.nih.gov/ij/>) and the tool 'region of interest'. To determine the distance of the maximum signal intensities of two dots (e.g. an Ist2 dot and a dot from the Golgi marker Sed5), a line was drawn in the merge picture thereby connecting the two nearest dots in one cell. The distance of the two maxima was determined in pixels. To determine the distance of the maximum signal intensity of an Ist2 dot and the ER membrane (e.g. stained by Scs2), a line with 3 pixel line width was drawn in an angle of 90° relative to the ER membrane. Using 'plot profile', the maximum of the signal intensity was measured in both channels (red and green channel). Thereby, the distance of the maxima in pixel was determined. These analyses were performed in at least 100 cells per strain.

Indirect immunofluorescence

Yeast cells were grown to mid-log phase at 25°C in YEAP medium supplemented with 2% (w/v) raffinose. After induction for 40 minutes with 2% galactose (w/v), 100 μ g/ml cycloheximide (Sigma) was added and samples were fixed at the indicated time points with 2.7% (v/v) formaldehyde for 1 hour at 25°C. After incubation at 30°C for 10 minutes with 0.3% (v/v) β -mercaptoethanol in buffer B (1.2 M sorbitol in PBS), 0.9 mg/ml zymolyase 20T (Seikagaku, Tokyo, Japan) in buffer B was added for 30 minutes. The spheroblasts were spotted onto polylysine-coated slides, dehydrated in 70% (v/v) ethanol at -20°C, and permeabilised with 0.5% NP-40 (v/v). The slides were probed with antibodies against HA (1:1000, Berkeley Antibody Company), Ist2 (1:1000, affinity purified rabbit serum raised against GST-Ist2 residues 589-946), or Kar2 [1:500 (Frey et al., 2001)] in PBS with 1% (w/v) BSA for 2 hours, goat-anti-mouse Alexa Fluor 488 (1:400, Molecular Probes) or goat-anti-rabbit Alexa Fluor 488 (1:400, Molecular Probes) for 1 hour, and stained with 0.1 mg/ml 496-diamido-2-phenylindole dihydrochloride (DAPI). The slides were mounted with 80% (v/v) glycerol in PBS. For the classification of localisation, at least 100 cells from each of three independent experiments were analysed.

Generation of yeast cell extracts and western blotting

Denaturing cell lysis and fractionation of yeast cells in supernatant and 25,000 g pellet were done as described (Franz et al., 2007; Frey et al., 2001). For fractionation, we used yeast lysis buffer [20 mM HEPES-KOH pH 7.6, 250 mM potassium acetate, 5 mM magnesium acetate, 1 mM EDTA, 1 mM DTT, 0.1 mM PMSF, Complete protease inhibitor (Roche)]. Western blotting was performed using antibodies against HA- (1:3000), Tub2- (1:500, rabbit serum raised against GST-Tub2 residues 407-457, gift from Elmar Schiebel, ZMBH, Heidelberg, Germany), GFP (1:20,000, affinity-purified rabbit serum raised against GFP, gift from Dirk Görlich, Max-Planck-Institute for Biophysical Chemistry, Göttingen, Germany), Ist2 (1:25,000), Sec61- [1:7500 (Frey et al., 2001)], Kar2 [1:20,000 (Frey et al., 2001)], Emp47 [1:5000, gift from Howard Riezman, University of Geneva, Switzerland (Schroder et al., 1995)] or glucose-6-phosphate dehydrogenase (G6PDH, 1:35,000, Sigma). For quantification of protein bands from western blots and Coomassie-blue-stained gels, the exposed blot or the stained gel were scanned followed by picture processing using the ImageJ software.

Cell fractionation by sucrose density centrifugation and flotation

ist2Δ cells constitutively expressing either Pma1-GFP, Sed5-GFP or Sec13-GFP were grown in selective medium containing 2% (w/v) raffinose. Expression of mCherry-Ist2 L942Q was induced by the addition of 2% (w/v) galactose for 2 hours. Cells from 10 OD₆₀₀ units were then treated with 10 mM Na₃N and NaF for 10 minutes, harvested, washed and resuspended in 1 ml of a buffer containing 10% (w/v) sucrose, 10 mM Tris-HCl pH 7.6, 5 mM MgCl₂ and Complete protease inhibitor (Roche). After lysis on ice with glass beads, the lysate was centrifuged (500 g, 10 minutes, 4°C) followed by another centrifugation (1200 g, 2 minutes, 4°C). 700 μ l of the supernatants were loaded on a 20-60% linear sucrose gradient (buffered with 10 mM Tris-HCl pH 7.6 and 5 mM MgCl₂). After centrifugation (100,000 g, 16 hours, 4°C) in an SW40-Rotor (Beckman), fractions were collected from the top. For flotation, a 25,000 g pellet of 100 OD₆₀₀ yeast cells was resuspended in 2 M sucrose in yeast lysis buffer, overlaid with a sucrose step gradient (see supplementary material Fig. S14), applied to ultracentrifugation (Beckman SW60-Rotor, 50,000 r.p.m., 16 hours, 4°C) and equal fractions were collected from top to bottom.

Peptide synthesis and CD spectroscopy

The peptide corresponding to residues 933-946 from wild-type Ist2 or mutant Ist2 L939P were obtained from Peptide Speciality Laboratories (Heidelberg, Germany). The amount of peptide was determined by weighing the yield of peptide synthesis on a micro scale. CD spectra were recorded on a Jasco J-715 spectropolarimeter using a bandwidth of 0.5 nm and a scanning speed of 200 nm per minute. The instrument was calibrated with (1S)-(-)-10-camphorsulfonic acid. Measurements were carried out at 25°C using a 0.1 cm path length quartz cuvette, with a peptide concentration of 150 µM in 5 mM potassium phosphate buffer at pH 7.6. Spectral units were transformed into molar ellipticity per residue.

Protein purification

Recombinant GFP and GFP-fusion proteins were purified from BL21-*E. coli* using an N-terminal H₆-tag. Protein expression was induced at 30°C by adding 1 mM IPTG. After 2.5 hours the cells were harvested, resuspended in bacterial lysis buffer (50 mM Tris-HCl pH 7.5, 250 mM NaCl, 2 mM imidazol, 0.5 mM EDTA, 10 mM β-mercaptoethanol) and lysed with a homogeniser (EmulsiFlex C5, Avestin). After ultracentrifugation (Beckman 45 Ti rotor, 32,000 rpm, 45 minutes, 4°C) the supernatant was incubated for 1 hour at 4°C with Ni-NTA-beads (Qiagen), the beads were washed several times with lysis buffer and the protein was eluted by incubation for 3 hours with lysis buffer containing 500 mM imidazol. Eluted protein was dialysed against a buffer with 25 mM HEPES-KOH pH 7.4, 250 mM potassium acetate.

Binding to proteinase K-treated membranes

Yeast cells from 30 OD₆₀₀ units were fractionated into supernatant and pellet as described above, except the yeast lysis buffer contained 50 mM potassium acetate and no proteinase inhibitors. The pellet fraction was then treated either with buffer or 50 µg/ml proteinase K (Merck) for 30 minutes at 37°C, washed three times, incubated for 3 hours with 200 ng/ml recombinant GFP or GFP-Ist2 (878-946) and fractionated in supernatant and 25,000 g pellet.

Liposome generation and binding experiments

All lipids were purchased at Avanti Polar Lipids. Lipids including 1 mol% rhodamine-labeled phosphatidylethanolamine (16:0) were dissolved in chloroform and dried in a rotary evaporator yielding a homogenous dried lipid film. Liposomes, with a final lipid concentration of 4 mM, were generated by dissolving this film in an appropriate volume of HK buffer (25 mM HEPES, 150 mM KCl, pH 7.4) containing 10% (w/v) sucrose. This crude liposome mixture was subjected to ten freeze-thaw cycles followed by 21 size-extrusion steps through a filter with 1 µm pore size (Avanti Polar Lipids). Liposome size was analysed via light scattering (Zetasizer 1000 HS; Malvern Instruments) and liposome concentration was determined by rhodamine fluorescence. Plasma membrane like lipid mixtures according to (van Meer, 1998) consisted of 50 mol% cholesterol from ovine wool, 12.5 mol% phosphatidylcholine from bovine liver, 9 mol% phosphatidylethanolamine (bovine liver), 5 mol% phosphatidylserine from porcine brain, 5 mol% phosphatidylinositol from bovine liver, 12.5 mol% sphingomyelin from poultry eggs and 5 mol% phosphatidylinositol(4,5)-bisphosphate from porcine brain.

For liposome binding assays, 25 µl of 4 mM liposomes were blocked with 3% (w/v) fatty-acid-free BSA (Roche) in HK buffer for 1 hour (25°C), washed, and the liposome pellet (25,000 g, 15 minutes, 25°C) was incubated for 4 hours with 100 µl of recombinant protein at a final protein concentration of 150 µg/ml in HK buffer (25°C). To determine the amount of bound GFP-Ist2 (878-946) (Fig. 7B), the liposomes were spun down and pellet and supernatant fractions were stained with Coomassie blue. For flow cytometry analysis (Fig. 7C), liposomes were incubated with recombinant protein as described above, washed, resuspended in HK buffer and analysed via flow cytometry (Temmerman and Nickel, 2009). Liposomes were gated by size and rhodamine fluorescence and the GFP fluorescence from the bound recombinant proteins was detected. In all assays, the relative GFP fluorescence of GFP-Ist2 (878-946) bound to liposomes was arbitrarily set to 100. All measurements were performed at least three times. Error bars indicate the s.d.

We are grateful to E. Schiebel, H. Riezman and D. Goerlich for antibodies and B. Schwappach, C. Walch-Solimena, T. Levine and E. Schiebel for plasmids. We thank P. Eggensperger for helpful comments on the manuscript and B. Dobberstein for his generous support. This work was supported by grants from the Deutsche Forschungsgemeinschaft (SE 811/4-1/2, SE 811/5-1/2).

References

Aronov, S., Gelin-Licht, R., Zipor, G., Haim, L., Safran, E. and Gerst, J. E. (2007). mRNAs encoding polarity and exocytosis factors are cotransported with the cortical endoplasmic reticulum to the incipient bud in *Saccharomyces cerevisiae*. *Mol. Cell Biol.* **27**, 3441-3455.

Athenstaedt, K., Zwyetick, D., Jandrositz, A., Kohlwein, S. D. and Daum, G. (1999). Identification and characterization of major lipid particle proteins of the yeast *Saccharomyces cerevisiae*. *J. Bacteriol.* **181**, 6441-6448.

Basson, M. E., Thorsness, M. and Rine, J. (1986). *Saccharomyces cerevisiae* contains two functional genes encoding 3-hydroxy-3-methylglutaryl-coenzyme A reductase. *Proc. Natl. Acad. Sci. USA* **83**, 5563-5567.

Baumann, N. A., Sullivan, D. P., Ohvo-Rekila, H., Simonot, C., Pottekat, A., Klaassen, Z., Beh, C. T. and Menon, A. K. (2005). Transport of newly synthesized sterol to the sterol-enriched plasma membrane occurs via nonvesicular equilibration. *Biochemistry* **44**, 5816-5826.

Behnia, R. and Munro, S. (2005). Organelle identity and the signposts for membrane traffic. *Nature* **438**, 597-604.

Byrne, K. P. and Wolfe, K. H. (2005). The yeast gene order browser: combining curated homology and syntenic context reveals gene fate in polyploid species. *Genome Res.* **15**, 1456-1461.

Chen, Y. H., Yang, J. T. and Chau, K. H. (1974). Determination of the helix and beta form of proteins in aqueous solution by circular dichroism. *Biochemistry* **13**, 3350-3359.

Chenna, R., Sugawara, H., Koike, T., Lopez, R., Gibson, T. J., Higgins, D. G. and Thompson, J. D. (2003). Multiple sequence alignment with the Clustal series of programs. *Nucleic Acids Res.* **31**, 3497-3500.

Damelin, M. and Silver, P. A. (2000). Mapping interactions between nuclear transport factors in living cells reveals pathways through the nuclear pore complex. *Mol. Cell* **5**, 133-140.

Entian, K. D., Schuster, T., Hegemann, J. H., Becher, D., Feldmann, H., Guldener, U., Gotz, R., Hansen, M., Hollenberg, C. P., Jansen, G. et al. (1999). Functional analysis of 150 deletion mutants in *Saccharomyces cerevisiae* by a systematic approach. *Mol. Gen. Genet.* **262**, 683-702.

Ford, M. G., Mills, I. G., Peter, B. J., Vallis, Y., Praefcke, G. J., Evans, P. R. and McMahon, H. T. (2002). Curvature of clathrin-coated pits driven by epsin. *Nature* **419**, 361-366.

Franz, A., Maass, K. and Seedorf, M. (2007). A complex peptide-sorting signal, but no mRNA signal, is required for the Sec-independent transport of Ist2 from the yeast ER to the plasma membrane. *FEBS Lett.* **581**, 401-405.

Frey, S., Pool, M. and Seedorf, M. (2001). Scp160p, an RNA-binding, polysome-associated protein, localizes to the endoplasmic reticulum of *Saccharomyces cerevisiae* in a microtubule-dependent manner. *J. Biol. Chem.* **276**, 15905-15912.

Galindo, B. E. and Vacquier, V. D. (2005). Phylogeny of the TMEM16 protein family: some members are overexpressed in cancer. *Int. J. Mol. Med.* **16**, 919-924.

Heo, W. D., Inoue, T., Park, W. S., Kim, M. L., Park, B. O., Wandless, T. J. and Meyer, T. (2006). PI(3,4,5)P3 and PI(4,5)P2 lipid target proteins with polybasic clusters to the plasma membrane. *Science* **314**, 1458-1461.

Juschke, C., Ferring, D., Jansen, R. P. and Seedorf, M. (2004). A novel transport pathway for a yeast plasma membrane protein encoded by a localized mRNA. *Curr. Biol.* **14**, 406-411.

Juschke, C., Wachter, A., Schwappach, B. and Seedorf, M. (2005). SEC18/NSF-independent, protein-sorting pathway from the yeast cortical ER to the plasma membrane. *J. Cell Biol.* **169**, 613-622.

Kahana, J. A., Schnapp, B. J. and Silver, P. A. (1995). Kinetics of spindle pole body separation in budding yeast. *Proc. Natl. Acad. Sci. USA* **92**, 9707-9711.

Koning, A. J., Lum, P. Y., Williams, J. M. and Wright, R. (1993). DiOC6 staining reveals organelle structure and dynamics in living yeast cells. *Cell Motil. Cytoskeleton* **25**, 111-128.

Lee, M. C., Orci, L., Hamamoto, S., Futai, E., Ravazzola, M. and Schekman, R. (2005). Sar1p N-terminal helix initiates membrane curvature and completes the fission of a COPII vesicle. *Cell* **122**, 605-617.

Levine, T. and Loewen, C. (2006). Inter-organelle membrane contact sites: through a glass, darkly. *Curr. Opin. Cell Biol.* **18**, 371-378.

Loewen, C. J., Roy, A. and Levine, T. P. (2003). A conserved ER targeting motif in three families of lipid binding proteins and in Opi1p binds VAP. *EMBO J.* **22**, 2025-2035.

Loewen, C. J., Young, B. P., Tavassoli, S. and Levine, T. P. (2007). Inheritance of cortical ER in yeast is required for normal septin organization. *J. Cell Biol.* **179**, 467-483.

Luedeke, C., Frei, S. B., Sbalzarini, I., Schwarz, H., Spang, A. and Barral, Y. (2005). Septin-dependent compartmentalization of the endoplasmic reticulum during yeast polarized growth. *J. Cell Biol.* **169**, 897-908.

McLaughlin, S., Wang, J., Gambhir, A. and Murray, D. (2002). PIP(2) and proteins: interactions, organization, and information flow. *Annu. Rev. Biophys. Biomol. Struct.* **31**, 151-175.

McMahon, H. T. and Gallop, J. L. (2005). Membrane curvature and mechanisms of dynamic cell membrane remodelling. *Nature* **438**, 590-596.

Normington, K., Kohno, K., Kozutsumi, Y., Gething, M. J. and Sambrook, J. (1989). *S. cerevisiae* encodes an essential protein homologous in sequence and function to mammalian BiP. *Cell* **57**, 1223-1236.

Novick, P., Field, C. and Schekman, R. (1980). Identification of 23 complementation groups required for post-translational events in the yeast secretory pathway. *Cell* **21**, 205-215.

Perktold, A., Zechmann, B., Daum, G. and Zellnig, G. (2007). Organelle association visualized by three-dimensional ultrastructural imaging of the yeast cell. *FEMS Yeast Res.* **7**, 629-638.

Pichler, H., Gaigg, B., Hrstnik, C., Achleitner, G., Kohlwein, S. D., Zellnig, G., Perktold, A. and Daum, G. (2001). A subfraction of the yeast endoplasmic reticulum associates with the plasma membrane and has a high capacity to synthesize lipids. *Eur. J. Biochem.* **268**, 2351-2361.

Preuss, D., Mulholland, J., Kaiser, C. A., Orlean, P., Albright, C., Rose, M. D., Robbins, P. W. and Botstein, D. (1991). Structure of the yeast endoplasmic reticulum:

- localization of ER proteins using immunofluorescence and immunoelectron microscopy. *Yeast* **7**, 891-911.
- Prinz, W. A., Grzyb, L., Veenhuis, M., Kahana, J. A., Silver, P. A. and Rapoport, T. A.** (2000). Mutants affecting the structure of the cortical endoplasmic reticulum in *Saccharomyces cerevisiae*. *J. Cell Biol.* **150**, 461-474.
- Proszynski, T. J., Klemm, R. W., Gravert, M., Hsu, P. P., Gloor, Y., Wagner, J., Kozak, K., Grabner, H., Walzer, K., Bagnat, M. et al.** (2005). A genome-wide visual screen reveals a role for sphingolipids and ergosterol in cell surface delivery in yeast. *Proc. Natl. Acad. Sci. USA* **102**, 17981-17986.
- Raychaudhuri, S., Im, Y. J., Hurley, J. H. and Prinz, W. A.** (2006). Nonvesicular sterol movement from plasma membrane to ER requires oxysterol-binding protein-related proteins and phosphoinositides. *J. Cell Biol.* **173**, 107-119.
- Sapay, N., Guermeur, Y. and Deleage, G.** (2006). Prediction of amphipathic in-plane membrane anchors in monotopic proteins using a SVM classifier. *BMC Bioinformatics* **7**, 255.
- Schnabl, M., Daum, G. and Pichler, H.** (2005). Multiple lipid transport pathways to the plasma membrane in yeast. *Biochim. Biophys. Acta* **1687**, 130-140.
- Schroder, S., Schimmoller, F., Singer-Kruger, B. and Riezman, H.** (1995). The Golgi-localization of yeast Emp47p depends on its di-lysine motif but is not affected by the ret1-1 mutation in alpha-COP. *J. Cell Biol.* **131**, 895-912.
- Schwappach, B., Stobrawa, S., Hechenberger, M., Steinmeyer, K. and Jentsch, T. J.** (1998). Golgi localization and functionally important domains in the NH2 and COOH terminus of the yeast CLC putative chloride channel Gef1p. *J. Biol. Chem.* **273**, 15110-15118.
- Shepard, K. A., Gerber, A. P., Jambhekar, A., Takizawa, P. A., Brown, P. O., Herschlag, D., DeRisi, J. L. and Vale, R. D.** (2003). Widespread cytoplasmic mRNA transport in yeast: identification of 22 bud-localized transcripts using DNA microarray analysis. *Proc. Natl. Acad. Sci. USA* **100**, 11429-11434.
- Sonnichsen, F. D., Van Eyk, J. E., Hodges, R. S. and Sykes, B. D.** (1992). Effect of trifluoroethanol on protein secondary structure: an NMR and CD study using a synthetic actin peptide. *Biochemistry* **31**, 8790-8798.
- Takizawa, P. A., DeRisi, J. L., Wilhelm, J. E. and Vale, R. D.** (2000). Plasma membrane compartmentalization in yeast by messenger RNA transport and a septin diffusion barrier. *Science* **290**, 341-344.
- Temmerman, K. and Nickel W.** (2009). A novel flow cytometric assay to quantify interactions between proteins and membrane lipids. *J. Lipid Res.* Epub ahead of print.
- Thomas, B. J. and Rothstein, R.** (1989). Elevated recombination rates in transcriptionally active DNA. *Cell* **56**, 619-630.
- van Meer, G.** (1998). Lipids of the Golgi membrane. *Trends Cell Biol.* **8**, 29-33.
- Voeltz, G. K., Rolls, M. M. and Rapoport, T. A.** (2002). Structural organization of the endoplasmic reticulum. *EMBO Rep.* **3**, 944-950.
- Wilhovsky, S., Gardner, R. and Hampton, R.** (2000). HRD gene dependence of endoplasmic reticulum-associated degradation. *Mol. Biol. Cell* **11**, 1697-1708.

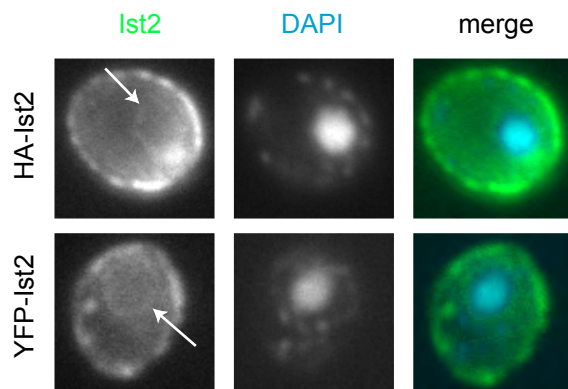


Fig. S1

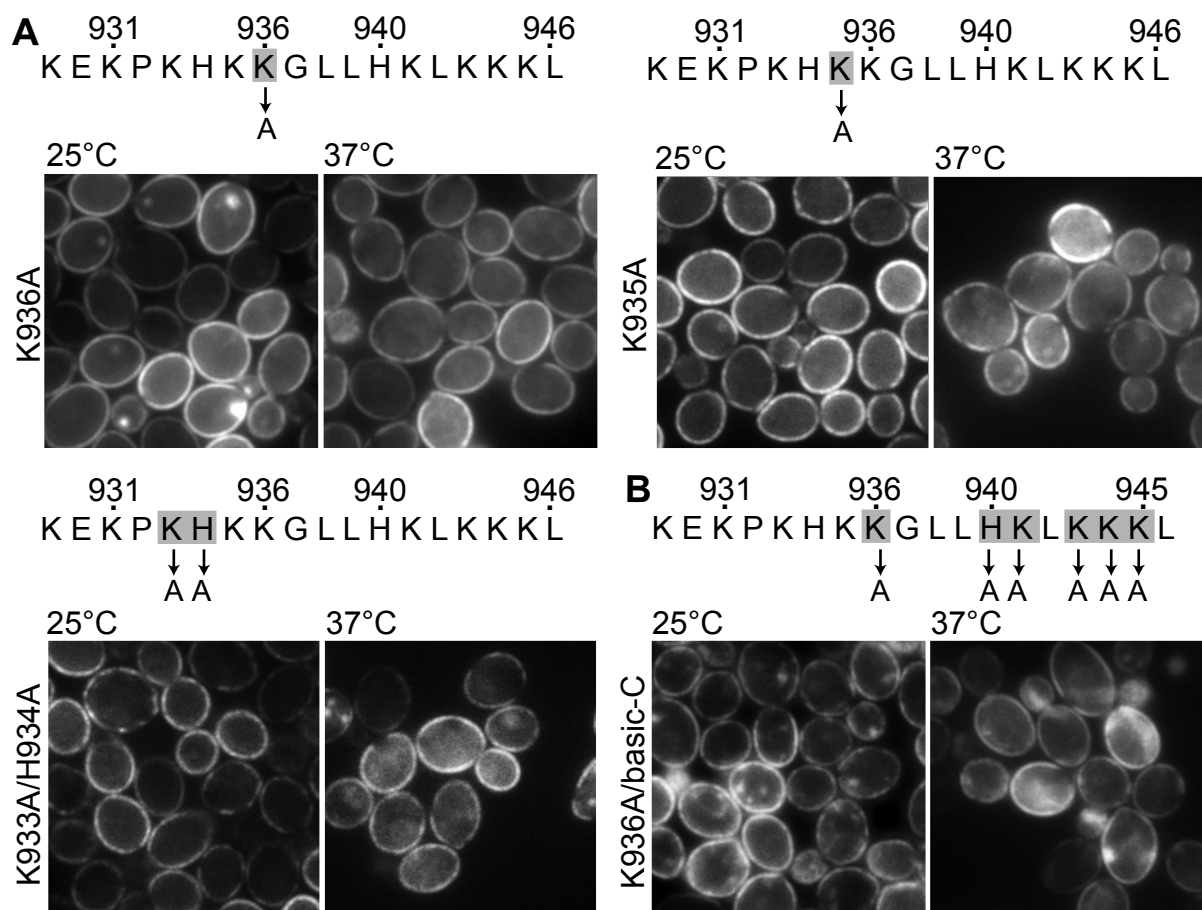


Fig. S2

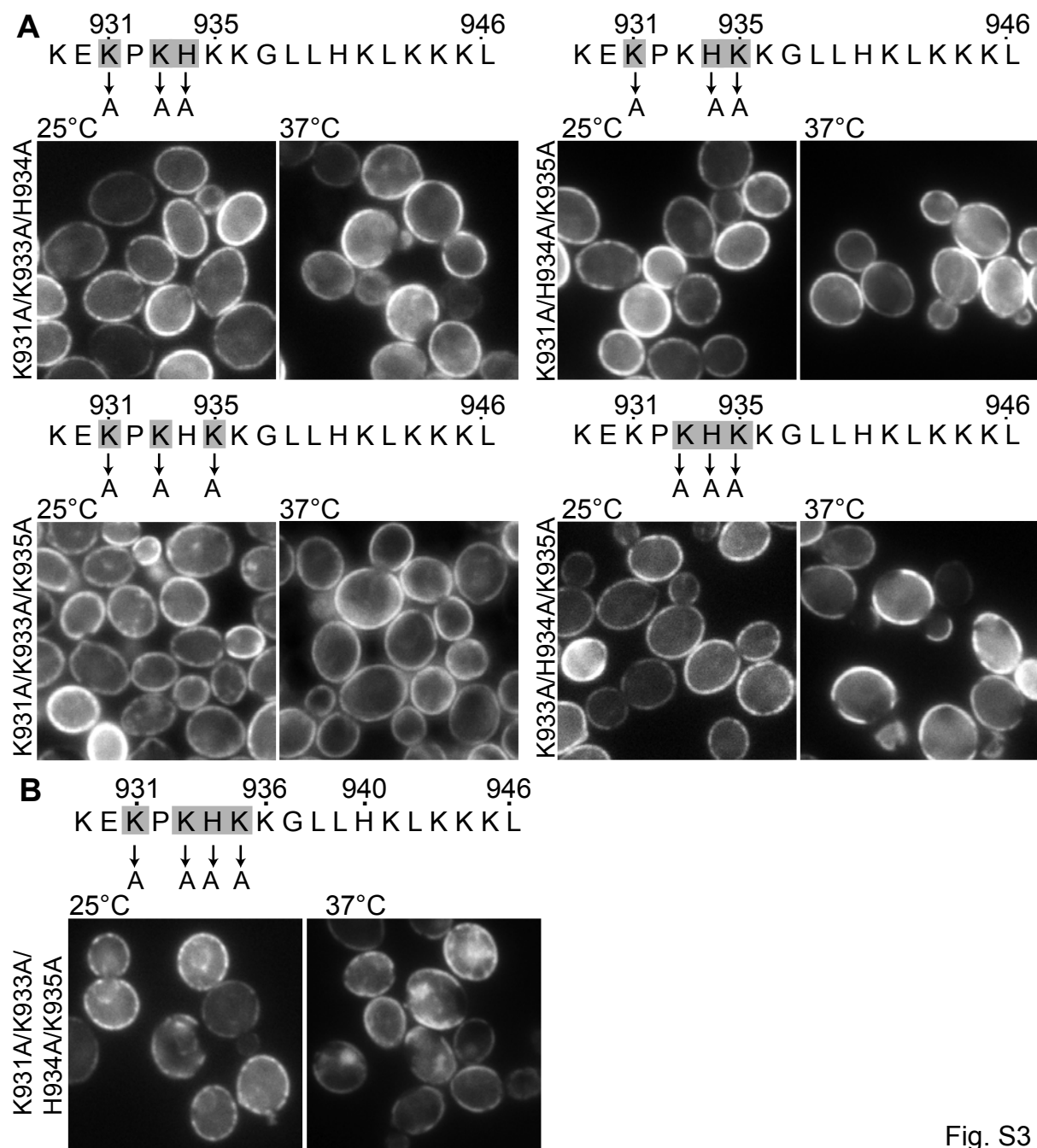


Fig. S3

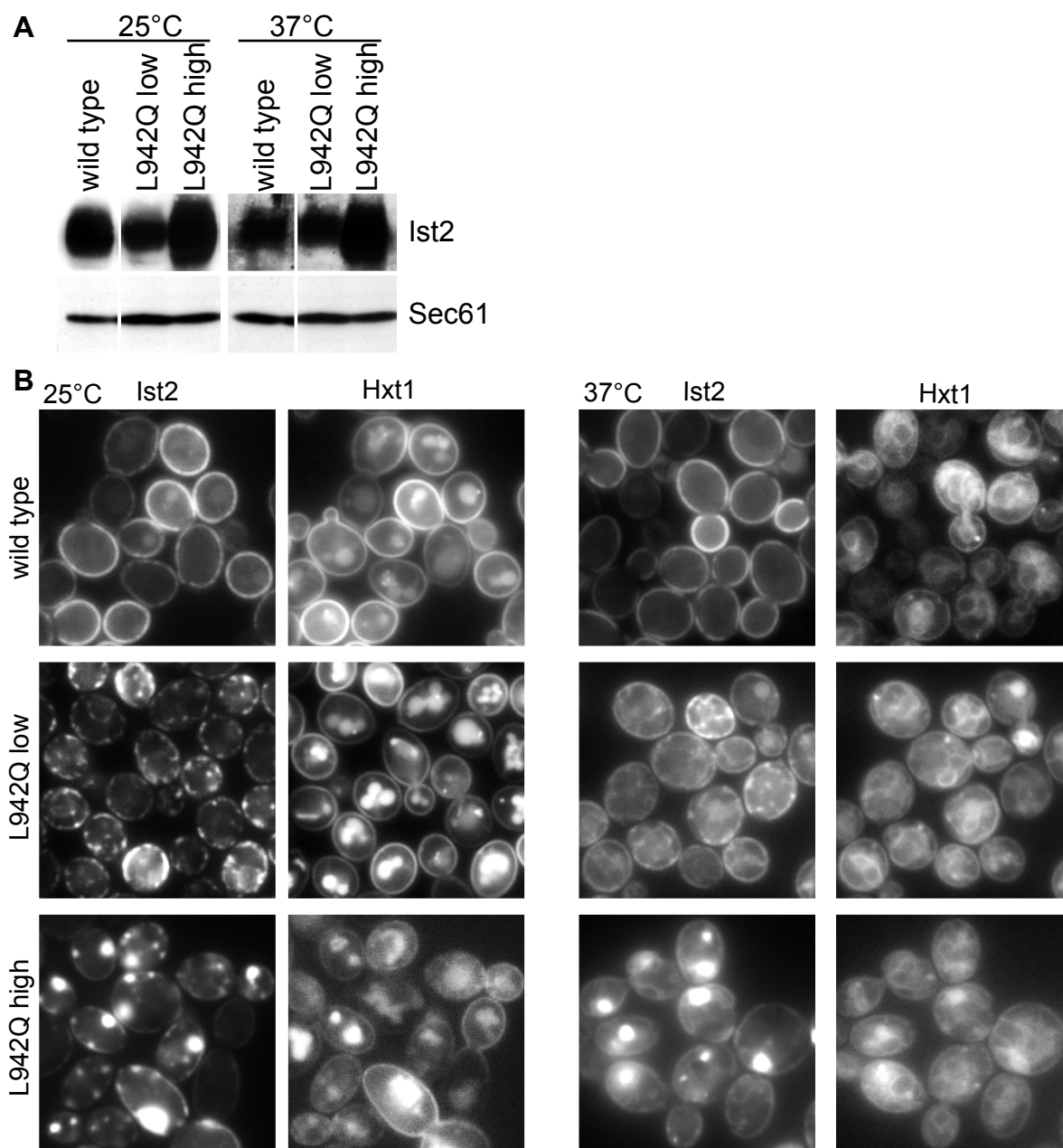


Fig. S4

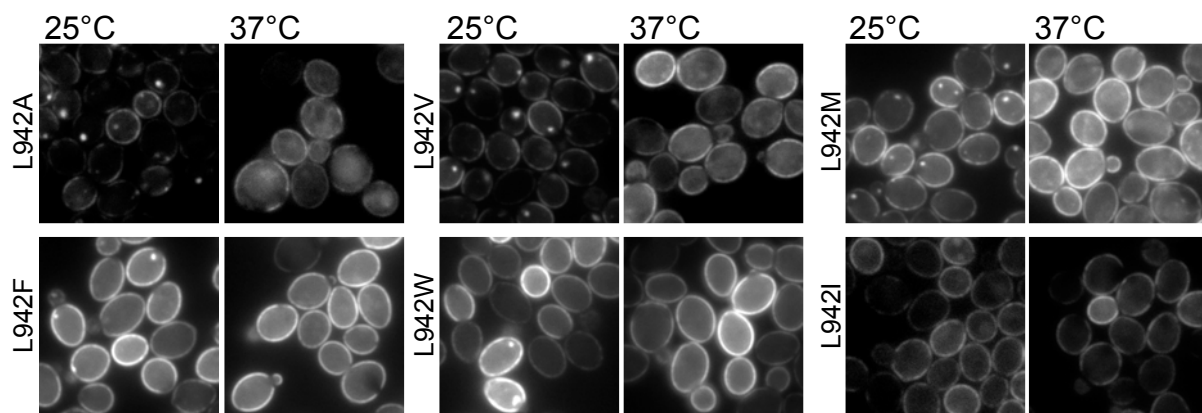


Fig. S5

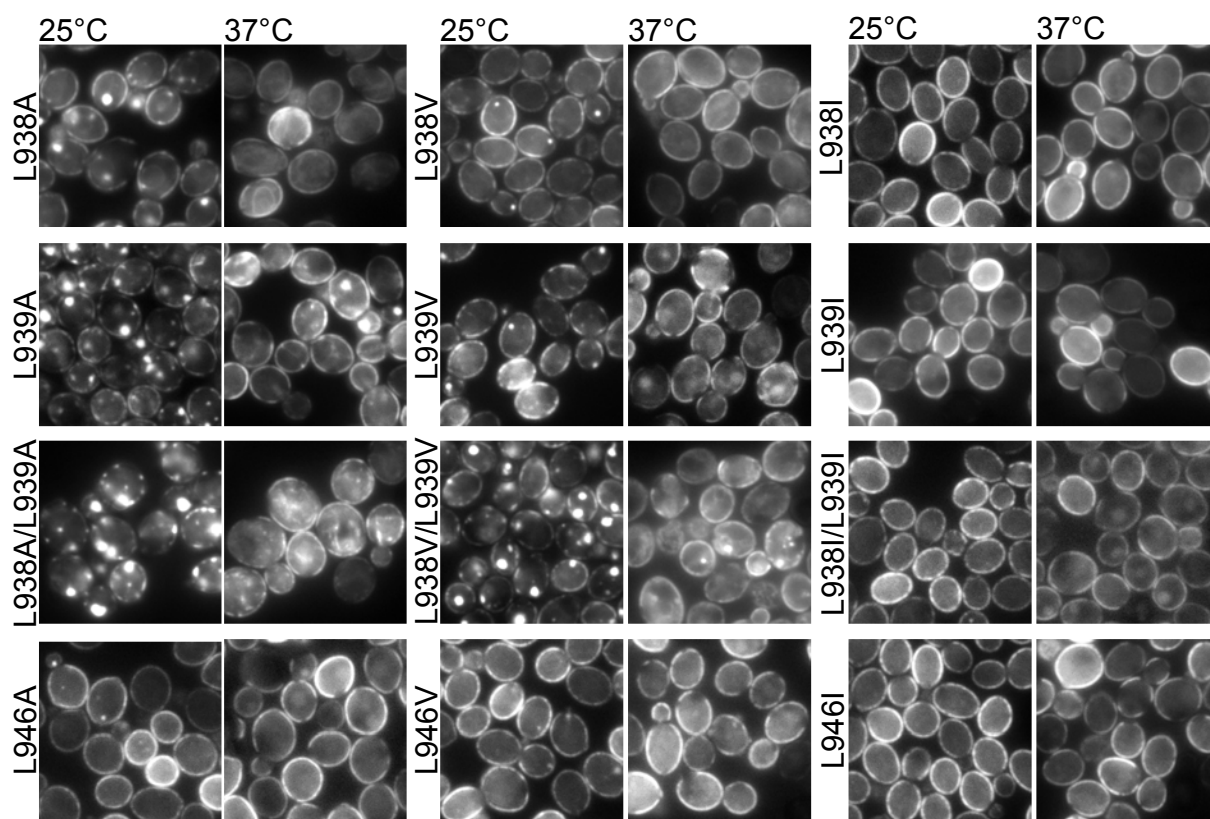


Fig. S6

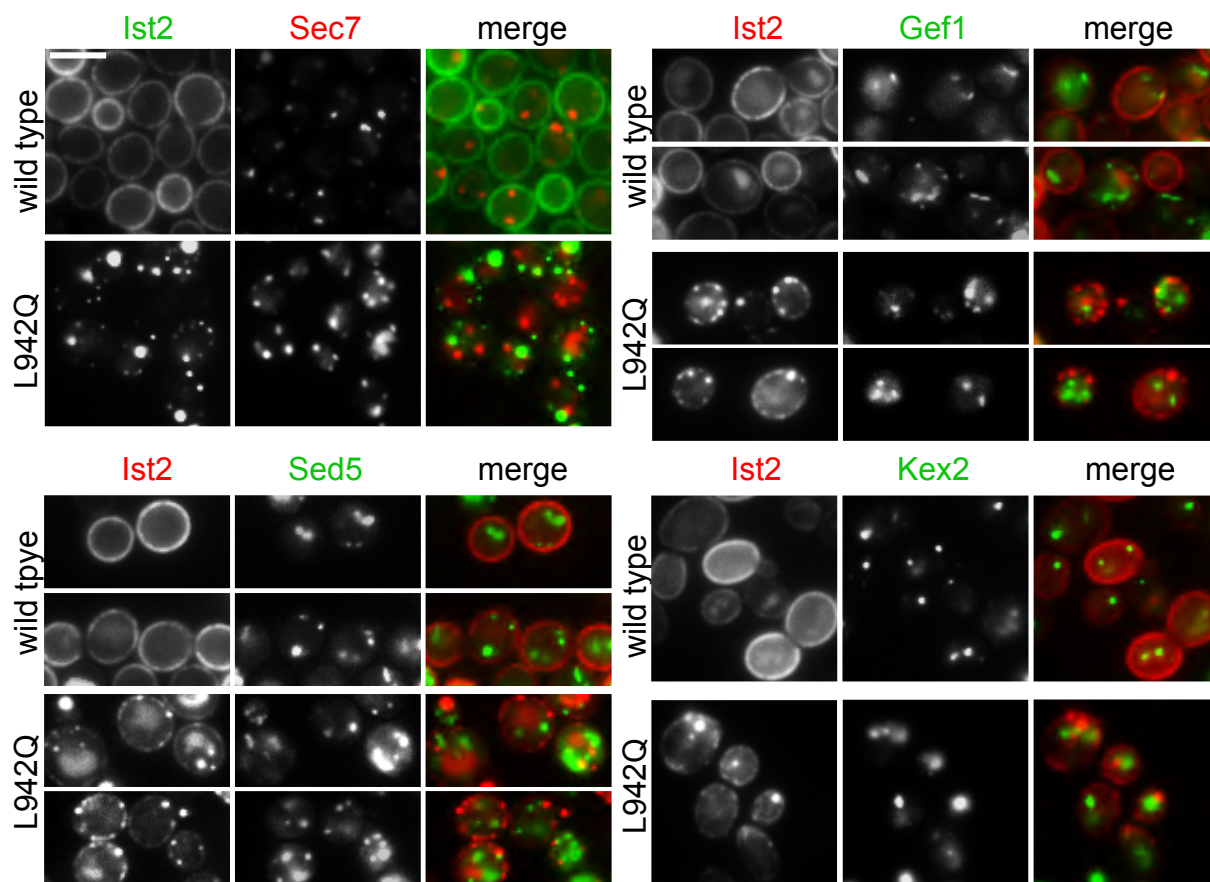


Fig. S7

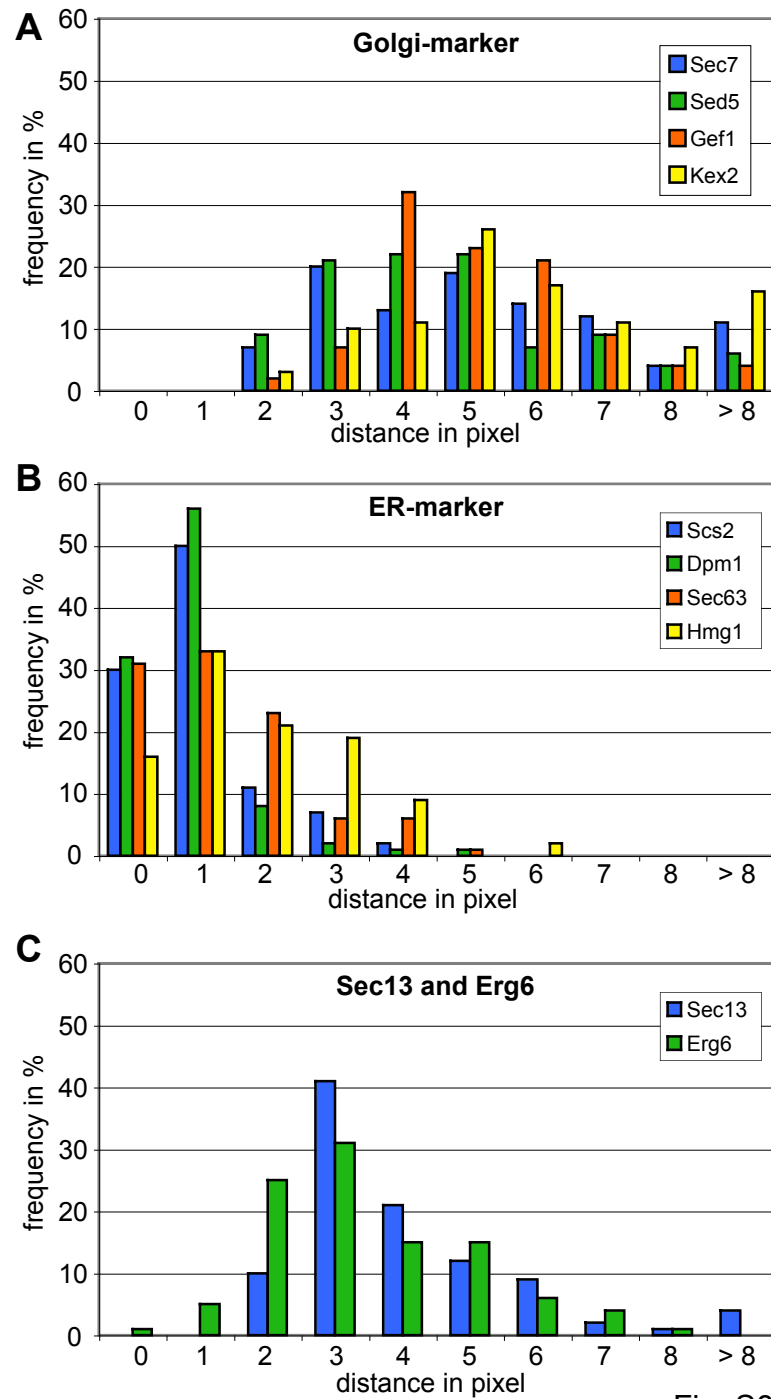
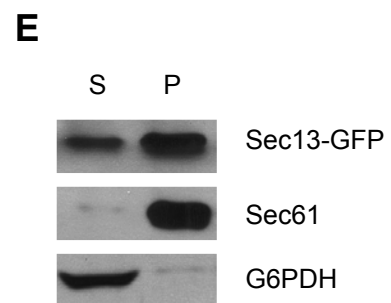
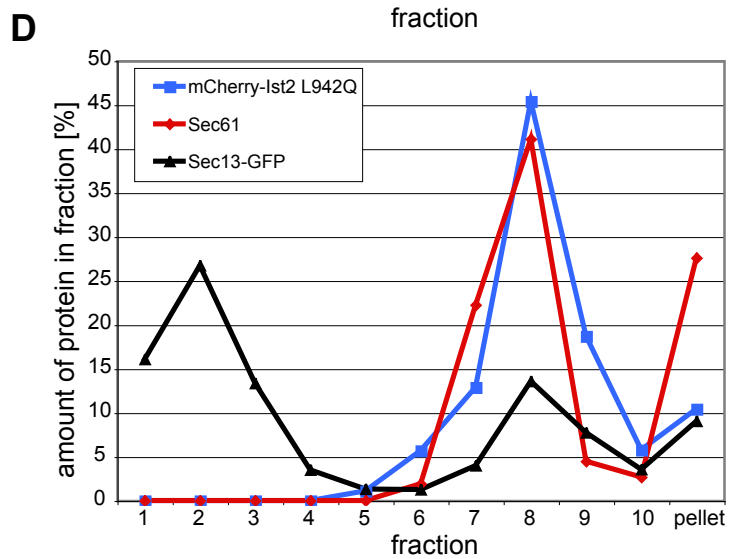
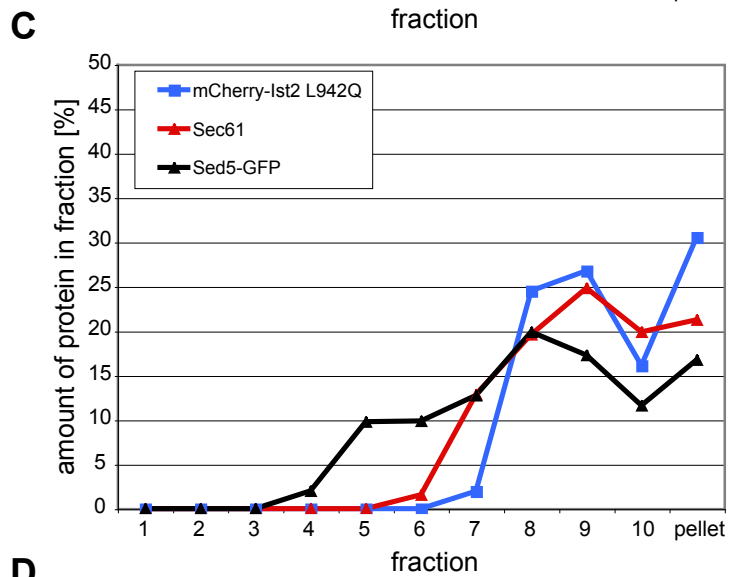
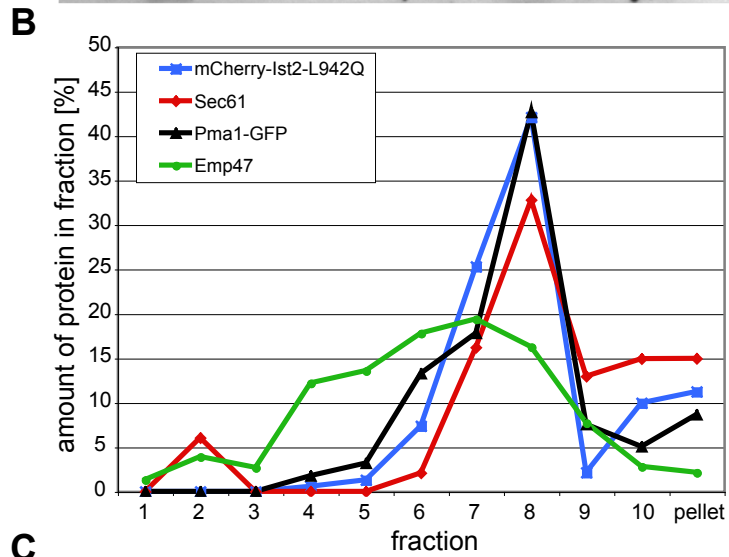
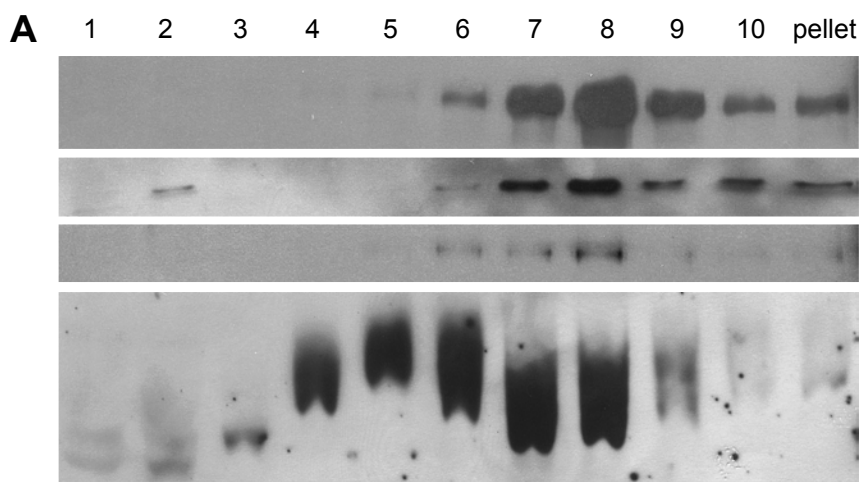


Fig. S8



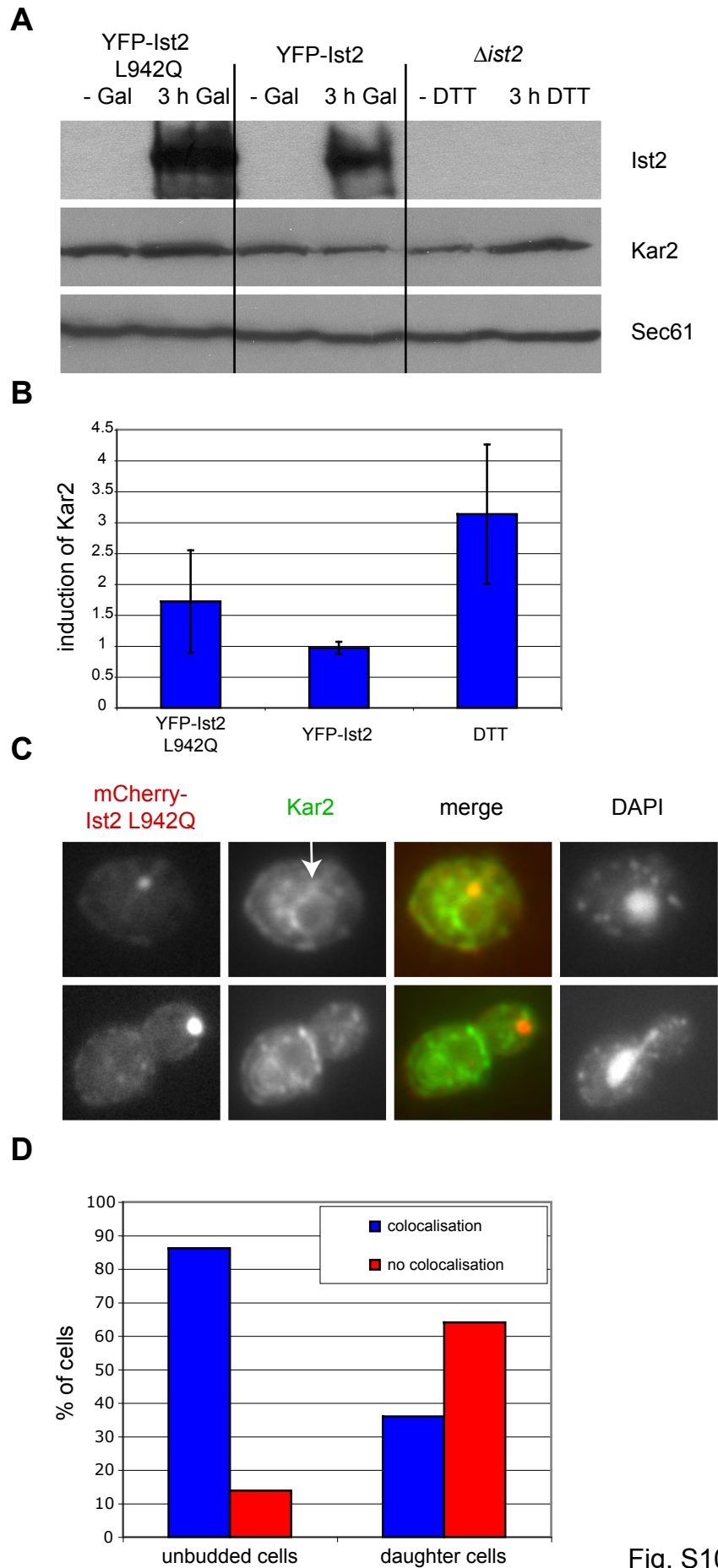


Fig. S10

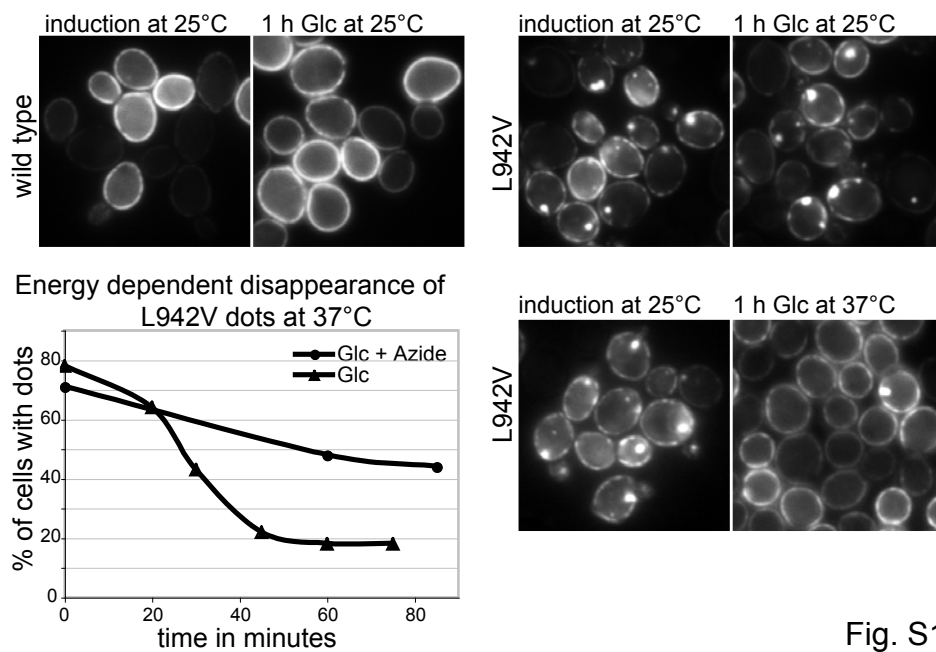


Fig. S11

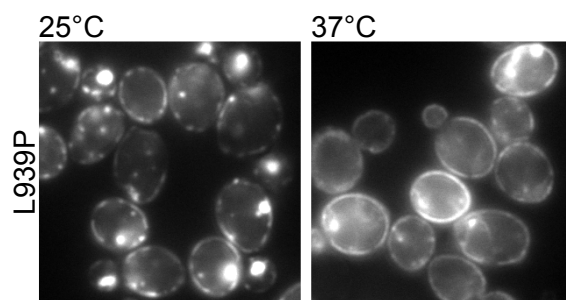


Fig. S12

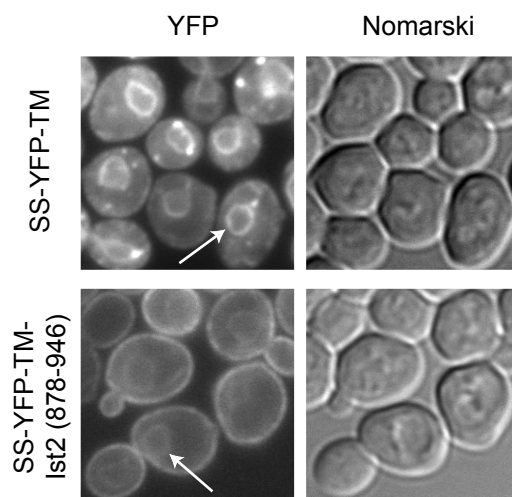


Fig. S13

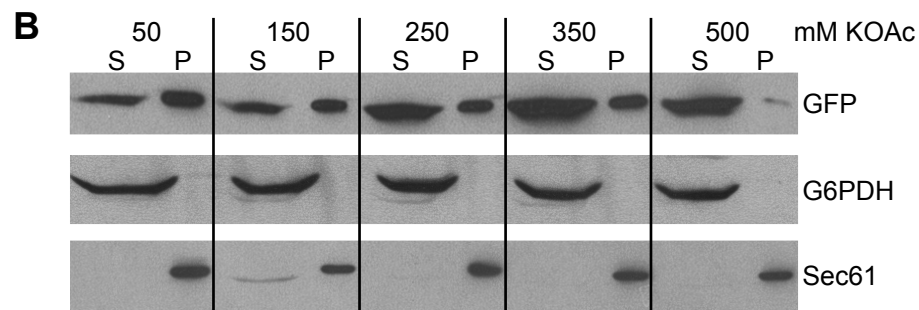
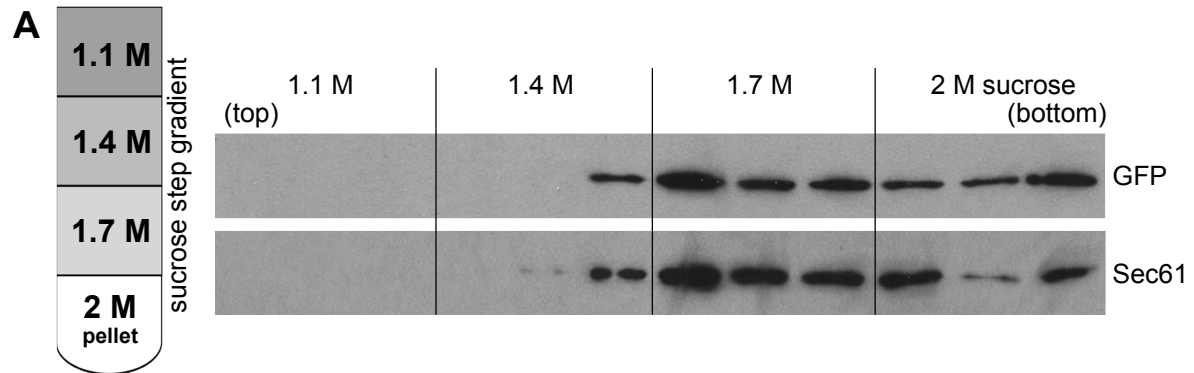


Fig. S14

Localisation of Ist2 protein [%]

	wild type YFP-Ist2	YFP-Ist2 L942Q low	YFP-Ist2 L942Q high
only peripheral signal	100	10	4
peripheral signal and dots	0	49	39
only small dots < 0.24 μ m	0	18	9
small and large dots	0	23	48

Table S1

Localisation of Ist2 protein [%]

allele	1-2 dots/cells	peripheral
WT	0	100
L942A	82	18
L942V	89	11
L942M	72	28
L942F	25	75
L942W	12	88
L942I	0	100

Table S2

Binding of plasma membrane lipids recruits the yeast integral membrane protein
Ist2 to the cortical ER

Marcel André Fischer, Koen Temmerman*, Ebru Ercan, Walter Nickel* and Matthias Seedorf

Zentrum für Molekulare Biologie der Universität Heidelberg, DKFZ-ZMBH Alliance
Im Neuenheimer Feld 282, 69120 Heidelberg, Germany

* Heidelberg University Biochemistry Center, Im Neuenheimer Feld 328,
69120 Heidelberg, Germany

Corresponding author: Matthias Seedorf

Phone: +49 6221 548299

Fax: +49 6221 545892

Email: m.seedorf@zmbh.uni-heidelberg.de

Character count: 58,093

Running title: Lipid-mediated sorting to yeast cortical ER

Key words: cortical ER, ER subdomain, lipid-binding motif, PI(4,5)P₂,
plasma membrane, sorting signal

Abstract

Recruitment of cytosolic proteins to individual membranes is governed by a combination of protein-protein and protein-membrane interactions. Many proteins recognize phosphatidylinositol 4,5-bisphosphate [PI(4,5)P₂] at the cytosolic surface of the plasma membrane (PM). Here, we show that a protein-lipid interaction can also serve as a dominant signal for the sorting of integral membrane proteins. Interaction with phosphatidylinositol phosphates (PIPs) at the PM is involved in the targeting of the polytopic yeast protein Ist2 to PM-associated domains of the cortical ER. Moreover, binding of PI(4,5)P₂ at the PM functions as a dominant mechanism that targets other integral membrane proteins to PM-associated domains of the cortical ER. This sorting to a subdomain of the ER abolishes proteasomal degradation and trafficking along the classical secretory (sec) pathway. In combination with the localization of *IST2* mRNA to the bud tip and other redundant signals in Ist2, binding of PIPs leads to efficient accumulation of Ist2 at domains of the cortical ER from where the protein may reach the PM independently of the function of the sec-pathway.

Introduction

Proteins recognize specific phospholipids, i.e. PIPs, with a number of structurally different PIP-binding domains and unstructured clusters of basic and hydrophobic residues (1, 2). This process plays a role in the anchorage of the cytoskeleton with the membrane surface and in the regulation of many trafficking and intracellular signaling events (3, 4). The distinct distribution of specific PIPs between organelles make these molecules well suited to contribute to organelle identity and to participate in the regulation of intracellular traffic (5, 6). For example a high proportion of PI(4,5)P₂ is located at the yeast PM and the highest concentration of phosphatidylinositol 4-phosphate [PI(4)P] is found at Golgi membranes (7). Phosphatidylinositol 3-phosphate [PI(3)P] and phosphatidylinositol 3,5-bisphosphate [PI(3,5)P₂] are found enriched at endosomal membranes and at the vacuole (8, 9).

As shown for the recruitment of proteins from the cytosol to the PM, the sorting of the polytopic yeast membrane protein Ist2 depends on interaction with PM lipids as well (10). Ist2 is the yeast member of the TMEM16 family, of which the mammalian TMEM16A and B proteins have been identified to be calcium-activated chloride channels (11-13).

These channels are expressed in multiple human tissues, e.g. glands and airway epithelia, where they play a role in fluid secretion (12, 13).

Ist2 is synthesized from a bud-localized mRNA, accumulates at PM-associated cortical ER and travels, by a yet unknown mechanism, to domains of the PM independently of the function of the classical secretory (sec) pathway (10, 14, 15). The yeast cortical ER is closely apposed to the PM and forms contacts with a distance of 30 nm or even less (16-18). For this reason in yeast it is very difficult to distinguish between localization at cortical ER and PM, but cell fractionation and protease protection experiments suggested that Ist2 reaches the PM (14). One step of this unconventional transport, the accumulation of Ist2 at PM-associated ER, is mediated by a C-terminal region of Ist2 (aa 878-946) (19), defining this sequence as the cortical sorting signal of Ist2 (CSS^{Ist2}).

IST2 mRNA contains one stem-loop that is recognized by the mRNA binding protein She2 and functions as mRNA localization signal (20, 21). This signal is part of the sequence encoding the CSS^{Ist2}. However, localization of Ist2 in *she2Δ* mutants and disruption of the secondary structure of the stem-loop mRNA sequence revealed that the function of the CSS^{Ist2} is independent of *IST2*

mRNA localization (19). Attached to the C termini of other membrane proteins, e.g. the furin protease Kex2, the CSS^{Ist2} mediates sec-independent transport from the perinuclear ER to patch-like structures in the cell periphery (10, 19), indicating that it is a dominant sorting signal. Whether these patches correspond to cortical ER or PM has not been resolved. Therefore, in the following we use the term peripheral in order to describe this localization. The CSS^{Ist2} is sufficient for an electrostatic interaction with PM lipids, which places Ist2 at domains of the cortical ER (10).

Here, we report that specific PIPs are involved in the interaction between CSS^{Ist2} and liposomes. In vivo, we show that the CSS^{Ist2} can be functionally replaced by a bona fide PI(4,5)P₂-specific lipid-binding domain from phospholipaseC-δ1 (PLC-δ1) but not by lipid-binding domains, which recognize PI(3)P or PI(4)P. Unexpectedly, the in-trans interaction between a PI(4,5)P₂-binding domain and PI(4,5)P₂ at the cytosolic surface of the PM functions as a dominant signal for the sorting of a number of integral membrane proteins. The interaction with lipids of the neighboring PM resulted in accumulation at cortical ER, bypassing proteosomal degradation and trafficking of integral membrane proteins along the classical sec pathway. Thus this in-trans interaction with lipids can serve as a dominant and general mechanism

for the sorting of integral membrane proteins with Ist2 being the first identified example using this novel pathway.

Results

Purified GFP-CSS^{Ist2} binds to PM-like liposomes containing PI(4,5)P₂

The cytosolically exposed C terminus of Ist2 contains a cortical sorting signal (Fig. 1A, in blue), which interacts with PM lipids (10). The N-terminal region of the CSS^{Ist2} contains single amino acid repeats comprised of threonine, histidine and serine residues (THS-cluster) and the C terminus is rich in lysine and leucine residues (K/L-sequence). Mutational analysis revealed that basic and hydrophobic residues of the K/L sequence as well as its amphipathic structure are required for interaction of the CSS^{Ist2} with PM lipids (10). Here, we wanted to identify the specific PM lipid that is responsible for this interaction. Therefore, we analyzed the binding of recombinant GFP-tagged CSS^{Ist2} to chemically defined liposomes, which were generated either from phosphatidylcholine (PC) or from a complex lipid composition resembling the PM, in the following named PM-like liposomes. Rhodamine-phosphatidylethanolamine (PE) labelled liposomes, with an average diameter of 200 nm, were sorted into the red channel of a FACS and the amount of liposome-bound GFP fluorescence was determined (22, 23). The

presence of 2.5 to 7.5 mol% PI(4,5)P₂ in PM-like liposomes led to a concentration-dependent binding of GFP-CSS^{Ist2}, whereas PI(4,5)P₂ in PC liposomes had almost no effect (Fig. 1B). On the one hand, this shows that binding of GFP-CSS^{Ist2} to liposomes requires PI(4,5)P₂ and on the other hand that a complex PM-like lipid composition is necessary for efficient binding. With PM-like liposomes containing 5 mol% PI(4,5)P₂ we measured a K_D for GFP-CSS^{Ist2} of 12.1 ± 3.3 μM.

Next, we replaced individual lipids of the PM-like liposomes containing 5 mol% PI(4,5)P₂ with PC and measured binding of GFP-CSS^{Ist2} to these liposomes. The exchange of PI(4,5)P₂ to PC abolished binding almost completely (Fig. 1C). The exchange of PE to PC had a minor positive effect, whereas the exchange of phosphatidylserine (PS) led to 30% reduction of binding, suggesting that the negative charge of PS contributes to the interaction between GFP-CSS^{Ist2} and membranes. The exchange of sphingomyelin (SM), cholesterol (CL) and both SM and CL to PC resulted in a 40 to 67% reduction of GFP-CSS^{Ist2} binding.

In order to function as a trafficking signal the CSS^{Ist2} requires a certain distance from the membrane, multimerization and a basic amphipathic α-helix (10, 19). Replacement of the THS-cluster (aa residues 878-928) in the CSS^{Ist2}

by an unrelated sequence of the PM-localized ATP-binding cassette transporter Ste6 with similar length (Ste6 aa residues 100-150) abolished most of the activity of the CSS^{Ist2} as cortical sorting signal. A replacement with a tetramerization domain of the Gcn4 leucine zipper variant of pLI (cc denotes the coiled-coil forming domain) however, led to peripheral accumulation of a Kex2-cc-GFP-(Ist2 929-946) reporter protein (19). In order to investigate whether tetramerization is required for interaction of the CSS^{Ist2} with PM-like liposomes as well, we purified different variants of the GFP-CSS^{Ist2} and tested their binding to liposomes. GFP-Ist2 (860-928) contains 18 additional residues, located N-terminal of the CSS^{Ist2} but lacks the K/L-sequence (928-946). This truncation abolished binding to liposomes completely (Fig. 2). A similar detrimental effect had the replacement of the THS-cluster with an unrelated sequence of Ste6, whereas the replacement with the tetramerization domain only moderately reduced binding to liposomes compared to GFP-CSS^{Ist2}. These data suggest that multiple copies of the basic amphipathic α -helix are required for efficient binding to PI(4,5)P₂ containing PM-like liposomes.

A bona-fide PI(4,5)P₂-binding domain replaces the function of the CSS^{Ist2}

In vitro binding assays, using either different lipids that were spotted on nitrocellulose membrane (PIP-strip, Fig. S1A), or PM-like liposomes that contained different PIPs (Fig. S1B), revealed a promiscuous interaction of GFP-CSS^{Ist2} with mono-, di- and tri-phosphorylated phosphatidylinositol species. However, in yeast cells GFP-CSS^{Ist2} accumulated at the PM but not at other membranes (10), suggesting a specific interaction with PM lipids.

In order to test to which PIP species the CSS^{Ist2} binds in cells, we replaced residues 878-946 of Ist2 with well-characterized lipid-binding domains and analyzed the localization of the resulting chimeras in wild type cells. We used domains that recognize PI(3)P at the vacuole (8, 24), PI(4)P at the Golgi (25), or PI(4,5)P₂ at the PM (25). The localization of these lipid-binding domains depends on the kinases generating the respective PIPs. However, additional organelle-specific components contribute to their specificity, e.g. the PI(4)P-binding pleckstrin homology (PH) domain from the four-phosphate-adaptor protein 1 (FAPP1) (26) interacts with Arf1 and binds PI(4,5)P₂ to a certain extent as well (27). Expression of GFP-Ist2 lacking the cortical sorting signal (GFP-Ist2^{ΔCSS}, see cartoon Fig. 3A) under control of the inducible

GAL1 promoter led to accumulation of GFP-Ist2^{ΔCSS} at peripheral dot-like structures (Fig. 3B). Attachment of a PI(3)P-binding FYVE-domain from the human early endosome antigen (EEA1) protein (24) to GFP-Ist2^{ΔCSS} led to accumulation in dot-like and membranous structures, partially surrounding the vacuole (Fig. 3B, the latter indicated with arrows), whereas attachment of the PI(4)P-binding FAPP1 PH domain to GFP-Ist2^{ΔCSS} resulted in localization at ill-defined intracellular structures only. The localization was strikingly different when we attached a PI(4,5)P₂-binding PH domain from PLC-δ1 (28, 29) to GFP-Ist2^{ΔCSS}. This chimera localized at peripheral structures, indistinguishable from the localization of wild type GFP-Ist2, arguing that in vivo, an interaction with PI(4,5)P₂ at the PM is sufficient for the rapid transport of Ist2 from the perinuclear to the cortical ER. A combination of full length Ist2, including the CSS^{Ist2} and the EEA1-FYVE domain resulted in localization at both cell periphery and structures, which partially surround the vacuole (Fig. 3B, indicated with arrows).

As the peripheral accumulation of GFP-Ist2 occurs *sec*-independently (14), we asked, whether this is also the case for GFP-Ist2^{ΔCSS} + PLC-δ1-PH. As a control for the block of the *sec*-pathway, we localized the hexose transporter Hxt1, which under permissive conditions reaches the PM (14). In *sec23-1* cells at 37°C, where *GAL1*-induced Hxt1-

RFP accumulated at intracellular ER-like structures, *GAL1*-induced GFP-Ist2^{ΔCSS} + PLC-δ1-PH reached the cell periphery (Fig. 3C). Most likely, the in-trans interaction with PI(4,5)P₂ at the PM leads to a trapping at PM-associated subdomains of the ER.

Based on the same peripheral, patch-like localization of GFP-Ist2 and GFP-Ist2^{ΔCSS} + PLC-δ1-PH this suggests that the CSS^{Ist2} in vivo functions as a PI(4,5)P₂ binding motif, which is dominant over ER export. As seen from the localization of PI(3)P-, PI(4)P- and PI(4,5)P₂-binding biosensors the block of COPII vesicle formation in *sec23-1* mutants at 37°C had no effect on the accumulation of PI(4,5)P₂ at the PM and PI(3)P at the vacuole (Fig. S2). However, the accumulation of PI(4)P at the Golgi was completely lost in *sec23-1* cells at 37°C.

At 37°C in *sec23-1* cells the dot-like accumulations of GFP-Ist2^{ΔCSS} + EEA1-FYVE disappeared and the majority of the protein localized at membranous structures around the vacuole (Fig. 3C). Most likely these structures correspond to junctions between ER and vacuole, suggesting that a direct interaction with PI(3)P traps GFP-Ist2^{ΔCSS} + EEA1-FYVE at a vacuole-associated subcompartment of the ER. In order to test whether indeed the expression of GFP-Ist2^{ΔCSS} +

EEA1-FYVE recruits ER to the vacuole, we localized the ER-marker RFP-HDEL, which is translocated by a signal sequence into the ER lumen, in cells expressing GFP-Ist2^{ΔCSS} + EEA1-FYVE. In addition to the characteristic perinuclear and cortical ER staining, we observed a significant accumulation of RFP-HDEL around vacuoles, at sites where GFP-Ist2^{ΔCSS} + EEA1-FYVE localized (Fig. 4A, indicated with arrows). The colocalization of a GFP-tagged version of this ER-marker with the lipid dye FM 4-64 in cells that express Ist2^{ΔCSS} + EEA1-FYVE confirmed that ER structures were recruited to the vacuole (data not shown). This efficient zippering of ER and vacuole is specific for the expression of GFP-Ist2^{ΔCSS} with a PI(3)P-binding EEA1-FYVE domain. The expression of GFP-Ist2^{ΔCSS} with a PI(4)P-binding FAPP1-PH domain led to accumulation at ill-defined structures, positive for the ER marker RFP-HDEL, however, efficient zippering between ER and vacuole was not observed (Fig. 4A).

Since the expression of GFP-Ist2^{ΔCSS} with a PI(3)P-binding EEA1-FYVE domain resulted in the zippering of ER and vacuole, we wondered whether the association between Ist2 and the PM is involved in the anchoring of cortical ER at the PM. However, the deletion of Ist2 had no obvious effect on the amount of cortical ER stained by RFP-HDEL (Fig. 4B). The ratio of RFP-HDEL

intensity between perinuclear and cortical ER in unbudded cells did not change in cells without Ist2 nor in cells expressing GFP-Ist2 or GFP-Ist2^{ΔCSS} + PLC-δ1-PH under control of the *GAL1* promoter (quantification in Tab. S1). To check whether Ist2 is involved in the inheritance of cortical ER into small and medium sized daughter cells, we compared the amount of RFP-HDEL in these daughter cells with the amount in the corresponding mother cells. Again, deletion of Ist2 or expression of GFP-Ist2 and GFP-Ist2^{ΔCSS} + PLC-δ1-PH had no effect on the amount of cortical ER in small and medium sized daughter cells that have not yet received a perinuclear ER (Tab. S1).

In order to test whether sorting via the PI(4,5)P₂-binding PH domain from PLC-δ1 results in a functional Ist2 protein, we analyzed whether different versions of Ist2 rescue a growth defect of *ist2Δ* on plates containing the cell wall drug calcofluor white (CFW). Ist2^{ΔCSS} only partially rescued the growth defect, whereas GFP-Ist2^{ΔCSS} + PLC-δ1-PH rescued it with the same efficiency as wild type Ist2 (Fig. 5). This establishes that GFP-Ist2^{ΔCSS} + PLC-δ1-PH is indeed a functional Ist2 protein with respect to growth in the presence of CFW. Attachment of EEA1-FYVE and FAPP1-PH domains to Ist2^{ΔCSS} had no effect. The in vitro liposome binding experiments showed that a

multimerization domain and the K/L-sequence in the CSS^{Ist2} are necessary for binding to PI(4,5)P₂-containing PM-like liposomes (Fig. 2). Therefore, we tested Ist2 without the K/L-sequence (Ist2 1-928). This version of Ist2 showed the same partial rescue as Ist2^{ΔCSS}, indicating that binding of Ist2 to lipids at the PM via the K/L-sequence is required for function of Ist2. The replacement of the THS cluster had no influence on the function of Ist2 in this assay.

A PI(4,5)P₂-binding domain in integral membrane proteins functions as a signal for sorting to PM-associated domains of the ER

Next, we asked whether a PI(4,5)P₂-specific lipid-binding domain can target other membrane proteins than Ist2 to PM-associated domains of the cortical ER. Attached to the C terminus of the Golgi-located protein Sys1 (30), the PI(4,5)P₂-specific lipid-binding domain of PLC-δ1-PH as well the CSS^{Ist2} relocated GAL1-induced Sys1-GFP from the Golgi to the cell periphery (Fig. 6A). This recruitment of integral membrane proteins to PM-associated domains of the cortical ER by binding to PI(4,5)P₂ at the PM is a general phenomenon. We observed the same effect as with Sys1, when we attached PLC-δ1-PH or CSS^{Ist2} to the C terminus of the Golgi- and endosome-located protein Kex2-GFP (Fig. 6A). This peripheral accumulation of Kex2-GFP +

PLC-δ1-PH occurred sec-independently (Fig. 6B). In *sec23-1* cells Hxt1-RFP was trapped at proliferating ER whereas Kex2-GFP + PLC-δ1-PH reached the cell periphery. This clearly indicates that binding of PI(4,5)P₂ targets Kex2-GFP without any transport along the sec-pathway to PM-associated subdomains of the ER. Moreover, this suggests that an in-trans interaction with organelle-specific lipids can function as a general mechanism for the distribution of integral membrane proteins into ER subdomains.

Additional factors besides PI(4,5)P₂ are involved in the transport of Ist2

PI(4,5)P₂ at the PM is created from PI(4)P by the lipid kinase Mss4 (31). Previous quantitation of total PI(4,5)P₂ in temperature-sensitive *mss4-102* and wild type cells, showed a two-fold reduction of PI(4,5)P₂ at 25°C and a ten-fold reduction at 38°C (25).

We confirmed the reduction of PM PI(4,5)P₂ in *mss4-102* cells by localizing the soluble PI(4,5)P₂-binding biosensor GFP-2x PLC-δ1-PH (25). In wild type cells GFP-2x PLC-δ1-PH localized at the PM, whereas in *mss4-102* at 25°C some of the GFP-2x PLC-δ1-PH was released from the PM into the cytosol (Fig. S3A). After 90 min at 38°C the peripheral signal vanished in all *mss4-102* cells, confirming the reduction of PI(4,5)P₂ at the

PM. However, this reduction of PI(4,5)P₂ had no effect on the accumulation of GFP-Ist2 and GFP-Ist2^{ΔCSS} + PLC-δ1-PH at the cell periphery (Fig. 6C). Compared to Ist2, the peripheral localization of Kex2-GFP + PLC-δ1-PH required a high level of PI(4,5)P₂ at the PM in many cells. Shifting *mss4-102* mutant cells for 90 min to 38°C abolished trafficking of GAL1-induced Kex2-GFP + PLC-δ1-PH to the periphery in the majority of cells (Fig. 6D). 72% of the *mss4-102* cells accumulated Kex2-GFP + PLC-δ1-PH only at intracellular dot-like structures, whereas 14% showed an intermediate phenotype with Kex2-GFP + PLC-δ1-PH at the periphery and in dots, and 14% had a peripheral distribution of Kex2-GFP + PLC-δ1-PH (Tab. S2). Similarly to GFP-2x PLC-δ1-PH, we observed a strong accumulation of GFP-2x CSS^{Ist2} at the PM of wild type cells (Fig. S3B). In order to test whether this PM localization depends on PI(4,5)P₂ or the PM pool of PI(4)P, we employed temperature-sensitive alleles of the lipid kinases *MSS4*, *STT4* and a double mutant of *STT4* and *PIK1*, in which PI(4,5)P₂, the PM pool of PI(4)P or both are largely depleted (25, 32). The localization of GFP-2x CSS^{Ist2} did not change in *mss4-102* and *stt4-4* mutants at 38°C (Fig. S3B). However, at restrictive temperature 22% of *stt4-4/pik1-63* cells lost the PM localization of GFP-2x CSS^{Ist2} and showed an intracellular accumulation (Fig. S3C).

Since the depletion of PI(4,5)P₂ in *mss4-102* cells did not abolish the peripheral accumulation of GFP-Ist2, we suggest that other signals in the N- and C-terminal regions of Ist2 and/or specific properties of its transmembrane part also contribute to peripheral accumulation. In order to test this idea, we analyzed the localization of GFP-Ist2^{ΔCSS} in *ist2Δ* cells. Compared to wild type Ist2, deletion of the CSS^{Ist2} led in 71% of the cells to localization at the perinuclear ER as well (Fig. 7A, quantification in Tab. S3), when expressed under control of the *IST2* promoter, thus confirming that the CSS^{Ist2} is required for efficient accumulation at the cortical ER. However, induction of GFP-Ist2^{ΔCSS} under the control of the *GAL1* promoter, which resulted in strong overexpression (Fig. 7B), led to accumulation in dots and patches that localized preferentially at the cell periphery. After one and two hours in galactose 24% and 58% of the cells showed a dot-like accumulation of GFP-Ist2^{ΔCSS} at the cell periphery only (Fig. 7A, quantification in Tab. S3). The number of cells with ring-like perinuclear fluorescence dropped in cells that overexpress GFP-Ist2^{ΔCSS} to 14% after one hour and this localization vanished completely after two hours of induction. This suggests a concentration dependent trapping of Ist2 at subdomains of the peripheral ER, where GFP-Ist2^{ΔCSS} may interact with yet unknown

components of ER-PM junctions. Colocalization of GFP-Ist2^{ΔCSS} dots with the ER marker RFP-HDEL confirmed that these dots are part of the ER (Fig. 7C). Moreover, we observed that large amounts of this ER marker were recruited into these peripheral dots, suggesting that the overexpression of GFP-Ist2^{ΔCSS} leads to a recruitment of ER at the cell periphery. Colocalization of GFP-Ist2^{ΔCSS} with Kar2 revealed that in contrast to RFP-HDEL the ER chaperone Kar2 was not enriched at these peripheral dots, indicating that GFP-Ist2^{ΔCSS} accumulated at subdomains of the cortical ER. The GFP-Ist2^{ΔCSS} dots did not overlap with the Golgi marker Sec7 (Fig. 7C). This is consistent with an accumulation of GFP-Ist2^{ΔCSS} at peripheral subdomains of the ER. Expression of GFP-Ist2^{ΔCSS} in wild type cells led to partial accumulation in peripheral patches (Fig. 7D). This suggests that GFP-Ist2^{ΔCSS} and Ist2 form a complex and that the CSS^{Ist2} in this complex mediates a distribution along the ER-PM interface.

The N terminus of the Ist2 orthologue TMEM16A binds lipids

Compared to Ist2 in yeast, the members of the mammalian TMEM16 protein family, which are characterized by a central region with eight transmembrane domains, have much shorter C termini than Ist2 (12, 13, 33). The last transmembrane domain of the longest reported

isoform of TMEM16A (1006 aa residues) ends at residue 925 (13) for example. This results in a cytosolically exposed C terminus of 81 residues. Sequence comparison with the C-terminal domain of Ist2, comprising 358 aa residues, revealed that the features of the CSS^{Ist2} are not conserved. Compared to Ist2, TMEM16A has a rather long N-terminal domain with the first predicted transmembrane domain starting at aa residue 354 (Fig. 8A). In order to test whether either the N- or C-terminus of TMEM16A interact with lipids as well, we fused these sequences to GFP and analyzed the binding to PM-like liposomes with and without 5 mol% PI(4,5)P₂. Similar as seen for GFP alone, GFP-TMEM16A 928-1006 showed no binding even at higher protein concentration (4 μM instead of 1 μM; Fig. 8B). This indicates that a PIP-specific lipid-binding signal is not present in the C terminus of TMEM16A. However, the situation was different when we investigated the N-terminal domain of TMEM16A. We fused the N terminus of TMEM16A to the C terminus of GFP resulting in a protein with similar arrangement of domains as in GFP-CSS^{Ist2}. For this GFP-TMEM16A 1-352 we observed a significant increase of binding. Although this binding was not as efficient as the binding of GFP-CSS^{Ist2}, this binding was dependent on the presence of PI(4,5)P₂ in the PM-like liposomes as well. Moreover, we positioned the N-terminal domain of

TMEM16A at the N terminus of GFP. Again, binding of TMEM16A 1-352-GFP was PI(4,5)P₂-dependent and under these conditions even more efficient than binding of GFP-CSS^{Ist2}. However, we have not investigated whether this binding is specific for PI(4,5)P₂ and whether a PM-like liposome is required for binding.

Attached to GFP-Ist2^{ΔCSS} the C-terminal domain of TMEM16A had no effect on the localization of GFP-Ist2^{ΔCSS} in *ist2Δ* cells (Fig. 8C). Consistent with a function as a lipid-binding motif, the N-terminal domain of TMEM16A targeted GFP-Ist2^{ΔCSS} from peripheral dot-like structures into more patch-like structures. At 25°C the signal of the N-terminally tagged TMEM16A 1-352-GFP-Ist2^{ΔCSS} was weak as compared to the C-terminally tagged GFP-Ist2^{ΔCSS}-TMEM16A 1-352. However, at 37°C both proteins were unstable and therefore we could not investigate their trafficking in temperature-sensitive sec-mutants.

The CSS^{Ist2} functions dominantly over ER degradation signals

Since binding to PI(4,5)P₂ at the cytosolic face of the PM traps membrane proteins at domains of the cortical ER and impedes on transport along the sec-pathway, we investigated whether such trapping interferes with proteosomal degradation of proteins as well. Misfolded and damaged ER

membrane proteins are removed from the ER membrane by dislocation into the cytosol and proteasomal degradation (34). A *GAL1*-induced C-terminally truncated aberrant version of Ste6 localized at the perinuclear ER (Fig. 9A), from where it disappeared rapidly. One hour after shift into glucose containing media, the majority of YFP-Ste6 1-150 was degraded (Fig. 9B). Attachment of CSS^{Ist2} or PLC-δ1-PH to the C terminus of YFP-Ste6 1-150 led to a relocation from the perinuclear ER to the cell periphery (Fig. 9A). Moreover, this relocation was accompanied by a dramatic stabilization of truncated Ste6 (Fig. 9B).

Discussion

The cytosolically exposed C terminus of the integral membrane protein Ist2 binds lipids at the PM and this interaction places Ist2 at the yeast cortical ER. Responsible for this binding is a basic and amphipathic sequence at the extreme C terminus of Ist2 (10). Efficient interaction with PI(4,5)P₂-containing PM-like liposomes and function of this sequence as CSS^{Ist2} required a multimerization domain. This suggests that an homooligomeric Ist2 complex at the ER membrane exposes a signal with high avidity for anionic lipids like PI(4)P and PI(4,5)P₂ at the cytosolic face of the PM. We could functionally replace this signal by a PI(4,5)P₂-specific PH domain but not by lipid-

binding domains recognizing PI(3)P at the vacuole or PI(4)P at the Golgi. This indicates that the CSS^{Ist2} interacts with lipids of the PM but not with membranes of the vacuole or the Golgi. In combination with any kind of ER-located transmembrane domain, this lipid-binding signal was sufficient for the recruitment of the protein to PM-associated domains of the cortical ER. We showed this phenomenon for Ist2, a truncated version of the ABC-like pheromone transporter Ste6, trans-Golgi-located Sys1 and Kex2. This sorting into a specific subdomain of the ER and the physical linkage of proteins with lipids at the cytoplasmic surface of the PM interferes with recruitment of these proteins into COPII vesicles and proteosomal degradation, defining PM-associated domains of the ER as a specific ER subcompartment.

Expression of Ist2^{ΔCSS} with a PI(3)P binding domain resulted in an efficient zippering between ER subdomains and vacuole. However, it remains open whether besides known protein-protein interactions, such as the ER protein Nvj1 and the vacuolar protein Vac8 (35, 36), this type of protein-lipid interaction contributes to the sorting of authentic ER proteins to ER-vacuole junctions. In *sec23-1* cells we observed that Ist2^{ΔCSS} + FAPP1-PH indeed had some affinity for the vacuole and the PM (data not shown). Under these artificial

conditions, where PI(4)P is no longer at the Golgi, some zippering between ER and vacuole may occur, however we did not observe any Ist2^{ΔCSS} + FAPP1-PH induced zippering between ER and vacuole in cells with intact secretion. Based on the observed recruitment of ER that contains Ist2^{ΔCSS} + EEA1-FYVE to the vacuole, a similar, Ist2-mediated mechanism could be involved in the recruitment of cortical ER to the PM and the spreading of cortical ER around the entire bud. However, we observed no variations in the amount of cortical ER nor did we see any variations in the inheritance of this organelle into daughters in cells with different amounts of Ist2. This suggests that redundant mechanisms, e.g. the interaction of translocon components, reticulons and Scs2 on the ER with exocyst and polarisome components on the PM are sufficient for the formation and inheritance of cortical ER (37-42).

Based on the patch-like localization of Ist2 and Ist2^{ΔCSS} + PLC-δ1-PH at the cell periphery in cells with reduced PI(4,5)P₂ levels at the PM (after 90 min at 38°C in *mss4-102* cells), we suggest the presence of additional sorting signals in Ist2^{ΔCSS} (residues 1-877). In *ist2Δ* cells at high expression, Ist2^{ΔCSS} accumulated at peripheral dot-like structures where the ER marker RFP-HDEL was enriched. Compared to this ER marker, the Ist2^{ΔCSS}-induced peripheral dot-like ER structures

showed no enrichment of the ER chaperone Kar2, indicating that Ist2^{ΔCSS} does not behave like a misfolded protein aggregate. These data rather suggest the presence of an additional signal in Ist2^{ΔCSS}, which mediates accumulation at dot-like subdomains of the cortical ER. Compared to the formation of karmellae, which are Kar2-positive proliferated membrane stacks around the nucleus, induced by overexpression of Hmg1 (43, 44), the peripheral ER structures, in which Ist2^{ΔCSS} accumulated, rather share features with Hmg2 induced ER subdomains: peripheral proliferation of the ER and exclusion of Kar2 (44). Compared to the expression of full length GFP-Ist2, which had no obvious impact on the distribution of RFP-HDEL, the lack of the C-terminal PM-binding site in Ist2^{ΔCSS} may favor homotypic interaction between cytoplasmic domains of Ist2^{ΔCSS} on apposing membranes and thereby the formation of membrane stacks. A concept of low affinity cytosolic protein interactions of membrane anchored proteins as driving force for changes of ER morphology has been described for yeast and mammalian cells (45). However, it remains unclear, which properties of Ist2 are responsible for this accumulation at peripheral ER subdomains.

Expression of Ist2^{ΔCSS} in wild type cells resulted in the localization of some Ist2^{ΔCSS} in patch-like

peripheral structures, suggesting that Ist2^{ΔCSS} can form a heterooligomeric complex with Ist2. In this complex wild type Ist2 provides the signal for targeting the complex to PM-associated domains of the cortical ER. Thus Ist2^{ΔCSS} contains signals for oligomerization. These signals in Ist2^{ΔCSS} are sufficient for support of wild type-like growth on CFW as long the K/L-sequence is present. The efficient recruitment of GFP-2x CSS^{Ist2} to the PM, as compared to the weak accumulation of monomeric GFP-CSS^{Ist2} (10), indicates that multiple copies of this signal confer a high affinity interaction with the PM. The reduction of either PI(4)P or PI(4,5)P₂ at the PM did not change the localization of GFP-2x CSS^{Ist2} in *stt4-4* or *mss4-102* cells shifted for 90 min to 38°C. However, after 40 min at 38°C 22% of *stt4-4/pik1-63* cells showed a delocalization of GFP-2x CSS^{Ist2} with accumulation in cytoplasm and at a single dot. Partial localization of GFP-CSS^{Ist2} at nucleoli (10) suggests that this dot corresponds to the nucleolus as well. Under these conditions in a similar *stt4-4/pik1-83* mutant the cellular levels of PI(4)P and PI(4,5)P₂ were reduced by 90% as compared to wild type (32). Since the reduction of PIPs at the PM affected the localization of the CSS^{Ist2} only in 22% of cells, we conclude that in addition to PIPs other components of the PM contribute to this localization as well. However, two arguments support the view that PI(4,5)P₂ is the major binding

site of the CSS^{Ist2} at the PM: the CSS^{Ist2} could be functionally replaced by a PI(4,5)P₂-specific PLC- δ 1-PH domain and binding of the CSS^{Ist2} to liposomes in vitro depends on PIPs and a PM-like composition of the liposomes. Since the binding of the CSS^{Ist2} to PIP containing liposomes requires a PM-like lipid composition, we suggest that specificity for the interaction between the CSS^{Ist2} and the PM over other cellular compartments containing PIPs is a result of the recognition of multiple binding sites at the PM.

The affinity of CSS^{Ist2} to PI(4,5)P₂-containing liposomes is significantly weaker than the affinity of the PLC- δ 1-PH domain. In the FACS-based in vitro lipid-binding assay we employed, the K_D of a single copy of the CSS^{Ist2} was 12.1 \pm 3.3 μ M as compared to the K_D of 2.7 \pm 0.5 μ M for a single copy of the PLC- δ 1-PH domain (23). However, it is important to note that the situation for ER resident Ist2 is different from the situation of a cytosolic version of the CSS^{Ist2} or of cytosolic proteins carrying a lipid-binding domain. Restricted to the ER membrane the lower affinity of the CSS^{Ist2} to the PM, as compared to the higher affinity of the PLC- δ 1-PH domain, is sufficient for efficient targeting of Ist2 to PM-associated domains of the cortical ER.

Whether Ist2 functions similar as the recently characterized mammalian homologues TMEM16A and B as a calcium-activated chloride channel remains to be investigated (11-13). The C terminus of TMEM16A does not share similarities with the C terminus of Ist2. This sequence is much shorter as the C terminus of Ist2, has an acidic pI of 5.2 instead of 10.6 for the CSS^{Ist2}, lacks the characteristic basic and amphipathic K/L-sequence and neither binds to PI(4,5)P₂-containing PM-like liposomes nor replaces the function of the CSS^{Ist2} as a localization signal. This was different for the N terminus of TMEM16A, of which the longest reported isoform has a 353 aa residues cytosolically exposed N-terminal domain with an pI of 9.1 (13). The binding of this domain to PI(4,5)P₂-containing PM-like liposomes was comparable with the binding of the CSS^{Ist2} to these liposomes. Moreover, positioned at either N or C terminus of Ist2 ^{Δ CSS} this domain conferred an enrichment of the resulting chimeras in patches at the cell periphery. However, the targeting of the resulting chimeras to peripheral patches was not as efficient as the targeting of Ist2 to cortical ER and these chimeras were unstable at 37°C. Moreover, we have not discriminated whether the N-terminal domain of TMEM16A provides an ER export signal or whether it functions in vivo as a PM-lipid binding signal. Without detailed further analysis it remains elusive whether the N termini of

TMEM16A and other TMEM16 family members contain lipid-binding signals, which function similar as the CSS^{Ist2}.

Ist2 in yeast utilizes the interaction with PI(4,5)P₂ and other components at the cytoplasmic face of the PM for rapid enrichment at PM-associated domains of the cortical ER. The protein may function at the interface between cortical ER and PM, e.g. as a calcium-activated chloride channel as deduced from the function of its putative orthologues TMEM16A and TMEM16B. Alternatively Ist2 may travel directly from the cortical ER to the PM in order to fulfill its function at this membrane. Based on the accessibility of Ist2 to external proteases, we suggested that Ist2 reaches the PM (14, 15).

Taken together, our data indicate that the interaction of integral membrane proteins with lipids at the PM is sufficient for the targeting of these proteins to PM-associated domains of the ER. This interaction with lipids at a neighboring membrane, e.g. with PI(4,5)P₂ at the PM, provides a general, simple and efficient mechanism for the sorting of integral membrane proteins into a subdomain of the cortical ER.

Materials and Methods

Yeast strains and media

The strains MSY383 (*sec23-1*, *pGAL1-HXT1-RFP::TRP1* (19)) and CJY3 (*ist2Δ::HIS3MX6* (14)) are isogenic derivatives of *W303* (46). The *mss4-102*, *stt4-4* and *stt4-4/pik1-63* mutants and their isogenic wildtype (used in Figs. 6 and S3) were gifts from J. Thorner. Preparation of media and yeast transformation were carried out as described in (47, 48).

Plasmids

All plasmids were cloned using standard molecular biology techniques and are described in Table S4. TMEM16A cDNA clone SC314998 (splice variant *abcd*) (13) was obtained from OriGene.

Generation of liposomes

Lipids including 1 mol% rhodamine labelled PE (16:0, Avanti Polar Lipids, ordering number 810158) were dissolved in chloroform and dried in a rotary evaporator yielding a homogenous dried lipid film. Liposomes, with a final lipid concentration of 4 mM, were generated by resolving this film in an appropriate volume HK-buffer (25 mM Hepes, 150 mM KCl, pH 7.4) containing 10% (w/v) sucrose. This crude liposome mixture was subjected to 10 freeze/thaw cycles followed by 21 size extrusion steps through a filter with 1000 nm pore size (Avanti Polar Lipids),

resulting in liposomes with an average diameter of 200 nm. Liposomes were analyzed via light scattering (Zetasizer 1000 HS; Malvern Instruments). Liposome concentration was determined by rhodamine fluorescence. All lipids were purchased from Avanti Polar Lipids. PM-like liposomes according to (49) consisted of 50 mol% CL from ovine wool (700000), 17.5 mol% PC from bovine liver (840055), 9 mol% PE from bovine liver (840026), 5 mol% PS from porcine brain (840032), 5 mol% phosphatidylinositol from bovine liver (840042), and 12.5 mol% SM from poultry eggs (860061). PI(4,5)P₂ (840046) and PI(4)P (840045) were from porcine brain. PI(3,4,5)P₃ (850164) and PI(3,5)P₂ (850146) had 18:0 and 20:4 fatty acid acyl chains.

Liposome binding

For liposome binding assays, liposomes were blocked with 3% (w/v) fatty acid free bovine serum albumin (Roche) in HK-buffer for 1 h (25°C), washed and incubated for 4 h with 100 µl of recombinant protein at a final protein concentration of 25 µg/ml in HK-buffer (25°C). Recombinant GFP and GFP-fusion proteins were purified via an N-terminal His₆-tag as described (10). Liposomes were then washed, resuspended in HK-buffer and analyzed via flow cytometry (23). Liposomes were gated by size and rhodamine fluorescence, and the GFP fluorescence from the bound recombinant

proteins was detected. In all assays the relative GFP fluorescence of His₆-GFP-CSS^{Ist2} bound to PM-like liposomes with 5 mol% PI(4,5)P₂ was set to 100 (in the figure axes shown as arbitrary units). In binding assays using 6 µM His₆-GFP-CSS^{Ist2} and PM-like liposomes including 5 mol% PI(4,5)P₂ 30% of the protein input is bound to the liposomes (10). For the liposome binding assays, an extra normalization factor was introduced, to allow for an exact comparison between binding to liposomes with different PIPs (Fig. S1) or between different protein concentrations, which were used for K_D measurements. Through a size gate in the scatter channel, a reference rhodamine signal was defined for GFP treated liposomes. The GFP-CSS^{Ist2} signal was then corrected with a factor based on the rhodamine signal ratio between GFP and GFP-CSS^{Ist2} treated liposomes. As such, equally accessible lipid surface areas can be compared. K_D measurements were performed using PM-like liposomes including 5 mol% PI(4,5)P₂. Liposomes were incubated with 9 different concentrations of His₆-GFP-CSS^{Ist2}, the K_D was determined using GraphPad Prism 4. Each titration curve was fitted to $Y = B_{\max} * X / (K_D + X)$ using a one site binding model. Y indicates the relative fluorescence and X the protein concentration of the respective sample. B_{max} represents the asymptotic maximum of the binding curve. All liposome measurements were performed at least 3

times. Error bars indicate the standard deviation.

Fluorescence microscopy

For *GAL1*-controlled protein expression, cells were grown to an OD_{600} of < 0.5 in YEAP medium containing 2% (w/v) raffinose. Protein expression was induced by the addition of 2% (w/v) galactose. For fluorescence microscopy exponentially growing yeast cells were mounted in medium and examined live. All constructs were observed with an inverted microscope (Leica DM IRE2), using an oil immersion objective (HCX PL APO CS 100/1.4 0.7, Leica). Pictures were taken using a Hamamatsu ORCA-ER CCD camera using Openlab software (Improvision). The following filters were used: GFP 470/40 (excitation) and 525/50 (emission), YFP 510/20 (excitation) and 560/40 (emission) and dsRed 510/40 (excitation) and 610 (emission). Picture processing was performed with Adobe Photoshop.

Indirect immunofluorescence

Following *GAL1*-driven induction of GFP-Ist2^{ΔCSS} Kar2 was detected as described (10). Kar2 was detected with goat-anti-rabbit AlexaFluor546 (1:400, Molecular Probes).

Lipid binding assays

PIP stripsTM (Molecular Probes) were incubated with recombinant His₆-GFP and His₆-GFP-CSS^{Ist2}

at a concentration of 5 ng/ml according to the manufacturers protocol. Protein was detected using a GFP-antibody (1:20000, immunoaffinity purified rabbit serum, gift from D. Goerlich).

Generation of yeast cell extracts and Western blotting

Denaturing cell lysis and SDS-PAGE were performed as described (19). Western blotting was carried out using GFP-, Kar2- (1:20000, (50)) or Sec61- (1:3000, (50)) antibodies.

Quantification of the amount of cortical ER

Cells expressing the ER-Marker dsRed-HDEL were subjected to fluorescence microscopy. Pictures were handled with the ImageJ software (<http://rsb.info.nih.gov/ij/>). A complete, unbudded yeast cell was marked and analyzed via the ROI manager yielding the marked area (A_{cell}) and the average fluorescence (F_{mean}). The product $A_{cell} * F_{mean}$ gives the total fluorescence of the cell F_{cell} . Similarly the same cell was analyzed by marking the cell without its cortical ER, such yielding the product $A_{perinuclear} * F_{mean}$ for the total fluorescence of the perinuclear ER $F_{perinuclear}$. The difference $F_{cell} - F_{perinuclear}$ gives the total fluorescence of the cortical ER $F_{cortical}$. For these unbudded cells the ratio $F_{perinuclear} / F_{cortical}$ was determined (Table S1). For budding cells, which did not yet have perinuclear ER inherited, the ratio $F_{cell (daughter)} / F_{cell}$

(mother) was determined similarly. All quantifications were performed in at least 100 cells per strain.

Table S1 gives the mean and the standard deviation of all quantifications.

Acknowledgements

We are grateful to P. Mayinger and E. Schiebel for plasmids, J. Thorner for the *mss4-102*, *stt4-4* and *stt4-4/pik1-63* mutants, D. Goerlich for the GFP antibody and C. Ungermann for reagents. We thank P. Eggensperger for helpful comments on the manuscript and B. Dobberstein for his generous support. This work was supported by a grant from the Deutsche Forschungsgemeinschaft (SE 811/5-1/2).

References

1. McLaughlin S, Murray D. Plasma membrane phosphoinositide organization by protein electrostatics. *Nature* 2005;438(7068):605-611.
2. Lemmon MA. Membrane recognition by phospholipid-binding domains. *Nat Rev Mol Cell Biol* 2008;9(2):99-111.
3. Sheetz MP, Sable JE, Dobereiner HG. Continuous membrane-cytoskeleton adhesion requires continuous accommodation to lipid and cytoskeleton dynamics. *Annu Rev Biophys Biomol Struct* 2006;35:417-434.
4. Di Paolo G, De Camilli P. Phosphoinositides in cell regulation and membrane dynamics. *Nature* 2006;443(7112):651-657.
5. Roth MG. Phosphoinositides in constitutive membrane traffic. *Physiol Rev* 2004;84(3):699-730.
6. Behnia R, Munro S. Organelle identity and the signposts for membrane traffic. *Nature* 2005;438(7068):597-604.
7. De Matteis MA, Godi A. PI-loting membrane traffic. *Nat Cell Biol* 2004;6(6):487-492.
8. Gillooly DJ, Morrow IC, Lindsay M, Gould R, Bryant NJ, Gaullier JM, Parton RG, Stenmark H. Localization of phosphatidylinositol 3-phosphate in yeast and mammalian cells. *EMBO J* 2000;19(17):4577-4588.
9. Lindmo K, Stenmark H. Regulation of membrane traffic by phosphoinositide 3-kinases. *J Cell Sci* 2006;119(Pt 4):605-614.
10. Maass K, Fischer MA, Seiler M, Temmerman K, Nickel W, Seedorf M. A signal comprising a basic cluster and an amphipathic α -helix interacts with lipids and is required for the transport of Ist2 to the yeast cortical ER. *J Cell Sci* 2009;122:625-635.
11. Schroeder BC, Cheng T, Jan YN, Jan LY. Expression cloning of TMEM16A as a calcium-activated chloride channel subunit. *Cell* 2008;134(6):1019-1029.
12. Yang YD, Cho H, Koo JY, Tak MH, Cho Y, Shim WS, Park SP, Lee J, Lee B, Kim BM, Raouf R, Shin YK, Oh U. TMEM16A confers receptor-activated calcium-dependent chloride conductance. *Nature* 2008;455(7217):1210-1215.
13. Caputo A, Caci E, Ferrera L, Pedemonte N, Barsanti C, Sondo E, Pfeiffer U, Ravazzolo R, Zegarra-Moran O, Galletta LJ. TMEM16A, a membrane protein associated with calcium-dependent chloride channel activity. *Science* 2008;322(5901):590-594.
14. Juschke C, Ferring D, Jansen RP, Seedorf M. A novel transport pathway for a yeast plasma membrane protein encoded by a localized mRNA. *Curr Biol* 2004;14(5):406-411.
15. Juschke C, Wachter A, Schwappach B, Seedorf M. SEC18/NSF-independent, protein-sorting pathway from the yeast cortical ER to the plasma membrane. *J Cell Biol* 2005;169(4):613-622.
16. Pichler H, Gaigg B, Hrstnik C, Achleitner G, Kohlwein SD, Zellnig G, Perktold A, Daum G. A subfraction of the yeast endoplasmic reticulum associates with the plasma membrane and has a high capacity to synthesize lipids. *Eur J Biochem* 2001;268(8):2351-2361.

17. Perktold A, Zechmann B, Daum G, Zellnig G. Organelle association visualized by three-dimensional ultrastructural imaging of the yeast cell. *FEMS Yeast Res* 2007;7(4):629-638.
18. Griffith J, Mari M, De Maziere A, Reggiori F. A cryosectioning procedure for the ultrastructural analysis and the immunogold labelling of yeast *Saccharomyces cerevisiae*. *Traffic* 2008;9(7):1060-1072.
19. Franz A, Maass K, Seedorf M. A complex peptide-sorting signal, but no mRNA signal, is required for the Sec-independent transport of Ist2 from the yeast ER to the plasma membrane. *FEBS Lett* 2007;581(3):401-405.
20. Olivier C, Poirier G, Gendron P, Boisgontier A, Major F, Chartrand P. Identification of a conserved RNA motif essential for She2p recognition and mRNA localization to the yeast bud. *Mol Cell Biol* 2005;25(11):4752-4766.
21. Jambhekar A, McDermott K, Sorber K, Shepard KA, Vale RD, Takizawa PA, DeRisi JL. Unbiased selection of localization elements reveals cis-acting determinants of mRNA bud localization in *Saccharomyces cerevisiae*. *Proc Natl Acad Sci U S A* 2005;102(50):18005-18010.
22. Temmerman K, Ebert AD, Muller HM, Sinning I, Tews I, Nickel W. A direct role for phosphatidylinositol-4,5-bisphosphate in unconventional secretion of fibroblast growth factor 2. *Traffic* 2008;9(7):1204-1217.
23. Temmerman K, Nickel W. A novel flow cytometric assay to quantify interactions between proteins and membrane lipids. *J Lipid Res* 2009.
24. Burd CG, Emr SD. Phosphatidylinositol(3)-phosphate signaling mediated by specific binding to RING FYVE domains. *Mol Cell* 1998;2(1):157-162.
25. Stefan CJ, Audhya A, Emr SD. The yeast synaptojanin-like proteins control the cellular distribution of phosphatidylinositol (4,5)-bisphosphate. *Mol Biol Cell* 2002;13(2):542-557.
26. Dowler S, Currie RA, Campbell DG, Deak M, Kular G, Downes CP, Alessi DR. Identification of pleckstrin-homology-domain-containing proteins with novel phosphoinositide-binding specificities. *Biochem J* 2000;351(Pt 1):19-31.
27. Levine TP, Munro S. Targeting of Golgi-specific pleckstrin homology domains involves both PtdIns 4-kinase-dependent and -independent components. *Curr Biol* 2002;12(9):695-704.
28. Lemmon MA, Ferguson KM, O'Brien R, Sigler PB, Schlessinger J. Specific and high-affinity binding of inositol phosphates to an isolated pleckstrin homology domain. *Proc Natl Acad Sci U S A* 1995;92(23):10472-10476.
29. Kavran JM, Klein DE, Lee A, Falasca M, Isakoff SJ, Skolnik EY, Lemmon MA. Specificity and promiscuity in phosphoinositide binding by pleckstrin homology domains. *J Biol Chem* 1998;273(46):30497-30508.
30. Votsmeier C, Gallwitz D. An acidic sequence of a putative yeast Golgi membrane protein binds COPII and facilitates ER export. *Embo J* 2001;20(23):6742-6750.
31. Homma K, Terui S, Minemura M, Qadota H, Anraku Y, Kanaho Y, Ohya Y. Phosphatidylinositol-4-phosphate 5-kinase localized on the plasma membrane is essential for yeast cell morphogenesis. *J Biol Chem* 1998;273(25):15779-15786.
32. Audhya A, Foti M, Emr SD. Distinct roles for the yeast phosphatidylinositol 4-kinases, Stt4p and Pik1p, in secretion, cell growth, and organelle membrane dynamics. *Mol Biol Cell* 2000;11(8):2673-2689.
33. Galindo BE, Vacquier VD. Phylogeny of the TMEM16 protein family: some members are overexpressed in cancer. *Int J Mol Med* 2005;16(5):919-924.
34. Nakatsukasa K, Brodsky JL. The recognition and retrotranslocation of misfolded proteins from the endoplasmic reticulum. *Traffic* 2008;9(6):861-870.
35. Pan X, Roberts P, Chen Y, Kvam E, Shulga N, Huang K, Lemmon S, Goldfarb DS. Nucleus-vacuole junctions in *Saccharomyces cerevisiae* are formed through the direct interaction of Vac8p with Nvj1p. *Mol Biol Cell* 2000;11(7):2445-2457.
36. Kvam E, Goldfarb DS. Structure and function of nucleus-vacuole junctions: outer-nuclear-membrane targeting of Nvj1p and a role in tryptophan uptake. *J Cell Sci* 2006;119(Pt 17):3622-3633.
37. Fehrenbacher KL, Davis D, Wu M, Boldogh I, Pon LA. Endoplasmic reticulum dynamics, inheritance, and cytoskeletal interactions in budding yeast. *Mol Biol Cell* 2002;13(3):854-865.

38. Du Y, Walker L, Novick P, Ferro-Novick S. Ptc1p regulates cortical ER inheritance via Sit2p. *Embo J* 2006;25(19):4413-4422.
39. Loewen CJ, Young BP, Tavassoli S, Levine TP. Inheritance of cortical ER in yeast is required for normal septin organization. *J Cell Biol* 2007;179(3):467-483.
40. Wiederkehr A, Du Y, Pypaert M, Ferro-Novick S, Novick P. Sec3p is needed for the spatial regulation of secretion and for the inheritance of the cortical endoplasmic reticulum. *Mol Biol Cell* 2003;14(12):4770-4782.
41. Reinke CA, Kozik P, Glick BS. Golgi inheritance in small buds of *Saccharomyces cerevisiae* is linked to endoplasmic reticulum inheritance. *Proc Natl Acad Sci U S A* 2004;101(52):18018-18023.
42. De Craene JO, Coleman J, Estrada de Martin P, Pypaert M, Anderson S, Yates JR, 3rd, Ferro-Novick S, Novick P. Rtn1p is involved in structuring the cortical endoplasmic reticulum. *Mol Biol Cell* 2006;17(7):3009-3020.
43. Wright R, Basson M, D'Ari L, Rine J. Increased amounts of HMG-CoA reductase induce "karmellae": a proliferation of stacked membrane pairs surrounding the yeast nucleus. *J Cell Biol* 1988;107(1):101-114.
44. Koning AJ, Roberts CJ, Wright RL. Different subcellular localization of *Saccharomyces cerevisiae* HMG-CoA reductase isozymes at elevated levels corresponds to distinct endoplasmic reticulum membrane proliferations. *Mol Biol Cell* 1996;7(5):769-789.
45. Snapp EL, Hegde RS, Francolini M, Lombardo F, Colombo S, Pedrazzini E, Borgese N, Lippincott-Schwartz J. Formation of stacked ER cisternae by low affinity protein interactions. *J Cell Biol* 2003;163(2):257-269.
46. Thomas BJ, Rothstein R. Elevated recombination rates in transcriptionally active DNA. *Cell* 1989;56(4):619-630.
47. Sherman F. Getting started with yeast. *Methods Enzymol* 2002;350:3-41.
48. Gietz RD, Woods RA. Transformation of yeast by lithium acetate/single-stranded carrier DNA/polyethylene glycol method. *Methods Enzymol* 2002;350:87-96.
49. van Meer G. Lipids of the Golgi membrane. *Trends Cell Biol* 1998;8(1):29-33.
50. Frey S, Pool M, Seedorf M. Scp160p, an RNA-binding, Polysome-associated Protein, Localizes to the Endoplasmic Reticulum of *Saccharomyces cerevisiae* in a Microtubule-dependent Manner. *J Biol Chem* 2001;276(19):15905-15912.
51. Madrid AS, Mancuso J, Cande WZ, Weis K. The role of the integral membrane nucleoporins Ndc1p and Pom152p in nuclear pore complex assembly and function. *J Cell Biol* 2006;173(3):361-371.

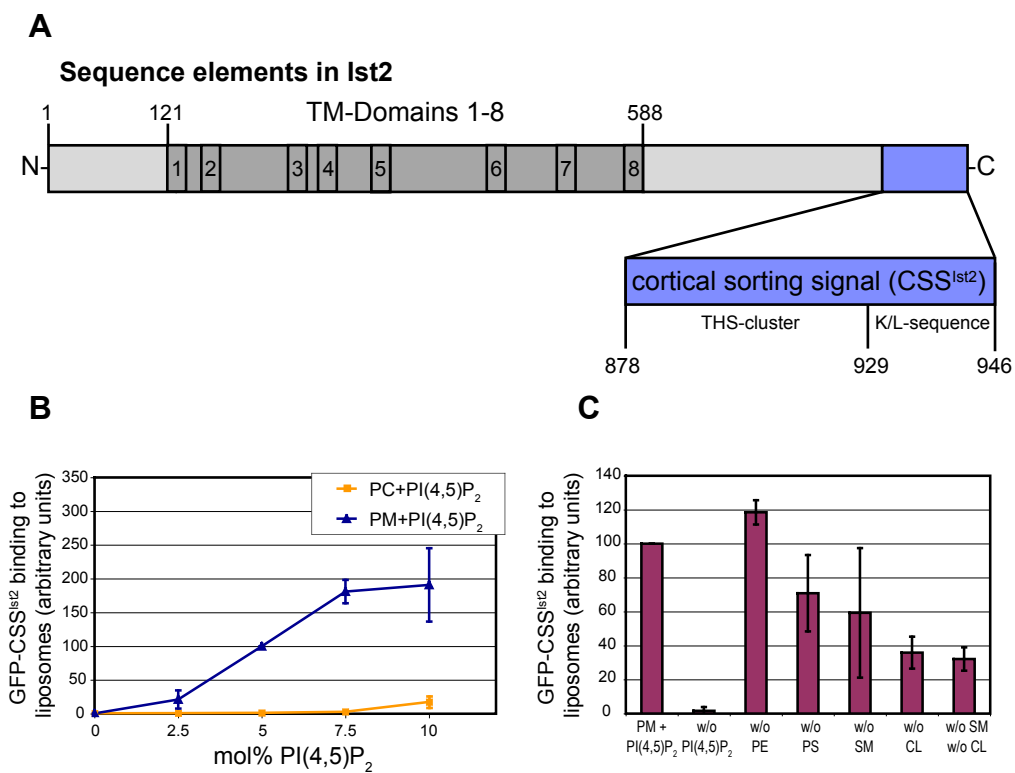


Fig. 1

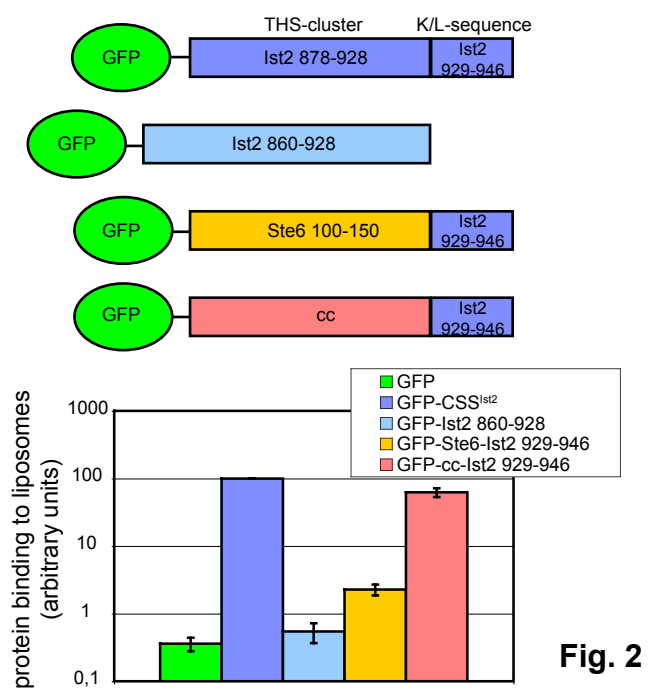
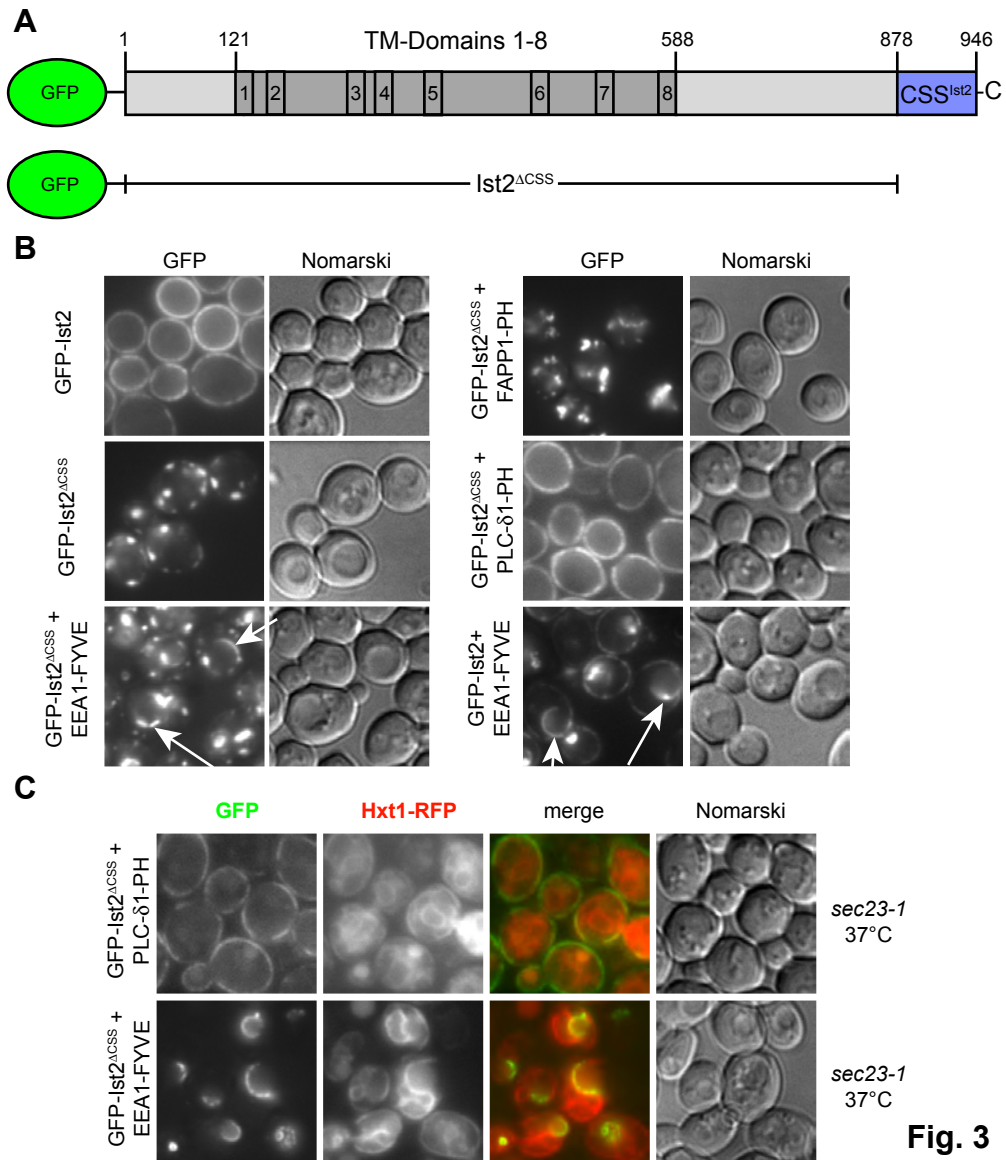


Fig. 2



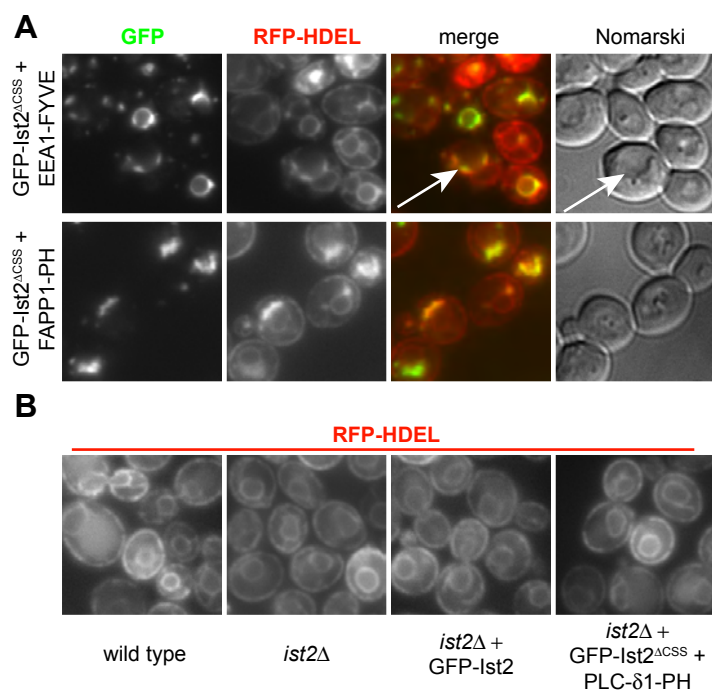


Fig. 4

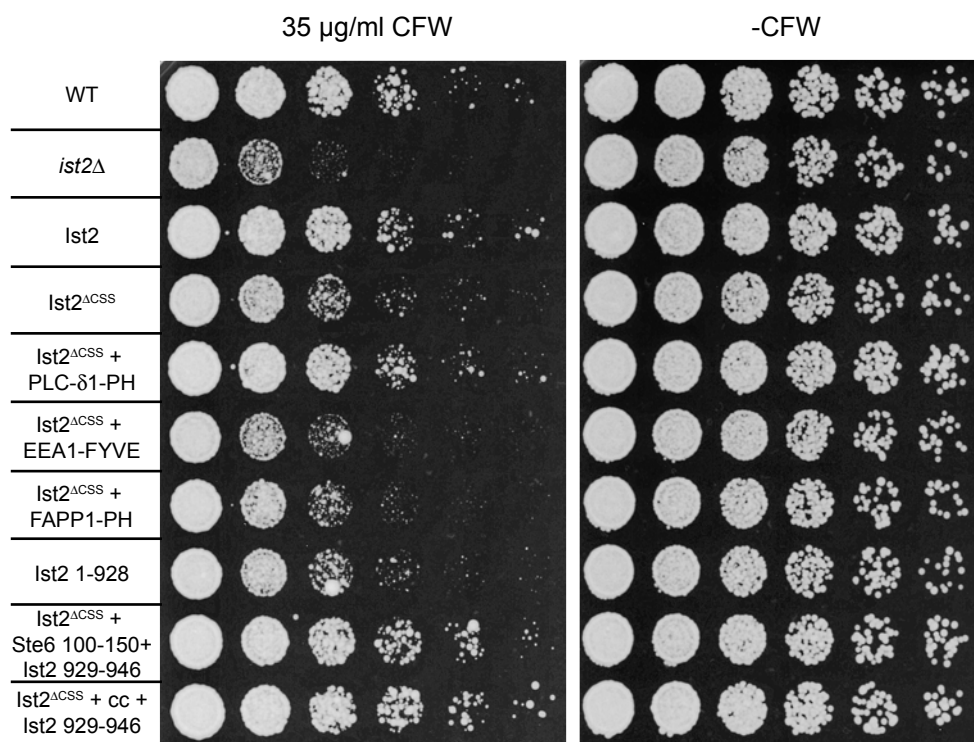


Fig. 5

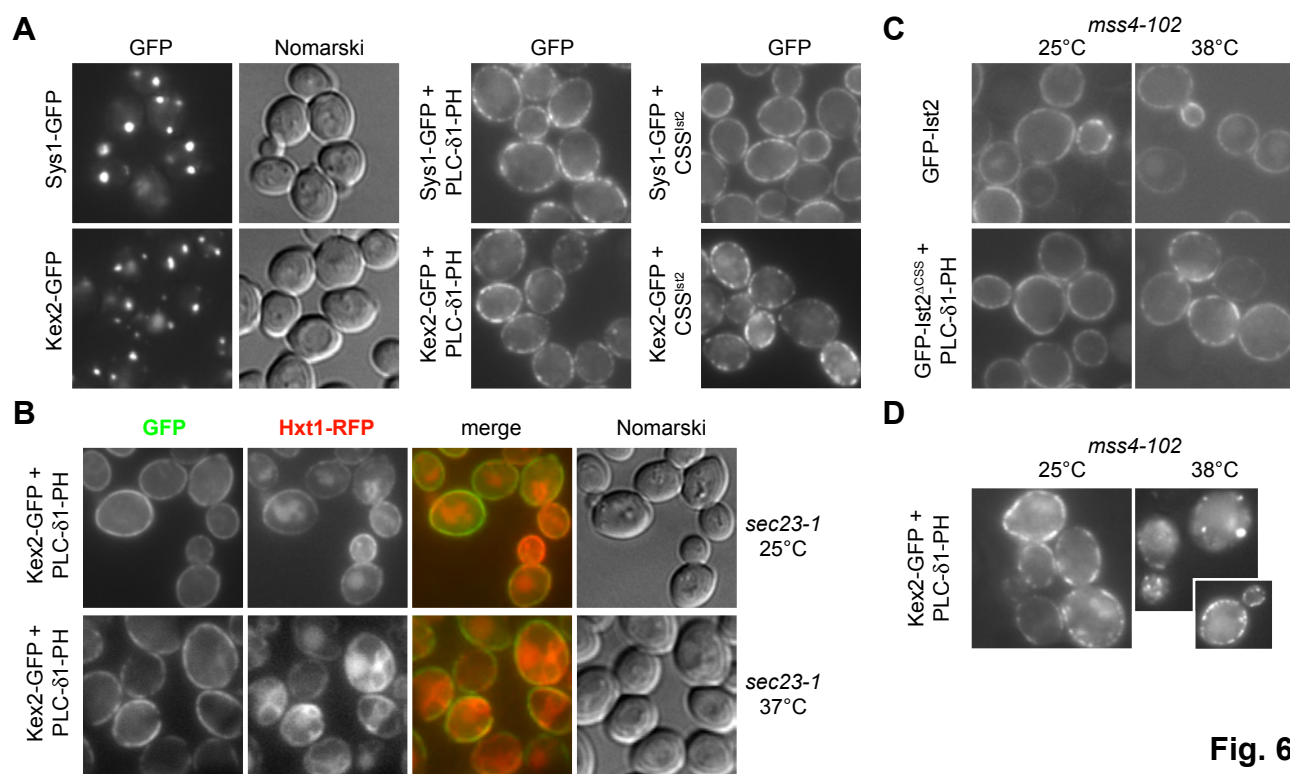


Fig. 6

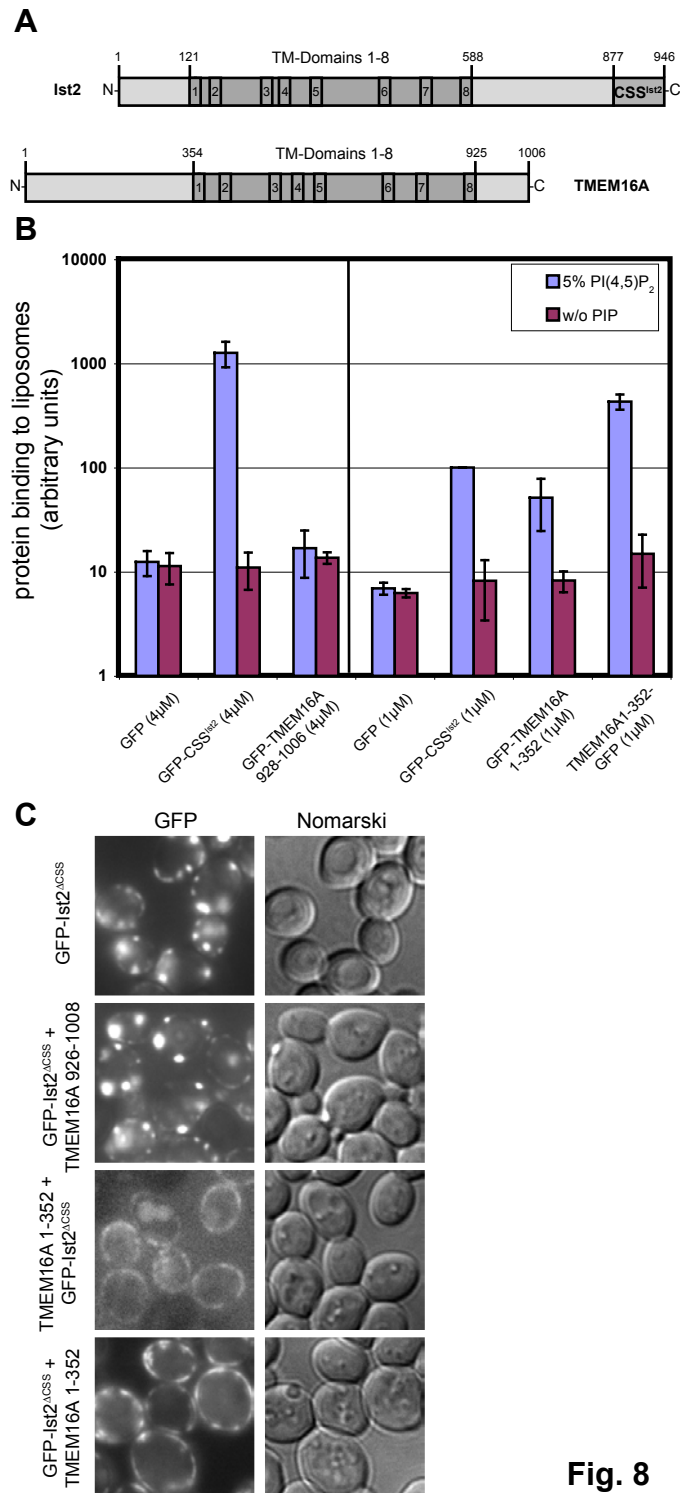


Fig. 8

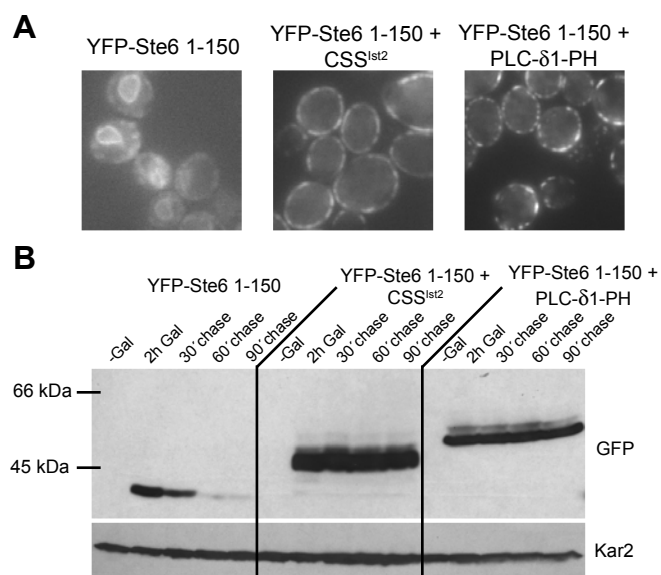


Fig. 9

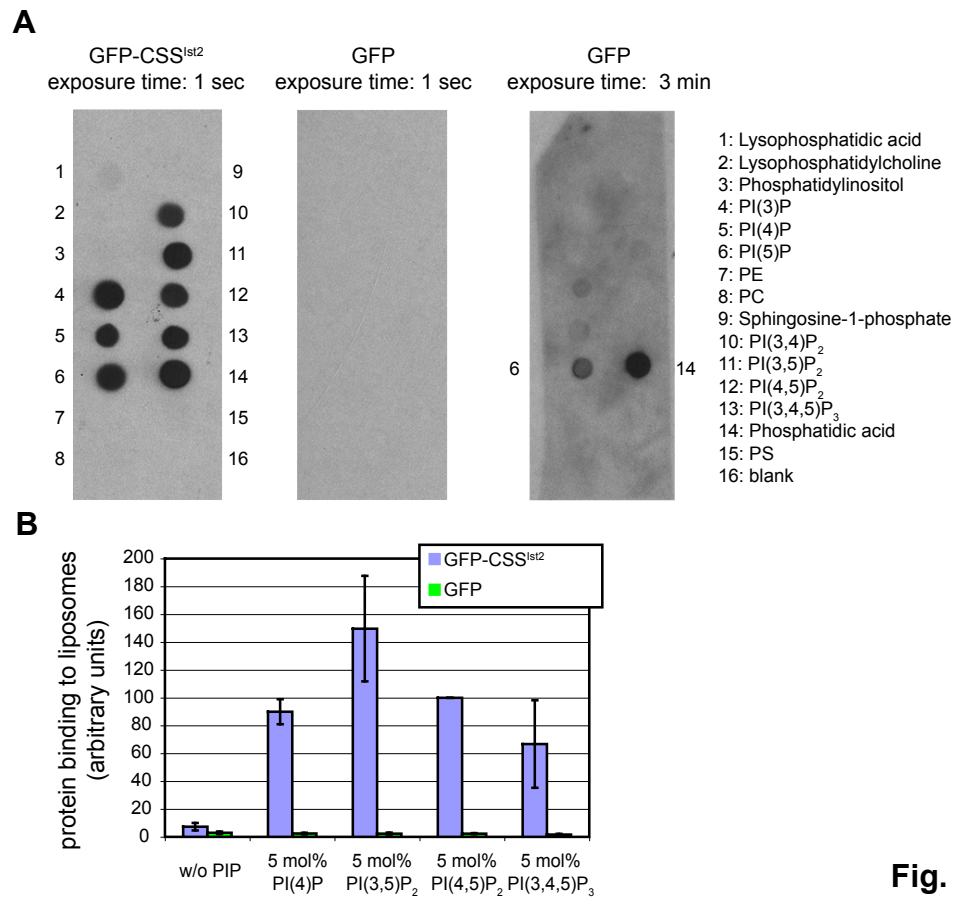


Fig. S1

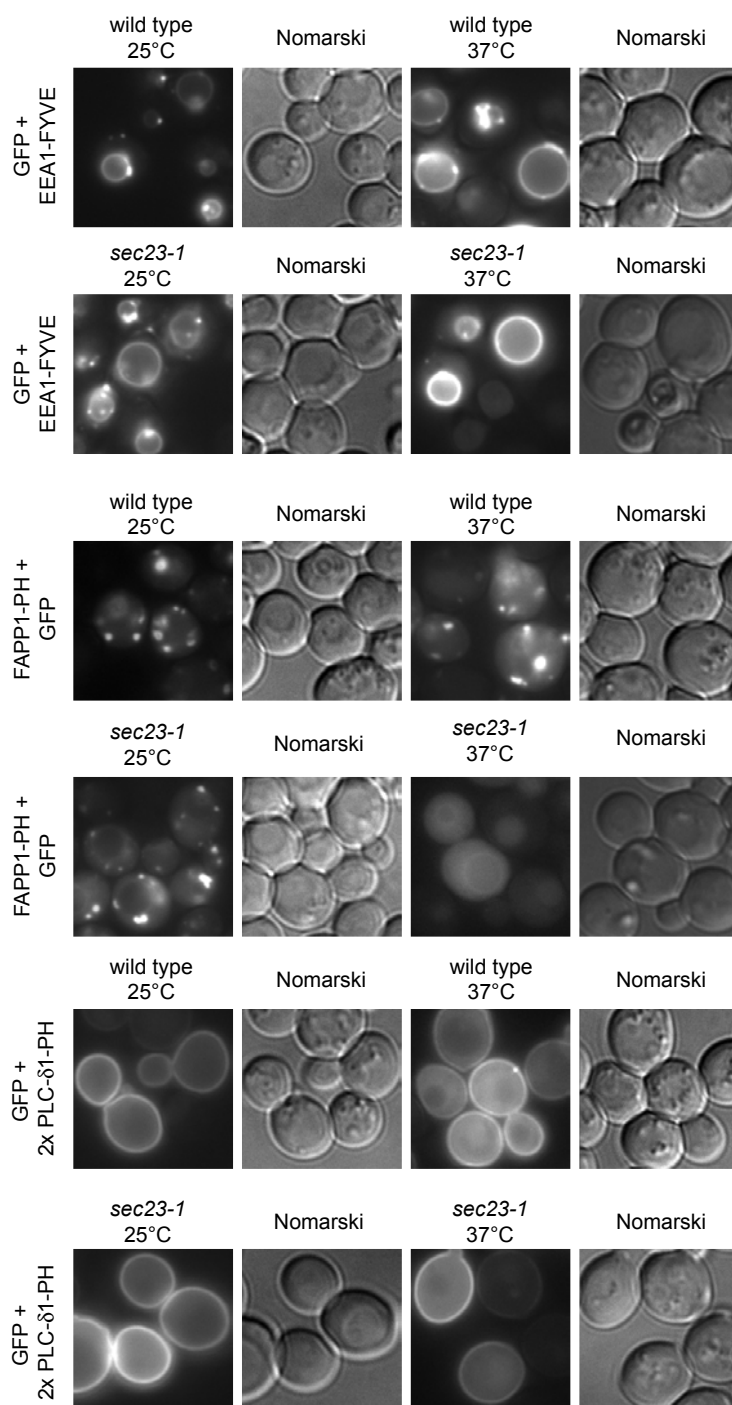


Fig. S2

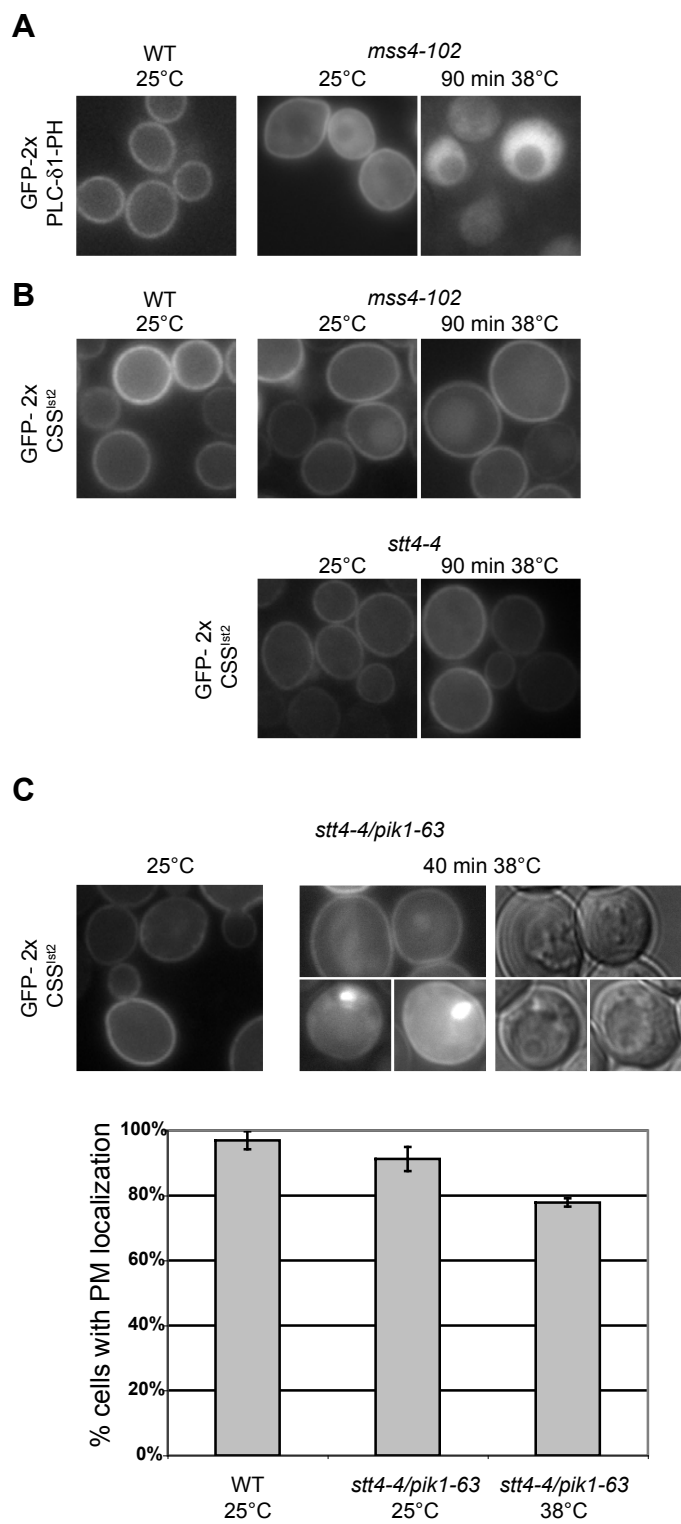


Fig. S3

Figure legends**Fig. 1: Binding of CSS^{Ist2} to PM-like liposomes depends on PI(4,5)P₂.**

(A) Cartoon of Ist2 protein with the positions of transmembrane domains indicated in boxes and the cortical sorting signal (CSS^{Ist2}) in blue. (B) Relative binding of recombinant GFP-CSS^{Ist2} to PM-like liposomes (PM) or to PC liposomes with increasing concentrations of PI(4,5)P₂. The binding of GFP-CSS^{Ist2} to PM-like liposomes with 5 mol% PI(4,5)P₂ was set to 100. (C) Relative binding of recombinant GFP-CSS^{Ist2} to PM-like liposomes containing 5 mol% PI(4,5)P₂ and to liposomes with an exchange of either PI(4,5)P₂, PE, PS, SM, CL or both SM and CL to PC.

Fig. 2: A multimeric form of the Ist2 K/L-sequence is sufficient for liposome binding.

Relative binding (in logarithmic scale) of recombinant GFP (green), GFP-CSS^{Ist2} (blue), GFP-Ist2 860-928 (light blue), GFP-Ste6 100-150 + Ist2 929-946 (yellow) and GFP-cc + Ist2 929-946 (pink) to PM-like liposomes containing 5 mol% PI(4,5)P₂. Ste6 100-150 corresponds to an intermembrane loop of Ste6. 'cc' depicts the tetramerization domain of the pLI Gcn4 leucine zipper.

Fig. 3: A PI(4,5)P₂-binding domain targets Ist2^{ΔCSS} to PM-associated ER domains.

(A) Cartoon of Ist2 and Ist2 lacking the CSS^{Ist2} (Ist2^{ΔCSS}). (B) Localization of GAL1-controlled GFP-Ist2, GFP-Ist2^{ΔCSS}, GFP-Ist2 with CSS^{Ist2} replaced by PLC-δ1-PH-, EEA1-FYVE-, or FAPP1-PH-domains and full-length Ist2 containing an additional EEA1-FYVE domain in *ist2Δ* cells at 25°C. Arrows indicate membranous structures partially surrounding vacuoles. (C) Fluorescence of GAL1-induced GFP-Ist2 with CSS^{Ist2} replaced by PLC-δ1-PH or the EEA1-FYVE domains in *sec23-1* at 37°C. GAL1-induced Hxt1-tandem-dimer RFP (labeled as Hxt1-RFP) serves as a control for the block of the secretory pathway.

Fig. 4: Expression of Ist2^{ΔCSS} + EEA1-FYVE leads to a zippering of ER and vacuole.

(A) Localization of the ER-marker DsRed-HDEL (labeled as RFP-HDEL) in *ist2Δ* cells expressing GAL1-induced GFP-Ist2 with CSS^{Ist2} replaced by EEA1-FYVE or FAPP1-PH at 25°C. Arrows indicate colocalization of the Ist2 fusion protein with dsRed-HDEL at the vacuole. (B) Localization of DsRed-HDEL in wild type-, *ist2Δ*-, and *ist2Δ* cells expressing GAL1-induced GFP-Ist2 and GFP-Ist2 with CSS^{Ist2} replaced by PLC-δ1-PH at 25°C.

Fig. 5: Ist2 and Ist2^{ACSS} + PLC- δ 1-PH rescue the CFW sensitivity of *ist2 Δ* cells. Five-fold serial dilutions of wild type-, *ist2 Δ* -, and *ist2 Δ* cells expressing genomically integrated Ist2, Ist2^{ACSS} and Ist2 with CSS^{Ist2} replaced by different lipid binding domains or multimerization elements under control of the *IST2* promoter were spotted on YPD plates and YPD plates containing 35 μ g/ml CFW. Cells were grown for two (w/o CFW) of three days (with CFW) at 25°C.

Fig. 6: The PI(4,5)P₂ binding PLC- δ 1-PH domain targets membrane proteins to the cell periphery. (A) Localization of *GAL1*-induced Sys1-GFP, Sys1-GFP + PLC- δ 1-PH, Sys1-GFP + CSS^{Ist2}, Kex2-GFP, Kex2-GFP + PLC- δ 1-PH, and Kex2-GFP + CSS^{Ist2} in wild type cells at 25°C. (B) Localization of *GAL1*-induced Kex2-GFP + PLC- δ 1-PH and Hxt1-tandem-dimer RFP in *sec23-1* cells at 25° or 37°C. (C) Localization of *GAL1*-induced GFP-Ist2 and GFP-Ist2^{ACSS} + PLC- δ 1-PH after 90 min induction in *mss4-102* cells at 25° and 38°C. (D) Localization of *GAL1*-induced Kex2-GFP + PLC- δ 1-PH in *mss4-102* cells after 90 min at 25° and 38°C. The insert shows a cell with only peripheral localization.

Fig. 7: GFP-Ist2^{ACSS} is recruited to the cell periphery in a concentration dependent manner via ER structures. (A) Localization of

GFP-Ist2 and GFP-Ist2^{ACSS} under the control of the *IST2* promoter (*pIST2*) in *ist2 Δ* cells at 25°C. Arrows indicate localization of GFP-Ist2^{ACSS} at the perinuclear ER. Localization of *GAL1*-induced GFP-Ist2^{ACSS} in *ist2 Δ* cells at 25°C after one and two hours in galactose. (B) Western blot of 0.25 OD₆₀₀ yeast total cell lysate from cells expressing GFP-Ist2 and GFP-Ist2^{ACSS} under the control of the *IST2* promoter and *GAL1*-induced GFP-Ist2^{ACSS}. Samples of *GAL1*-induced cells were taken 1 and 2 hours after induction. GFP-Ist2, GFP-Ist2^{ACSS} and Sec61 were detected with antibodies specific for GFP and Sec61. (C) Colocalization of 2 hours *GAL1*-induced GFP-Ist2^{ACSS} with DsRed-HDEL (RFP-HDEL), Kar2 (indirect immunofluorescence) and Sec7-DsRed (Sec7-RFP) in *ist2 Δ* cells at 25°C. (D) Localization of 2 hours *GAL1*-induced GFP-Ist2^{ACSS} in wild type and *ist2 Δ* cells at 25°C.

Fig. 8: The cytosolic N-terminal region of TMEM16A binds to PI(4,5)P₂ containing PM-like liposomes. (A) Cartoon of the Ist2 protein and its mammalian homologue TMEM16A. (B) Relative binding of 1 μ M recombinant GFP, GFP-CSS^{Ist2}, GFP-TMEM16A 1-352 and TMEM16A 1-352-GFP and 4 μ M recombinant GFP, GFP-CSS^{Ist2} and GFP-TMEM16A 928-1006 to PM-like liposomes with or without 5 mol% PI(4,5)P₂. TMEM16A 1-352-GFP contains between TMEM16A 1-352 and

GFP a (GGGGS)₂ spacer. **(C)** Localization of *GAL1*-induced GFP-Ist2^{ΔCSS}, GFP-Ist2^{ΔCSS}-TMEM16A 926-1008, TMEM16A 1-352-GFP-Ist2^{ΔCSS} and GFP-Ist2^{ΔCSS}-TMEM16A 1-352 in *ist2Δ* cells at 25°C.

Fig. 9: The PI(4,5)P₂ binding PLC-δ1-PH domain is a dominant sorting signal abolishing proteasomal degradation **(A)** Localization of *GAL1*-induced YFP-Ste6 1-150, YFP-Ste6 1-150 +

CSS^{Ist2} and YFP-Ste6 1-150 + PLC-δ1-PH in *ist2Δ* cells at 25°C. **(B)** Western blot of 0.5 OD₆₀₀ yeast total cell lysate from cells expressing galactose-induced YFP-Ste6 1-150, YFP-Ste6 1-150 + CSS^{Ist2} or YFP-Ste6 1-150 + PLC-δ1-PH. Samples were taken before induction (-Gal) and 2 h after induction (2 h Gal). Glucose was added and samples were taken after 30, 60, and 90 min. YFP-Ste6 proteins and Kar2 were detected with antibodies against GFP and Kar2.

Supplementary figures and tables

Fig. S1: CSS^{Ist2} binds to different PIPs in vitro. (A) Nitrocellulose membranes with immobilized purified lipids (“PIP-strips”) were incubated with 5 ng/ml recombinant GFP or GFP-CSS^{Ist2} according to the manufacturers protocol. Lipid bound recombinant protein was detected with GFP-specific antibodies by chemiluminescence. PIP-strips incubated with GFP were exposed for 1 s and for 3 min, whereas the PIP-strip incubated with GFP-CSS^{Ist2} was exposed for 1 s only. The weak binding of GFP and GFP-CSS^{Ist2} to phosphatidic acid may be a result of the presence of the His₆-tag. (B) Relative binding of recombinant GFP and GFP-CSS^{Ist2} to PM-like liposomes. Liposomes were either lacking PIPs or containing 5 mol% of PI(4)P, PI(3,5)P₂, PI(4,5)P₂, and PI(3,4,5)P₃. The binding of GFP-CSS^{Ist2} to PM-like liposomes containing 5 mol% PI(4,5)P₂ was set to 100.

Fig. S2: PI(3)P- and PI(4,5)P₂-localization are not affected in *sec23-1* mutant cells. Localization of constitutively expressed GFP-EEA1-FYVE, FAPP1-PH-GFP and GFP-2x PLC- δ 1-PH in wild type (*W303*) and *sec23-1* cells at 25°C and 37°C.

Fig. S3: Localization of GFP-2x CSS^{Ist2} in lipid kinase mutants. (A) Fluorescence of GFP-2x PLC- δ 1-PH in wild type cells at 25°C and in *mss4-102* cells at 25° and after 90 min at 38°C. (B) Fluorescence of GFP-2x CSS^{Ist2} in wild type cells at 25°C and in *mss4-102* and *stt4-4* cells at 25° and after 90 min at 38°C. (C) Fluorescence of GFP-2x CSS^{Ist2} in *stt4-4/pik1-63* cells at 25°C and after 40 min at 38°C. The number of cells with PM localization was quantified. Cells with the majority of the GFP fluorescence at the PM (38°C, top panel) and cells with PM and intracellular signal (38°C, bottom right) were counted as cells with PM localization. An example for a cells with intracellular signal only is shown at 38°C bottom left.

Table S1: Quantification of ER-fluorescence of wild type-, *ist2Δ*-, *ist2Δ* overexpressing *Ist2*-, and *ist2Δ* overexpressing *Ist2*^{ΔCSS} + PLC-δ-PH cells. The ratio of perinuclear fluorescence (PF) / cortical fluorescence (CF) was determined in unbudded cells (n > 100 for every strain, see Material and Methods). In cells with small and medium sized buds, which lack perinuclear ER, the ratio of CF in daughter cell / ER fluorescence in mother cell was determined (n > 100 for every strain).

	PF / CF unbudded cells	CF in daughter cells / ER fluorescence in mother cells
wild type	1,52 ± 0,28	0,412 ± 0,078
<i>ist2Δ</i>	1,48 ± 0,31	0,399 ± 0,062
<i>ist2Δ</i> + <i>Ist2</i>	1,51 ± 0,33	0,382 ± 0,083
<i>ist2Δ</i> + <i>Ist2</i> ^{ΔCSS} + PLC-δ1-PH	1,48 ± 0,25	0,405 ± 0,102

Table S2: Quantification of Kex2-GFP + PLC-δ1-PH localizations in wild type (n = 102) and *mss4-102* (n = 128) cells at 38°C after 90 min galactose induction.

	wild type 38°C	<i>mss4-102</i> 38°C
Cells with peripheral signal only	96%	14%
Cells with intracellular dots only	0%	72%
Intermediate phenotype	4%	14%

Table S3: Quantification of localizations of GFP-*Ist2* (n = 108) and GFP-*Ist2*^{ΔCSS} (n = 105) expressed under control of their endogenous UTRs and of one and two hours *GAL1*-induced GFP-*Ist2*^{ΔCSS} (n = 105 and n = 113) in *ist2Δ* cells at 25°C.

	GFP- <i>Ist2</i>	GFP- <i>Ist2</i> ^{ΔCSS}	GFP- <i>Ist2</i> ^{ΔCSS} 1 hour Gal	GFP- <i>Ist2</i> ^{ΔCSS} 2 hours Gal
Cells with peripheral patches only	100%	21%	18%	13%
Cells with peripheral dots only	0%	6%	24%	58%
Cells with intracellular and peripheral dots	0%	2%	44%	29%
Cells with perinuclear ER signal	0%	71%	14%	0%

Table S4: Plasmids used in this study

Name	Backbone	Insert	Source
	pRS424	pPRC1-GFP-EEA1-FYVE	P.Mayingier
	pRS426	pPRC1-FAPP1-PH-GFP	P.Mayingier
	pRS426	pPRC1-GFP-2x PLC- δ 1-PH	P.Mayingier
	YIPlac	ss-dsRED-HDEL	E.Schiebel (51)
pAF17	pRS306	pGAL1-yEmCitrine-STE6 1-150; NUF2 3'UTR	this study
pAF18	pRS303	pGAL1-KEX2-yEGFP3-CSS ^{IST2} ; IST2 3'UTR	(19)
pAF25	pRS306	pGAL1-yEmCitrine-STE6 1-150 + CSS ^{IST2} ; NUF2 3'UTR	this study
pAF47	pRS303	pGAL1-SYS1-yEGFP3; IST2 3'UTR	this study
pAF49	pRS303	pGAL1-SYS1-yEGFP3 + CSS ^{IST2} ; IST2 3'UTR	this study
pCJ149	pRS303	pGAL1-KEX2-yEGFP3; IST2 3'UTR	(19)
pKM81	pRS306	pIST2-IST2; IST2 3'UTR	this study
pKM154	pRS415	pADH1-SEC7-dsRed	(10)
pMF40	pET15b	His ₆ -EGFP (recombinant expression)	(10)
pMF61	pET15b	His ₆ -EGFP- CSS ^{IST2} (recombinant expression)	(10)
pMF93	pET15b	His ₆ -EGFP-STE6 100-150 + IST2 (929-946) (recombinant expression)	this study
pMF104	pRS306	pGAL1-yEGFP3-IST2; IST2 3'UTR	this study
pMF111	pET15b	His ₆ -EGFP-IST2 (860-928) (recombinant expression)	this study
pMF135	pET15b	His ₆ -EGFP-GCN4 Leucine Zipper-IST2 (929-946) (recombinant expression)	this study
pMF212	pRS306	pGAL1-yEGFP3-IST2 ^{ACSS} + PLC- δ 1-PH; IST2 3'UTR	this study
pMF216	pRS303	pGAL1-KEX2-yEGFP3 + PLC- δ 1-PH; IST2 3'UTR	this study
pMF218	pRS306	pGAL1-yEGFP3-IST2 ^{ACSS} + EEA1-FYVE; IST2 3'UTR	this study
pMF220	pRS306	pGAL1-yEGFP3-IST2 ^{ACSS} + FAPP1-PH; IST2 3'UTR	this study
pMF225	pRS306	pGAL1-yEGFP3-IST2 ^{ACSS} ; IST2 3'UTR	this study
pMF229	pRS306	pIST2-yEGFP3-IST2; IST2 3'UTR	this study
pMF231	pRS306	pGAL1-yEmCitrine-STE6 1-150 + PLC- δ 1-PH; NUF2 3'UTR	this study
pMF232	pRS306	pIST2-yEGFP3-IST2 ^{ACSS} ; IST2 3'UTR	this study
pMF234	pRS303	pGAL1-SYS1-yEGFP3 + PLC- δ 1-PH; IST2 3'UTR	this study
pMF259	pET15b	His ₆ -EGFP- TMEM16A 1-352 (recombinant expression)	this study
pMF260	pET15b	His ₆ -EGFP- TMEM16A 928-1006 (recombinant expression)	this study
pMF262	pRS306	pGAL1- TMEM16A 1-352 - yEGFP3-IST2 ^{ACSS} ; IST2 3'UTR	this study
pMF264	pRS306	pGAL1-yEGFP3-IST2 ^{ACSS} - TMEM16A 1-352; IST2 3'UTR	this study

pMF266	pRS306	pGAL1-yEGFP3-IST2 ^{ΔCSS} - TMEM16A 928-1006; IST2 3'UTR	this study
pMF272	pRS306	pGAL1-IST2 ^{ΔCSS} + EEA1-FYVE; IST2 3'UTR	this study
pMF275	pRS306	pGAL1-yEGFP3-IST2 + EEA1-FYVE; IST2 3'UTR	this study
pMF279	pRS306	pIST2-IST2 ^{ΔCSS} ; IST2 3'UTR	this study
pMF280	pRS306	pIST2-IST2 ^{ΔCSS} + PLC-δ1-PH; IST2 3'UTR	this study
pMF281	pRS306	pIST2-IST2 ^{ΔCSS} + EEA1-FYVE; IST2 3'UTR	this study
pMF282	pRS306	pIST2-IST2 ^{ΔCSS} + FAPP1-PH; IST2 3'UTR	this study
pMF284	pRS306	pIST2-IST2 1-928; IST2 3'UTR	this study
pMF286	pRS306	pIST2-IST2 ^{ΔCSS} + GCN4 Leucine Zipper + IST2 (929-946); IST2 3'UTR	this study
pMF288	pRS306	pIST2-IST2 ^{ΔCSS} + STE6 100-150 + IST2 (929-946); IST2 3'UTR	this study
pMF291	pRS304	ss-GFP-HDEL	this study
pMF301	pRS304	pADH1-mCherry-GOS1; NUF2 3'UTR	this study
pMF303	pRS316	pIST2-EGFP-2x CSS ^{Ist2} ; IST2 3'UTR	this study
pMF305	pET15b	His ₆ - TMEM16A 1-352 – (GGGGS) ₂ - EGFP (recombinant expression)	this study

3 Discussion

After translation, Ist2 rapidly accumulates at the cortical ER in a process independent of the *IST2* mRNA transport (Franz et al., 2007; Maass et al., 2009). The aim of this thesis was to find the molecular mechanism responsible for this rapid accumulation of Ist2 at the cortical ER. Two major questions have been addressed within this thesis:

(1) What mediates the rapid transport of Ist2 to the cell periphery and which interactions between cellular factors and Ist2 are necessary and sufficient for this accumulation?

In this thesis I was able to show that the CSS^{Ist2} acts as a lipid-binding motif, which binds to lipids, in particular PIPs, of the PM *in vivo* and *in vitro*. The CSS^{Ist2} can functionally be replaced by a PtdIns[4,5]P₂ binding PH domain from the δ_1 subunit of Phospholipase C. The chimeric protein localized under all tested conditions like wild type Ist2 and it complements cell wall defects of *ist2*-knockout strains, which are caused by calcofluor white. Both, CSS^{Ist2} and the PLC- δ_1 -PH domain, can redirect different Golgi- and ER localized membrane proteins efficiently to the cortical ER, dominant over ER export and proteasomal degradation.

(2) Which structural properties are present within the cortical sorting signal of Ist2? Which amino acids are really crucial for Ist2 transport and are they exposed in a certain domain fold?

I could show that for lipid binding the CSS^{Ist2} has to be present in a multimeric state. The K/L-sequence of the CSS^{Ist2} exposes an amphipathic helix, which is necessary for transport of Ist2. Mutations within the CSS^{Ist2}, which impair the basicity of the K/L-sequence and the structure of the amphipathic helix, lead to transport defects to cell periphery (Maass et al., 2009). A CSS^{Ist2} carrying such mutations largely lacks lipid-binding properties.

3.1 Lipid mediated sorting of integral membrane proteins

3.1.1 The cortical sorting signal of Ist2 is a lipid-binding motif

The CSS^{Ist2} is necessary and sufficient for the localization of Ist2 in patch-like structures in the cell periphery (Franz et al., 2007). It can redirect other integral membrane proteins to the cell periphery in a dominant manner (Franz et al., 2007). In order to test, where the soluble CSS^{Ist2} localizes and whether it binds to factors in the cell periphery, it was expressed as a GFP-fusion protein. GFP-CSS^{Ist2} localized to the cytosol, to intracellular structures and to a smooth ring in the cell periphery (Maass et al., 2009, Fig. 6A, 6B).

The intracellular structures GFP-CSS^{Ist2} localized to could be identified as nucleoli, as this portion of GFP-CSS^{Ist2} colocalized with the nucleolar marker RFP-Nop1 (from Ed Hurt, data not shown). GFP-CSS^{Ist2} is extremely basic (see Fig. 6). Therefore, the basic amino acids might act as a nuclear localization signal (Makkerh et al., 1996) and GFP-CSS^{Ist2} could enter the nucleus, where it might bind via its positive residues to negatively charged RNA.

Although translated on cytosolic ribosomes without a transmembrane region, GFP-CSS^{Ist2} partly localized to a smooth ring in the cell periphery. This structure can either be the cortical ER or the PM. However, the cortical ER of yeast does not appear as a smooth ring, but rather as peripheral patches (Prinz et al., 2000). In contrast, cytosolic proteins, which are recruited to the yeast PM, appear as a smooth ring, as shown for the GFP-labeled PtdIns[4,5]P₂ binding PH domain from the δ_1 subunit of Phospholipase C (Levine and Munro, 2002). Therefore, it is most likely that GFP-CSS^{Ist2} *in vivo* binds to the PM.

The membrane binding properties of GFP-CSS^{Ist2} could be confirmed by fractionating cells expressing GFP-CSS^{Ist2} into the cytosolic supernatant and the pellet fraction containing the membranes. GFP-CSS^{Ist2} partly was found in the pellet fraction, the membrane association was confirmed via floatation of GFP-CSS^{Ist2} in a sucrose step gradient (Maass et al., 2009, Fig. 6C, S14A).

Which factor of the PM does the GFP-CSS^{Ist2} bind to? Biological membranes are made of lipid bilayers with a variety of integral or peripheral membrane proteins. In order to test whether GFP-CSS^{Ist2} binds to proteins or to lipids of the PM, I performed a biochemical *in vitro* approach. In this experiment the binding of recombinant GFP-CSS^{Ist2} to yeast microsomes was tested. GFP-CSS^{Ist2} bound to yeast microsomes isolated from *ist2 Δ* cells. This binding occurred as well, when the microsomes were pretreated with proteinase K (Maass et al., 2009, Fig 7A). Under these conditions the proteins on the surface of the yeast microsomes were completely digested, as judged from Western-Blot against the polytopic membrane protein Sec61 (Maass et al., 2009, Fig 7A). This protein-independent binding of GFP-CSS^{Ist2} to isolated yeast microsomes suggests that lipids mediate the interaction between the CSS^{Ist2} and membranes.

To confirm the binding of GFP-CSS^{Ist2} to lipids of the PM, a FACS-based liposome-binding assay (Temmerman et al., 2008; Temmerman and Nickel, 2009) was used. GFP-CSS^{Ist2} showed a binding to liposomes with a PM-like lipid composition, whereas GFP did not (Maass et al., 2009, Fig 7B, 7C). This binding was strongly dependent on the presence of PIPs and a PM-like lipid background (Fischer et al., 2009, Fig. 1B). An interaction between the negatively charged PIPs (McLaughlin and Murray, 2005) and the GFP-CSS^{Ist2} can thereby be explained via the high number of basic residues within the CSS^{Ist2} (see Fig. 6). In fact, the membrane binding of GFP-CSS^{Ist2} is salt dependent and therefore electrostatic (Maass et al., 2009, Fig S14B), indicating that charged residues in GFP-CSS^{Ist2} facilitate the binding to the PIPs of the PM.

However, the binding to PM-like liposomes containing different PIPs revealed a rather promiscuous interaction with PtdIns[4]P, PtdIns[3,5]P₂, PtdIns[4,5]P₂ and PtdIns[3,4,5]P₃, which was confirmed via binding experiments to immobilized lipids (Fischer et al., 2009, Fig. S1).

Different PIPs are enriched in particular organelles, serving as markers for organelle identity (Fig. 4, Behnia and Munro, 2005; Di Paolo and De Camilli, 2006; Munro, 2002; Strahl and Thorner, 2007). Despite interacting promiscuously with different PIPs *in vitro*, GFP-CSS^{Ist2} localizes to the PM *in vivo*. Binding of GFP-CSS^{Ist2} to PIP-containing liposomes, however, strongly depends on a PM-like lipid composition of the liposomes and is impaired by the lack of the PM components PtdSer, sterols and sphingolipids (Fischer et al., 2009, Fig. 1B). This might explain, why *in vivo* the GFP-CSS^{Ist2} localizes to the PM, but not to other PIP-containing organelles.

3.1.2 Transport to subdomains of the ER is a novel transport mechanism

The finding that the CSS^{Ist2} binds to PIPs in a PM-like lipid environment raises the question, whether CSS^{Ist2} *in vivo* also binds PIPs at the PM and whether this process then mediates the sorting of the full-length Ist2 protein to the cell periphery. In order to test, whether the lipid-binding domain can be sufficient to mediate the transport of the Ist2 protein to domains of the cortical ER, the CSS^{Ist2} was replaced by different characterized lipid-binding domains. The domains used in this swapping-experiments bind to PtdIns[4]P at the Golgi apparatus (Stefan et al., 2002), PtdIns[3]P at the vacuole (Burd and Emr, 1998) and PtdIns[4,5]P₂ at the PM (Stefan et al., 2002). Replacement of CSS^{Ist2} with the PtdIns[4,5]P₂ binding PH domain from the δ_1 subunit of Phospholipase C (PLC- δ_1 -PH) resulted in a peripheral patch-like localization of Ist2 1-877 + PLC- δ_1 -PH (Ist2^{ACSS} + PLC- δ_1 -PH) in *ist2* Δ cells and in *sec23^{ts}* cells at both restrictive and permissive temperature (Fischer et al., 2009, Fig. 3). This localization was indistinguishable from wild type Ist2 under similar conditions. Moreover, Ist2^{ACSS} + PLC- δ_1 -PH and wild type Ist2 complemented cell wall defects of *ist2* Δ cells induced by the drug calcofluor white (Elorza et al., 1983) (Fischer et al., 2009, Fig. 5). This establishes that a protein domain that binds to PtdIns[4,5]P₂ at the PM can replace the CSS^{Ist2} in transport assays and with respect to calcofluor white sensitivity.

The chimeric protein Ist2^{ACSS} + PLC- δ_1 -PH lacks the CSS^{Ist2} and the stem-loop element within the mRNA sequence, which confers the localization of the mRNA to the daughter cell (see 1.4.4). Because the mRNA of Ist2^{ACSS} + PLC- δ_1 -PH is not localized, the finding that the PLC- δ_1 -PH domain can replace the CSS^{Ist2} is limited to the transport of proteins in the mother cell. The CSS^{Ist2} is necessary and sufficient for the accumulation of Ist2 and reporter proteins at the cell periphery (Franz et al., 2007). After translation at the

perinuclear ER of mother cells, Ist2 would use its CSS^{Ist2} as a PM-lipid-binding motif, which places the protein at domains of the cortical ER closely adjacent to the PM. Whether also in daughter cells a lipid binding domain can be sufficient to mediate the transport of Ist2 to domains of the cortical ER, cannot be tested with this experimental setup. However, GFP-CSS^{Ist2} partly localizes to the PM in mother cells, as well as in daughter cells (Maass et al., 2009, Fig. 6A, 6B). Therefore, it is likely that the affinity of the CSS^{Ist2} to PM lipids might also be sufficient to mediate the peripheral accumulation of Ist2 in daughter cells. This process could even be facilitated by the local translation of Ist2 at the cortical ER of daughter cells under wild type conditions.

In order to test, whether the localization of Ist2 depends on a PIP-binding domain specific for PM-lipids, the CSS^{Ist2} was also replaced with the PtdIns[4]P binding PH domain from the four-phosphate adaptor protein 1 (FAPP1-PH) and the PtdIns[3]P binding FYVE domain from the human early endosome antigen (EEA1-FYVE). Ist2^{ACSS} + FAPP1-PH localized to ill-defined dots, which recruit the ER-marker RFP-HDEL (Fischer et al., 2009, Fig. 3B, 4A). Ist2^{ACSS} + EEA1-FYVE localized to dot-like structures and partially to the vacuole (Fischer et al., 2009, Fig. 3B). However, the vacuolar localization did not depend on transport along the secretory pathway (Fischer et al., 2009, Fig. 3C) and was characterized by a recruitment of ER to these domains (Fischer et al., 2009, Fig. 4A). This establishes that Ist2^{ACSS} + EEA1-FYVE localizes within a subdomain of the ER with the EEA1-FYVE domain binding to PtdIns[3]P at the vacuolar membrane. This then leads to a massive recruitment of ER to the vacuolar membrane (Fischer et al., 2009, Fig. 4A). However, the interaction between Ist2^{ACSS} + EEA1-FYVE and the vacuole, which leads to a zippering between both ER and vacuole, is clearly different from the described nuclear-vacuolar junctions in yeast. These are established via a protein-protein interaction of the ER protein Nvj1 and the vacuolar protein Vac8 (Kvam and Goldfarb, 2006; Pan et al., 2000). These NVJs are not accompanied by a massive ER recruitment to the vacuole as seen for the protein-lipid interaction between Ist2^{ACSS} + EEA1-FYVE and vacuolar PtdIns[3]P. Moreover, Nvj1-GFP does not colocalize with RFP-Ist2^{ACSS} + EEA1-FYVE (data not shown).

These assays establish that Ist2^{ACSS} can be sorted into different subcompartments of the ER via different lipid-binding domains. This mechanism is dependent on an interaction of a transmembrane spanning protein with a lipid on ER-adjacent organelles. In the context of the Ist2 protein the CSS^{Ist2} acts as a lipid-binding motif interacting with PIPs at the PM. This leads to the recruitment of Ist2 to PM-adjacent domains of the cortical ER.

Only very few examples of integral membrane proteins that bind to lipids via cytosolic motifs or domains, have been described in the literature. In mammalian cells synaptotagmins are integral membrane proteins present on the surface of synaptic vesicles, where they trigger the fusion of synaptic vesicles with the PM. Synaptotagmins possess two C2 domains, of which the C-terminal C2B domain binds to PtdIns[4,5]P₂ and

PtdIns[3,4,5]P₃ at the PM, thereby increasing the speed of vesicle fusion (Bai et al., 2004; Schiavo et al., 1996). The localization of synaptotagmin IV depends on the C2B domain, although it is unclear, whether PIP-binding directly evokes this localization (Fukuda et al., 2001). In yeast the integral type II membrane protein Eft1 binds PtdIns[3]P via a polybasic cluster of lysine residues near its transmembrane region (Wurmser and Emr, 2002). Eft1 regulates the cytoplasm-to-vacuole targeting pathway via its lipid-binding motif. Whether the localization of Eft1 depends on PIP binding, is not clear. The yeast ER protein Scs2, which is involved in cortical ER inheritance (Loewen et al., 2007), binds PtdIns[4]P *in vitro*. However, in mutants lacking PIP-binding activity the localization is not changed compared to wild type Scs2 (Kagiwada and Hashimoto, 2007).

Therefore, Ist2 is the first described example of an integral membrane protein localizing to subcompartments of the ER via a lipid-binding motif. This novel sorting pathway depends on the interaction with lipids of other organelles adjacent to the ER. A polybasic motif binding to PIPs of the PM places the transmembrane protein Ist2 to subdomains of the cortical ER.

In order to test the hypothesis that lipid mediated protein sorting can be a general mechanism for partitioning transmembrane proteins within the ER, the Golgi-localized reporter proteins Kex2 and Sys1 were tagged with PLC- δ_1 -PH on their cytosolic C-terminus. Kex2-GFP + PLC- δ_1 -PH and Sys1-GFP + PLC- δ_1 -PH both accumulated efficiently at the cell periphery (Fischer et al., 2009, Fig. 6A). As shown for the CSS^{Ist2} (Franz et al., 2007), the PLC- δ_1 -PH domain acts dominant over the DXE ER-export signal of Sys1 (Votsmeier and Gallwitz, 2001) and the tyrosine Golgi retention signal of Kex2 (Wilcox et al., 1992). In order to test, whether the transport into subdomains of the ER can also stabilize unstable proteins, a C-terminally truncated version of the ABC transporter Ste6 was used. Ste6 1-150 showed a weak accumulation at perinuclear and cortical ER and was rapidly degraded (Fischer et al., 2009, Fig. 9). However, when fusing CSS^{Ist2} or PLC- δ_1 -PH to the cytosolic C-terminus of Ste6 1-150, these fusion proteins were efficiently redirected to the cell periphery. Moreover, Ste6 1-150 (Fischer et al., 2009, Fig. 9) was massively stabilized as fusion protein with CSS^{Ist2} or PLC- δ_1 -PH. This establishes that a lipid-binding domain can confer a bypass of protein degradation to reporter proteins.

An interaction with PtdIns[4,5]P₂ at the PM resulted in an accumulation of the reporter proteins Kex2, Sys1 and Ste6 1-150 at the cortical ER, bypassing ER export and proteasomal degradation. A binding to lipids of adjacent organelles can be a dominant and general mechanism for protein distribution into ER subdomains, with Ist2 being the first identified example using this mechanism.

3.2 Signals and factors involved in Ist2 sorting

The CSS^{Ist2} acts as a lipid-binding motif interacting with PIPs at the PM. Moreover, it can be replaced by a protein domain, which binds to PtdIns[4,5]P₂ at the PM. This raises the question, whether an interaction between the CSS^{Ist2} and PIPs at the PM is the only determinant for the localization of Ist2 at domains of the cortical ER. In order to test this hypothesis, Ist2 was localized in the temperature sensitive lipid kinase mutants *mss4-102* (*mss4^{ts}*), *stt4-4* (*stt4^{ts}*) and *stt4-4/pik1-63* (*stt4^{ts}/pik1^{ts}*), in which the PM pools of PtdIns[4,5]P₂, PtdIns[4]P or both are largely depleted (Audhya et al., 2000; Stefan et al., 2002). However, in all of these mutants the localization of Ist2 remained unchanged (Fischer et al., 2009, Fig. 6C, data not shown). Therefore, the interaction of the CSS^{Ist2} with PIPs at the PM is not the only determinant for Ist2 localization. In order to test, whether additional information in Ist2^{ACSS} targets the protein to domains of the cortical ER, Ist2^{ACSS} + PLC-δ₁-PH was localized in *mss4^{ts}* cells. Under restrictive conditions, which lead to a 10-fold reduction of PtdIns[4,5]P₂ at the PM (Stefan 2002), Ist2^{ACSS} + PLC-δ₁-PH still localized at the PM. However, this was not the case for Kex2-GFP + PLC-δ₁-PH, which localized to dot-like structures in *mss4^{ts}* cells at 38°C (Fischer et al., 2009, Fig. 6D). The localization of Kex2-GFP + PLC-δ₁-PH is sensitive to a depletion of PtdIns[4,5]P₂ at the PM, whereas the localization of Ist2^{ACSS} + PLC-δ₁-PH is not. This established that additional signals in Ist2^{ACSS}, which mediate the localization of Ist2 at the cell periphery, have to be present.

Overexpressed GFP-Ist2^{ACSS} localizes to dot-like structures in the cell periphery. These structures colocalize with the ER-Marker RFP-HDEL (Fischer et al., 2009, Fig. 7A, C). This dot-like localization leads to two conclusions: (1) the lack of the CSS^{Ist2} leads to a localization defect. The protein is no longer distributed in peripheral patches, but in dots. Moreover, Ist2^{ACSS} can only partially rescue the calcofluor sensitivity of *ist2Δ* cells as compared to full length Ist2 (Fischer et al., 2009, Fig. 5). This establishes that Ist2^{ACSS} is not a functional protein with respect to transport assays and calcofluor sensitivity. The CSS^{Ist2} is necessary for the sorting of Ist2^{ACSS} to domains of the cell periphery. This is consistent with the finding that the CSS^{Ist2} is a dominant signal in transport assays with other integral ER or Golgi membrane proteins (Franz et al., 2007). (2) Even without the presence of the CSS^{Ist2}, overexpressed Ist2^{ACSS} does localize to the cell periphery and partially rescues the calcofluor sensitivity of *ist2Δ* cells. This establishes that additional signals in Ist2^{ACSS} do contribute to the sorting of Ist2 to subdomains of the ER. Ist2^{ACSS} colocalizes with the ER-Marker RFP-HDEL, but not with Golgi specific markers (Fischer et al., 2009, Fig. 7C). Ist2^{ACSS} even recruits RFP-HDEL into the dot-like structures in the cell periphery. This establishes that Ist2^{ACSS} is not exported from the ER, but leads to a proliferation of ER structures in the cell periphery. However, the ER luminal chaperon Kar2 is largely excluded from these dots, pointing out that Ist2^{ACSS} most probably is not

aggregated, but rather a functional protein. The proliferation of peripheral ER structures has previously been described for overexpression of a subunit of the HMG-CoA-Reductase, Hmg2 (Koning et al., 1996).

The strong proliferation of peripheral ER is dependent on the expression level of Ist2^{ACSS} (Fischer et al., 2009, Fig. 7A, 7B). In this case a high concentration of Ist2^{ACSS}, which may be supported by multimerization (see also 3.3.2), might favor an interaction of cytoplasmic domains in Ist2^{ACSS}, subsequently driving the formation of membrane stacks in the cell periphery. At least in mammalian cells such concept for the proliferation of organized stack-like sER structures was described. These structures can be generated via overexpression of ER resident membrane proteins, which undergo weak homodimeric interactions with their cytoplasmic domains (Snapp et al., 2003). These cytosolic low affinity interactions can be enhanced by fusion of GFP, which itself has the potential to undergo homodimerization (Zacharias et al., 2002; Snapp et al., 2003).

At this point it remains unclear, which parts of Ist2^{ACSS} are involved in the accumulation of Ist2 at domains of the cortical ER. The exact mapping of the additional sorting signals in Ist2^{ACSS} turned out to be rather difficult. GFP-Ist2^{ACSS} shows multiple phenotypes dependent on the expression level (Fischer et al., 2009, Table S3). Further truncations in N- and C-terminal regions of Ist2^{ACSS} for all constructs led to mixed phenotypes with protein at the perinuclear ER and in intracellular and peripheral dot-like structures (data not shown). However, with this experimental setup that relies on overexpression of these constructs it remained elusive, whether these observed phenotypes depend on expression level or on truncations in N- and C-termini of Ist2^{ACSS}. In initial experiments overexpressed Ist2 120-591, which lacks both cytosolic termini, also partly localized in peripheral dots (data not shown), suggesting that some targeting information is present within the transmembrane regions of Ist2. The partition of certain proteins into ER subdomains at least in mammalian cells depends solely on the length of their transmembrane regions (Ronchi et al., 2008). Whether this is also true for Ist2 120-591, has not been investigated in further detail. The length of the transmembrane regions within Ist2 120-591 might contribute to the peripheral targeting of the Ist2 protein. In addition, Ist2 120-591 might carry signals directly interacting with additional factors in the cell periphery.

The CSS^{Ist2} can, in transport assays and with respect to calcofluor white sensitivity, functionally be replaced by a protein domain, which binds to PtdIns[4,5]P₂ at the PM. Moreover, an additional sorting signal in Ist2^{ACSS} contributes to the localization of Ist2. *In vitro* the interaction of GFP-CSS^{Ist2} with liposomes does not depend on a particular PIP but is rather promiscuous, as long as a PIP of whatever kind is present in a PM-like lipid background of the liposomes. *In vivo* GFP-CSS^{Ist2} partly localizes to the PM (Maass et al., 2009, Fig. 6A) and the dimeric GFP-2x CSS^{Ist2} localizes exclusively to the PM (Fischer et al., 2009, Fig. S3B). The major PIPs at the PM are PtdIns[4,5]P₂ and PtdIns[4]P (see 1.3.4). Is the CSS^{Ist2} a PIP-binding motif, which is sufficient to mediate the accumulation

of Ist2 at domains of the cortical ER? In order to test, whether the PM localization of GFP-2x CSS^{Ist2} depends on the presence of PIPs at the PM, GFP-2x CSS^{Ist2} was localized in the lipid kinase mutants *mss4^{ts}*, *stt4^{ts}* and *stt4^{ts}/pik1^{ts}*. Under restrictive conditions in the *mss4^{ts}* and the *stt4^{ts}* cells the PM localization of GFP-2x CSS^{Ist2} was not diminished (Fischer et al., 2009, Fig. S3B). However, in 22% of the *stt4^{ts}/pik1^{ts}* cells at the restrictive temperature GFP-2x CSS^{Ist2} was delocalized into the cytoplasm and an intracellular dot, which might correspond to the nucleolus (Fischer et al., 2009, Fig. S3C). Under these conditions in a similar temperature sensitive mutant the cellular levels of PtdIns[4,5]P₂ and PtdIns[4]P were decreased by 90% as compared to wild type cells (Audhya et al., 2000). These experiments show that neither PtdIns[4,5]P₂ nor the PM pool of PtdIns[4]P are solely responsible for the localization of GFP-2x CSS^{Ist2} at the PM. However, depleting both PIPs at the PM leads to a mild effect on GFP-2x CSS^{Ist2} localization. Therefore, PM PIPs are indeed one determining factor in the PM localization of the CSS^{Ist2}, but an interaction with PIPs is not the only determinant for its localization. Additional factors, which keep GFP-2x CSS^{Ist2} bound to the PM, have to be present under conditions with PIPs largely depleted from the PM. Although in *stt4^{ts}/pik1^{ts}* cells at restrictive temperature the levels of PtdIns[4,5]P₂ and PtdIns[4]P are largely decreased, GFP-2x CSS^{Ist2} still is bound to the PM in 78% of the cells. As both negatively charged PIPs, PtdIns[4,5]P₂ and PtdIns[4]P, have to be depleted to show a delocalization of GFP-2x CSS^{Ist2} in some cells, one might speculate, whether the polybasic sorting signal of Ist2 is also *in vivo* rather unspecific for different PIPs as shown *in vitro*. Negatively charged PtdSer is highly abundant in the inner leaflet of the yeast PM and might in the case of decreased PtdIns[4,5]P₂ and PtdIns[4]P keep GFP-2x CSS^{Ist2} at the PM.

In vitro data show a rather promiscuous interaction between the CSS^{Ist2} and different PIPs (Fischer et al., 2009, Fig. S1). However, even under conditions with depleted PM PIPs GFP-2x CSS^{Ist2} does not delocalize from the PM to other organelles, which are still enriched in PIPs (e.g. PtdIns[3]P at the vacuole). Since the binding of GFP-2x CSS^{Ist2} to PIP containing liposomes is strongly dependent on a PM-like lipid composition, the PM might be favored over other PIP containing organelles because of the recognition of multiple binding partners at the PM.

However, whether under conditions with depleted PIPs the GFP-2x CSS^{Ist2} directly binds to lipids (e.g. PtdSer) or proteins at the PM, whether the remaining PIPs might be sufficient to confer PM localization or whether the CSS^{Ist2} itself might penetrate the PM via structural motifs like an amphipathic helix (see 3.3.1), remains unclear at this point.

Taken together, multiple signals in Ist2 seem to be involved in the localization at domains of the cortical ER. But which of these signals are the most crucial ones for Ist2 transport and function? Ist2^{ΔCSS} localizes to the general ER, when expressed weakly and to peripheral dot-like structures when overexpressed (Fischer et al., 2009, Fig. 7A, 7B). *ist2Δ* cells expressing Ist2^{ΔCSS} are more sensitive against calcofluor white than cells expressing

wild type Ist2. Moreover, amino acid mutations, which lead to a mislocalization of the protein, could up to this point exclusively been found in the K/L sequence of the CSS^{Ist2} (Maass et al., 2009). This establishes that a functional CSS^{Ist2} is necessary for the accumulation of Ist2 at domains of the cortical ER. Moreover, in other ER and Golgi localized reporter proteins the CSS^{Ist2} was found to be a dominant signal for the targeting of these reporters to domains of the cortical ER (Franz et al., 2007). In the Ist2 protein the CSS^{Ist2} can functionally be replaced by the PLC- δ 1-PH domain, which binds to PtdIns[4,5]P₂ at the PM. However, PLC- δ 1-PH associates to PM-like liposomes containing PtdIns[4,5]P₂ with a K_D of 2.7 μ M as compared to 12.1 μ M for the CSS^{Ist2}. The high-affinity interaction of PLC- δ 1-PH with the PM might therefore mimic the function of the CSS^{Ist2} with respect to transport assays and resistance to calcofluor white. Nevertheless interaction with PIPs is one function of the CSS^{Ist2}, but other factors contribute to the peripheral localization of GFP-2x CSS^{Ist2} as well. *In vivo*, multiple interaction partners of the CSS^{Ist2} might stabilize or increase the rather low affinity interaction to PIPs at the PM. This model is in agreement with the coincidence detection model, in which a strong interaction between proteins and lipids is a consequence of the combination of many weak interactions (Carlton and Cullen, 2005; Di Paolo and De Camilli, 2006; Krauss and Haucke, 2007).

The finding that multiple signals within Ist2 confer transport of the protein to domains of the cortical ER, also explains, why a single, nonessential gene is not solely responsible for the peripheral accumulation of GFP-Ist2 (see 2.1). The CSS^{Ist2} does interact with PIPs at the PM. Moreover, PIPs are not the only factor driving the accumulation of Ist2 at the cell periphery. Other factors bound by Ist2^{ACSS} or the CSS^{Ist2} also play a role in Ist2 transport. However, the presence of multiple binding sites in Ist2 leads to some redundancy in the accumulation of Ist2 at the cell periphery. If factors involved in Ist2 transport are indeed encoded by nonessential genes, these might have been missed, because of this redundancy. Additional binding sites in Ist2 for other factors beside PIPs, in combination with *IST2* mRNA transport, a multimerization and an amphipathic helix (see 3.3.1) might lead to a high affinity interaction between CSS^{Ist2} and the PM, which finally drives Ist2 transport to domains of the cortical ER.

The sequence of the Ist2 protein carries some known consensus sequences for the sorting of integral membrane proteins. Within the amino acids 81-83, Ist2 has a DXE ER export motif. However, the finding that export from the ER is no prerequisite for Ist2 transport (Juschke et al., 2004) and the fact that most of the functional DXE signals are located in the C-terminus of ER-exported proteins (see 1.2.2), renders the functionality of this motif in Ist2 unlikely. At amino acids 903-905 Ist2 exposes an RXR ER retention signal and a C-terminal KKXX ER retrieval signal. The reporter protein Prm1 tagged with the Ist2 C-terminus containing the Ist2 sorting signal could in part enter the cis-Golgi apparatus, but was not transported to the trans-Golgi apparatus as judged from the glycosylation pattern

(Juschke et al., 2005). This suggests that the RXR-signal, the KKXX-signal or both are functional *in vivo*.

3.3 Structural properties and multimerization of Ist2

3.3.1 Domains within the CSS^{Ist2}

Which domains and structural properties in Ist2 confer its accumulation at the cell periphery? Two domains in Ist2 have been described. The DUF590 domain, which covers the amino acids 369-605 (source: <http://pfam.sanger.ac.uk/>) of Ist2, is homologous to other members of the TMEM16 family. However, the exact function of this protein domain is not known. The CSS^{Ist2} is the only described functional protein domain in Ist2. It is necessary for the transport of Ist2 and other reporter proteins to the cell periphery (Franz et al., 2007). The Ist2 structure has not yet been solved by X-Ray crystallography or NMR studies. Structure predictions of Ist2 predict eight transmembrane domains (Krogh et al., 2001) and the cytosolic N- and C-termini to be largely unstructured (Cole et al., 2008). Also the CSS^{Ist2} as the only described functional domain is predicted as unstructured (Cole et al., 2008), except the C-terminal eleven amino acids, which are suggested to form an amphipathic helix (Sapay et al., 2006).

The CSS^{Ist2} has a function as a complex sorting signal (Franz et al., 2007). However, it is unclear, whether it also adopts a certain domain fold. In order to find domain borders within the whole cytosolic C-terminus, GST-Ist2 589-946 was subjected to limited proteolysis. GST-Ist2 589-946 is accessible to Proteinase K after the amino acid T886 (Fig. 7+8), suggesting a domain border in this region of the protein. GFP-Ist2 1-591 + 878-946 is efficiently transported to the cell periphery and Ist2 1-591 + 895-946 is not (Franz A., Diploma Thesis 2005). Therefore, between the amino acids R878 and H895 (see also Fig. 6) a domain border has to be present, which separates the functional sorting signal of Ist2 from the rest of the protein. The performed limited proteolysis experiments suggest that this domain border might be present within the threonine stretch of Ist2 at the amino acids T886/T887.

In order to investigate, whether the predicted amphipathic helix (Sapay et al., 2006) in the Ist2 amino acids 936-946 is present and functional *in vivo*, circular dichroism (CD) spectroscopy and a mutational analysis within this region of the protein were combined. In aqueous solution the CD spectrum of a peptide consisting of Ist2 933-946 showed a random coil structure (Maass et al., 2009, Fig. 5C) as compared to reference spectra (Chen et al., 1974). When subjecting Ist2 933-946 to increasing concentrations of Trifluoroethanol (TFE) from 0% to 50% (v/v), a transition into an α -helical state could be observed (Maass et al., 2009, Fig. 5C). The precise effect of TFE on a protein is unclear.

TFE is a hydrophilic agent, but it can nonetheless mimic certain biophysical properties of a lipid bilayer. For example the dielectric constant of TFE is similar to the dielectric constant of phospholipid aliphatic sidechains (Sonnichsen et al., 1992). Therefore, Ist2 933-946 can under changing environmental conditions adopt a helical conformation. This suggests that the extreme C-terminus of Ist2 indeed can function as an amphipathic helix, at least under certain conditions as for example at membranes.

In parallel a mutational analysis within the K/L-Sequence of the CSS^{Ist2} corroborated that the extreme C-terminus of Ist2 indeed adopts an amphipathic helix, which is required for the localization of Ist2. Three major classes of mutations within the K/L-Sequence were found: (1) Mutations in certain hydrophobic residues led to dot-like accumulations of Ist2. In particular the hydrophobic amino acids L938, L939 and L942 are crucial for Ist2 transport to domains of the cortical ER and they have to be placed on one side of the Ist2 amphipathic helix. (2) Amino acid insertions, which lead to the misassembly of the amphipathic helix, cause dot-like accumulations of the mutated Ist2 protein. (3) Mutations in a cluster of basic residues N-terminal of the amphipathic helix (K931A/K933A/H934A/K935A/K936A) caused a partial perinuclear localization of Ist2 (Maass et al., 2009).

These data strongly suggest that the formation of an amphipathic helix within the K/L-sequence of Ist2 is crucial for the accumulation of Ist2 at the cell periphery. This is supported by CD-measurements using Ist2 933-946 with the mutation L939P. This peptide does not undergo a transition from an unstructured to a helical state in 50% TFE (Maass et al., 2009, Fig. 5D). GFP-Ist2 L939P localizes in dot-like structures in the cell periphery (Maass et al., 2009).

In order to test, whether the mislocalization of the aforementioned mutants is caused due to a lack in lipid-binding properties, liposome binding studies using PM-like liposomes containing 5 mol% PtdIns[4,5]P₂ were carried out. These experiments revealed that variants of GFP-CSS^{Ist2} carrying such mutations show strongly decreased liposome binding properties compared to wild type GFP-CSS^{Ist2}. The strongest impairment on lipid binding was found in GFP-CSS^{Ist2} (K931A/K933A/H934A/K935A/K936A). Furthermore, a GFP-CSS^{Ist2} carrying additional amino acid insertions, which interfere with the amphipathic helix of GFP-CSS^{Ist2}, showed a strongly decreased liposome binding (Maass et al., 2009, Fig. 7C). This establishes a functional connection between the structural properties of the CSS^{Ist2}, namely the amphipathic helix, and its lipid-binding properties. Multiple activities within the K/L-sequence are required for binding of PtdIns[4,5]P₂ containing liposomes. Basic residues within a polybasic cluster from amino acids 931-936 are required as well as the formation of an amphipathic helix. This finding is consistent with the fact that multiple binding sites are required for accumulation of GFP-2x CSS^{Ist2} at the PM (see 3.2).

A polybasic cluster in Ist2 931-936 is required for the transport of Ist2 from the perinuclear to the cortical ER. Mutations in these amino acids strongly decrease the binding to

PtdIns[4,5]P₂ containing liposomes. This suggests that the interaction with negatively charged PIPs at the PM could *in vivo* be mediated by these amino acids. In mammalian cells many cytosolic GTPases are recruited to PIPs at the PM via two or three polybasic clusters interconnected with hydrophobic amino acids (Heo et al., 2006), a motif also found in the K/L-sequence of Ist2. In a large number of the examined proteins in this study additional lipid-binding properties as prenylation or myristoylation facilitate the PM binding. In the case of the Ist2 protein, these additional lipid-binding properties might be caused by the fact that Ist2 is already embedded into the lipid bilayer via its transmembrane domains and also by the formation of an amphipathic helix. However, whether the amphipathic helix of Ist2 penetrates into the PM was not formally shown. Nonetheless its activity is necessary for the efficient accumulation of Ist2 at domains of the cortical ER. For a variety of proteins their interaction with different membranes is driven by the formation of an amphipathic helix sometimes in combination with electrostatic interactions (Antonny et al., 1997; McMahon and Gallop, 2005; Thiyagarajan et al., 2004). In a yet speculative model the basic amino acids within the K/L-sequence of CSS^{Ist2} might mediate a low affinity electrostatic interaction between Ist2 at the ER and PIPs at the PM. This interaction is subsequently stabilized by the penetration of the Ist2 amphipathic into the PM, stably localizing Ist2 at domains of the cortical ER adjacent to the PM.

3.3.2 Multimerization of Ist2

It was suggested that Ist2 forms multimeric complexes, as coexpressed HA-Ist2 and myc-Ist2 can be co-immunoprecipitated (Franz et al., 2007). In which part of the Ist2 molecule does multimerization occur? Two lines of evidence have established that a multimerization function of Ist2 is present within the T/H/S-cluster of the CSS^{Ist2}: (1) the introduction of a cysteine at position 916 of Ist2 and subsequent crosslinking experiments with the cysteine-specific homobifunctional crosslinker bismaleimido-hexane (BMH) leads to the formation of Ist2 oligomers, whereas wild type Ist2 is not crosslinked to oligomers. As judged from the molecular weight in SDS-PAGE, crosslinked Ist2 S916C can be found in complexes resembling a dimeric form of Ist2 S916C after treatment with BMH (Seedorf M., personal communication). (2) A tetramerization domain (cc) from the Gcn4-pLI Leucine Zipper (Harbury et al., 1993) can functionally replace the T/H/S-cluster. Kex2-cc-GFP-Ist2 929-946 efficiently accumulates at the cell periphery, whereas replacement of the T/H/S-cluster with an unrelated sequence from the ABC transporter Ste6 led to partial intracellular accumulation (Franz et al., 2007; Franz A., personal communication) of Kex2-Ste6 100-150-GFP-Ist2 929-946.

In order to address the question, whether a multimerization of the T/H/S-cluster in CSS^{Ist2} is not only a prerequisite for efficient transport to the cell periphery, but also a prerequisite for lipid binding, liposome-binding experiments with different replacements of domains

within GFP-CSS^{Ist2} were carried out. GFP-cc-Ist2 929-946 efficiently bound to PtdIns[4,5]P₂ containing liposomes in a range comparable to the wild type GFP-CSS^{Ist2} (Fischer et al., 2009, Fig. 2). In GFP-cc-Ist2 929-946 the T/H/S-cluster from the CSS^{Ist2} is replaced with a tetramerization domain from the Gcn4-pLI Leucine Zipper (Harbury et al., 1993). Replacement of the T/H/S-cluster with an unrelated spacer of the similar length led to inefficient liposome binding of GFP-Ste6 100-150-Ist2 929-946. Moreover, a truncated version of GFP-CSS^{Ist2} lacking its K/L-sequence does not exhibit any lipid-binding property at all (Fischer et al., 2009, Fig. 2). These experiments establish that for efficient liposome binding a multimeric K/L-sequence is necessary. This finding is in agreement with transport assays using the reporter protein Kex2. Kex2 can be efficiently redirected to the cell periphery by a multimeric K/L-sequence, but not by a monomeric K/L-sequence (Franz et al., 2007; Franz A., personal communication). Also *in vivo* GFP-2x CSS^{Ist2} shows a stronger accumulation at the PM as compared to monomeric GFP-CSS^{Ist2} (Fischer et al., 2009, Fig. S3; Maass et al., 2009, Fig. 6A).

These data, in combination with the aforementioned crosslinking experiments, suggest that the T/H/S-cluster of the CSS^{Ist2} has a function as a multimerization domain within Ist2. In order to test whether other parts of Ist2 can also act as multimerization signals, the T/H/S-cluster of the full-length Ist2 protein was replaced with either the cc-multimerization element or the unrelated Spacer Ste6 100-150. The resulting proteins Ist2^{ACSS} + cc + Ist2 929-946 and Ist2^{ACSS} + Ste6 100-150 + Ist2 929-946 both conferred sensitivity to calcofluor white in the same way as wild type Ist2 did (Fischer et al., 2009, Fig. 5). Moreover, GFP-fusion proteins localized to patch-like domains of the cell periphery (data not shown). These data suggest that the T/H/S-cluster is not the only multimerization element within Ist2. Moreover, GFP-Ist2^{ACSS} expressed at extremely low levels localizes to both perinuclear and cortical ER (Fischer et al., 2009, Fig. 7A). Overexpression of GFP-Ist2^{ACSS} leads to the formation of dot-like proliferated ER-structures in the cell periphery in *ist2Δ* cells (Fischer et al., 2009, Fig. 7A). This shows that for the peripheral localization of GFP-Ist2^{ACSS} a high expression level is necessary. GFP-Ist2^{ACSS} might upon high expression levels multimerize and as a multimeric complex expose signals, which lead to the accumulation of the protein at peripheral ER structures. Furthermore, in contrast to *ist2Δ* cells, overexpressed GFP-Ist2^{ACSS} in wild type cells localized to some peripheral dots, but also to patch-like structures in the cell periphery. This suggests a heterooligomerization between GFP-Ist2^{ACSS} and wild type Ist2. These data establish that a multimerization signal is not only present within the T/H/S-cluster, but also in Ist2^{ACSS}.

The multimerization of the proteins EEA1 and dynamin is a prerequisite for a high affinity interaction with PIPs (Dumas et al., 2001; Klein et al., 1998). The ability of protein complexes to expose multiple binding sites to the membrane thereby strongly increases the affinity of the protein complex for PIP-containing membranes (Carlton and Cullen, 2005). Also in the case of Ist2 multimerization domains within the protein might mediate such

high-affinity interactions. The formation of Ist2 oligomers would then lead to an integration of PIP binding sites within the CSS^{Ist2} leading to a high affinity membrane interaction, which might even further be stabilized by the amphipathic helix in Ist2.

Under *in vivo* conditions the formation of Ist2 multimers might be supported by the mRNA transport into the bud tip. This leads to a very restricted area of Ist2 translation sites and a high local concentration of Ist2, which might finally lead to the formation of multimeric Ist2 complexes.

3.4 Model for Ist2 transport to the cortical ER

The results of this thesis, in combination with other studies (Franz et al., 2007; Maass et al., 2009) have elucidated a model for the accumulation of Ist2 at the cortical ER:

Under wild type conditions the *IST2* mRNA is transported to the bud-tip dependent on the She-machinery, followed by a local translation of Ist2 at the cortical ER of the daughter cell (Takizawa et al., 2000, Juschke et al., 2004). However, Ist2 can also be translated at the perinuclear ER of mother cells followed by a rapid accumulation at the cortical ER of mother cells (Maass et al., 2009). Whether Ist2 is translated at the perinuclear ER of mother cells or at the cortical ER of the daughter cell, depends on the stage of the cell cycle. In non-budding mother cells Ist2 translation can more often be detected at the perinuclear ER than in budding cells (Maass et al., 2009). This might be explained by the fact that the *IST2* mRNA is cotransported with ER tubules into the daughter cell (Lange et al., 2008; Schmid et al., 2006). As cortical ER inheritance into the daughter cell is only occurring in the S- and the G2-phase of the cell cycle, in non-budding cells Ist2 might be easier to detect at the perinuclear ER of non-budding cells, because the mRNA is not transported at this stage of the cell cycle and therefore not preferentially locally translated at the cortical ER of daughter cells. However, under both conditions, Ist2 efficiently accumulates at domains of the cortical ER in a process that depends on its cortical sorting signal. It was previously shown with fluorescence loss in photobleaching experiments that half of the ER polytopic integral membrane protein Sec61-GFP exchanges between the perinuclear and cortical ER of mother cells within 40 seconds (Luedeke et al., 2005). This establishes that integral ER membrane proteins can exchange between both compartments rapidly. Therefore, Ist2 would subsequent to its translation be able to rapidly diffuse throughout the ER and exchange between perinuclear and cortical ER via ER tubules. In half of the cells translating Ist2 at the perinuclear ER of mother cells, the perinuclear signal disappears 3 minutes after stop of translation by treating the cells with cycloheximide (Maass et al., 2009). This establishes that Ist2 is rapidly accumulating at the cell periphery subsequent to translation. Via diffusion Ist2 could enter junctions between the ER and the PM, which are of a distance of less than 30 nm (Perktold et al., 2007; Pichler et al., 2001).

In these junctions, multiple binding sites within the CSS^{Ist2} interact with PIPs and other factors at the PM. This confers a strong interaction with the PM, which leads to a trapping of Ist2 at domains of the cortical ER (Maass et al., 2009; Fischer et al., 2009). This diffusion and trapping mechanism is established by an interaction between the CSS^{Ist2} and factors at the PM.

At least three different activities of Ist2 contribute to the accumulation of the protein at the cell periphery. Multiple multimerization elements, of which at least one is necessary for efficient lipid binding, act within Ist2 (Fig. 9, labeled 1) (Franz et al., 2007; Fischer et al., 2009). An Ist2 protein complex with high avidity (Lemmon and Ferguson, 2000) to the PM could much more efficiently bind to PIPs, as shown for other multimeric proteins (Dumas et al., 2001; Klein et al., 1998) as well. The efficient binding to PIPs of the PM leads to an efficient trapping of the Ist2 protein in domains of the cortical ER (Fig. 9, labeled 2). Which positive residues create the binding site for PIPs? Two polybasic clusters are present within the K/L-sequence of Ist2 (Fig. 6). A mutational analysis revealed that mutating basic residues within the first polybasic cluster to alanines (K931A/K933A/H934A/K935A/K936A) led to a partial perinuclear localization of Ist2, whereas mutating the second polybasic cluster had a much milder effect (Maass et al., 2009). Moreover, GFP-CSS^{Ist2} (K931A/K933A/H934A/K935A/K936A) showed a drastic reduction in binding to PtdIns[4,5]P₂ containing liposomes (Maass et al., 2009, Fig. 7C). Therefore, most likely this polybasic cluster is responsible for binding PIPs at the PM. This cluster is directly upstream of the amphipathic helix, which is predicted to start at the lysine at position 936. Therefore, these lysine residues might electrostatically interact with the headgroups of PIPs, whereas the C-terminal amphipathic (Fig. 9, labeled 3) helix might penetrate the lipid bilayer of the PM. Two binding sites, lysines conferring an electrostatic interaction with PIPs, and the amphipathic helix penetrating the lipid bilayer, would also explain the following observation: in *stt4^{ts}/pik1^{ts}* cells with largely decreased levels of PtdIns[4,5]P₂ and PtdIns[4]P, GFP-2x CSS^{Ist2} remains bound to the PM in the majority of cells (Fischer et al., 2009, Fig. S3). Interactions of lysine residues with the few residual PIP headgroups and in particular the penetration of the amphipathic helix into the PM might be sufficient to confer a PM localization of GFP-2x CSS^{Ist2} under these conditions. However, also an interaction of the amphipathic helix or other parts of the CSS^{Ist2} with proteins at the PM might be possible, although direct evidence for this does not exist. The different activities in Ist2 that contribute to the accumulation of the protein at the cell periphery are outlined in Figure 9.

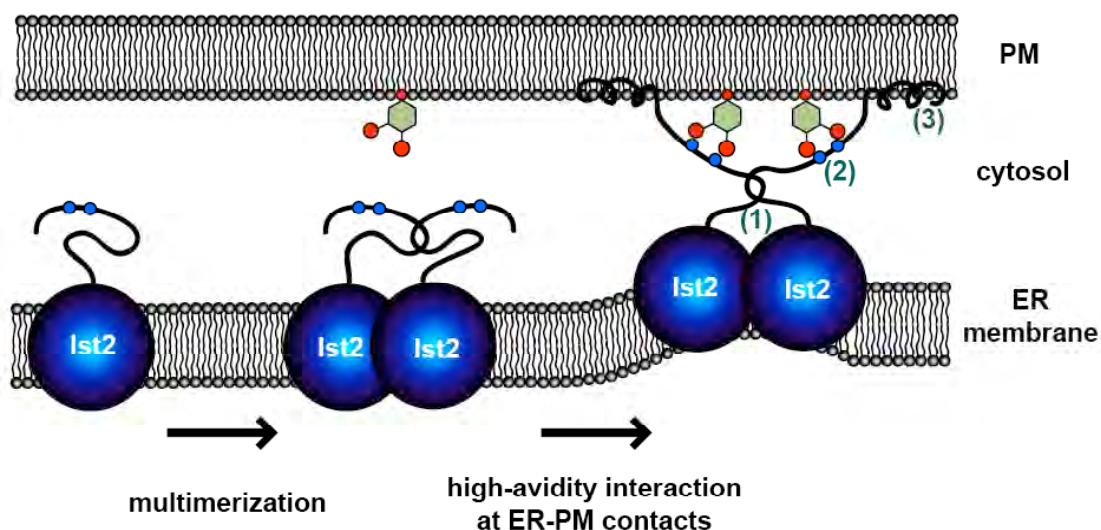


Fig. 9: Model for the transport of Ist2. Subsequent to its translation, Ist2 multimerizes (1). The Ist2 protein complex diffuses throughout the ER, also reaching organelle junctions between the ER and the PM. At these junctions a multimeric Ist2 complex exposes a signal with high avidity to the PM, in particular to negatively charged PIPs (2). Positively charged amino acids (blue) interact with negatively charged PIP headgroups (red). This interaction is stabilized by the exposure of an amphipathic helix (3), which might penetrate the PM.

This proposed model is in agreement with the observed phenomenon that Ist2 and reporter proteins, to which Ist2^c or the CSS^{Ist2} are fused, accumulate at patch-like structures in the cell periphery independently of a functional secretory pathway and without being transported through the TGN (Franz et al., 2007; Juschke et al., 2004; Juschke et al., 2005). The accumulation at the cell periphery in this model would simply be achieved by an efficient trapping of diffusing ER membrane proteins at domains of the cortical ER, which are adjacent to the PM.

GFP-Ist2 is accessible to proteases given to intact yeast cells. Whether Ist2 is protease sensitive residing in organelle junctions between the cortical ER and the PM, or whether Ist2 is localized to the PM, remains unclear at this point. Ist2 might function at domains of the cortical ER, nonetheless a transfer to domains of the PM subsequent to Ist2 transport to the cortical ER, cannot be excluded.

3.5 Localization and function of Ist2

What is its molecular function of Ist2 and does it exhibit this function at the cortical ER or the PM? Ist2 is localized in the cell periphery in patch-like structures, which colocalize with the cortical ER (Juschke et al., 2004). The cortical ER and the PM are in close apposition to each other. At ER-PM junctions the distance between both organelles is less than 30 nm, which is more than order of magnitude below the diffraction barrier of fluorescence microscopy. Initial localization of HA-Ist2 in immuno-electron microscopy

(EM) suggested an accumulation at both cortical ER and PM (Reggiori F., unpublished data). However, even with this technique distinguishing the cortical ER from the PM is very hard (Griffith et al., 2008). After translation Ist2 rapidly accumulates at domains of the cortical ER (Maass et al., 2009). Does Ist2 maintain this localization or is it translocated to the PM? Ist2 is protease accessible (Juschke et al., 2004). This led to the suggestion that Ist2 localizes at the PM (Juschke et al., 2004; Takizawa et al., 2000). It is unclear, whether also domains of the cortical ER, which are in close apposition to the PM, might be accessible to proteases. This would favor a model for Ist2 function, in which Ist2 stays in protease accessible domains of the cortical ER without being translocated to the PM. From its localization at the interface between ER and PM it is likely that Ist2 couples processes between both organelles. This functional coupling could finally lead to scenario, in which Ist2 itself is transported to domains of the PM in a process independently of the secretory pathway system. This transport of Ist2 to the PM could be achieved by Sec18 (NSF)-independent vesicular transport from the cortical ER to the PM. Alternatively, a local transient and highly regulated fusion between both organelles might be used to transfer Ist2 from the cortical ER to the PM. However, whether such mechanism exists, remains unclear at this point. A direct extraction of Ist2 from the cortical ER and subsequent insertion into the PM is unlikely from the thermodynamic point of view, because it would be extremely energy-consuming to transfer a protein with 8 transmembrane regions through the aqueous cytosol.

What is the molecular function of Ist2? Few data have been generated to address this question. As a protein interacting with the PM from the cortical ER, Ist2 might have a function in coupling processes between the ER and the PM.

Firstly, Ist2 might as well as the mammalian TMEM16A and TMEM16B proteins function as an anion channel. Ist2 might mediate chloride ion flux processes over the cortical ER membrane or the PM. A function as a chloride channel might explain the observed phenotypes of Ist2 that have been linked to ion tolerance or ion homeostasis (Entian et al., 1999; Kim et al., 2005). The coupling of anion influx processes from the cell exterior into the ER has not been described so far. However, such coupling is described for cation transport in mammalian cells. Influx of calcium from the cell exterior into the ER involves a coupling between ER and PM. The calcium sensing proteins STIM1 or STIM2 are resident in the ER and upon drop of ER calcium concentration, undergo a conformational change (Brandman et al., 2007; Navarro-Borelly et al., 2008), leading to an interaction with the Orai channel at the PM (Putney et al., 2007; Lewis 2007; Frischauf et al., 2008) and to a massive recruitment ER to the cell periphery (Liou et al., 2005; Wu 2006; Brandman et al., 2007). Calcium, which is imported into the cell via Orai, can then subsequently be imported into the ER via the SERCA system (Frischauf et al., 2008). However, in mammalian cells the recruitment of ER to the cell periphery is a rather transient process, whereas in yeast the peripheral cortical ER is stably localized beneath the

PM (Prinz et al., 2000). Moreover, a SERCA system is not found in yeast. Ist2 might, however, act as a chloride channel in the ER or the PM mediating anion ion flux processes over both membranes in a similar manner as the STIM/Orai machinery mediates ion flux for the cation calcium.

Secondly, sterols can be transported from the ER to the PM in nonvesicular transport pathways (Baumann et al., 2005). Sterol transfer might occur at junctions between the ER and the PM in a process mediated by proteins of the Osh family (Raychaudhuri et al., 2006). The localization of Osh proteins is regulated by Scs2 (Loewen et al., 2003). As Ist2 can be co-immunoprecipitated with Scs2 (Maass K., PhD Thesis 2008), Ist2 might together with Scs2 be involved in creating a microenvironment between the ER and the PM, which facilitates the lipid transfer between both membranes. However, a detailed analysis of sterol distribution was not performed in cells lacking Ist2 yet.

Thirdly, during its transport process Ist2 is localized in domains of the cortical ER, where it interacts with the PM. This evokes another possible function of Ist2 as a direct consequence of the localization at the ER-PM interface: is Ist2 necessary for the placement of the cortical ER beneath the PM or for the inheritance of the cortical ER? This hypothesis is supported by the fact that Ist2 physically interacts with Scs2 (Maass K., PhD Thesis 2008), a protein involved in cortical ER inheritance and morphology (Loewen et al., 2007). Moreover, Ist2^{ACSS} + EEA1-FYVE localizes partially to ER structures adjacent to the vacuole, thereby recruiting the ER marker RFP-HDEL to ER, which is closely apposed to the vacuole (Fischer et al., 2009, Fig. 4A). If a PtdIns[3]P-binding transmembrane protein has the potential to recruit ER to the vacuole, Ist2 as a PM binding protein might recruit cortical ER to the cell periphery, thereby being the determining factor for the attachment of cortical ER in the cell periphery.

In order to test, whether Ist2 is involved in cortical ER maintenance or inheritance, the ER-marker RFP-HDEL was localized in *ist2Δ* cells, wild type cells and cells overexpressing Ist2 or Ist2^{ACSS} + PLC- δ_1 -PH. In all of these cells the ER morphology remained unchanged as judged from fluorescence microscopy. Moreover, the ratio of cortical ER versus perinuclear ER in non-budding cells did not change and the inheritance of ER into daughter cells was not impaired (Fischer et al., 2009, Fig. 4A and Table S1). Therefore, Ist2 is not solely responsible for the inheritance or maintenance of cortical ER. If Ist2 is involved in this process, other redundant factors might take over this role in cells lacking Ist2. These factors might be proteins that are required or involved this process, as Scs2, Sec3, Aux1/Swa2, Ice2, reticulons or translocon components (De Craene et al., 2006; Du et al., 2004; Du et al., 2001; Estrada de Martin et al., 2005; Guo and Novick, 2004; Loewen et al., 2007; Toikkanen et al., 2003; Voeltz et al., 2006; Wiederkehr et al., 2003).

3.6 Lipid mediated sorting of eukaryotic membrane proteins

Is the transport of proteins to peripheral ER subdomains via binding of PM lipids a general mechanism? The finding that in yeast integral membrane proteins can be transported to domains of the cortical ER via binding of PM lipids, raises the question whether also in mammalian cells proteins can be recruited to peripheral ER subdomains via this mechanism as well. Two recent studies have shown that the CSS^{Ist2} can redirect UNC93B1, which is involved in signaling of certain toll-receptors, from endolysosomes to the cell periphery of mammalian cells (Ewald et al., 2008; Kim et al., 2008). These studies claimed that the fusion proteins localized to the PM. However, no surface assay was performed in order to detect the fusion protein of UNC93B1 and the CSS^{Ist2} at the PM of mammalian cells. A detailed analysis of the function of the CSS^{Ist2} in higher eukaryotic cells was not performed yet.

The most obvious mammalian candidates for a transport to peripheral ER subdomains via binding of PM lipids in mammalian cells are STIM1 and STIM2. At least under certain conditions they reside in ER patches, which are adjacent to the PM (Liou et al., 2005). However, the recruitment of STIM proteins upon drop of ER calcium concentration is stabilized via a direct interaction to the PM localized calcium channel Orai (Penna et al., 2008)

Neither STIM1 nor STIM2 were shown to bind PM lipids up to now. However, STIM2 shares some characteristic similarities to Ist2. The extreme C-termini of STIM1 and STIM2 are polybasic and STIM2 is predicted to form an amphipathic helix as well (Sapay et al., 2006). Moreover, STIM2 was bioinformatically identified to share a K x [LIWF] [LIWF] x x [LIWF] feature in its amino acid sequence. This motif is present in the K/L-sequence of the CSS^{Ist2} and Ist2 homologues from closely related yeast species and it was identified to be essential for sorting of Ist2 (Maass K., PhD Thesis 2008; Seiler M., personal communication). However, a detailed analysis of the lipid-binding properties of both STIM1 and STIM2 is necessary in order to test whether lipid binding contributes to their accumulation at peripheral ER structures.

Beside the STIM proteins also members from the TMEM16 family might be sorted to the peripheral ER of mammalian cells via binding to PM lipids, similar to Ist2 in yeast. However, a K x [LIWF] [LIWF] x x [LIWF] or a similar motif, cannot be found in the N- or C-terminus of TMEM16A. In order to test, whether TMEM16A nevertheless carries a lipid-binding motif similar to Ist2, liposome-binding experiments were carried out. Compared to Ist2, TMEM16A has a rather short C-terminal region following the last transmembrane domain (Fig. 5). Fused to GFP, the TMEM16A C-terminus did not significantly bind to PtdIns[4,5]P₂ containing liposomes (Fischer et al., 2009, Fig. 8B). However, fusion of the N-terminal 352 amino acids of TMEM16A to either the N-terminus or the C-terminus of GFP led to a significant binding of liposomes, which was dependent

on the presence of PtdIns[4,5]P₂. GFP-TMEM16A 1-352 bound to PtdIns[4,5]P₂ containing liposomes slightly weaker as compared to GFP-CSS^{Ist2}. TMEM16A 1-352-GFP exhibited even stronger lipid-binding properties than GFP-CSS^{Ist2} (Fischer et al., 2009, Fig. 8B). It has to be noted that in these experiments the TMEM16A *abcd* splice isoform was used, which is more basic within its N-terminal region than other splice isoforms of TMEM16A (Caputo et al., 2008). In order to test, whether N- or C-termini of TMEM16A have a function as a peripheral targeting signal *in vivo*, they were fused to Ist2^{ACSS}. Ist2^{ACSS} accumulated at dot-like structures in the cell periphery. This localization was not changed upon fusion of the TMEM16A C-terminus to Ist2^{ACSS}. However, both Ist2^{ACSS}-TMEM16A 1-352 and TMEM16A 1-352-Ist2^{ACSS} showed an accumulation at peripheral dots and also peripheral patches (Fischer et al., 2009, Fig. 8C). This suggests that at least in part the TMEM16A N-terminus might take over the function of the CSS^{Ist2} and target Ist2^{ACSS} to the cell periphery as a lipid-binding motif. However, fusion proteins of TMEM16A 1-352 and Ist2^{ACSS} were unstable at 37°C, making experiments in temperature sensitive *sec*-mutants impossible. Therefore, it was not resolved, whether the peripheral targeting function of TMEM16A 1-352 is due to its lipid-binding properties or whether an ER export signal is present in this protein, allowing transport of the fusion proteins to the PM via the secretory pathway, which would lead to peripheral accumulation as well.

Despite its function as a lipid-binding motif *in vitro* and its peripheral targeting function *in vivo*, it is unclear, whether TMEM16A is transported to domains of the peripheral ER in mammalian cells as well. GFP-TMEM16A localizes at the PM (Schroeder et al., 2008; Yang et al., 2008) and currently there is no evidence that during its transport to the PM peripheral ER structures are formed or involved.

3.7 Future perspectives

This thesis has revealed that the yeast transmembrane protein Ist2 is accumulating at domains of the yeast cortical ER via a binding to lipids of the adjacent PM. However, many open questions about Ist2 still remain, in particular concerning the function and localization of Ist2.

Which function does Ist2 have? From the similarity to the TMEM16 family Ist2 might be a calcium-activated chloride channel. The genetic power of yeast will be of great usage to characterize, in which pathways Ist2 is involved and whether these are related to ion flux processes. In order to test, whether Ist2 indeed has a channel function, reconstitution experiments of Ist2 into lipid bilayers would be beneficial. If Ist2 functions as a channel, it would be of great interest over which organelle membrane Ist2 mediates ion flux.

This leads to the question, where Ist2 is localized. Is Ist2 exclusively localized in protease accessible sites of the cortical ER or is at least a part of the protein transferred to the PM in a Sec18 (NSF)-independent process? Fluorescence microscopy cannot resolve the cortical ER from the PM and even immuno-EM does not give a clear answer about the localization of Ist2. The development of enzymatic or immunological assays, which allow the sensitive distinction between localization within the cortical ER or the PM, would be beneficial. Also novel microscopy methods like STED microscopy might enable the distinction between both organelles.

Ist2 carries additional signals, which confer its peripheral accumulation beside the interaction with PIPs at the PM. Where are these signals and which are the cellular binding partners of Ist2? Biochemical analyses and genetic screens might help to reveal different, yet unknown factors, which are involved in the transport of Ist2 to the cell periphery.

Finally, the conservation of the Ist2 pathway is of greatest interest. Are there other proteins in yeast or especially in mammalian cells, which use the binding to PM lipids as a mechanism for their accumulation at the peripheral ER? Lipid binding experiments with STIM1 and STIM2 as well as the detailed analysis of the lipid-binding properties of TMEM16A and their relevance in mammalian cells will elucidate, whether this novel sorting mechanism of Ist2 is conserved from yeast to mammalian cells.

4 Abbreviation list

aa	amino acid
Arf	Adenosine diphosphate ribosylation factor
ATP	Adenosine triphosphate
b	base pairs
BFA	Brefeldin A
BiP	heavy chain binding protein
BMH	bismaleimidohexane
C	Celsius
CaCC	calcium activated chloride channel
cc	coiled-coil region from the Gcn4-pLI protein
CD	circular dichroism
CFP	cyan fluorescent protein
CFTR	cystic fibrosis transmembrane conductance regulator
CDP	cytidin diphosphate
COP	coat protein complex
CSS ^{Ist2}	cortical sorting signal of Ist2
Da	Dalton
DAG	diacylglycerol
DIM	detergent-insoluble membranes
DNA	desoxyribonucleic acid
DUF	domain of unknown function
<i>E. coli</i>	<i>Escherichia. coli</i>
EDTA	Ethylenediaminetetraacetic acid
EEA1	human early endosome antigen 1
e.g.	for example
ER	endoplasmic reticulum
ERAD	endoplasmic reticulum associated degradation
ERGIC	endoplasmic reticulum to Golgi intermediate compartment
ERJ	endoplasmic reticulum-organelle junction
ESI	electrospray ionization
F	Farad
f	femto
FACS	fluorescence activated cell sorting
FAPP1	four-phosphate adaptor protein 1
FGF-2	fibroblast growth factor 2
Fig.	Figure
g	Earth's gravity
g	gram
G1	gap1
G2	gap2
GDP	Guanosine diphosphate
GFP	green fluorescent protein
GPI	glycosylphosphatidylinositol
GST	glutathione-S-transferase
GTP	Guanosine triphosphate
h	hour
HA	hemagglutinin

HC	Hartwell-complete
HEK	human embryonic kidney
HMG-CoA	3-hydroxy-3-methyl-glutaryl coenzyme A
HPLC	high performance liquid chromatography
HSPG	Heparan sulfate proteoglycan
k	kilo
K _D	dissociation constant
Kir	inwardly rectifying potassium
IP ₃	inositol triphosphate
IPC	inositol-phosphoceramide
Ist2 ^c	cytosolic C-terminus of Ist2
l	liter
LB	lysogeny broth
M	mitosis / molar
m	meter / mili
μ	micro
MAM	mitochondrial associated membranes
min	minute
MIPC	mannose-inositol-phosphoceramide
M(IP) ₂ C	mannose-(inositol phosphate) ₂ -ceramide
MVB	multivesicular body
mRNA	messenger ribonucleic acid
MS	mass spectrometry
myc	myelocytomatosis oncogene
n	nano
NMR	nuclear magnetic resonance
NSF	N-ethylmaleimide sensitive factor
NV junction	nuclear-vacuolar junction
ORF	open reading frame
Osh	oxysterol binding protein homologue
P	phosphate
PAGE	polyacrylamide-gel electrophoresis
PAM	plasma membrane associated membranes
PBS	phosphate buffered saline
pH	<i>pontius hydrogenii</i>
PH	pleckstrin homology
PIP	phosphoinositide
PITP	phosphatidylinositol transfer protein
PLC	phospholipase C
PM	plasma membrane
PMN	piecemeal microautophagy of the nucleus
PMSF	Phenyl-methylsulfonyl fluoride
PtdCho	phosphatidylcholine
PtdEtn	phosphatidylethanolamine
PtdIns	phosphatidylinositol
PtdSer	phosphatidylserine
PVC	prevacuolar compartment
rER	rough endoplasmic reticulum
RFP	red fluorescent protein
rpm	rounds per minute
S	synthesis

s	second
<i>S. cerevisiae</i>	<i>Saccharomyces cerevisiae</i>
SDS	sodium dodecyl sulfate
<i>sec</i>	secretory pathway
sER	smooth endoplasmic reticulum
SERCA	sarcoplasmic/endoplasmic reticulum calcium ATPase
SNAP	soluble N-ethylmaleimide sensitive factor attachment protein
SNARE	soluble N-ethylmaleimide sensitive factor attachment protein receptor
SRP	signal recognition particle
STED	stimulated emission depletion
STIM	stromal interaction molecule
TCA	trichloro acetic acid
TFA	trifluoro acetic acid
TFE	trifluoro ethanol
TGN	trans Golgi network
TM	transmembrane
TMEM	transmembrane protein with unknown function
<i>ts</i>	temperature sensitive
U	Unit
UTR	untranslated region
UV	ultraviolet
V	volt
VSV-G	vesicular stomatitis virus glycoprotein
(v/v)	volume per volume
(w/v)	weight per volume
yEGFP	yeast enhanced green fluorescent protein
YFP	yellow fluorescent protein
YPD	yeast peptone dextrose
Ω	Ohm

5 List of tables and figures

5.1 List of tables

Table 1: Number of ERJs per cell.	5
Table 2: Characterized ER export signals for transmembrane proteins.	11
Table 3: Lipid-binding domains.	22
Table 4: Phenotypes observed in the yeast knockout library screen.	32

5.2 List of figures

Figure 1: ER-organelle junctions (ERJs).	2
Figure 2: Overview of the early secretory pathway.	7
Figure 3: Structure of PtdIns and possible phosphorylation sites at the inositol ring.	18
Figure 4: Distribution of PIPs in yeast.	19
Figure 5: Alignment of Ist2 and the <i>abcd</i> splice variant of TMEM16A.	24
Figure 6: Ist2 and its cortical sorting signal.	28
Figure 7: Limited proteolysis of GST-Ist2 589-946.	39
Figure 8: Peptides identified via mass spectrometry.	40
Figure 9: Model for the transport of Ist2.	118

6 References

- Achleitner, G., B. Gaigg, A. Krasser, E. Kainersdorfer, S.D. Kohlwein, A. Perktold, G. Zellnig, and G. Daum. 1999. Association between the endoplasmic reticulum and mitochondria of yeast facilitates interorganelle transport of phospholipids through membrane contact. *Eur J Biochem.* 264:545-53.
- Adelman, M.R., D.D. Sabatini, and G. Blobel. 1973. Ribosome-membrane interaction. Nondestructive disassembly of rat liver rough microsomes into ribosomal and membranous components. *J Cell Biol.* 56:206-29.
- Antonny, B., S. Beraud-Dufour, P. Chardin, and M. Chabre. 1997. N-terminal hydrophobic residues of the G-protein ADP-ribosylation factor-1 insert into membrane phospholipids upon GDP to GTP exchange. *Biochemistry.* 36:4675-84.
- Antonny, B., D. Madden, S. Hamamoto, L. Orci, and R. Schekman. 2001. Dynamics of the COPII coat with GTP and stable analogues. *Nat Cell Biol.* 3:531-7.
- Appenzeller, C., H. Andersson, F. Kappeler, and H.P. Hauri. 1999. The lectin ERGIC-53 is a cargo transport receptor for glycoproteins. *Nat Cell Biol.* 1:330-4.
- Aronov, S., R. Gelin-Licht, G. Zipor, L. Haim, E. Safran, and J.E. Gerst. 2007. mRNAs encoding polarity and exocytosis factors are cotransported with the cortical endoplasmic reticulum to the incipient bud in *Saccharomyces cerevisiae*. *Mol Cell Biol.* 27:3441-55.
- Athenstaedt, K., and G. Daum. 2006. The life cycle of neutral lipids: synthesis, storage and degradation. *Cell Mol Life Sci.* 63:1355-69.
- Audhya, A., and S.D. Emr. 2002. Stt4 PI 4-kinase localizes to the plasma membrane and functions in the Pkc1-mediated MAP kinase cascade. *Dev Cell.* 2:593-605.
- Audhya, A., M. Foti, and S.D. Emr. 2000. Distinct roles for the yeast phosphatidylinositol 4-kinases, Stt4p and Pik1p, in secretion, cell growth, and organelle membrane dynamics. *Mol Biol Cell.* 11:2673-89.
- Audhya, A., R. Loewith, A.B. Parsons, L. Gao, M. Tabuchi, H. Zhou, C. Boone, M.N. Hall, and S.D. Emr. 2004. Genome-wide lethality screen identifies new PI4,5P2 effectors that regulate the actin cytoskeleton. *Embo J.* 23:3747-57.
- Backhaus, R., C. Zehe, S. Wegehingel, A. Kehlenbach, B. Schwappach, and W. Nickel. 2004. Unconventional protein secretion: membrane translocation of FGF-2 does not require protein unfolding. *J Cell Sci.* 117:1727-36.
- Bai, J., W.C. Tucker, and E.R. Chapman. 2004. PIP2 increases the speed of response of synaptotagmin and steers its membrane-penetration activity toward the plasma membrane. *Nat Struct Mol Biol.* 11:36-44.

- Baldwin, T.A., and H.L. Ostergaard. 2002. The protein-tyrosine phosphatase CD45 reaches the cell surface via golgi-dependent and -independent pathways. *J Biol Chem.* 277:50333-40.
- Bankaitis, V.A., J.R. Aitken, A.E. Cleves, and W. Dowhan. 1990. An essential role for a phospholipid transfer protein in yeast Golgi function. *Nature.* 347:561-2.
- Bankaitis, V.A., D.E. Malehorn, S.D. Emr, and R. Greene. 1989. The *Saccharomyces cerevisiae* SEC14 gene encodes a cytosolic factor that is required for transport of secretory proteins from the yeast Golgi complex. *J Cell Biol.* 108:1271-81.
- Barlowe, C. 2003. Signals for COPII-dependent export from the ER: what's the ticket out? *Trends Cell Biol.* 13:295-300.
- Barlowe, C., L. Orci, T. Yeung, M. Hosobuchi, S. Hamamoto, N. Salama, M.F. Rexach, M. Ravazzola, M. Amherdt, and R. Schekman. 1994. COPII: a membrane coat formed by Sec proteins that drive vesicle budding from the endoplasmic reticulum. *Cell.* 77:895-907.
- Barral, Y., V. Mermall, M.S. Mooseker, and M. Snyder. 2000. Compartmentalization of the cell cortex by septins is required for maintenance of cell polarity in yeast. *Mol Cell.* 5:841-51.
- Baudin, A., O. Ozier-Kalogeropoulos, A. Denouel, F. Lacroute, and C. Cullin. 1993. A simple and efficient method for direct gene deletion in *Saccharomyces cerevisiae*. *Nucleic Acids Res.* 21:3329-30.
- Baumann, N.A., D.P. Sullivan, H. Ohvo-Rekila, C. Simonot, A. Pottekat, Z. Klaassen, C.T. Beh, and A.K. Menon. 2005. Transport of newly synthesized sterol to the sterol-enriched plasma membrane occurs via nonvesicular equilibration. *Biochemistry.* 44:5816-26.
- Beh, C.T., and J. Rine. 2004. A role for yeast oxysterol-binding protein homologs in endocytosis and in the maintenance of intracellular sterol-lipid distribution. *J Cell Sci.* 117:2983-96.
- Behnia, R., and S. Munro. 2005. Organelle identity and the signposts for membrane traffic. *Nature.* 438:597-604.
- Belden, W.J., and C. Barlowe. 2001. Role of Erv29p in collecting soluble secretory proteins into ER-derived transport vesicles. *Science.* 294:1528-31.
- Bera, T.K., S. Das, H. Maeda, R. Beers, C.D. Wolfgang, V. Kumar, Y. Hahn, B. Lee, and I. Pastan. 2004. NGEF, a gene encoding a membrane protein detected only in prostate cancer and normal prostate. *Proc Natl Acad Sci U S A.* 101:3059-64.
- Bialkowska, A., and A. Kurlandzka. 2002. Additional copies of the NOG2 and IST2 genes suppress the deficiency of cohesin Irr1p/Scc3p in *Saccharomyces cerevisiae*. *Acta Biochim Pol.* 49:421-5.

- Bielli, A., C.J. Haney, G. Gabreski, S.C. Watkins, S.I. Bannykh, and M. Aridor. 2005. Regulation of Sar1 NH2 terminus by GTP binding and hydrolysis promotes membrane deformation to control COPII vesicle fission. *J Cell Biol.* 171:919-24.
- Blobel, G., and B. Dobberstein. 1975. Transfer of proteins across membranes. I. Presence of proteolytically processed and unprocessed nascent immunoglobulin light chains on membrane-bound ribosomes of murine myeloma. *J Cell Biol.* 67:835-51.
- Bohl, F., C. Kruse, A. Frank, D. Ferring, and R.P. Jansen. 2000. She2p, a novel RNA-binding protein tethers ASH1 mRNA to the Myo4p myosin motor via She3p. *Embo J.* 19:5514-24.
- Bonnon, C., L. Goutebroze, N. Denisenko-Nehrbass, J.A. Girault, and C. Faivre-Sarrailh. 2003. The paranodal complex of F3/contactin and caspr/paranodin traffics to the cell surface via a non-conventional pathway. *J Biol Chem.* 278:48339-47.
- Borgese, N., S. Colombo, and E. Pedrazzini. 2003. The tale of tail-anchored proteins: coming from the cytosol and looking for a membrane. *J Cell Biol.* 161:1013-9.
- Brandhorst, D., D. Zwilling, S.O. Rizzoli, U. Lippert, T. Lang, and R. Jahn. 2006. Homotypic fusion of early endosomes: SNAREs do not determine fusion specificity. *Proc Natl Acad Sci U S A.* 103:2701-6.
- Brandman, O., J. Liou, W.S. Park, and T. Meyer. 2007. STIM2 is a feedback regulator that stabilizes basal cytosolic and endoplasmic reticulum Ca²⁺ levels. *Cell.* 131:1327-39.
- Brugger, B., R. Sandhoff, S. Wegehingel, K. Gorgas, J. Malsam, J.B. Helms, W.D. Lehmann, W. Nickel, and F.T. Wieland. 2000. Evidence for segregation of sphingomyelin and cholesterol during formation of COPI-coated vesicles. *J Cell Biol.* 151:507-18.
- Burd, C.G., and S.D. Emr. 1998. Phosphatidylinositol(3)-phosphate signaling mediated by specific binding to RING FYVE domains. *Mol Cell.* 2:157-62.
- Burda, P., S.M. Padilla, S. Sarkar, and S.D. Emr. 2002. Retromer function in endosome-to-Golgi retrograde transport is regulated by the yeast Vps34 PtdIns 3-kinase. *J Cell Sci.* 115:3889-900.
- Buvelot Frei, S., P.B. Rahl, M. Nussbaum, B.J. Briggs, M. Calero, S. Janeczko, A.D. Regan, C.Z. Chen, Y. Barral, G.R. Whittaker, and R.N. Collins. 2006. Bioinformatic and comparative localization of Rab proteins reveals functional insights into the uncharacterized GTPases Ypt10p and Ypt11p. *Mol Cell Biol.* 26:7299-317.
- Cabrera, M., M. Muniz, J. Hidalgo, L. Vega, M.E. Martin, and A. Velasco. 2003. The retrieval function of the KDEL receptor requires PKA phosphorylation of its C-terminus. *Mol Biol Cell.* 14:4114-25.

- Cai, H., K. Reinisch, and S. Ferro-Novick. 2007. Coats, tethers, Rabs, and SNAREs work together to mediate the intracellular destination of a transport vesicle. *Dev Cell*. 12:671-82.
- Cameroni, E., C. De Virgilio, and O. Deloche. 2006. Phosphatidylinositol 4-phosphate is required for translation initiation in *Saccharomyces cerevisiae*. *J Biol Chem*. 281:38139-49.
- Caputo, A., E. Caci, L. Ferrera, N. Pedemonte, C. Barsanti, E. Sondo, U. Pfeffer, R. Ravazzolo, O. Zegarra-Moran, and L.J. Galiotta. 2008. TMEM16A, a membrane protein associated with calcium-dependent chloride channel activity. *Science*. 322:590-4.
- Caramelo, J.J., and A.J. Parodi. 2008. Getting in and out from calnexin/calreticulin cycles. *J Biol Chem*. 283:10221-5.
- Carlton, J.G., and P.J. Cullen. 2005. Coincidence detection in phosphoinositide signaling. *Trends Cell Biol*. 15:540-7.
- Catrein, I., R. Herrmann, A. Bosserhoff, and T. Ruppert. 2005. Experimental proof for a signal peptidase I like activity in *Mycoplasma pneumoniae*, but absence of a gene encoding a conserved bacterial type I SPase. *FEBS J*. 272:2892-900.
- Chang, F.S., G.S. Han, G.M. Carman, and K.J. Blumer. 2005. A WASp-binding type II phosphatidylinositol 4-kinase required for actin polymerization-driven endosome motility. *J Cell Biol*. 171:133-42.
- Cheever, M.L., T.K. Sato, T. de Beer, T.G. Kutateladze, S.D. Emr, and M. Overduin. 2001. Phox domain interaction with PtdIns(3)P targets the Vam7 t-SNARE to vacuole membranes. *Nat Cell Biol*. 3:613-8.
- Chen, P., S.K. Sapperstein, J.D. Choi, and S. Michaelis. 1997. Biogenesis of the *Saccharomyces cerevisiae* mating pheromone α -factor. *J Cell Biol*. 136:251-69.
- Chen, Y.H., J.T. Yang, and K.H. Chau. 1974. Determination of the helix and beta form of proteins in aqueous solution by circular dichroism. *Biochemistry*. 13:3350-9.
- Chung, J.H., R.L. Lester, and R.C. Dickson. 2003. Sphingolipid requirement for generation of a functional v1 component of the vacuolar ATPase. *J Biol Chem*. 278:28872-81.
- Cleves, A.E., T.P. McGee, E.A. Whitters, K.M. Champion, J.R. Aitken, W. Dowhan, M. Goebel, and V.A. Bankaitis. 1991. Mutations in the CDP-choline pathway for phospholipid biosynthesis bypass the requirement for an essential phospholipid transfer protein. *Cell*. 64:789-800.
- Cole, C., J.D. Barber, and G.J. Barton. 2008. The Jpred 3 secondary structure prediction server. *Nucleic Acids Res*. 36:W197-201.
- Cooper, D.N., and S.H. Barondes. 1990. Evidence for export of a muscle lectin from cytosol to extracellular matrix and for a novel secretory mechanism. *J Cell Biol*. 110:1681-91.

- Cosson, P., and F. Letourneur. 1994. Coatamer interaction with di-lysine endoplasmic reticulum retention motifs. *Science*. 263:1629-31.
- Cowart, L.A., and L.M. Obeid. 2007. Yeast sphingolipids: recent developments in understanding biosynthesis, regulation, and function. *Biochim Biophys Acta*. 1771:421-31.
- Cutler, N.S., J. Heitman, and M.E. Cardenas. 1997. STT4 is an essential phosphatidylinositol 4-kinase that is a target of wortmannin in *Saccharomyces cerevisiae*. *J Biol Chem*. 272:27671-7.
- Daleke, D.L. 2003. Regulation of transbilayer plasma membrane phospholipid asymmetry. *J Lipid Res*. 44:233-42.
- Daum, G., N.D. Lees, M. Bard, and R. Dickson. 1998. Biochemistry, cell biology and molecular biology of lipids of *Saccharomyces cerevisiae*. *Yeast*. 14:1471-510.
- de Brito, O.M., and L. Scorrano. 2008. Mitofusin 2 tethers endoplasmic reticulum to mitochondria. *Nature*. 456:605-10.
- De Craene, J.O., J. Coleman, P. Estrada de Martin, M. Pypaert, S. Anderson, J.R. Yates, 3rd, S. Ferro-Novick, and P. Novick. 2006. Rtn1p is involved in structuring the cortical endoplasmic reticulum. *Mol Biol Cell*. 17:3009-20.
- Demmel, L., M. Gravert, E. Ercan, B. Habermann, T. Muller-Reichert, V. Kukhtina, V. Haucke, T. Baust, M. Sohrmann, Y. Kalaidzidis, C. Klose, M. Beck, M. Peter, and C. Walch-Solimena. 2008. The clathrin adaptor Gga2p is a phosphatidylinositol 4-phosphate effector at the Golgi exit. *Mol Biol Cell*. 19:1991-2002.
- Desrivieres, S., F.T. Cooke, P.J. Parker, and M.N. Hall. 1998. MSS4, a phosphatidylinositol-4-phosphate 5-kinase required for organization of the actin cytoskeleton in *Saccharomyces cerevisiae*. *J Biol Chem*. 273:15787-93.
- Di Paolo, G., and P. De Camilli. 2006. Phosphoinositides in cell regulation and membrane dynamics. *Nature*. 443:651-7.
- Dickson, R.C., and R.L. Lester. 2002. Sphingolipid functions in *Saccharomyces cerevisiae*. *Biochim Biophys Acta*. 1583:13-25.
- Dove, S.K., F.T. Cooke, M.R. Douglas, L.G. Sayers, P.J. Parker, and R.H. Michell. 1997. Osmotic stress activates phosphatidylinositol-3,5-bisphosphate synthesis. *Nature*. 390:187-92.
- Du, Y., S. Ferro-Novick, and P. Novick. 2004. Dynamics and inheritance of the endoplasmic reticulum. *J Cell Sci*. 117:2871-8.
- Du, Y., M. Pypaert, P. Novick, and S. Ferro-Novick. 2001. Aux1p/Swa2p is required for cortical endoplasmic reticulum inheritance in *Saccharomyces cerevisiae*. *Mol Biol Cell*. 12:2614-28.

- Dumas, J.J., E. Merithew, E. Sudharshan, D. Rajamani, S. Hayes, D. Lawe, S. Corvera, and D.G. Lambright. 2001. Multivalent endosome targeting by homodimeric EEA1. *Mol Cell*. 8:947-58.
- Dutzler, R., E.B. Campbell, M. Cadene, B.T. Chait, and R. MacKinnon. 2002. X-ray structure of a Cl⁻ chloride channel at 3.0 Å reveals the molecular basis of anion selectivity. *Nature*. 415:287-94.
- Ellgaard, L., and A. Helenius. 2003. Quality control in the endoplasmic reticulum. *Nat Rev Mol Cell Biol*. 4:181-91.
- Elorza, M.V., H. Rico, and R. Sentandreu. 1983. Calcofluor white alters the assembly of chitin fibrils in *Saccharomyces cerevisiae* and *Candida albicans* cells. *J Gen Microbiol*. 129:1577-82.
- Entian, K.D., T. Schuster, J.H. Hegemann, D. Becher, H. Feldmann, U. Guldener, R. Gotz, M. Hansen, C.P. Hollenberg, G. Jansen, W. Kramer, S. Klein, P. Kotter, J. Kricke, H. Launhardt, G. Mannhaupt, A. Maiertl, P. Meyer, W. Mewes, T. Munder, R.K. Niedenthal, M. Ramezani Rad, A. Rohmer, A. Romer, A. Hinnen, and et al. 1999. Functional analysis of 150 deletion mutants in *Saccharomyces cerevisiae* by a systematic approach. *Mol Gen Genet*. 262:683-702.
- Estrada de Martin, P., Y. Du, P. Novick, and S. Ferro-Novick. 2005. Ice2p is important for the distribution and structure of the cortical ER network in *Saccharomyces cerevisiae*. *J Cell Sci*. 118:65-77.
- Estrada, P., J. Kim, J. Coleman, L. Walker, B. Dunn, P. Takizawa, P. Novick, and S. Ferro-Novick. 2003. Myo4p and She3p are required for cortical ER inheritance in *Saccharomyces cerevisiae*. *J Cell Biol*. 163:1255-66.
- Ewald, S.E., B.L. Lee, L. Lau, K.E. Wickliffe, G.P. Shi, H.A. Chapman, and G.M. Barton. 2008. The ectodomain of Toll-like receptor 9 is cleaved to generate a functional receptor. *Nature*. 456:658-62.
- Fang, M., B.G. Kearns, A. Gedvilaite, S. Kagiwada, M. Kearns, M.K. Fung, and V.A. Bankaitis. 1996. Kes1p shares homology with human oxysterol binding protein and participates in a novel regulatory pathway for yeast Golgi-derived transport vesicle biogenesis. *Embo J*. 15:6447-59.
- Fatal, N., L. Karhinen, E. Jokitalo, and M. Makarow. 2004. Active and specific recruitment of a soluble cargo protein for endoplasmic reticulum exit in the absence of functional COPII component Sec24p. *J Cell Sci*. 117:1665-73.
- Faty, M., M. Fink, and Y. Barral. 2002. Septins: a ring to part mother and daughter. *Curr Genet*. 41:123-31.
- Faulhammer, F., G. Konrad, B. Brankatschk, S. Tahirovic, A. Knodler, and P. Mayinger. 2005. Cell growth-dependent coordination of lipid signaling and glycosylation is mediated by interactions between Sac1p and Dpm1p. *J Cell Biol*. 168:185-91.

- Fehrenbacher, K.L., D. Davis, M. Wu, I. Boldogh, and L.A. Pon. 2002. Endoplasmic reticulum dynamics, inheritance, and cytoskeletal interactions in budding yeast. *Mol Biol Cell*. 13:854-65.
- Ferguson, K.M., M.A. Lemmon, J. Schlessinger, and P.B. Sigler. 1995. Structure of the high affinity complex of inositol trisphosphate with a phospholipase C pleckstrin homology domain. *Cell*. 83:1037-46.
- Ficarro, S.B., M.L. McClelland, P.T. Stukenberg, D.J. Burke, M.M. Ross, J. Shabanowitz, D.F. Hunt, and F.M. White. 2002. Phosphoproteome analysis by mass spectrometry and its application to *Saccharomyces cerevisiae*. *Nat Biotechnol*. 20:301-5.
- Fischer, M.A., K. Temmerman, E. Ercan, W. Nickel and M. Seedorf. 2009. Binding of plasma membrane lipids recruits the yeast integral membrane protein Ist2 to the cortical ER. *Traffic*. In press.
- Florkiewicz, R.Z., R.A. Majack, R.D. Buechler, and E. Florkiewicz. 1995. Quantitative export of FGF-2 occurs through an alternative, energy-dependent, non-ER/Golgi pathway. *J Cell Physiol*. 162:388-99.
- Franz, A., K. Maass, and M. Seedorf. 2007. A complex peptide-sorting signal, but no mRNA signal, is required for the Sec-independent transport of Ist2 from the yeast ER to the plasma membrane. *FEBS Lett*. 581:401-5.
- Franz, A. 2005. Analyse der Cis-Elemente im C-Terminus von Ist2 für den SEC-unabhängigen Transport in die Plasmamembran. Diploma Thesis, University of Heidelberg.
- Frischauf, I., R. Schindl, I. Derler, J. Bergsmann, M. Fahrner, and C. Romanin. 2008. The STIM/Orai coupling machinery. *Channels (Austin)*. 2:261-8.
- Fromme, J.C., and R. Schekman. 2005. COPII-coated vesicles: flexible enough for large cargo? *Curr Opin Cell Biol*. 17:345-52.
- Fukuda, M., K. Ibata, and K. Mikoshiba. 2001. A unique spacer domain of synaptotagmin IV is essential for Golgi localization. *J Neurochem*. 77:730-40.
- Gaigg, B., R. Simbeni, C. Hrastnik, F. Paltauf, and G. Daum. 1995. Characterization of a microsomal subfraction associated with mitochondria of the yeast, *Saccharomyces cerevisiae*. Involvement in synthesis and import of phospholipids into mitochondria. *Biochim Biophys Acta*. 1234:214-20.
- Gaigg, B., B. Timischl, L. Corbino, and R. Schneiter. 2005. Synthesis of sphingolipids with very long chain fatty acids but not ergosterol is required for routing of newly synthesized plasma membrane ATPase to the cell surface of yeast. *J Biol Chem*. 280:22515-22.
- Gary, J.D., A.E. Wurmser, C.J. Bonangelino, L.S. Weisman, and S.D. Emr. 1998. Fab1p is essential for PtdIns(3)P 5-kinase activity and the maintenance of vacuolar size and membrane homeostasis. *J Cell Biol*. 143:65-79.

- Gaynor, P.M., and G.M. Carman. 1990. Phosphatidylethanolamine methyltransferase and phospholipid methyltransferase activities from *Saccharomyces cerevisiae*. Enzymological and kinetic properties. *Biochim Biophys Acta*. 1045:156-63.
- Gething, M.J. 1999. Role and regulation of the ER chaperone BiP. *Semin Cell Dev Biol*. 10:465-72.
- Gillooly, D.J., I.C. Morrow, M. Lindsay, R. Gould, N.J. Bryant, J.M. Gaullier, R.G. Parton, and H. Stenmark. 2000. Localization of phosphatidylinositol 3-phosphate in yeast and mammalian cells. *Embo J*. 19:4577-88.
- Gorlich, D., S. Prehn, E. Hartmann, K.U. Kalies, and T.A. Rapoport. 1992. A mammalian homolog of SEC61p and SECYp is associated with ribosomes and nascent polypeptides during translocation. *Cell*. 71:489-503.
- Guo, W., and P. Novick. 2004. The exocyst meets the translocon: a regulatory circuit for secretion and protein synthesis? *Trends Cell Biol*. 14:61-3.
- Gusarova, V., J.L. Brodsky, and E.A. Fisher. 2003. Apolipoprotein B100 exit from the endoplasmic reticulum (ER) is COPII-dependent, and its lipidation to very low density lipoprotein occurs post-ER. *J Biol Chem*. 278:48051-8.
- Hama, H., E.A. Schnieders, J. Thorner, J.Y. Takemoto, and D.B. DeWald. 1999. Direct involvement of phosphatidylinositol 4-phosphate in secretion in the yeast *Saccharomyces cerevisiae*. *J Biol Chem*. 274:34294-300.
- Harbury, P.B., T. Zhang, P.S. Kim, and T. Alber. 1993. A switch between two-, three-, and four-stranded coiled coils in GCN4 leucine zipper mutants. *Science*. 262:1401-7.
- Hasdemir, B., D.J. Fitzgerald, I.A. Prior, A.V. Tepikin, and R.D. Burgoyne. 2005. Traffic of Kv4 K⁺ channels mediated by KChIP1 is via a novel post-ER vesicular pathway. *J Cell Biol*. 171:459-69.
- Hegedus, T., A. Aleksandrov, L. Cui, M. Gentzsch, X.B. Chang, and J.R. Riordan. 2006. F508del CFTR with two altered RXR motifs escapes from ER quality control but its channel activity is thermally sensitive. *Biochim Biophys Acta*. 1758:565-72.
- Helenius, J., and M. Aebi. 2002. Transmembrane movement of dolichol linked carbohydrates during N-glycoprotein biosynthesis in the endoplasmic reticulum. *Semin Cell Dev Biol*. 13:171-8.
- Heo, W.D., T. Inoue, W.S. Park, M.L. Kim, B.O. Park, T.J. Wandless, and T. Meyer. 2006. PI(3,4,5)P₃ and PI(4,5)P₂ lipids target proteins with polybasic clusters to the plasma membrane. *Science*. 314:1458-61.
- Homma, K., S. Terui, M. Minemura, H. Qadota, Y. Anraku, Y. Kanaho, and Y. Ohya. 1998. Phosphatidylinositol-4-phosphate 5-kinase localized on the plasma membrane is essential for yeast cell morphogenesis. *J Biol Chem*. 273:15779-86.

- Horvath, A., C. Sutterlin, U. Manning-Krieg, N.R. Movva, and H. Riezman. 1994. Ceramide synthesis enhances transport of GPI-anchored proteins to the Golgi apparatus in yeast. *Embo J.* 13:3687-95.
- Im, Y.J., S. Raychaudhuri, W.A. Prinz, and J.H. Hurley. 2005. Structural mechanism for sterol sensing and transport by OSBP-related proteins. *Nature.* 437:154-8.
- Jansen, R.P., C. Dowzer, C. Michaelis, M. Galova, and K. Nasmyth. 1996. Mother cell-specific HO expression in budding yeast depends on the unconventional myosin myo4p and other cytoplasmic proteins. *Cell.* 84:687-97.
- Johnston, G.C., J.A. Prendergast, and R.A. Singer. 1991. The *Saccharomyces cerevisiae* MYO2 gene encodes an essential myosin for vectorial transport of vesicles. *J Cell Biol.* 113:539-51.
- Joshi, A.S., J. Zhou, V.M. Gohil, S. Chen, and M.L. Greenberg. 2009. Cellular functions of cardiolipin in yeast. *Biochim Biophys Acta.* 1793:212-8.
- Juschke, C., D. Ferring, R.P. Jansen, and M. Seedorf. 2004. A novel transport pathway for a yeast plasma membrane protein encoded by a localized mRNA. *Curr Biol.* 14:406-11.
- Juschke, C., A. Wachter, B. Schwappach, and M. Seedorf. 2005. SEC18/NSF-independent, protein-sorting pathway from the yeast cortical ER to the plasma membrane. *J Cell Biol.* 169:613-22.
- Juschke, C. 2005. Charakterisierung des Transportweges von Ist2p zur Plasmamembran in *Saccharomyces cerevisiae*. PhD Thesis, University of Heidelberg.
- Kagiwada, S., and M. Hashimoto. 2007. The yeast VAP homolog Scs2p has a phosphoinositide-binding ability that is correlated with its activity. *Biochem Biophys Res Commun.* 364:870-6.
- Kappeler, F., D.R. Klopfenstein, M. Foguet, J.P. Paccard, and H.P. Hauri. 1997. The recycling of ERGIC-53 in the early secretory pathway. ERGIC-53 carries a cytosolic endoplasmic reticulum-exit determinant interacting with COPII. *J Biol Chem.* 272:31801-8.
- Karhinen, L., R.N. Bastos, E. Jokitalo, and M. Makarow. 2005. Endoplasmic reticulum exit of a secretory glycoprotein in the absence of sec24p family proteins in yeast. *Traffic.* 6:562-74.
- Katzmann, D.J., C.J. Stefan, M. Babst, and S.D. Emr. 2003. Vps27 recruits ESCRT machinery to endosomes during MVB sorting. *J Cell Biol.* 162:413-23.
- Keenan, R.J., D.M. Freymann, R.M. Stroud, and P. Walter. 2001. The signal recognition particle. *Annu Rev Biochem.* 70:755-75.
- Kim, Y., S. Chattopadhyay, S. Locke, and D.A. Pearce. 2005. Interaction among Btn1p, Btn2p, and Ist2p reveals potential interplay among the vacuole, amino acid levels, and ion homeostasis in the yeast *Saccharomyces cerevisiae*. *Eukaryot Cell.* 4:281-8.

- Kim, Y.M., M.M. Brinkmann, M.E. Paquet, and H.L. Ploegh. 2008. UNC93B1 delivers nucleotide-sensing toll-like receptors to endolysosomes. *Nature*. 452:234-8.
- Klein, D.E., A. Lee, D.W. Frank, M.S. Marks, and M.A. Lemmon. 1998. The pleckstrin homology domains of dynamin isoforms require oligomerization for high affinity phosphoinositide binding. *J Biol Chem*. 273:27725-33.
- Knauer, R., and L. Lehle. 1999. The oligosaccharyltransferase complex from yeast. *Biochim Biophys Acta*. 1426:259-73.
- Kohlwein, S.D., K. Kuchler, C. Sperka-Gottlieb, S.A. Henry, and F. Paltauf. 1988. Identification of mitochondrial and microsomal phosphatidylserine synthase in *Saccharomyces cerevisiae* as the gene product of the CHO1 structural gene. *J Bacteriol*. 170:3778-81.
- Koning, A.J., C.J. Roberts, and R.L. Wright. 1996. Different subcellular localization of *Saccharomyces cerevisiae* HMG-CoA reductase isozymes at elevated levels corresponds to distinct endoplasmic reticulum membrane proliferations. *Mol Biol Cell*. 7:769-89.
- Konrad, G., T. Schlecker, F. Faulhammer, and P. Mayinger. 2002. Retention of the yeast Sac1p phosphatase in the endoplasmic reticulum causes distinct changes in cellular phosphoinositide levels and stimulates microsomal ATP transport. *J Biol Chem*. 277:10547-54.
- Krauss, M., and V. Haucke. 2007. Phosphoinositides: regulators of membrane traffic and protein function. *FEBS Lett*. 581:2105-11.
- Krogh, A., B. Larsson, G. von Heijne, and E.L. Sonnhammer. 2001. Predicting transmembrane protein topology with a hidden Markov model: application to complete genomes. *J Mol Biol*. 305:567-80.
- Kuchler, K., G. Daum, and F. Paltauf. 1986. Subcellular and submitochondrial localization of phospholipid-synthesizing enzymes in *Saccharomyces cerevisiae*. *J Bacteriol*. 165:901-10.
- Kvam, E., and D.S. Goldfarb. 2004. Nvj1p is the outer-nuclear-membrane receptor for oxysterol-binding protein homolog Osh1p in *Saccharomyces cerevisiae*. *J Cell Sci*. 117:4959-68.
- Kvam, E., and D.S. Goldfarb. 2006. Nucleus-vacuole junctions in yeast: anatomy of a membrane contact site. *Biochem Soc Trans*. 34:340-2.
- Lange, S., Y. Katayama, M. Schmid, O. Burkacky, C. Brauchle, D.C. Lamb, and R.P. Jansen. 2008. Simultaneous transport of different localized mRNA species revealed by live-cell imaging. *Traffic*. 9:1256-67.
- Lee, M.C., E.A. Miller, J. Goldberg, L. Orci, and R. Schekman. 2004. Bi-directional protein transport between the ER and Golgi. *Annu Rev Cell Dev Biol*. 20:87-123.

- Lee, M.C., L. Orci, S. Hamamoto, E. Futai, M. Ravazzola, and R. Schekman. 2005. Sar1p N-terminal helix initiates membrane curvature and completes the fission of a COPII vesicle. *Cell*. 122:605-17.
- Lemmon, M.A. 2008. Membrane recognition by phospholipid-binding domains. *Nat Rev Mol Cell Biol*. 9:99-111.
- Lemmon, M.A., and K.M. Ferguson. 2000. Signal-dependent membrane targeting by pleckstrin homology (PH) domains. *Biochem J*. 350 Pt 1:1-18.
- Lemmon, M.A., K.M. Ferguson, R. O'Brien, P.B. Sigler, and J. Schlessinger. 1995. Specific and high-affinity binding of inositol phosphates to an isolated pleckstrin homology domain. *Proc Natl Acad Sci U S A*. 92:10472-6.
- Levine, T. 2004. Short-range intracellular trafficking of small molecules across endoplasmic reticulum junctions. *Trends Cell Biol*. 14:483-90.
- Levine, T.P., and S. Munro. 2001. Dual targeting of Osh1p, a yeast homologue of oxysterol-binding protein, to both the Golgi and the nucleus-vacuole junction. *Mol Biol Cell*. 12:1633-44.
- Levine, T.P., and S. Munro. 2002. Targeting of Golgi-specific pleckstrin homology domains involves both PtdIns 4-kinase-dependent and -independent components. *Curr Biol*. 12:695-704.
- Lewis, R.S. 2007. The molecular choreography of a store-operated calcium channel. *Nature*. 446:284-7.
- Li, X., M.P. Rivas, M. Fang, J. Marchena, B. Mehrotra, A. Chaudhary, L. Feng, G.D. Prestwich, and V.A. Bankaitis. 2002. Analysis of oxysterol binding protein homologue Kes1p function in regulation of Sec14p-dependent protein transport from the yeast Golgi complex. *J Cell Biol*. 157:63-77.
- Li, Y., and W.A. Prinz. 2004. ATP-binding cassette (ABC) transporters mediate nonvesicular, raft-modulated sterol movement from the plasma membrane to the endoplasmic reticulum. *J Biol Chem*. 279:45226-34.
- Liou, J., M.L. Kim, W.D. Heo, J.T. Jones, J.W. Myers, J.E. Ferrell, Jr., and T. Meyer. 2005. STIM is a Ca²⁺ sensor essential for Ca²⁺-store-depletion-triggered Ca²⁺ influx. *Curr Biol*. 15:1235-41.
- Lippincott-Schwartz, J., and W. Liu. 2006. Insights into COPI coat assembly and function in living cells. *Trends Cell Biol*. 16:e1-4.
- Loewen, C.J., A. Roy, and T.P. Levine. 2003. A conserved ER targeting motif in three families of lipid binding proteins and in Opi1p binds VAP. *Embo J*. 22:2025-35.
- Loewen, C.J., B.P. Young, S. Tavassoli, and T.P. Levine. 2007. Inheritance of cortical ER in yeast is required for normal septin organization. *J Cell Biol*. 179:467-83.

- Lowe, M., and F.A. Barr. 2007. Inheritance and biogenesis of organelles in the secretory pathway. *Nat Rev Mol Cell Biol.* 8:429-39.
- Luedeke, C., S.B. Frei, I. Sbalzarini, H. Schwarz, A. Spang, and Y. Barral. 2005. Septin-dependent compartmentalization of the endoplasmic reticulum during yeast polarized growth. *J Cell Biol.* 169:897-908.
- Ma, D., N. Zerangue, Y.F. Lin, A. Collins, M. Yu, Y.N. Jan, and L.Y. Jan. 2001. Role of ER export signals in controlling surface potassium channel numbers. *Science.* 291:316-9.
- Ma, D., N. Zerangue, K. Raab-Graham, S.R. Fried, Y.N. Jan, and L.Y. Jan. 2002. Diverse trafficking patterns due to multiple traffic motifs in G protein-activated inwardly rectifying potassium channels from brain and heart. *Neuron.* 33:715-29.
- Maass, K., M.A. Fischer, M. Seiler, K. Temmerman, W. Nickel, and M. Seedorf. 2009. A signal comprising a basic cluster and an amphipathic α -helix interacts with lipids and is required for the transport of Ist2 to the yeast cortical ER. *J Cell Sci.* 122:625-35.
- Maass, K. 2008. Untersuchungen zum Sortierungsweg von Ist2 in *Saccharomyces cerevisiae*. PhD Thesis, University of Heidelberg.
- Madden, K., and M. Snyder. 1998. Cell polarity and morphogenesis in budding yeast. *Annu Rev Microbiol.* 52:687-744.
- Makkerh, J.P., C. Dingwall, and R.A. Laskey. 1996. Comparative mutagenesis of nuclear localization signals reveals the importance of neutral and acidic amino acids. *Curr Biol.* 6:1025-7.
- Malkus, P., F. Jiang, and R. Schekman. 2002. Concentrative sorting of secretory cargo proteins into COPII-coated vesicles. *J Cell Biol.* 159:915-21.
- Malsam, J., S. Kreye, and T.H. Sollner. 2008. Membrane fusion: SNAREs and regulation. *Cell Mol Life Sci.* 65:2814-32.
- Martinez-Menarguez, J.A., H.J. Geuze, J.W. Slot, and J. Klumperman. 1999. Vesicular tubular clusters between the ER and Golgi mediate concentration of soluble secretory proteins by exclusion from COPI-coated vesicles. *Cell.* 98:81-90.
- McGrath, J.P., and A. Varshavsky. 1989. The yeast STE6 gene encodes a homologue of the mammalian multidrug resistance P-glycoprotein. *Nature.* 340:400-4.
- McLaughlin, S., and D. Murray. 2005. Plasma membrane phosphoinositide organization by protein electrostatics. *Nature.* 438:605-11.
- McMahon, H.T., and J.L. Gallop. 2005. Membrane curvature and mechanisms of dynamic cell membrane remodelling. *Nature.* 438:590-6.

- Michelsen, K., T. Mrowiec, K.E. Duderstadt, S. Frey, D.L. Minor, M.P. Mayer, and B. Schwappach. 2006. A multimeric membrane protein reveals 14-3-3 isoform specificity in forward transport in yeast. *Traffic*. 7:903-16.
- Michelsen, K., H. Yuan, and B. Schwappach. 2005. Hide and run. Arginine-based endoplasmic-reticulum-sorting motifs in the assembly of heteromultimeric membrane proteins. *EMBO Rep*. 6:717-22.
- Middleton, R.E., D.J. Pheasant, and C. Miller. 1996. Homodimeric architecture of a ClC-type chloride ion channel. *Nature*. 383:337-40.
- Miller, E.A., T.H. Beilharz, P.N. Malkus, M.C. Lee, S. Hamamoto, L. Orci, and R. Schekman. 2003. Multiple cargo binding sites on the COPII subunit Sec24p ensure capture of diverse membrane proteins into transport vesicles. *Cell*. 114:497-509.
- Miller, J.D., H. Wilhelm, L. Gierasch, R. Gilmore, and P. Walter. 1993. GTP binding and hydrolysis by the signal recognition particle during initiation of protein translocation. *Nature*. 366:351-4.
- Mitsui, K., K. Hatakeyama, M. Matsushita, and H. Kanazawa. 2009. *Saccharomyces cerevisiae* Na⁺/H⁺ antiporter Nha1p associates with lipid rafts and requires sphingolipid for stable localization to the plasma membrane. *J Biochem*.
- Mizuta, K., S. Tsutsumi, H. Inoue, Y. Sakamoto, K. Miyatake, K. Miyawaki, S. Noji, N. Kamata, and M. Itakura. 2007. Molecular characterization of GDD1/TMEM16E, the gene product responsible for autosomal dominant gnathodiaphyseal dysplasia. *Biochem Biophys Res Commun*. 357:126-32.
- Mousley, C.J., K.R. Tyeryar, P. Vincent-Pope, and V.A. Bankaitis. 2007. The Sec14-superfamily and the regulatory interface between phospholipid metabolism and membrane trafficking. *Biochim Biophys Acta*. 1771:727-36.
- Mrowiec, T., and B. Schwappach. 2006. 14-3-3 proteins in membrane protein transport. *Biol Chem*. 387:1227-36.
- Munro, S. 2002. Organelle identity and the targeting of peripheral membrane proteins. *Curr Opin Cell Biol*. 14:506-14.
- Nakamura, H., K. Miura, Y. Fukuda, I. Shibuya, A. Ohta, and M. Takagi. 2000. Phosphatidylserine synthesis required for the maximal tryptophan transport activity in *Saccharomyces cerevisiae*. *Biosci Biotechnol Biochem*. 64:167-72.
- Navarro-Borelly, L., A. Somasundaram, M. Yamashita, D. Ren, R.J. Miller, and M. Prakriya. 2008. STIM1-Orai1 interactions and Orai1 conformational changes revealed by live-cell FRET microscopy. *J Physiol*. 586:5383-401.
- Ng, D.T., J.D. Brown, and P. Walter. 1996. Signal sequences specify the targeting route to the endoplasmic reticulum membrane. *J Cell Biol*. 134:269-78.

- Nice, D.C., T.K. Sato, P.E. Stromhaug, S.D. Emr, and D.J. Klionsky. 2002. Cooperative binding of the cytoplasm to vacuole targeting pathway proteins, Cvt13 and Cvt20, to phosphatidylinositol 3-phosphate at the pre-autophagosomal structure is required for selective autophagy. *J Biol Chem.* 277:30198-207.
- Nichols, W.C., U. Seligsohn, A. Zivelin, V.H. Terry, C.E. Hertel, M.A. Wheatley, M.J. Moussalli, H.P. Hauri, N. Ciavarella, R.J. Kaufman, and D. Ginsburg. 1998. Mutations in the ER-Golgi intermediate compartment protein ERGIC-53 cause combined deficiency of coagulation factors V and VIII. *Cell.* 93:61-70.
- Nickel, W., and C. Rabouille. 2009. Mechanisms of regulated unconventional protein secretion. *Nat Rev Mol Cell Biol.* 10:148-55.
- Nickel, W., and M. Seedorf. 2008. Unconventional mechanisms of protein transport to the cell surface of eukaryotic cells. *Annu Rev Cell Dev Biol.* 24:287-308.
- Niessing, D., S. Huttelmaier, D. Zenklusen, R.H. Singer, and S.K. Burley. 2004. She2p is a novel RNA binding protein with a basic helical hairpin motif. *Cell.* 119:491-502.
- Nikawa, J., and S. Yamashita. 1997. Phosphatidylinositol synthase from yeast. *Biochim Biophys Acta.* 1348:173-8.
- Nishikawa, S., J.L. Brodsky, and K. Nakatsukasa. 2005. Roles of molecular chaperones in endoplasmic reticulum (ER) quality control and ER-associated degradation (ERAD). *J Biochem.* 137:551-5.
- Novick, P., C. Field, and R. Schekman. 1980. Identification of 23 complementation groups required for post-translational events in the yeast secretory pathway. *Cell.* 21:205-15.
- Odorizzi, G., M. Babst, and S.D. Emr. 1998. Fab1p PtdIns(3)P 5-kinase function essential for protein sorting in the multivesicular body. *Cell.* 95:847-58.
- Odorizzi, G., M. Babst, and S.D. Emr. 2000. Phosphoinositide signaling and the regulation of membrane trafficking in yeast. *Trends Biochem Sci.* 25:229-35.
- Oeffinger, M., K.E. Wei, R. Rogers, J.A. DeGrasse, B.T. Chait, J.D. Aitchison, and M.P. Rout. 2007. Comprehensive analysis of diverse ribonucleoprotein complexes. *Nat Methods.* 4:951-6.
- Olivier, C., G. Poirier, P. Gendron, A. Boisgontier, F. Major, and P. Chartrand. 2005. Identification of a conserved RNA motif essential for She2p recognition and mRNA localization to the yeast bud. *Mol Cell Biol.* 25:4752-66.
- Opekarova, M., K. Malinska, L. Novakova, and W. Tanner. 2005. Differential effect of phosphatidylethanolamine depletion on raft proteins: further evidence for diversity of rafts in *Saccharomyces cerevisiae*. *Biochim Biophys Acta.* 1711:87-95.
- Orci, L., R. Montesano, P. Meda, F. Malaisse-Lagae, D. Brown, A. Perrelet, and P. Vassalli. 1981. Heterogeneous distribution of filipin--cholesterol complexes across the cisternae of the Golgi apparatus. *Proc Natl Acad Sci U S A.* 78:293-7.

- Osborne, A.R., T.A. Rapoport, and B. van den Berg. 2005. Protein translocation by the Sec61/SecY channel. *Annu Rev Cell Dev Biol.* 21:529-50.
- Pagano, A., F. Letourneur, D. Garcia-Estefania, J.L. Carpentier, L. Orci, and J.P. Paccaud. 1999. Sec24 proteins and sorting at the endoplasmic reticulum. *J Biol Chem.* 274:7833-40.
- Palade, G.E. 1958. Microsomes and Ribonucleoprotein Particles. 1st Symposium of Biophysical Society. *Pergamon Press, Elmsford, New York.*
- Palmer, R.E., E. Hogan, and D. Koshland. 1990. Mitotic transmission of artificial chromosomes in cdc mutants of the yeast, *Saccharomyces cerevisiae*. *Genetics.* 125:763-74.
- Pan, X., P. Roberts, Y. Chen, E. Kvam, N. Shulga, K. Huang, S. Lemmon, and D.S. Goldfarb. 2000. Nucleus-vacuole junctions in *Saccharomyces cerevisiae* are formed through the direct interaction of Vac8p with Nvj1p. *Mol Biol Cell.* 11:2445-57.
- Paravicini, G., M. Cooper, L. Friedli, D.J. Smith, J.L. Carpentier, L.S. Klig, and M.A. Payton. 1992. The osmotic integrity of the yeast cell requires a functional PKC1 gene product. *Mol Cell Biol.* 12:4896-905.
- Parrish, W.R., C.J. Stefan, and S.D. Emr. 2004. Essential role for the myotubularin-related phosphatase Ymr1p and the synaptojanin-like phosphatases Sjl2p and Sjl3p in regulation of phosphatidylinositol 3-phosphate in yeast. *Mol Biol Cell.* 15:3567-79.
- Peng, J., D. Schwartz, J.E. Elias, C.C. Thoreen, D. Cheng, G. Marsischky, J. Roelofs, D. Finley, and S.P. Gygi. 2003. A proteomics approach to understanding protein ubiquitination. *Nat Biotechnol.* 21:921-6.
- Penna, A., A. Demuro, A.V. Yeromin, S.L. Zhang, O. Safrina, I. Parker, and M.D. Cahalan. 2008. The CRAC channel consists of a tetramer formed by Stim-induced dimerization of Orai dimers. *Nature.* 456:116-20.
- Perktold, A., B. Zechmann, G. Daum, and G. Zellnig. 2007. Organelle association visualized by three-dimensional ultrastructural imaging of the yeast cell. *FEMS Yeast Res.* 7:629-38.
- Pichler, H., B. Gaigg, C. Hrastnik, G. Achleitner, S.D. Kohlwein, G. Zellnig, A. Perktold, and G. Daum. 2001. A subfraction of the yeast endoplasmic reticulum associates with the plasma membrane and has a high capacity to synthesize lipids. *Eur J Biochem.* 268:2351-61.
- Pineau, L., L. Bonifait, J.M. Berjeaud, P. Alimardani-Theuil, T. Berges, and T. Ferreira. 2008. A lipid-mediated quality control process in the Golgi apparatus in yeast. *Mol Biol Cell.* 19:807-21.
- Ploegh, H.L. 2007. A lipid-based model for the creation of an escape hatch from the endoplasmic reticulum. *Nature.* 448:435-8.

- Pool, M.R. 2003. Getting to the membrane: how is co-translational protein targeting to the endoplasmic reticulum regulated? *Biochem Soc Trans.* 31:1232-7.
- Pool, M.R., J. Stumm, T.A. Fulga, I. Sinning, and B. Dobberstein. 2002. Distinct modes of signal recognition particle interaction with the ribosome. *Science.* 297:1345-8.
- Preuss, D., J. Mulholland, C.A. Kaiser, P. Orlean, C. Albright, M.D. Rose, P.W. Robbins, and D. Botstein. 1991. Structure of the yeast endoplasmic reticulum: localization of ER proteins using immunofluorescence and immunoelectron microscopy. *Yeast.* 7:891-911.
- Prinz, W.A., L. Grzyb, M. Veenhuis, J.A. Kahana, P.A. Silver, and T.A. Rapoport. 2000. Mutants affecting the structure of the cortical endoplasmic reticulum in *Saccharomyces cerevisiae*. *J Cell Biol.* 150:461-74.
- Putney, J.W., Jr. 2007. Recent breakthroughs in the molecular mechanism of capacitative calcium entry (with thoughts on how we got here). *Cell Calcium.* 42:103-10.
- Rajakumari, S., K. Grillitsch, and G. Daum. 2008. Synthesis and turnover of non-polar lipids in yeast. *Prog Lipid Res.* 47:157-71.
- Raychaudhuri, S., Y.J. Im, J.H. Hurley, and W.A. Prinz. 2006. Nonvesicular sterol movement from plasma membrane to ER requires oxysterol-binding protein-related proteins and phosphoinositides. *J Cell Biol.* 173:107-19.
- Roberts, P., S. Moshitch-Moshkovitz, E. Kvam, E. O'Toole, M. Winey, and D.S. Goldfarb. 2003. Piecemeal microautophagy of nucleus in *Saccharomyces cerevisiae*. *Mol Biol Cell.* 14:129-41.
- Robinson, J.S., D.J. Klionsky, L.M. Banta, and S.D. Emr. 1988. Protein sorting in *Saccharomyces cerevisiae*: isolation of mutants defective in the delivery and processing of multiple vacuolar hydrolases. *Mol Cell Biol.* 8:4936-48.
- Rock, J.R., C.R. Futtner, and B.D. Harfe. 2008. The transmembrane protein TMEM16A is required for normal development of the murine trachea. *Dev Biol.* 321:141-9.
- Romisch, K. 2005. Endoplasmic reticulum-associated degradation. *Annu Rev Cell Dev Biol.* 21:435-56.
- Ronchi, P., S. Colombo, M. Francolini, and N. Borgese. 2008. Transmembrane domain-dependent partitioning of membrane proteins within the endoplasmic reticulum. *J Cell Biol.* 181:105-18.
- Rossi, D., V. Barone, E. Giacomello, V. Cusimano, and V. Sorrentino. 2008. The sarcoplasmic reticulum: an organized patchwork of specialized domains. *Traffic.* 9:1044-9.
- Rothman, J.H., I. Howald, and T.H. Stevens. 1989. Characterization of genes required for protein sorting and vacuolar function in the yeast *Saccharomyces cerevisiae*. *Embo J.* 8:2057-65.

- Routt, S.M., M.M. Ryan, K. Tyeryar, K.E. Rizzieri, C. Mousley, O. Roumanie, P.J. Brennwald, and V.A. Bankaitis. 2005. Nonclassical PITPs activate PLD via the Stt4p PtdIns-4-kinase and modulate function of late stages of exocytosis in vegetative yeast. *Traffic*. 6:1157-72.
- Rubartelli, A., F. Cozzolino, M. Talio, and R. Sitia. 1990. A novel secretory pathway for interleukin-1 beta, a protein lacking a signal sequence. *Embo J*. 9:1503-10.
- Sambrook, J., D.W. Russell. 2001. Molecular Cloning. A Laboratory Manual. *Cold Spring Harbor Laboratory Press, Cold Spring Harbor, New York*. Third Edition.
- Sapay, N., Y. Guermeur, and G. Deleage. 2006. Prediction of amphipathic in-plane membrane anchors in monotopic proteins using a SVM classifier. *BMC Bioinformatics*. 7:255.
- Sato, K., and A. Nakano. 2002. Emp47p and its close homolog Emp46p have a tyrosine-containing endoplasmic reticulum exit signal and function in glycoprotein secretion in *Saccharomyces cerevisiae*. *Mol Biol Cell*. 13:2518-32.
- Sato, K., and A. Nakano. 2003. Oligomerization of a cargo receptor directs protein sorting into COPII-coated transport vesicles. *Mol Biol Cell*. 14:3055-63.
- Sato, S., I. Burdett, and R.C. Hughes. 1993. Secretion of the baby hamster kidney 30-kDa galactose-binding lectin from polarized and nonpolarized cells: a pathway independent of the endoplasmic reticulum-Golgi complex. *Exp Cell Res*. 207:8-18.
- Schafer, T., H. Zentgraf, C. Zehe, B. Brugger, J. Bernhagen, and W. Nickel. 2004. Unconventional secretion of fibroblast growth factor 2 is mediated by direct translocation across the plasma membrane of mammalian cells. *J Biol Chem*. 279:6244-51.
- Schekman, R., and P. Novick. 2004. 23 genes, 23 years later. *Cell*. 116:S13-5, 1 p following S19.
- Schiavo, G., Q.M. Gu, G.D. Prestwich, T.H. Sollner, and J.E. Rothman. 1996. Calcium-dependent switching of the specificity of phosphoinositide binding to synaptotagmin. *Proc Natl Acad Sci U S A*. 93:13327-32.
- Schimmoller, F., B. Singer-Kruger, S. Schroder, U. Kruger, C. Barlowe, and H. Riezman. 1995. The absence of Emp24p, a component of ER-derived COPII-coated vesicles, causes a defect in transport of selected proteins to the Golgi. *Embo J*. 14:1329-39.
- Schmid, M., A. Jaedicke, T.G. Du, and R.P. Jansen. 2006. Coordination of endoplasmic reticulum and mRNA localization to the yeast bud. *Curr Biol*. 16:1538-43.
- Schnabl, M., G. Daum, and H. Pichler. 2005. Multiple lipid transport pathways to the plasma membrane in yeast. *Biochim Biophys Acta*. 1687:130-40.
- Schroeder, B.C., T. Cheng, Y.N. Jan, and L.Y. Jan. 2008. Expression cloning of TMEM16A as a calcium-activated chloride channel subunit. *Cell*. 134:1019-29.

- Schu, P.V., K. Takegawa, M.J. Fry, J.H. Stack, M.D. Waterfield, and S.D. Emr. 1993. Phosphatidylinositol 3-kinase encoded by yeast VPS34 gene essential for protein sorting. *Science*. 260:88-91.
- Schulz, T.A., and W.A. Prinz. 2007. Sterol transport in yeast and the oxysterol binding protein homologue (OSH) family. *Biochim Biophys Acta*. 1771:769-80.
- Sciorra, V.A., A. Audhya, A.B. Parsons, N. Segev, C. Boone, and S.D. Emr. 2005. Synthetic genetic array analysis of the PtdIns 4-kinase Pik1p identifies components in a Golgi-specific Ypt31/rab-GTPase signaling pathway. *Mol Biol Cell*. 16:776-93.
- Seelenmeyer, C., S. Wegehangel, I. Tews, M. Kunzler, M. Aebi, and W. Nickel. 2005. Cell surface counter receptors are essential components of the unconventional export machinery of galectin-1. *J Cell Biol*. 171:373-81.
- Sevier, C.S., O.A. Weisz, M. Davis, and C.E. Machamer. 2000. Efficient export of the vesicular stomatitis virus G protein from the endoplasmic reticulum requires a signal in the cytoplasmic tail that includes both tyrosine-based and di-acidic motifs. *Mol Biol Cell*. 11:13-22.
- Shepard, K.A., A.P. Gerber, A. Jambhekar, P.A. Takizawa, P.O. Brown, D. Herschlag, J.L. DeRisi, and R.D. Vale. 2003. Widespread cytoplasmic mRNA transport in yeast: identification of 22 bud-localized transcripts using DNA microarray analysis. *Proc Natl Acad Sci U S A*. 100:11429-34.
- Shi, J., C.W. Heegaard, J.T. Rasmussen, and G.E. Gilbert. 2004. Lactadherin binds selectively to membranes containing phosphatidyl-L-serine and increased curvature. *Biochim Biophys Acta*. 1667:82-90.
- Shibata, Y., G.K. Voeltz, and T.A. Rapoport. 2006. Rough sheets and smooth tubules. *Cell*. 126:435-9.
- Siddiqi, S.A., F.S. Gorelick, J.T. Mahan, and C.M. Mansbach, 2nd. 2003. COPII proteins are required for Golgi fusion but not for endoplasmic reticulum budding of the pre-chylomicron transport vesicle. *J Cell Sci*. 116:415-27.
- Siders, W.M., J.C. Klimovitz, and S.B. Mizel. 1993. Characterization of the structural requirements and cell type specificity of IL-1 alpha and IL-1 beta secretion. *J Biol Chem*. 268:22170-4.
- Sikorski, R.S., and P. Hieter. 1989. A system of shuttle vectors and yeast host strains designed for efficient manipulation of DNA in *Saccharomyces cerevisiae*. *Genetics*. 122:19-27.
- Simon, S.M., and G. Blobel. 1991. A protein-conducting channel in the endoplasmic reticulum. *Cell*. 65:371-80.
- Snapp, E.L., R.S. Hegde, M. Francolini, F. Lombardo, S. Colombo, E. Pedrazzini, N. Borgese, and J. Lippincott-Schwartz. 2003. Formation of stacked ER cisternae by low affinity protein interactions. *J Cell Biol*. 163:257-69.

- Sollner, T., S.W. Whiteheart, M. Brunner, H. Erdjument-Bromage, S. Geromanos, P. Tempst, and J.E. Rothman. 1993. SNAP receptors implicated in vesicle targeting and fusion. *Nature*. 362:318-24.
- Sonnichsen, F.D., J.E. Van Eyk, R.S. Hodges, and B.D. Sykes. 1992. Effect of trifluoroethanol on protein secondary structure: an NMR and CD study using a synthetic actin peptide. *Biochemistry*. 31:8790-8.
- Sorensen, J.B., K. Wiederhold, E.M. Muller, I. Milosevic, G. Nagy, B.L. de Groot, H. Grubmuller, and D. Fasshauer. 2006. Sequential N- to C-terminal SNARE complex assembly drives priming and fusion of secretory vesicles. *Embo J*. 25:955-66.
- Staehelin, L.A. 1997. The plant ER: a dynamic organelle composed of a large number of discrete functional domains. *Plant J*. 11:1151-65.
- Stagg, S.M., C. Gurkan, D.M. Fowler, P. LaPointe, T.R. Foss, C.S. Potter, B. Carragher, and W.E. Balch. 2006. Structure of the Sec13/31 COPII coat cage. *Nature*. 439:234-8.
- Stefan, C.J., A. Audhya, and S.D. Emr. 2002. The yeast synaptojanin-like proteins control the cellular distribution of phosphatidylinositol (4,5)-bisphosphate. *Mol Biol Cell*. 13:542-57.
- Stephens, D.J., and R. Pepperkok. 2002. Imaging of procollagen transport reveals COPI-dependent cargo sorting during ER-to-Golgi transport in mammalian cells. *J Cell Sci*. 115:1149-60.
- Strahl, T., H. Hama, D.B. DeWald, and J. Thorner. 2005. Yeast phosphatidylinositol 4-kinase, Pik1, has essential roles at the Golgi and in the nucleus. *J Cell Biol*. 171:967-79.
- Strahl, T., and J. Thorner. 2007. Synthesis and function of membrane phosphoinositides in budding yeast, *Saccharomyces cerevisiae*. *Biochim Biophys Acta*. 1771:353-404.
- Sullivan, D.P., H. Ohvo-Rekila, N.A. Baumann, C.T. Beh, and A.K. Menon. 2006. Sterol trafficking between the endoplasmic reticulum and plasma membrane in yeast. *Biochem Soc Trans*. 34:356-8.
- Tahirovic, S., M. Schorr, and P. Mayinger. 2005. Regulation of intracellular phosphatidylinositol-4-phosphate by the Sac1 lipid phosphatase. *Traffic*. 6:116-30.
- Takizawa, P.A., J.L. DeRisi, J.E. Wilhelm, and R.D. Vale. 2000. Plasma membrane compartmentalization in yeast by messenger RNA transport and a septin diffusion barrier. *Science*. 290:341-4.
- Takizawa, P.A., and R.D. Vale. 2000. The myosin motor, Myo4p, binds Ash1 mRNA via the adapter protein, She3p. *Proc Natl Acad Sci U S A*. 97:5273-8.
- Temmerman, K., A.D. Ebert, H.M. Muller, I. Sinning, I. Tews, and W. Nickel. 2008. A direct role for phosphatidylinositol-4,5-bisphosphate in unconventional secretion of fibroblast growth factor 2. *Traffic*. 9:1204-17.

- Temmerman, K., and W. Nickel. 2009. A novel flow cytometric assay to quantify interactions between proteins and membrane lipids. *J Lipid Res.*
- Thiyagarajan, M.M., R.P. Stracquatano, A.N. Pronin, D.S. Evanko, J.L. Benovic, and P.B. Wedegaertner. 2004. A predicted amphipathic helix mediates plasma membrane localization of GRK5. *J Biol Chem.* 279:17989-95.
- Toikkanen, J.H., K.J. Miller, H. Soderlund, J. Jantti, and S. Keranen. 2003. The beta subunit of the Sec61p endoplasmic reticulum translocon interacts with the exocyst complex in *Saccharomyces cerevisiae*. *J Biol Chem.* 278:20946-53.
- Tsai, B., Y. Ye, and T.A. Rapoport. 2002. Retro-translocation of proteins from the endoplasmic reticulum into the cytosol. *Nat Rev Mol Cell Biol.* 3:246-55.
- Tyorinoja, K., T. Nurminen, and H. Suomalainen. 1974. The cell-envelope glycolipids of baker's yeast. *Biochem J.* 141:133-9.
- Urbani, L., and R.D. Simoni. 1990. Cholesterol and vesicular stomatitis virus G protein take separate routes from the endoplasmic reticulum to the plasma membrane. *J Biol Chem.* 265:1919-23.
- Van den Berg, B., W.M. Clemons, Jr., I. Collinson, Y. Modis, E. Hartmann, S.C. Harrison, and T.A. Rapoport. 2004. X-ray structure of a protein-conducting channel. *Nature.* 427:36-44.
- Vembar, S.S., and J.L. Brodsky. 2008. One step at a time: endoplasmic reticulum-associated degradation. *Nat Rev Mol Cell Biol.* 9:944-57.
- Voelker, D.R. 1997. Phosphatidylserine decarboxylase. *Biochim Biophys Acta.* 1348:236-44.
- Voelker, D.R. 2005. Bridging gaps in phospholipid transport. *Trends Biochem Sci.* 30:396-404.
- Voeltz, G.K., W.A. Prinz, Y. Shibata, J.M. Rist, and T.A. Rapoport. 2006. A class of membrane proteins shaping the tubular endoplasmic reticulum. *Cell.* 124:573-86.
- Voeltz, G.K., M.M. Rolls, and T.A. Rapoport. 2002. Structural organization of the endoplasmic reticulum. *EMBO Rep.* 3:944-50.
- Votsmeier, C., and D. Gallwitz. 2001. An acidic sequence of a putative yeast Golgi membrane protein binds COPII and facilitates ER export. *Embo J.* 20:6742-50.
- Wach, A., A. Brachat, R. Pohlmann, and P. Philippsen. 1994. New heterologous modules for classical or PCR-based gene disruptions in *Saccharomyces cerevisiae*. *Yeast.* 10:1793-808.
- Wachter, A., and B. Schwappach. 2005. The yeast CLC chloride channel is proteolytically processed by the furin-like protease Kex2p in the first extracellular loop. *FEBS Lett.* 579:1149-53.

- Wahlman, J., G.N. DeMartino, W.R. Skach, N.J. Bulleid, J.L. Brodsky, and A.E. Johnson. 2007. Real-time fluorescence detection of ERAD substrate retrotranslocation in a mammalian in vitro system. *Cell*. 129:943-55.
- Walch-Solimena, C., and P. Novick. 1999. The yeast phosphatidylinositol-4-OH kinase pik1 regulates secretion at the Golgi. *Nat Cell Biol*. 1:523-5.
- Wang, X., J. Matteson, Y. An, B. Moyer, J.S. Yoo, S. Bannykh, I.A. Wilson, J.R. Riordan, and W.E. Balch. 2004. COPII-dependent export of cystic fibrosis transmembrane conductance regulator from the ER uses a di-acidic exit code. *J Cell Biol*. 167:65-74.
- Wenk, M.R., and P. De Camilli. 2004. Protein-lipid interactions and phosphoinositide metabolism in membrane traffic: insights from vesicle recycling in nerve terminals. *Proc Natl Acad Sci U S A*. 101:8262-9.
- Wickner, W., and R. Schekman. 2008. Membrane fusion. *Nat Struct Mol Biol*. 15:658-664.
- Wiederkehr, A., Y. Du, M. Pypaert, S. Ferro-Novick, and P. Novick. 2003. Sec3p is needed for the spatial regulation of secretion and for the inheritance of the cortical endoplasmic reticulum. *Mol Biol Cell*. 14:4770-82.
- Wieland, F.T., M.L. Gleason, T.A. Serafini, and J.E. Rothman. 1987. The rate of bulk flow from the endoplasmic reticulum to the cell surface. *Cell*. 50:289-300.
- Wilcox, C.A., K. Redding, R. Wright, and R.S. Fuller. 1992. Mutation of a tyrosine localization signal in the cytosolic tail of yeast Kex2 protease disrupts Golgi retention and results in default transport to the vacuole. *Mol Biol Cell*. 3:1353-71.
- Wu, M.M., J. Buchanan, R.M. Luik, and R.S. Lewis. 2006. Ca²⁺ store depletion causes STIM1 to accumulate in ER regions closely associated with the plasma membrane. *J Cell Biol*. 174:803-13.
- Wurmser, A.E., and S.D. Emr. 2002. Novel PtdIns(3)P-binding protein Etf1 functions as an effector of the Vps34 PtdIns 3-kinase in autophagy. *J Cell Biol*. 158:761-72.
- Yamamoto, A., D.B. DeWald, I.V. Boronenkov, R.A. Anderson, S.D. Emr, and D. Koshland. 1995. Novel PI(4)P 5-kinase homologue, Fab1p, essential for normal vacuole function and morphology in yeast. *Mol Biol Cell*. 6:525-39.
- Yang, Y.D., H. Cho, J.Y. Koo, M.H. Tak, Y. Cho, W.S. Shim, S.P. Park, J. Lee, B. Lee, B.M. Kim, R. Raouf, Y.K. Shin, and U. Oh. 2008. TMEM16A confers receptor-activated calcium-dependent chloride conductance. *Nature*. 455:1210-5.
- Yin, H.L., and P.A. Janmey. 2003. Phosphoinositide regulation of the actin cytoskeleton. *Annu Rev Physiol*. 65:761-89.
- Yoshida, S., Y. Ohya, M. Goebel, A. Nakano, and Y. Anraku. 1994. A novel gene, STT4, encodes a phosphatidylinositol 4-kinase in the PKC1 protein kinase pathway of *Saccharomyces cerevisiae*. *J Biol Chem*. 269:1166-72.

- Yuan, H., K. Michelsen, and B. Schwappach. 2003. 14-3-3 dimers probe the assembly status of multimeric membrane proteins. *Curr Biol.* 13:638-46.
- Zacharias, D.A., J.D. Violin, A.C. Newton, and R.Y. Tsien. 2002. Partitioning of lipid-modified monomeric GFPs into membrane microdomains of live cells. *Science.* 296:913-6.
- Zanolari, B., S. Friant, K. Funato, C. Sutterlin, B.J. Stevenson, and H. Riezman. 2000. Sphingoid base synthesis requirement for endocytosis in *Saccharomyces cerevisiae*. *Embo J.* 19:2824-33.
- Zehe, C., A. Engling, S. Wegehingel, T. Schafer, and W. Nickel. 2006. Cell-surface heparan sulfate proteoglycans are essential components of the unconventional export machinery of FGF-2. *Proc Natl Acad Sci U S A.* 103:15479-84.
- Zerangue, N., B. Schwappach, Y.N. Jan, and L.Y. Jan. 1999. A new ER trafficking signal regulates the subunit stoichiometry of plasma membrane K(ATP) channels. *Neuron.* 22:537-48.
- Zhang, G., M.G. Kazanietz, P.M. Blumberg, and J.H. Hurley. 1995. Crystal structure of the cys2 activator-binding domain of protein kinase C delta in complex with phorbol ester. *Cell.* 81:917-24.
- Zhang, X., R.L. Lester, and R.C. Dickson. 2004. Pil1p and Lsp1p negatively regulate the 3-phosphoinositide-dependent protein kinase-like kinase Pkh1p and downstream signaling pathways Pkc1p and Ypk1p. *J Biol Chem.* 279:22030-8.
- Zhao, C., J.T. Slevin, and S.W. Whiteheart. 2007. Cellular functions of NSF: not just SNAPs and SNAREs. *FEBS Lett.* 581:2140-9.
- Zheng, B., J.N. Wu, W. Schober, D.E. Lewis, and T. Vida. 1998. Isolation of yeast mutants defective for localization of vacuolar vital dyes. *Proc Natl Acad Sci U S A.* 95:11721-6.

7 Acknowledgements

Approaching the end of the thesis, and looking back to the last years, I would like to thank these people, who supported this thesis by discussions, knowledge, funding or simply by their presence:

My entire family, for continuous support and for keeping an interested smile on their face when trying to explain them what all this is about. Especially a deep thanks to my mother, without whom I never could have and would have walked this way.

Matthias Seedorf, for offering me a project and a position, sharing all his yeast wisdom, believing in the lipid story, and investing so many hours of his time.

Bernhard Dobberstein for his support, advice and for fruitful discussions.

Blanche Schwappach, Walter Nickel and Marius Lemberg, for being PhD examiners and/or TAC members. Especially a big thanks to Blanche for sticking by this project, although being 1000 miles away.

Every single member of the Dobberstein/Seedorf lab, for a great working atmosphere. It was an honor and a great fun to be a member of this lab. And don't forget about my hat. Especially thanks to Gerry for providing countless yeast plates and plasmids.

Walter Nickel and Koen Temmerman, for a very fruitful collaboration, without which chapter 2.3 would probably not have been possible.

In particular Koen for having so much fun in the lab and for calling me a guinea pig in his thesis. The guinea pig is still holding the higher Snooker break.

Everyone who feels forgotten in this chapter, for not blaming me.

Dana, for providing thousands of encouraging words, all her patience and her equanimity, when I needed it most.